The Role of Floor Systems in Tall Concrete-Timber Buildings

A Variant Study on the Relationship between Dynamic behavior, Sustainability, and Construction Cost

Master's thesis report

M.E. Snijders

Delft University of Technology

TU Delft

The Role of Floor Systems in Tall Concrete-Timber Buildings

A Variant Study on the Relationship between Dynamic behavior, Sustainability, and Construction Cost

by

M.E. Snijders

to obtain the degree of Master of Science in Civil Engineering
at Delft University of Technology
to be defended publicly on March 24th 2025 at 9:45 AM.

Name	Maria Elisabeth Snijders
Student number	4713710
Product duration	May 2024 - March 2025
Date	March 17th 2025

Graduation Committee

Dr. Ir. Roel Schipper (Chair)	TU Delft CITG - Applied mechanics
Dr. Ir. Marc Ottelé	TU Delft CITG - Materials & Environment
Dr. Ir. Michele Mirra	TU Delft CITG - Biobased Structures and Materials

Preface

The completion of this thesis marks the final step in my master's studies. This research was conducted as part of my graduation from the Delft University of Technology's Civil Engineering Master's program, track Building Engineering. It has been an exciting journey exploring the role of floor systems in tall concrete-timber buildings, driven by my interest in sustainable construction and its implementation in high-rise structures. With the growing focus on hybrid buildings as a more sustainable solution, I was eager to investigate how different floor systems influence key design aspects such as dynamic performance, environmental impact, and cost. This research contributes to a holistic approach to building design.

Readers interested in the different floor systems applicable to tall buildings are encouraged to refer to Chapter 3. Those looking for the study's outcomes can find them in Chapter 9 and the conclusions and recommendations are provided in Chapters 10 and 11.

Conducting this research has been both challenging and rewarding. Along the way, I encountered setbacks that sometimes required me to take a step back before making further progress, like clearly defining the problem or choosing the right methodology. The process of modelling, making assumptions, and balancing workload and output presented its difficulties. However, overcoming these challenges has deepened my understanding of structural engineering and sustainability in high-rise construction. On a personal level, this experience has allowed me to develop my analytical skills and recognize the value of collaboration.

I would like to express my sincere gratitude to my supervisors, Roel Schipper, Marc Ottelé, and Michele Mirra, for their continuous support, valuable insights, and constructive feedback throughout this process. Additionally, I am thankful to Anneloes Klapwijk for her mental support and encouragement in developing my soft skills and maintaining balance. I also extend my thanks to the faculty of Civil Engineering and Geosciences at Delft University of Technology for providing the necessary resources to complete this study. Furthermore, I appreciate the contributions of industry professionals and university staff who shared their expertise, helping me refine my research approach. Lastly, I am deeply grateful to my family for their unwavering support and encouragement.

I hope this thesis provides valuable insights for researchers, engineers, and designers working on the integration of timber in high-rise construction. I look forward to seeing how this field evolves and how sustainable innovations will shape the future of tall buildings.

Unless the Lord builds the house, the builders labor in vain.

Marisa Snijders
Nieuw-Beijerland, March 2025

Summary

The increasing demand for sustainable and high-rise buildings has led to the development of hybrid concrete-timber structures. These buildings incorporate a concrete core and columns for stability, combined with timber and concrete floor systems, providing an opportunity to balance sustainability, structural efficiency, and cost-effectiveness. While this approach presents opportunities, it also introduces several challenges related to structural dynamics, fire safety, environmental impact, and construction costs.

A key issue in concrete-timber hybrid buildings is their lower weight due to timber floors that are lighter than concrete floors, which makes them more susceptible to wind-induced vibrations. Additionally, the irregular mass distribution caused by alternating timber and concrete floors over the height of the building influences the dynamic response of the building. From an environmental perspective, timber is often regarded as a sustainable material due to its carbon storage capability. However, the extent to which hybrid systems reduce overall carbon emissions compared to concrete buildings remains uncertain. Furthermore, construction costs are closely tied to structural and environmental performance, impacting the feasibility of such buildings.

Despite growing interest in hybrid concrete-timber high-rises, existing research lacks an integrated approach that examines the relationships between dynamic behavior, environmental impact, and construction cost. Although individual aspects have been studied, the correlation between these design factors remains unclear. Additionally, the influence of parameters such as building height, floor type, and concrete-timber distribution on these design aspects has not been extensively explored.

This research aims to support the integral design of hybrid concrete-timber high-rises by offering a structured approach to evaluating key design choices and their implications. The findings contribute to a more holistic approach to hybrid building design, supporting designers, policymakers, and researchers in optimizing hybrid systems.

This thesis explores the influence of key building parameters on the design aspects of tall concrete-timber buildings during the early design phase. The goal is to identify relationships between dynamic behavior, environmental performance, and building cost by analyzing various building variants. The studied parameters include building height, floor plan, floor type, and the percentage of concrete floors. To achieve this, three hypotheses are formulated that connect the design aspects with the percentage of concrete floors. By analyzing different percentage of concrete in the floor systems, the study aims to provide insights into the complex interactions between these aspects.

The methodology consists of three parts. First, building variants are designed based on predefined parameters, using structural calculations for floor systems, concrete cores, and foundations. Second, models are developed to determine the dependent variables: dynamic behavior (first natural frequency), environmental performance (Environmental Cost Index through Life Cycle Assessment), and construction cost. Based on the results of the models relationships between independent and dependent variables are analyzed to identify trends and interactions. Finally, correlations between the three design aspects are examined to provide insights into their interdependencies.

The results indicate that building height is the most significant factor influencing dynamic behavior, environmental performance, and construction cost. This is evident from the distinct scatter plots for each building height. The ECI value for buildings between 70 and 90m ranges from 12 to 28 €/m², while for buildings of 110m, it ranges from 20 to 33 €/m². Construction costs for buildings between 70 and 90m range from 735 to 875 €/m², and between 850 and 1000 €/m² for buildings of 110m. By analyzing the results, no significant correlation between construction cost and other parameters was found, as the effect ranges of the parameters are similar. Moreover, the dynamic behavior of the buildings remains within safe limits. Additionally, variations in foundation piles and core dimensions significantly impact the environmental cost index (ECI) and construction cost, making their inclusion essential for accurate comparisons. Finally, the model effectively analyzes specific parameters, thereby

providing clear insights into their influence on design aspects.

Keywords: Tall Timber-Concrete Hybrid Buildings, Environmental performance, Environmental Cost Index, Construction cost, Wind-induced Dynamic Behavior.

Contents

List of Figures

Part I

Research outline

1

Introduction

1.1. Trends driving tall hybrid buildings

Over the past decade there has been a notable increase in tall hybrid buildings, which combine both concrete and timber. A hybrid building is defined as a structure that uses multiple building materials for its load-bearing structure. The growth of these buildings can be explained by various trends, policies, and technical developments in the construction sector. During the last century, the rapid increase in population has led to urbanization and land scarcity in cities [1]. To meet society's needs, urban areas can be densified through high-rise construction. Another challenge society faces is climate change, driven primarily by anthropogenic carbon emissions [2]. The construction industry and its operations play a significant role in this context, as illustrated by Figure 1.1. In 2018, they were responsible for 39% of global greenhouse gas emissions, from which 11% is emitted during the production of building materials and construction [3].

Recent innovations have led to Engineering Timber Products (ETP) with improved material properties, which are suitable for high-rise structures. The development of these products, such as cross-laminated timber (CLT), shown in Figure 1.2 enables the production of larger structural elements. This makes it feasible to construct taller timber buildings [4]. Another compelling reason for using these timber elements is their low embedded carbon footprint. Embodied carbon refers to the carbon emissions released by the building materials and processes during production, construction, and maintenance of the building over its lifespan. Unlike concrete and steel, timber absorbs CO2 during its growth process, contributing to a more sustainable building material. Reducing the embodied carbon will positively impact the carbon footprint of a building, while also lowering raw material consumption and contribute to the circular economy [5]. In summary, the use of engineered timber products in tall buildings offers a solution to societal challenges, such as urbanization and the climate crisis.

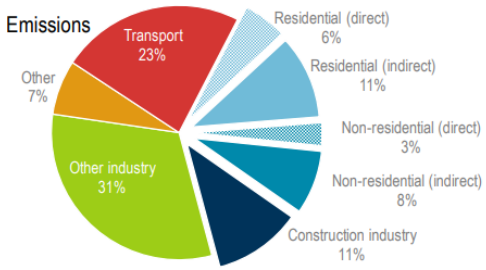

Figure 1.1: Global share construction industry emissions, 2018 [2]

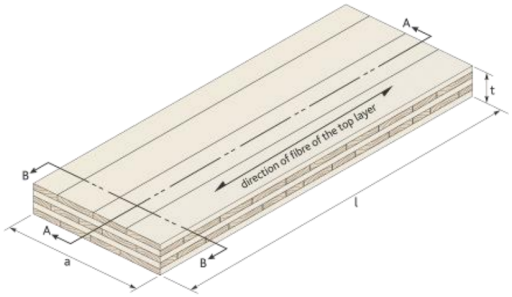

Figure 1.2: CLT panel [6]

1.2. Challenges in concrete-timber hybrid buildings

Using timber as the primary structural material in high-rise buildings is not yet common, as it presents several challenges. Timber typically has lower stiffness and mass compared to concrete and steel, making the building more vulnerable to dynamic wind loads, which can result in undesirable vibrations within the building. Moreover, the uncertainty surrounding timber's combustibility raises concerns about fire safety, necessitating additional measures to ensure adequate fire resistance and to mitigate fire hazards [7].

In response to these challenges, the design of a tall concrete-timber hybrid building has been proposed. This hybrid structure aims to combine the sustainability of timber with the strength of concrete, leveraging their individual advantages to enhance overall building performance.

Designing a tall concrete-timber building is a complex multidisciplinary task, involving the integration of various, potentially conflicting, objectives from different disciplines. This process requires a detailed approach and deep understanding of material properties and structural behaviour. Since requirements related to safety, reliability, fire, sound, sustainability, and cost are all integrated into the structural system, a well-balanced, holistic design approach is essential. Because of this complex integral design, constructing tall concrete-timber hybrid buildings is not yet common practice [8].

1.3. Literature

Despite advancements in hybrid building design, several uncertainties persist due to limited experience and ongoing challenges in the field. The literature can be grouped into two main areas: the first focuses on current developments in building practices, and the second examines the effects of hybridization on specific disciplines related to the challenges outlined before.

The first field focuses on the analysis of existing hybrid timber-concrete buildings, revealing that most use central cores within prismatic floor plans, with shear frame systems being the most common structural approach [9]. Currently the tallest concrete-timber hybrid building has this type of hybrid system. This building, the Ascent MKE has a height of 87 meters and is shown in Figure 1.3. Additional studies aim to identify the most effective structural systems. For buildings between 10 and 50 stories, core and braced systems are found to be efficient in terms of material use and embodied carbon. In contrast, for taller structures, trussed tube systems demonstrate greater efficiency [10, 11].

Much of the existing research in the second field focuses on one or two aspects rather than an integrated design approach, resulting in a lack of comprehensive understanding. Several studies examine both the dynamic and environmental performance of hybrid buildings. One study highlights how the combination of timber and concrete floors can enhance seismic resilience in tall structures, primarily due to reduced weight, which also contributes to a smaller carbon footprint compared to traditional all-concrete designs [12]. Other research indicates that replacing concrete with timber floors benefits the dynamic behavior. The arrangement of alternating timber and concrete floors throughout a building's height also impacts dynamic performance [13]. These types of studies demonstrate how various parameters influence specific design aspects and how these insights can be applied in practice.

1.4. Limitations in research

Several limitations in the literature can be noted. Firstly, understanding the influence of several key parameters on different design aspects is essential. While the effects of various floor types have been studied, the use of alternating concrete and timber floors remains underexplored, particularly as they have not yet been implemented in practice. This presents a unique opportunity to examine how such alternations affect different design aspects.

Secondly, as several research investigates the dynamic behavior of hybrid building designs in combination with examining the environmental performance, currently, there is no established correlation between these design aspects, highlighting the need for deeper insights into how adjustments in specific areas can impact outcomes in another design aspect. Besides, the intersection of parameters and construction costs and the relation with other design aspects is another area that warrants further investigation, as existing literature has not thoroughly examined these relationships.

By addressing these gaps, this research contributes to a new understanding of the correlations between different design aspects in tall concrete-timber hybrid buildings, aligning with the complex, multidisciplinary nature of integral design.

1.5. Problem statement

The trend towards constructing taller and more environmentally friendly buildings can be achieved by integrating timber and concrete construction materials. One approach is to use a structural system that combines a concrete core and columns for stiffness and lateral load resistance, along with a floor system that incorporates both timber and concrete floors at various levels as shown in Figure 1.4.

Several issues are related to this structural system. Tall buildings with timber floors are typically lighter than concrete buildings, which makes them more susceptible to wind-induced vibrations [14]. Additionally, irregular mass distribution can lead to a distinct dynamic response. Besides, incorporating a specific fire safety design approach for structures with both timber and concrete floors is crucial to guarantee the fire safety of the building. While timber elements are often assumed to contribute to environmental sustainability, a question remains whether combining timber and concrete floors can significantly help reduce carbon emissions. Additionally, construction cost is directly linked to both structural and environmental performance, and together, these aspects influence the overall feasibility of the building.

As the demand for sustainable, efficient, and resilient building designs continues to grow, understanding the interplay between various design aspects, such as dynamic behavior, environmental performance, and cost, is critical. In this thesis, these design aspects are combined, emphasizing the relevance of their correlation for various building variants. By examining different variants, it explores the impact of several key parameters on these design aspects. This approach aligns with the holistic, integrated design strategy essential for these hybrid buildings.

Figure 1.3: Ascent MKE Courtesy: Thornton Tomasetti

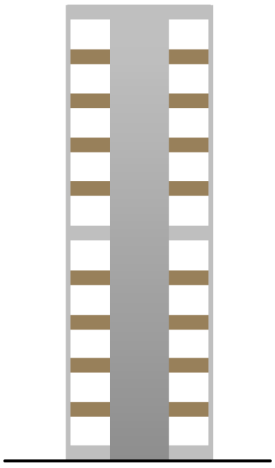

Figure 1.4: Tall Concrete-timber building with alternating floors

1.6. Relevance

Solving the challenges associated with hybrid concrete-timber buildings is of significant relevance in today's construction and architectural landscape. This thesis provides designers with guidelines for creating hybrid structural systems that combine timber and concrete. By examining different floor types and alternations, it encourages practitioners to adopt innovative practices that enhance techniques, materials, and overall project outcomes.

The findings reveal how adjustments to specific parameters impact various design aspects, helping to identify modifications that can improve performance. As current codes and standards lack proven solutions for conflicting design issues, design teams must seek balanced compromises. This research

aids stakeholders in the early design stages by aligning goals toward an integrated, holistic approach.

The findings of this research can inform policies by demonstrating how specific building materials impact environmental performance. By promoting the use of these materials, the study can facilitate the approval process for such buildings through quantitative analysis. It will illustrate how hybrid systems can be constructed in practice, thereby aligning policy with contemporary design practices.

This research will also identify and address existing gaps in the literature that have not been thoroughly explored. It will provide valuable data and insights on a specific structural system, enriching the literature by integrating multiple disciplines and offering a broader, interconnected viewpoint. By combining literature from various fields, the thesis will enhance understanding and encourage cross-disciplinary collaboration in the study of hybrid building systems.

2

Research approach

The following chapter presents the study's approach. First, Section 2.1 outlines the goal of this thesis, followed by the hypotheses in Section 2.2. Section 2.3 introduces the sub-questions that support the hypotheses. Next, Section 2.4 explains the methodology, detailing the setup and workflow of the thesis, which will generate the results needed to verify the hypotheses. Finally, the scope of the study is discussed.

2.1. Goal

The purpose of this study is to establish the correlations between building parameters and design aspects for tall concrete-timber buildings during the early design phase. The building parameters include height, floor plan, floor type, and the percentage of concrete floors, while the design aspects focus on dynamic behaviour, environmental performance, and building cost.

2.2. Hypotheses

To achieve the goal, three hypotheses are defined, each focusing on the relationship between two design aspects as shown in Figure 2.1. These hypotheses serve to clarify the research goal and provide direction for the thesis, ensuring they can be verified in the concluding chapter.

Environmental Performance – Dynamic Behaviour:
There is an inverse linear relationship between the environmental cost index (ECI) and the first natural frequency as the percentage of concrete floors increases for a specific building height.

Dynamic Behaviour – Construction Cost:
For a given building height, the relationship between the first natural frequency and the construction cost follows a linear trend with increasing percentage of concrete floors.

Environmental Performance – Construction Cost:
A specific floor system with an optimal percentage of concrete floors achieves a balance between the ECI value and building cost.

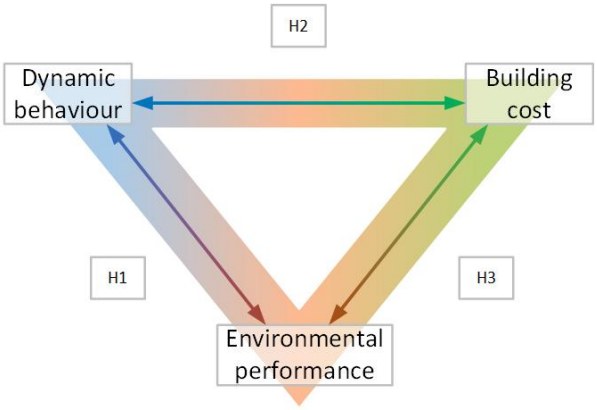

Figure 2.1: Design aspects

2.3. Sub-questions

To work toward the goal, several sub-questions are formulated and answered throughout the report. The study is divided into two parts: the literature study and the variant study, each with its respective sub-questions.

Literature study

1. How are fire safety standards integrated into the design of tall hybrid concrete-timber buildings?
2. What modelling technique is used to analyse the dynamic behaviour and obtain the natural frequency and accelerations of tall hybrid concrete-timber buildings?
3. How do concrete and timber floor types differ in environmental performance when considering production and end-of-life scenarios?
4. What parts must be included to make an accurate estimation in early design stage of the building cost of tall hybrid concrete-timber buildings?

Variant study

5. What is the relation between the mass of the floor type and the concrete core thickness and the number of foundation piles?
6. How do floor type and floor alternations influence the dynamic behavior of these buildings?
7. What impact do the parameters: floor type, floor alternations and building height have on a building's environmental performance?
8. How do floor alternations affect the construction cost?

2.4. Methodology and report outline

In this part, the methodology of the thesis is outlined. The purpose of this section is to provide a clear understanding of the approach, calculations, modelling procedures and analyses used to address the research question. In Figure 2.2 an overview is given of all the parts with including steps.

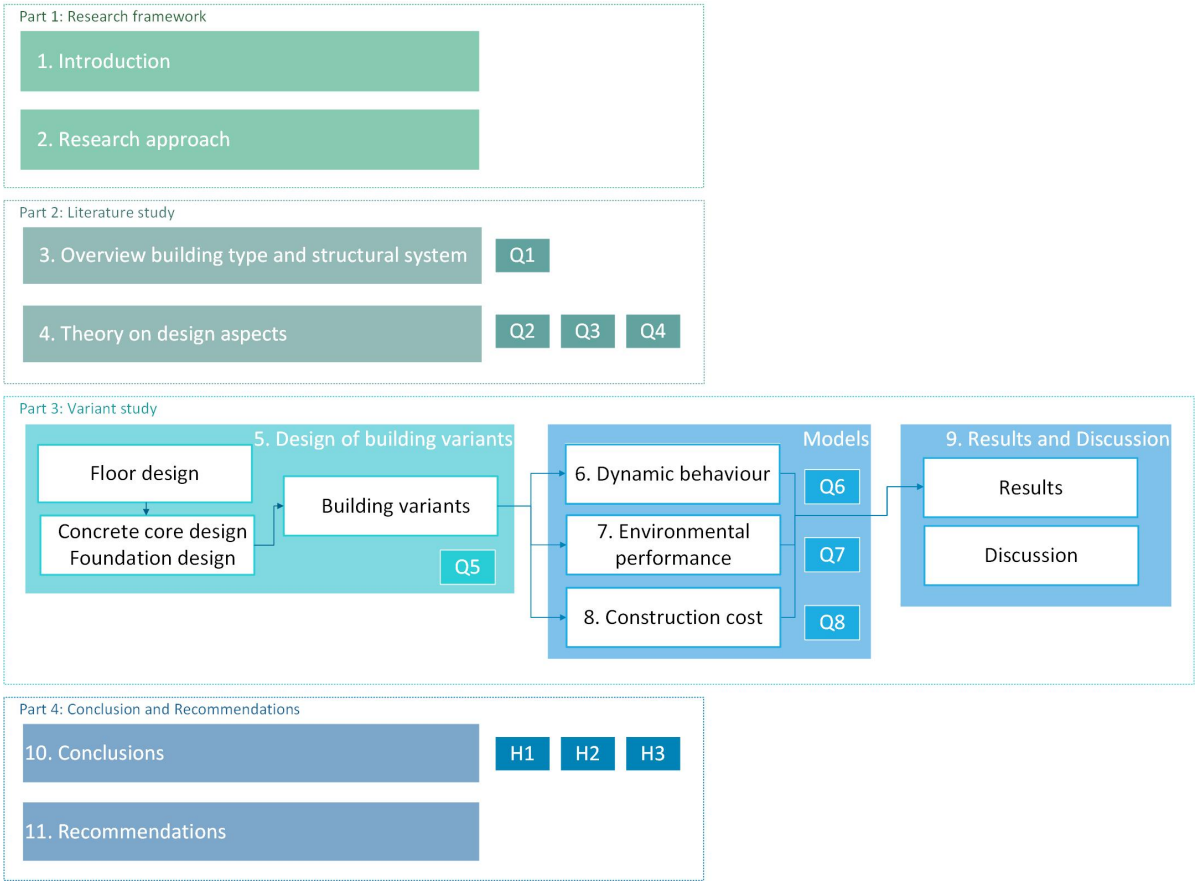

Figure 2.2: Overview methodology

2.4.1 Part 1: Research framework

Part 1 gives the framework of the thesis. It includes an introduction of the topic in Chapter 1 and the current chapter gives the research approach, including the goal, hypothesis, methodology and scope.

2.4.2 Part 2: Literature study

Part 2 focuses on the literature study, which provides further information on the parameters and design aspects in respectively Chapters 3 and 4. These chapters provide insights and background on the research approach and at the end subquestions 1 to 4 are answered.

2.4.3 Part 3: Relation between independent and dependent variables

Part 3, the variant study, consists of three subparts. The first section, outlined in Chapter 5, focuses on the dimensioning of structural elements based on the defined parameters and boundary conditions, with the goal of developing the building variants. This subpart is divided into three sections:

1. **Floor design** – The dimensions of the floor elements are calculated using the Calculatis software from Stora Enso.
2. **Concrete core and foundation design** – The dimensions of the stability system's structural elements, including the concrete core and the number of foundation piles, are determined using Karamba3D (a Grasshopper plugin) in combination with Python.

3. **Calculation of dependent variable** – Several dependent variables are derived from the developed building variants, serving as input for the second subpart of the variant study.

The Cooltoren serves as the reference for the geometry of the building variants. At the end of this chapter, subquestion 5 is answered.

In subpart 2, the calculations for the three dependent variables are divided into three chapters. A common aspect across all three models is that they utilize input data from the building variants, supplemented by additional external data. Python software is used to develop and process these models. Each model generates one output-dependent variable that represents a specific design aspect, corresponding to three distinct dependent variables.

1. **Dynamic behavior (Chapter 6)** – Represented by the first natural frequency of the building variant, calculated using a continuous model that describes the building's dynamic behavior. A Python script processes input from the mass and stiffness properties of the building variants. At the end of this chapter, subquestion 6 is answered.
2. **Environmental performance (Chapter 7)** – Represented by the Environmental Cost Index (ECI), calculated through a Life Cycle Assessment (LCA). This assessment relies on material quantities and Environmental Product Declarations (EPDs) as input. At the end of this chapter, subquestion 7 is answered.
3. **Building cost (Chapter 8)** – Represented by the construction costs associated with building the variants. A construction process is developed, incorporating three elements: materials, equipment, and labor required for each step. At the end of this chapter, subquestion 8 is answered.

In the third subparts, based on the output from the models, the relationships between the independent and dependent variables are visualized in graphs in Chapter 9. These visualizations provide a foundation for discussing the results and the hypotheses.

2.4.4 Part 4: Conclusion and Recommendations

The analysis of the results from Part 3 aims to identify potential correlations between the various design aspects, providing a basis for drawing conclusions related to the hypotheses. In Chapter 10, these hypotheses are evaluated, determining whether they can be verified. Chapter 11 then presents recommendations for practical applications and theoretical guidance for further research.

2.5. Scope

The research conducted in this thesis is constrained by several limitations, which are categorized into structural constraints, parameter choices, and design aspects.

2.5.1 Structural design

The building consists of a concrete core and concrete columns, with only the floors and beams varying across different designs, ensuring that creep is not an issue. Several simplifications are made in the design of the building variants; for instance, column dimensions remain consistent throughout the height of the building and across all variants. The development of the building variants is guided by strength, stability, and fire resistance as base and boundary conditions. Fire resistance is considered solely for the structural elements within the load-bearing systems, excluding aspects such as façade flashover. To maintain consistency, fire safety design measures are standardized across all building variants, while other elements, such as egress routes and venting systems, are not included.

2.5.2 Parameters

The number of parameters and building variants is intentionally limited. The building height is constrained by the chosen structural system, which consists of a concrete core with shear walls. This system is feasible only up to a certain height, beyond which the dimensions become impractical. The minimum height is set at 70 m, as this is the threshold for high-rise buildings in the Netherlands. Additionally, floor alternations are restricted to the repetition of timber and concrete floor types throughout the building's height.

2.5.3 Design aspects

The research focuses on three design aspects, with one key issue being how to quantify these aspects. It was decided to use a single dependent variable to represent each design aspect. However, a limitation of this approach is that it may not fully capture the complete essence of each design aspect.

Part II

Literature study

3

Overview of Building Type and Structural System

This Chapter 3 helps to improve the understanding of the the scope, boundary conditions, and independent parameters, progressing from a macro to a micro level. It begins by defining the building type in Section 3, followed by the structural system in Section 3.2, and then the structural elements and materials in Section 3.3. This chapter concludes with Section 3.4, which addresses the fire safety of buildings and forms a bridge to the next chapter.

3.1. Introduction to concrete-timber hybrid buildings

This section begins at the macro level, concentrating on the overall building. The topic is introduced by defining a concrete-timber hybrid building, followed by an overview of the development of tall timber buildings in recent history. Next, several recently constructed buildings are highlighted. Finally, since this thesis focuses on hybrid timber-concrete structures, the trends related to the structural systems of this building type are explored. The goal of this chapter is to provide a general introduction to the type of building and historical developments.

3.1.1 Definition of tall concrete-timber hybrid building

Buildings can be defined by different characteristics. A building can be defined based on the material that is used in the structural system. Three building types are defined [15] and shown in Figure 3.1:

- Single material building
- Mixed building
- Composite building

A composite building uses two or more material over the height of the building, with the dominant material based on the mass ratio in the building. The concrete-timber composite building that is used in this thesis is an example of a composite building with a concrete core and columns and timber floors. On the other hand, a mass timber buildings with concrete linking beams is defined as a timber-concrete composite building [16].

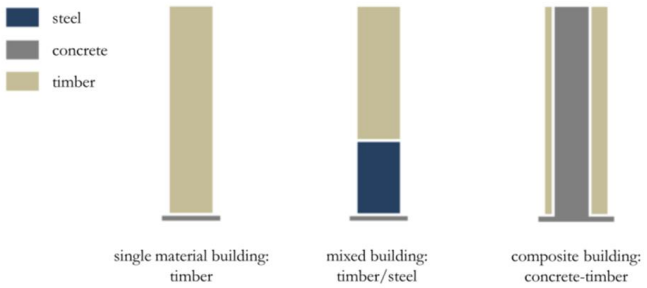

Figure 3.1: Buildings categorized by material [16]

Another way to define a building is by its length. A building is perceived as tall as it exceeds the height of buildings of the same material. Due to the lower mass and stiffness, timber buildings need a structural system that would be used in relatively taller concrete or steel buildings. Therefore, timber buildings are defined as tall at a lower height compared to concrete and steel buildings. The Council on Tall Buildings and Urban Habitat defines a timber building as a tall building starting from 8 storeys. However, concrete and steel buildings are considered tall based on relative height, proportion, and the technologies used in their design, such as vertical transportation technologies and structural wind bracing [16].

3.1.2 Trends in tall timber buildings in history

This subsection outlines the development of tall timber buildings in the past two decades and highlights the observed trends. Kuzmanovska et al. identified the trends in timber buildings by studying 49 timber buildings across Europe, Canada, and the United States revealed an increase in height across four generations [17].

- Generation 1: buildings constructed between 2009 - 2013
- Generation 2: buildings constructed between 2014 - 2016
- Generation 3: buildings constructed between 2017 - 2018
- Generation 4: buildings constructed between 2018 - 2020

The first generation of timber buildings, were predominantly constructed using load-bearing CLT floors and walls and CLT slab systems, with a maximum of 9 stories. This is because CLT floors are inefficient at transferring compression perpendicular to the grain when supporting increasing vertical loads. However, this trend shifted through the generations towards post-beam systems, with the last generation having 67% of the buildings having a post-beam system. A post-beam system is a structural system that transfers loads through vertical elements (posts) and horizontal bending elements (beams). This system aligns with the fact that, over the course of the generations, the dominant building shape has remained rectangular with regular extrusions.

Another noticeable trend is the increasing use of concrete cores in timber buildings, which is partly driven by fire safety requirements for taller structures. Additionally, concrete cores often make tall timber buildings more feasible. The use of CLT cores has declined from 63% to 43% over the four generations, especially in buildings taller than 16 storeys. This suggests that the growing building height over time has influenced the choice of materials and structural systems in timber buildings.

Furthermore, there has been a significant rise in the number of buildings featuring podiums, the lower section of a building that can be constructed from either concrete or steel. The percentage of timber buildings with a concrete podium has increased from 25% to 60%. However, this trend does not appear to correlate with building height [17].

In 2022, there were 84 timber buildings with at least 8 stories [15]. The Council on Tall Buildings and Urban Habitat (CTBUH) categorized these buildings, as shown in Figure 3.3 [15]. The buildings can be divided per function which are residential buildings, office buildings and buildings with mixed-usage as shown in Figure 3.2. Europe holds the majority of the timber buildings, with 71%, followed by North

America at 18% and Australia at 10%. Regarding structural material, 44% are all-timber buildings, 36% are concrete-timber hybrid buildings, 12% are concrete-steel-timber hybrid buildings, and 8% are steel-timber hybrid buildings.

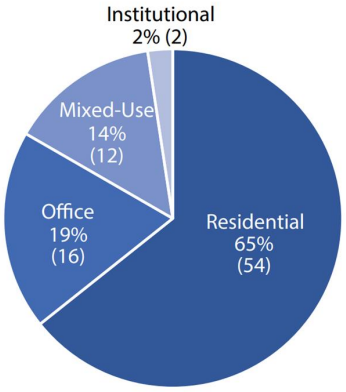

Figure 3.2: Function of tall timber buildings [15]

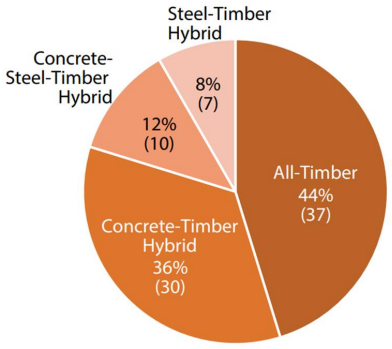

Figure 3.3: Structural type of tall timber buildings [15]

3.1.3 Constructed concrete-timber hybrid buildings

In recent years, the construction of iconic hybrid structures combining timber and concrete has gained significant attention. By analysing the architectural and structural design of three tall timber-concrete hybrid buildings built in recent years, important design parameters can be discovered and further insight can be gained into the design and construction of such structures. These buildings are described in Appendix A, Section A.1. The first building is the Treet building which uses a post-beam system and the second and third building which are the Brock Commons and Ascent MKE both use a hybrid structure with a concrete core and CLT floors. Over the past years, these three buildings have emerged as prominent examples of tall timber structures. Notably, they all incorporate concrete components to enhance the dynamic response to wind loads.

3.1.4 Structural systems in tall timber buildings

The structural systems used in tall timber buildings that exceed 49 m are summarized in Table A.1 in Appendix A. Notably, the majority of these buildings utilize concrete cores for the structural system, thereby falling under the classification of hybrid timber-concrete structures. Furthermore, when it comes to flooring, the predominant choice in most buildings is CLT slabs.

3.2. Structural system of tall hybrid timber-concrete buildings

This section dives further into the structural system of the concrete-timber hybrid building and with that transfers from the macro to the meso level with addressing the function of different structural components. The goal of this section is to give insight in how the structural elements work together to resist the loads.

3.2.1 Core wall system

Tall buildings can be defined as core wall systems when they consist of several shear walls forming a core, to which a frame of columns and beams is connected, as illustrated in Figure 3.4. Compared to a full timber building with the same structural system, a hybrid building offers a higher bearing capacity [18]. And when compared to a structural system with glulam trusses, a core wall system provides greater architectural freedom and spatial flexibility. For example the core can also house utility services and fulfill egress route requirements.

An example of a tall timber-concrete building that uses a concrete wall system is Brock Commons, shown in Figure A.3 in Appendix A. This structural system serves as the basis for designing various building variants. The core wall system is simple and allows for the incorporation of timber floors in tall buildings. This approach enables comparison with more conventional concrete buildings. Additionally, this system allows for adapting the original design of an existing concrete tall building, the Cooltoren in Rotterdam.

3.2.2 Load transfer by structural elements

The load transfer by structural elements can be divided in the transfer of horizontal and vertical loads. In a building with a concrete core, horizontal wind loads are transmitted from the façade through the diaphragm action of the CLT floor panels to the beams, and then to the core walls. The core then transfers these horizontal loads to the foundation by bending and shear deformation. Figure 3.5 shows the floor plan of the building with the wind load acting on the facade. This load is transferred to the concrete core (dark gray) through the diaphragm action of the CLT panels. This diaphragm action generates the bending of the diaphragm that results in tension and compression forces within the floor panels.

The flexibility of the diaphragm affects the overall stiffness of the building and with that influences the building's dynamic behaviour. Using more flexible timber floors reduces the building's stiffness, leading to a lower natural frequency compared to using more rigid concrete floors [19]. Buildings with a lower natural frequency are more susceptible to wind-induced vibrations. This assumption is justified as CLT is quite stiff in its plane, especially compared to its density with respect to concrete, it is justified to not account for the differences in flexibility between different floor types.

The primary contributors to vertical loads are the self-weight of the structure and the variable floor loads. These loads are transferred from the floors to the beams, which then pass the loads to the columns and core. Finally, the columns and core transfer these vertical loads to the foundation piles.

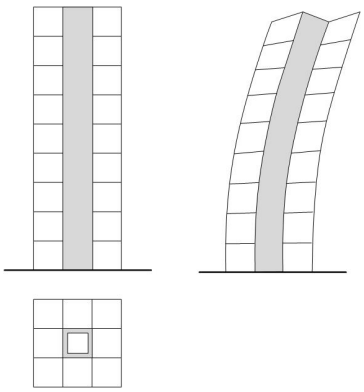

Figure 3.4: Timber-Concrete hybrid building

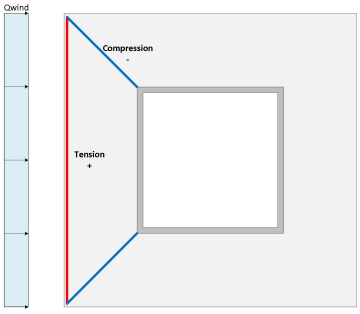

Figure 3.5: Diaphragm action in CLT panel floor

3.3. Materials and floor systems for tall timber buildings

This section begins at the micro level, focusing on the materials used in building construction. It then expands to explore the types of timber floor systems suitable for tall buildings. The aim is to provide an overview of the development of structural timber products, introduce the floor systems analyzed in this thesis.

3.3.1 Timber products development

Engineered timber, also referred to as mass timber, is a construction material in which the properties of the wood are optimized for specific applications through advanced processing techniques. The development of engineering wood products arose over the last 25 years and changed the way timber is applied in the construction industry. Many different products are developed over the past years that all have their specific optimal application. Examples of these products are glued laminated timber (glulam), cross laminated timber (CLT), laminated veneer lumber (LVL) or oriented stranded board (OSB). Several of these products are shown in Figure 3.6. The products are generally created by adhesive bonding of lamellea, veneers or wood chips to create beams, boards or other structural components. The advantages of engineering wood products are that bigger elements can be produced with more homogeneous mechanical properties. The wood that is used in these products is known as clear wood which has less imperfections. This allows for higher load-carrying abilities making it a more sufficient material [20]. The increase in structural properties results in the possibility to built taller buildings [4]. The introduction of these products also impacts the construction process as construction time reduces and building costs are lowered. Next, two of these products are explained in greater detail as these are commonly used as structural element in tall buildings.

Figure 3.6: Engineering Wood Products [21]

3.3.2 Glulam

Glued laminated timber is an engineered wood product made by glueing together multiple layers of timber, known as lamellae, with adhesives. These lamellae are arranged parallel to the grain. An example of a glulam beam is shown in Figure 3.10. Lamellae have higher-quality wood compared to solid timber structural elements due to the reduced amount and size of defects, ensuring greater uniformity and minimizing variability in the mechanical properties of the final product. Glulam beams can be manufactured in larger cross-sections than traditional sawn timber, and they have better and more homogeneous structural properties. They also exhibit less shrinkage and fewer cracks, making them more resistant to moisture and wood pests [22].

3.3.3 Cross Laminated Timber

Cross Laminated Timber is an engineering wood product first introduced in the early 1990s. It is a rigid massive wooden panel with high stability and freedom of dimensions and shape. It consists of layers of softwood lamellae glued together. The layers are mostly oriented perpendicular to the layer below. The panel sizes are available with a width up to 3 m and a length up to 18 m. The typical thickness of

a panel is between 105 and 245 mm. Figure 3.7 illustrates a typical CLT panel and Figure 3.8 shows a cross section of a CLT panel. The panels can be used as floor slabs or shear walls or cores that can transfer gravity loads and lateral loads [6].

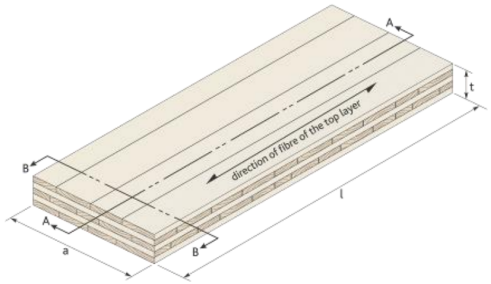

Figure 3.7: 3D view of CLT panel [6]

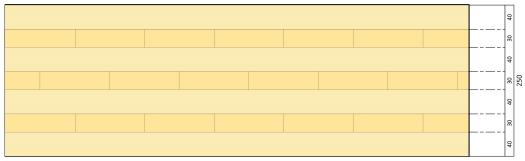

Figure 3.8: Cross-section of CLT panel [6]

One of the advantages of CLT over other engineering wood products is that the entire construction elements can be prefabricated with high in-plane and out-of-plane strength and stiffness properties due to the cross laminating of the lamellae. this makes it possible to make floors that span in two directions and walls that can resist both lateral loads and gravity loads[6]. Other benefits of CLT elements are:

- Short on site construction time.
- Little residual waste.
- Products with high dimensional accuracy.
- Freedom of size and shape.
- Exceptional thermal performance.
- Low self-weight compared to concrete and steel.

Building with cross-laminated timber also has some drawbacks, which are:

- Water and fire protection of CLT products required on construction site.
- High production cost.
- Making alternations during construction is challenging and undesirable.
- High delivery costs.
- The utilities must be fitted in advance.

Mechanical properties

The mechanical properties of CLT panels depends on several factors like wood species, moisture content and the strength of individual layers. Timber is an anisotropic material meaning it has different mechanical properties in different directions relative to the grain. The mechanical properties of GL24h that are used in the CLT panels are shown in Table E.5 in Appendix E.

Strength

In the Eurocode structural classes are defined based on the species and bending and mean bending strength. The mechanical properties of glulam are governed by the proprieties of the sawn timber. Glulam beams are categorized into different strength classes.

Stiffness

The stiffness of a glulam beam can be determined using several methods. The Mechanically Jointed Beams Theory is used to calculate the effective bending stiffness. This method uses the combined stiffness's of the lamellae. The second method is the Shear Analogy Method, that used the Euler Timoshenko beam theory and which is accurate for deep beams. With this method, both the effective bending stiffness and the effective shear stiffness are calculated [22].

3.3.4 CLT with concrete screed

It is common practice to combine a CLT floor with a concrete screed, as shown in Figure 3.9. This topping, usually 4 to 7 cm thick, serves to minimize human-induced vibrations, which can cause noise and it enhances the floor's mass and stiffness. In Europe, it is typical to pour concrete screed over a sound absorption layer and rigid insulation to maximize benefits [22].

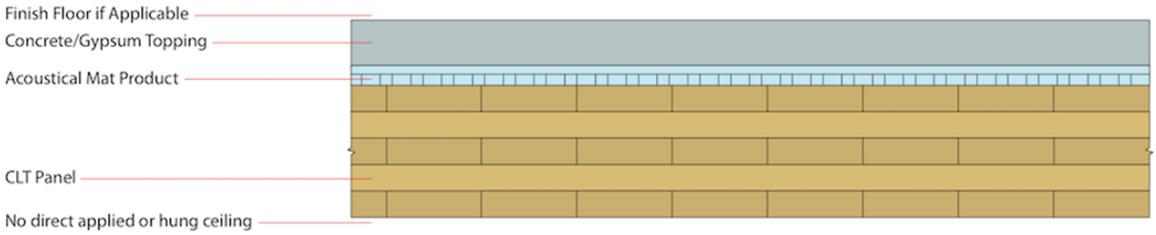

Figure 3.9: CLT with concrete screed [23]

Material properties

The CLT floor supports the additional weight of the concrete screed. Given the thinness of the screed, it is assumed that it does not significantly contribute to the load transfer. Therefore, a CLT floor with a concrete screed is designed as a CLT floor with an added permanent load. The screed helps for fulfilling the vibration verification requirements of the CLT floors. The mechanical properties of the CLT panels remain the same as those without the concrete screed.

3.3.5 Timber-Concrete Composite

A Timber-Concrete Composite (TCC) panel floor consists of a timber floor panel topped with a reinforced concrete slab as shown in Figure 3.11. This floor type typically transfers uniaxial bending loads, resulting in tension in the timber panel at the bottom and compression in the concrete layer at the top. The structural efficiency of this floor type is achieved by creating composite action between the two materials. This composite action is facilitated by shear connectors, which ensure effective load transfer between the concrete and timber components. Normal-weight concrete is used with minimal reinforcement to prevent cracking, and the concrete is often poured on-site [24].

Figure 3.10: Glulam beam [22]

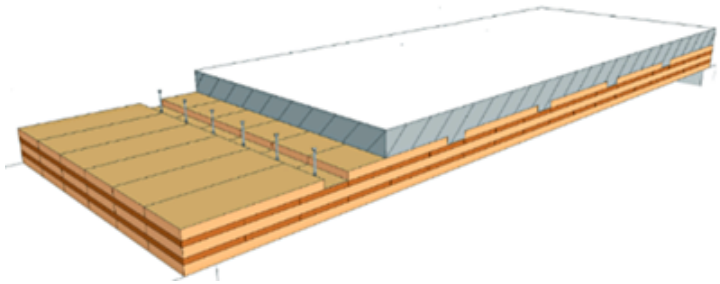

Figure 3.11: Timber Concrete composite panel [24]

Connection between timber elements

In Appendix B, several examples are provided of connections between different types of timber panels, as well as connections between timber beams and panels, and between timber beams and concrete columns and walls. The choice of connection type is crucial in the design process, as it influences the floor stack height. Additionally, different connection types may be selected based on manufacturing preferences.

3.4. Fire safety in building design

This section explores the fire safety considerations for tall concrete-timber buildings. Rules for fire-safe building design are introduced to address a wide range of risks, including loss of human life, material damage, and environmental harm. As a result, governments have established safety objectives concerning these risks. These objectives lead to functional requirements, which can be divided into two categories:

- Fire safety design of buildings: This includes all the measures and systems implemented in buildings to prevent and control fire hazards. It involves a combination of various measures, such as escape routes and detection systems, to achieve the overall safety level required by building regulations [25].
- Fire resistance of structures: The term 'fire resistance' refers to the ability of a building element to continue performing its function as a barrier or structural component during a fire [26].

3.4.1 Fire resistance of elements

The fire resistance of structural elements is defined through two aspects:

- The fire separation and smoke resistance of an element.
- The load-bearing capacity during a fire event.

Fire separation function

This fire separation function is associated with the term 'Resistance to fire penetration and fire spread' (Weerstand tegen branddoorslag en brandoverslag, WBDBO) used in the Netherlands, which refers to objective: resistance against fire spreading between spaces. To reach this goal, passive fire protection measures are used that enhance the fire resistance of structures. According to EN 13501-2, building materials are classified into three categories based on their performance characteristics:

- Integrity, E (flame tightness)
- Thermal insulation resistance, I (temperature)
- Thermal resistance, W (radiation)

Load bearing capacity of structural elements

To determine whether the load-bearing capacity of a structural element is sufficient during fire load, a defined process is followed. It starts with the development of a local fire and progresses through several steps to understand the mechanical response of a structural element. The steps are:

1. Ignition of the fire.
2. Fire development.
3. Thermal response of structural element.
4. Mechanical properties of structural element under fire load.
5. Mechanical response of structural element under fire load.

Fire resistance requirements

The Environment Buildings Decree (Besluit Bouwwerken Leefomgeving, Bbl) provides fire safety requirements for buildings, detailed in Section 4.2.2 on structural safety during fires (Articles 4.16-4.18) [27]. These requirements are shown in Table 3.1 and they align with those previously stated in the 2012 Building Decree. The basis for the fire resistance period is that elements are not allowed to fail to prevent progressive collapse. The building must remain standing while people are still inside, which include the evacuation period and the time needed for the fire department to search and rescue. Summerized, the Available Safe Time (AST) must be longer than the Required Safe Time (RST). This requirement leads to a longer fire resistance period of 30-120 minutes, which exceeds the evacuation time. These fire safety requirements are only quantified for buildings up to 70 meters [28].

Table 3.1: Fire resistance requirements [27]

Highest residential area compared to adjacent grounds (m)	Fire resistant period in terms of structural failure (min)
<7	60
7 - 13	90
>13	120

The Environment Buildings Decree requires that buildings taller than 70 meters have the same level of fire safety as those below 70 meters, but it does not provide concrete standards. Therefore, a Dutch Technical Agreement (Nederlandse Technische Afspraak, NTA) has been created, offering specific practical guidelines and recommendations. Additionally, the 'Guide to Fire Safety in High-Rise Buildings' (Handreiking Brandveiligheid in Hoge Gebouwen) specifies that structures must meet a 120-minute performance requirement [29]. The guide provides general, concrete guidelines. It assumes a compartment fire as the critical incident in the reference situation to which the facility level of the 2012 Building Decree is applicable. Additionally, the guide follows the Building Decree's regulations to achieve the following safety objectives [27]:

1. Prevent the spread of fire to neighbouring properties.
2. Maintain the integrity of the structure or building.
3. Limit the spread of fire and smoke.
4. Preserve escape and access routes.

For these objectives, acceptable failure is defined in terms of risk. This means that these goals must be achieved for a specified duration. The guide does not provide customized fire safety solutions like those found in fire safety engineering. Therefore, the probability of failure for risk objectives is not further addressed, but it is essential to minimize these risks. The safety standards in tall buildings exceeding 70 meters can only be maintained at an acceptable and practical level through the implementation of additional measures such as [29]:

- Automatic fire suppression systems in fire compartments.
- Overpressure systems in escape routes, ensuring these routes are redundant.
- Supporting fire safety systems to enable efficient evacuation.
- Supporting fire safety systems to facilitate effective emergency response.

Table 3.2: Design fire resistance rating for structural elements

Structural element	Separating function (min)	Fire resistance rating (min)
Floor	X	120
Beam	120	120
Column	120	120
Wall	X	120

3.4.2 Fire safety design of building

The protective measures belonging to the fire safety of buildings can be divided into two categories, corresponding to the stated in the introduction of this section. These are active and passive fire protection systems.

Active fire protection systems

Active fire proofing measures are related to the fire safety design of the building. The type and extent of these systems depend on the building's specific performance requirements and national regulations. One goal of these measures is to prevent a localized fire from developing into a compartment fire.

Passive fire protection systems

The focus is on the structural resistance to fire load (R) of structural elements. One example of enhancing the fire resistance of structural elements is the use of fireproofing materials. Fireproofing materials improve the fire resistance of structural elements by delaying heat transfer and the subsequent increase in structural temperature. These materials allow the structural elements to have lower a fire resistance rating, enabling smaller dimensions.

3.5. Preliminary conclusions

This section presents conclusions based on the results of the previous sections in this chapter. It is divided into two parts: trends in tall concrete-timber buildings and fire safety. At the end, the corresponding subquestion is answered.

The trend of hybrid concrete-timber buildings has shown a significant increase in height, growing from a maximum of 9 stories in 2009 to 24 stories in 2022. This increase in height is often accompanied by the inclusion of a concrete core. Tall hybrid concrete-timber buildings primarily utilize CLT (Cross-Laminated Timber) floor panels.

Fire safety design for these buildings is standardized based on the fire resistance of structural elements, with additional active and passive fire protection systems required for buildings taller than 70 meters.

Sub-question 1:
How are fire safety standards integrated into the design of tall hybrid concrete-timber buildings?

Answer:
In the tall hybrid concrete-timber buildings that have been build the combination of both active and passive fire protection systems are incorporated. For buildings taller than 70 m it is advised to use an active fire protection system, like a sprinkler system.

4

Theory on design aspects

This chapter presents the theoretical background on the design aspects of dynamic behavior, environmental performance, and building cost. It aims to deepen the understanding of these aspects, explore their representation through quantitative dependent variables, and establish the methodology for addressing the problem. Section 4.1 covers dynamic behavior, Section 4.2 examines environmental performance, and Section 4.3 discusses construction costs.

4.1. Dynamic behaviour of tall buildings

The dynamic behaviour of tall buildings refers to their response to rapidly varying external loads, leading to disturbing or damaging vibrations. The loads that are important for tall buildings:

- Wind
- Earthquakes
- Walking
- Collisions

Buildings become more susceptible to these dynamic actions as they become more slender and lighter. Taller buildings are more prone to wind effects like gust effect and vortex shedding. Timber floors reduce both weight and stiffness in buildings, potentially increasing susceptibility to wind-induced vibrations and causing discomfort for occupants. Walking on lighter and less stiff floors can result in unwanted vibrations, and earthquakes can induce internal forces that may cause structural failure [30, 31].

4.1.1 Dynamic models

The dynamic response of a high-rise building can be modeled using different systems. These are discrete systems or continuous systems.

Single-degree-of-freedom system

To understand the dynamic behavior of a building, a simplified model is used: a single-degree-of-freedom (SDOF). The physical representation of the model is a damped mass-spring system, consisting of a mass m, a spring stiffness k, and a viscous damper c, as shown in Figure 4.1. The displacement is depicted as $x(t)$ [32].

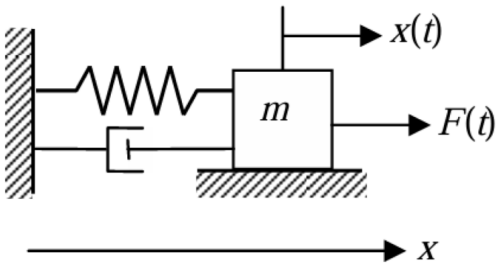

Figure 4.1: Simplified model of tall building [33]

The equation of motion for the SDOF system is given in Formula 4.1 with $F(t)$ representing the load on the system.

$$m\frac{\delta^2 x}{\delta t^2} + c\frac{\delta x}{\delta t} + kx = F(t) \tag{4.1}$$

The homogeneous equation is rewritten in Formula 4.2.

$$\ddot{x} + 2\zeta\omega_n\dot{x} + \omega_n^2 x = \frac{F(t)}{m} \tag{4.2}$$

With;
$\dot{x} = \frac{\delta x}{\delta t}$ = First derivative of x to t
$\ddot{x} = \frac{\delta^2 x}{\delta t^2}$ = Second derivative of x to t

The natural frequency of the system is given as ω_n and the damping ratio is ζ.

$$\omega_n = \sqrt{\frac{k}{m}} \tag{4.3}$$

$$\zeta = \frac{c}{c_{cr}} = \frac{c}{2\sqrt{km}} \tag{4.4}$$

The solution to the equation of motion of the SDOF is a summation of the homogeneous and particular solution as shown in Formula 4.5. With constants A and B depending on the initial conditions.

$$x(t) = x_{hom}(t) + x_{part}(t) \tag{4.5}$$

The homogeneous solution to the homogeneous equation is given in Formula 4.6, with the constants A and B are depending on the initial conditions.

$$x_{hom}(t) = Acos(\omega_n t) + Bsin(\omega_n t) \tag{4.6}$$

Multiple-degree-of-freedom system

A multiple-degree-of-freedom model (MDOF) is more appropriate to describe the behaviour of a real building as it has more than one degree of freedom. The physical representation of this MDOF system contains multiple masses that are linked by viscous dampers as shown in Figure 4.2. The masses all have their own degree of freedom [34].

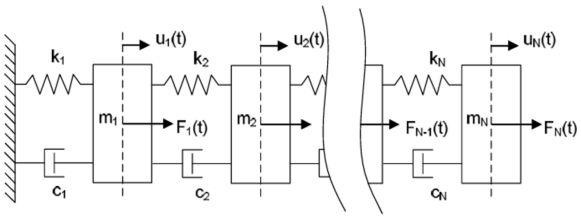

Figure 4.2: NDOF system [35]

The equation of motion for this MDOF system is given in Formula 4.7 with **M** diagonal mass matrix. **K** and **C** the symmetrical stiffness and damping matrix. Vector x is the displacement vector, $\dot{x}$ is the velocity vector and $\ddot{x}$ the acceleration vector.

$$\mathbf{M}\underline{\ddot{x}} + \mathbf{C}\underline{\dot{x}} + \mathbf{K}\underline{x} = \underline{F}(t) \tag{4.7}$$

The general solution to this equation is the sum of the homogeneous and particular solution. For the modal analysis only the homogeneous solution is relevant. The free vibration solution to the undamped system is given in Formula 4.8. In this solution the space variation and time variation functions are decoupled.

$$\underline{x}(t) = \underline{\hat{x}} sin(\omega t + \phi) \tag{4.8}$$

With $\hat{x}$ = eigenvectors with unknown natural frequency ω and phase angle ϕ. Substituting this solution into the equation of motion results in Formula 4.9:

$$\left(-\omega^2\mathbf{M} + \mathbf{K}\right) \underline{\hat{x}} sin(\omega t + \phi) = \underline{0} \tag{4.9}$$

This equation must be satisfied for all $t > 0$, which implies than $sin(\omega t + \phi) \neq 0$ at every moment. This results in a homogeneous system of linear algebraic equations for ϕ which is called the eigenvalue problem as given in Formula 4.10. The trivial solution to this equation is $\phi = 0$, which is the static state result.

$$\left(-\mathbf{M}\omega 2 + \mathbf{K}\right) \Phi = 0 \tag{4.10}$$

For the non-trivial solution the determinant of A must be equal to 0 as given in Formula 4.11. This is called the characteristic equation. From this natural frequencies of the system are found.

$$det(A) = Det(-\mathbf{M}\omega^2\lambda + \mathbf{K}) = 0 \tag{4.11}$$

With $\lambda = \omega^2$

The output for a N-degrees of freedom are the natural frequencies ω_1 to ω_n. For each natural frequency the corresponding eigenvectors x_1 to x_n are found by substituting the natural frequency in Formula 4.8. The eigenvalues represent the principal modes of vibration. When solving the eigenvalue problem, we assumed a synchronic harmonic motion as a free vibration, in other words all degrees of freedom have their maximum values at the same time, this also holds for their minimum values and zeros [36]. The eigenvalue problem for systems with multiple degrees of freedom is typically solved with a numerical

method. The results in an Ω-matrix for the eigenvalues λ and the eigenvectors E. For a system with n degrees of freedom there appear to be n principal modes of vibration (eigenmodes). The eigenmodes are visualized in Figure 4.3. Thus, the free vibration is the summation of all possible eigenmodes given in Formula 4.12.

$$\underline{x}(t) = \underline{\hat{x}_1} A_1 sin(\omega_1 t + \phi_1) + \underline{\hat{x}_2} A_2 sin(\omega_2 t + \phi_2) + \cdots + \underline{\hat{x}_n} A_n sin(\omega_n t + \phi_n) \tag{4.12}$$

A shortened version is shown in Formula 4.13.

$$\underline{x}(t) = \sum_{i=1}^{n} \underline{\hat{x}_i} A_i sin(\omega_i t + \phi_i) = E sin(\omega t + \phi) \tag{4.13}$$

A and ϕ are found from initial conditions: $X(0)$ and $\dot{x}(0)$.

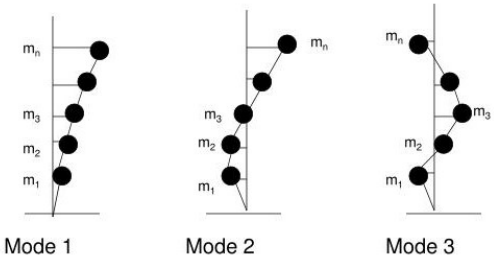

Figure 4.3: Eigenmodes [37]

Continious system

A tall building can also be modeled as a continuous system, which has an infinite number of degrees of freedom and, therefore, an infinite number of natural frequencies. Figure 4.4 illustrates this model, where wind load $q(z,t)$, self weight ρA and stiffness EI are distributed along the building height. A tall building can be approximated as a bending beam, whose dynamic behavior is described by a fourth-order partial differential equation [34]. The solution to this equation is provided in Appendix G.

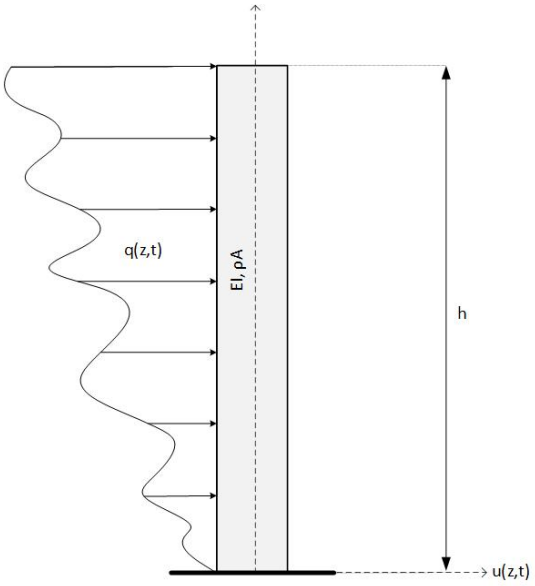

Figure 4.4: Model continuous system

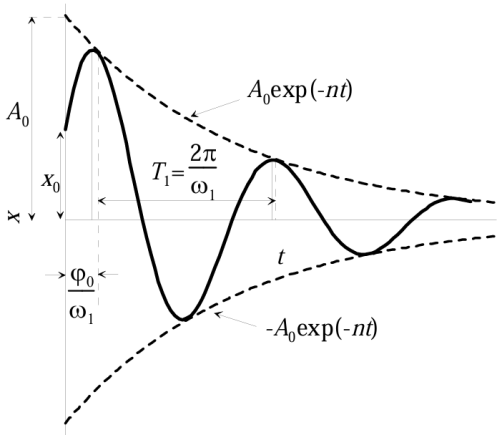

Figure 4.5: Free vibration of 1DOF system with damping [33]

4.1.2 Damping

Damping is a crucial factor in the dynamic behavior of a tall building, as it can significantly reduce vibrations. It is defined as the dissipation of vibratory energy in a mechanical system [38]. Damping in a tall building can be defined in different ways. One way is illustrated in Figure 4.5, in which the damping of a single degree of freedom system is mathematically presented by a viscous damper. The system is subjected to a sinusoidal load and the damping ratio is a measure that is used to describe the energy dissipation in a system. It is depending on the damping factor c and the critical damping c_{cr} of the system as given in Formula 4.4 for slender buildings.

Damping in tall buildings

For tall buildings, the damping coefficient is small, resulting in an underdamped system. This system exhibits a decaying periodic motion as shown in Figure 4.5. Damping lowers the mechanical response of the building due to dynamic wind load. Figure 4.6 demonstrates this by the mechanical admittance response that decreases as global damping increases [39]. With a decrease in mechanical admittance follows a decrease in vibrations in the building. Tall buildings generally have low damping values. It is assumed that the damping has little influence on the natural frequency and the mode shapes of the models of the building variants. This is shown by the frequency of a damped SDOF system is given in Formula 4.14. When the damping coefficient is small, the damped frequency is approximated by the natural frequency, which is given in Formula 4.3.

$$\omega_1 = \omega_n \sqrt{1 - \zeta^2} \approx \omega_n \quad for \quad \zeta < 0.1 \tag{4.14}$$

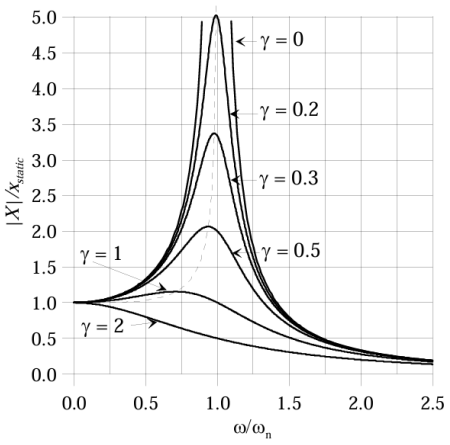

Figure 4.6: SDOF dynamic amplification factor for dynamic response [33]

4.1.3 Wind loading

The wind speed increases with height, making tall buildings more susceptible to the effects of wind. Figure 6.3 shows the power spectra for both turbulent wind velocity variations and earthquake velocity variations, along with the corresponding frequencies. High-rise buildings have low first natural frequencies in the range of 0.1 to 1 Hz, making them more vulnerable to wind as it has a similar frequency range [40]. This can cuase resonance in a building. The dynamic response of a building can be divided into three distinct components: along-wind, across-wind and torsional response. The consequential along wind, across wind and torsional response of the buildings are the most important applications for structural engineering [41].

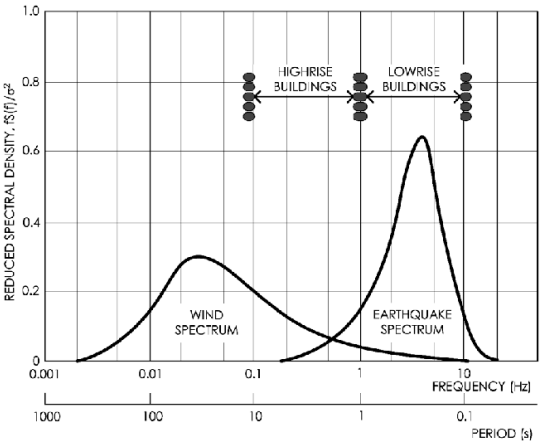

Figure 4.7: Frequency range of structures excited by wind and earthquakes [40]

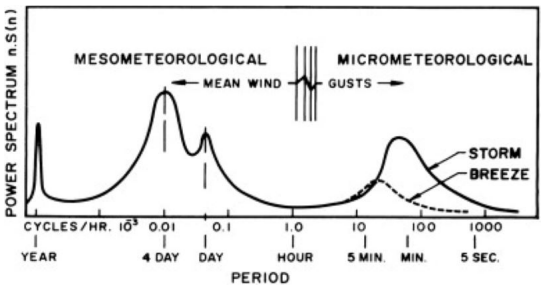

Figure 4.8: Spectrum of wind speed variations within the atmospheric boundary layer [42]

4.1.4 Parameters influencing dynamic behavior

The dynamic response of a high-rise building depends on several building characteristics. These building characteristics and their dependence on each other is visualised in Figure 4.9. This paragraph explores the impact of intermediate variables on the dynamic behavior of a building, focusing specifically on mass and stiffness as the thesis is limited to the system's free vibration. Based on a literature review, the effect of the selected parameters on these two intermediate variables is examined. Geometry and damping are not included in the thesis, as they are not included in the modal analysis.

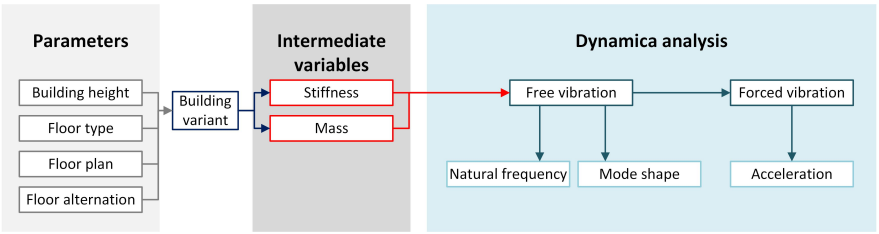

Figure 4.9: Overview building characteristics for dynamic behavior of tall building

Influence of mass and stiffness

This thesis primarily focuses on the intermediate variables of mass and stiffness. The mass is directly influenced by the parameters, while stiffness is indirectly affected through its dependence on the dimensions of the concrete core, which in turn depend on the four parameters. When a building is modeled as a SDOF system, the impact of mass and stiffness on dynamic behavior becomes clear. A reduction in mass leads to an increase in natural frequency, while a reduction in stiffness leads to a decrease in natural frequency, as demonstrated in Formula 4.3.

4.2. Environmental performance of buildings

One of the goals of the United Nations (UN) is to achieve a sustainable planet and society [3]. Sustainable development is defined as development that meets the needs of the present without compromising the ability of future generations to meet their own needs [43]. This concept is broken down into three aspects, known as the 3 P's [44]:

- People: Social aspects
- Planet: Environmental aspects
- Profit: Economic growth

The environmental performance of a building refers to the environmental impact it has throughout its life cycle, focusing on the 'Planet' aspect of sustainability.

4.2.1 Environmental Cost Indicator

The Environmental Cost Index (ECI), known as the 'milieukostenindicator' (MKI) in Dutch, is selected to compare and quantify the environmental impact of buildings. The ECI monetizes the environmental impact of building materials, and it is used to calculate the environmental performance of buildings (MilieuPrestatie Gebouwen, MPG). A reason for selecting this variable is its clarity. In the Netherlands, the MPG calculation is mandatory for the application for a building permit for all new office and residential buildings. The MPG value is expressed in euros per m² per year [45, 44].

The ECI describes the shadow cost that would be made to compensate negative effect of a product on the environment. To calculate the ECI value a Life Cycle Analysis (LCA) is conducted. The LCA is a tool to quantify environmental impact of product based on environmental impact categories. The background and rules for this procedure are found in EN15804, EN159978, ISO14025. The framework of the LCA is shown in Figure 4.10. The various steps of the LCA and how to calculate the ECI value are explained by following these steps, which are:

1. Goal and scope
2. Life Cycle Inventory (LCI)
3. Life Cycle Impact Assessment (LCIA)
4. Life Cycle Interpretation

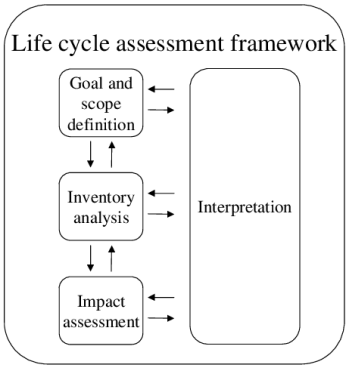

Figure 4.10: Life Cycle Assessment Framework ISO14040 standard

4.2.2 Goal and scope

Goal

The goal of the LCA study must first be defined. The goal comprise three elements:

- Description of the intended application.
- Explanation of the reason for performing LCA.
- Description of audience for which LCA is intended.

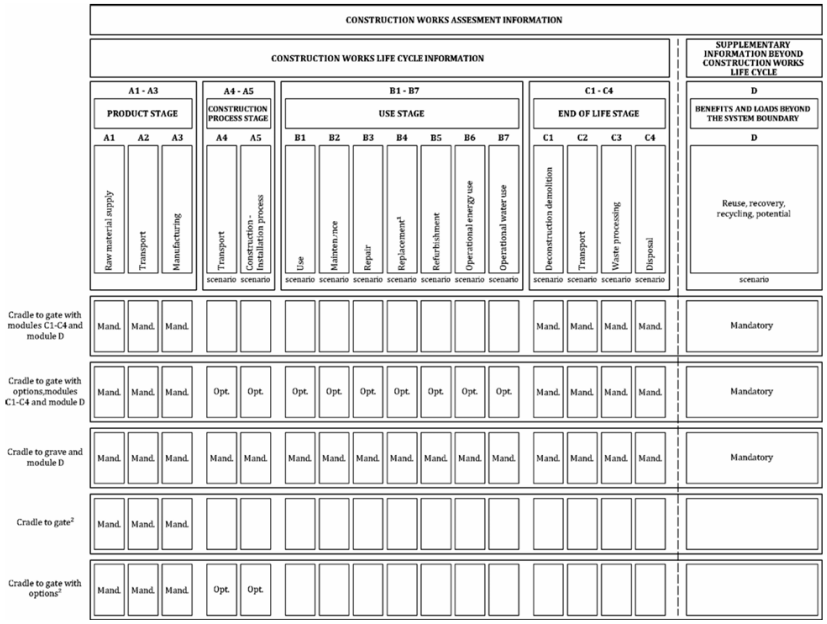

Figure 4.11: Types of EPD with respect to life cycle stages covered and life cycle stages and modules for the construction works assessment [46]

Scope

The scope of the LCA includes six elements. These are the functional unit, the system boundaries, LCA methodology, resources of LCI data, quality of LCI data and quality of the review of the analysis. These elements are discussed below.

Functional unit

The functional unit is broadly defined as the required function of the product. It is the base for comparing products. The functional unit includes:

- The function of the product.
- The elements of the product that are included or excluded, accompanied with a reasoning.
- The expected life span of the product and the elements of the product. This includes how much maintenance, repair or replacement is needed during the life span.
- Requirements for the external environment of the elements of the product to fulfil their function during life span.

System boundaries

The system boundaries define which processes and product related materials and equipment are included in the LCA. The life cycle stages as defined in EN15804, shown in Figure 4.11 and written down below are a base for defining these boundaries. The life cycle stages are:

1. Production stage (A1-3)
2. Construction process stage (A4-A5)
3. Use stage (B1-B7)
4. End-of-life stage (C1-C4)
5. Benefits and loads beyond the system boundary (D)

Based on the Dutch legislation, the mandatory stages are the production stage (A1-3), the end-of-life stage (C3-4) and the benefits and loads beyond the system boundary stage (D). The combination of these stages is defined as ‘Cradle-to-Gate with modules C1-4 and D’. These stages are minimal for an Environmental Product Declaration (EPD) of a product. An EPD provides quantified environmental impact information of a product over its life cycle, depending on the processes and materials used by the

manufacturer. Based on a LCA, an EPD includes the product's environmental profile with numerical data for each life cycle stage. The environmental impact categories included in an EPD can vary, meaning EPDs for the same product from different manufacturers may not be directly comparable. It must be defined which stages are included and to what extend these stages are considered. This can be visualised in a process flow diagram of the required resources (inputs), processes, and by-products and emissions (wastes) involved in the products life cycle stages. For stages C and D a realistic prediction scenario must be selected as it is unknown what will happen in the future to the product in these stages.

LCA methodology

In the methodology of the LCA is described which environmental impact categories are included in the LCA. Each Environmental Impact Category (EIC) addresses a negative effect on the environmental during one of the life-cycle stages of the product. These impacts are grouped in categories each addressing a specific type of environmental effect. Some of the environmental impact categories are:

1. Climate change - total
2. Climate change - fossil fuel
3. Climate change - biogenic
4. Climate change - land use and land use change
5. Ozone Depletion
6. Acidification
7. Eutrophication aquatic freshwater
8. Eutrophication aquatic marine
9. Eutrophication terrestrial
10. Photochemical ozone formation
11. Depletion of abiotic resources - minerals and metals
12. Depletion of abiotic resources - fossil fuels
13. Water use

These 13 environmental impact categories are mandatory for conducting an EPD of a product. Additionally, the methodology outlines how the LCI data is aggregated and internally weighted within various environmental impact categories. It also specifies the weight assigned to each category to calculate its contribution to the overall impact score.

Resources of LCI data
The reliability of the LCA is based on the resources of the LCI data. The production of a product needs many materials and processes, which results in many data input for the LCA of the product. The sources of data can be based on measurements, calculations, and estimations.

Level of quality of LCI data
One must reflect on the quality of the LCI data. This reflection includes the completive and representativeness of data. Ideally the data covers the geographic region and is recently collected and reproducible.

Quality of the review of analysis
It is determined whether a critical review of the performed LCA study is required, along with the reasoning for this decision.

Life Cycle Inventory

The Life Cycle Inventory (LCI) data documents the quantities of inputs involved in the life cycle phases of a product, including raw materials, energy, and processes. The database comprises LCI data for construction materials and processes. However, it limits the estimation of the output, the environmental impact, of complete constructions, as it only includes LCI data for a limited number of raw materials and

elements. The National Environmental Database (NMD) is designed for environmental impact assessment of products and buildings. It contains information about the environmental impact of materials, processes, and products across several impact categories for production stages A1-3.

Life Cycle Impact Assessment

In the Life Cycle Impact Assessment (LCIA) the LCI data collected is assigned to the environmental impact categories, and for each of those categories an indicator compound is defined against which all other compounds are weighed. For this weighing specific criteria are used. The ECI value is a weighted value of the contributions of each environmental impact category.

Life Cycle Interpretation

The life Cycle Interpretation phase includes a discussion about the results obtained in the LCI and LCIA phases of the study. In addition to this, completeness, sensitivity and possible limitations of the used methods must be discussed. Finally conclusions and recommendations are given.

4.3. Construction cost

This section provides the theoretical background on building costs required for the cost analysis. It begins by explaining the components that make up the building costs. Next, it discusses how these cost can be determined. Following this, it discusses the construction methods commonly employed in tall buildings.

4.3.1 Investment cost of high-rise buildings

The financial feasibility of high-rise buildings globally depends on the ratio between investment costs and revenues. Costs cannot be separated from revenues, as revenues are derived from the market value of the apartments in buildings. According to NEN2699, the investment costs are comprised of [47]:

- Land costs
- Construction costs
- Furnishing costs
- Additional costs
- Unforeseen costs
- Taxes
- Financing

According to NEN 2699, construction costs can be divided into direct and indirect costs. The direct construction costs (DC) include all physical components of the building, such as labor, materials, equipment, and subcontractor costs. The indirect construction costs include general construction site costs and general company expenses, expressed as a percentage of direct construction costs. For high-rise buildings, this is approximately 12%, but it can vary greatly depending on the construction site and equipment, as well as the project and building duration. The general business operating expenses is typically around 8%. Additionally, profit and risk are calculated as averaging 4% over direct construction costs. The direct and indirect cost combined with the profit and risk make up the total construction cost [48]. To this the additional costs are added. These typically range from 25-30% of the total costs. Including VAT, which results in the final budget sum. An overview of these costs is given in Table 4.1.

Table 4.1: Investment cost overview

Construction costs		
Direct construction costs (DC)	100	
Indirect construction costs		
General construction site costs (% over DC)	12	
General business operating expenses (% over DC)	6	
Profit and risk	4	+
Total construction costs	122	
Additional costs		
Preparation and guidance		
Taxes		
Insurances		
Financing		
Risk insurance		
Unforeseen	25-30	+
Subtotal	162	
VAT 21% of 162	34	+
Budget sum including VAT	191	%

There are two reasons why the ratio between revenues and investment costs is more important for high-

rise buildings compared to low-rise buildings. The first reason is that investment costs are higher due to requirements for high-rise buildings, including: extra installations, elevators, water pumps, facade systems, longer construction time, complex execution, and safety. The second reason is lower surface efficiency due to smaller lettable floor space (Verhuurbare VloerOppervlak, VVO). This is due to larger space requirements for vertical transport, load-bearing structural elements, and installation shafts. This lettable floor space has a direct relationship with revenues [49, 50].

4.3.2 Estimation of Construction Costs

To estimate the total construction cost in the early design phase, two methods are commonly used. The first method involves using key figures (kengetallen) to provide an initial cost estimate during the initiation or concept phase. Based on a dataset of reference projects, these key figures can be generated, typically presented as cost per m² or m³, allowing for an indication of the total construction cost. However, significant deviations are possible due to differing conditions of the new project [51].

Another method calculates the costs per construction component, depending on the level of detail available during the respective phase. The building is divided into product and element groups according to the element classification and coding system of NL-SFB. This subdivision is linked to the 'Element Method' (Elementenmethode), which categorizes construction costs at the element level, as shown in Table 4.2 [52].

Table 4.2: Subdivision direct construction cost

Direct construction cost
Project preparation and material provisions
Soil and foundation facilities
Primary structural elements
Recesses
Finishes
Mechanical installations
Electrical installations
Fixed other facilities
Terrain facilities

The construction costs are calculated by multiplying the unit price by the quantity of the specific element. This method can be used when making design changes as there is a relationship between the building components. This allows for the consideration of alternatives. The level of detail in construction cost calculations depends on the design phase. In the preliminary design phase (VO), costs are calculated per structural element per m³ or m². This data includes material, equipment, and labor costs, based on data available within the company. Other sources, such as bouwkosten.nl or archidat.nl, can also be consulted for costs per element or labor hours. The margin of error for cost estimates in this phase is typically +/- 15%. In a later phase, suppliers provide quotes for materials and equipment, and the number of labor hours is determined. This allows for a more accurate cost estimate.

4.3.3 Direct construction cost

A breakdown of the total construction cost by element group, along with their share of the total construction cost, is presented in Table 4.3.

Table 4.3: Construction cost break down

Direct construction cost	**Percentage (%)**
Foundation	10
Structural system	20
Facade	25
Installations	25
Other (construction, finishing, furnishing, etc.)	20
Total	100

The construction cost increases with height, as depicted in Figure 4.12, which shows the cumulative percentage rise of these components. This graph is derived from reference data involving concrete high-rise buildings in the Netherlands [49].

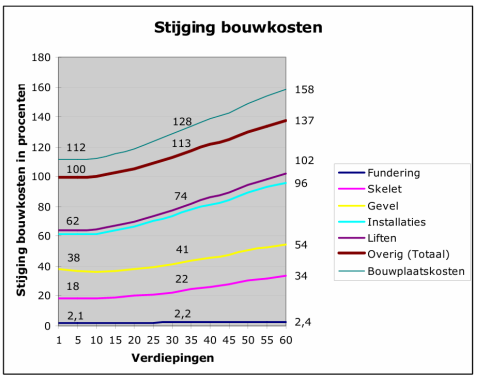

Figure 4.12: Cumulative increase of construction cost per storey [49]

The effect of building height on the cost of the foundation and the structural system is studied as this is the focus of this thesis. An increase in foundation costs, averaging 2% per 10 floors, can be attributed to four reasons [49]:

- Greater self-weight necessitates larger dimensions.
- Increased foundation depth.
- Increased number of piles.
- Thicker foundation slab.

The construction costs of the structural system and floors increase by 10-15% per 10 floors due to larger dimensions of structural elements and increasing wind loads leading to larger dimensions of stability elements.

4.3.4 Construction Method

The construction method refers to the approach used to realize a building. The choice depends on numerous factors, allowing the same building to be constructed in various ways. The factors that are project-specific are [53]:

- Structural system
- Materials
- In-situ or prefab
- Logistics
- Location
- Construction time
- Construction costs

Based on these factors, the most suitable construction technique is selected. The most common construction techniques for concrete high-rise buildings in the Netherlands are divided into in situ and industrialized methods ang given below. All these construction methods have their own advantages and limitations [54].

In situ

- Tunnelling
- Climbing formwork
- Self-climbing formwork (hydraulic)

- Slipform

Industrialized

- Prefabricated with tower crane
- Prefabricated wiht rising factory (hijsloods)

In situ construction techniques

In-situ construction involves pouring concrete on-site, creating a monolithic structure. This method allows for last-minute changes to installations before pouring. However, it also has drawbacks, such as lower concrete quality due to exposure to unprotected conditions and the requirement for adequate curing time before the formwork can be removed. The strength required for the removal of the formwork is achieved after about 48 to 72 hours [55].

Prefabricated construction techniques

Prefabricated construction involves building with pre-manufactured elements. These elements are produced in a factory and assembled on-site. Advantages include high product quality, a clean construction site, and fast execution. Disadvantages include numerous lifting operations and additional attention needed for connections to guarantee sufficient stability [53]. CLT and glulam elements are manufactured in a factory, where finishing details such as recesses are also integrated into the elements. This prefabrication process greatly enhances construction speed. Buildings from CLT panles can be constructed significantly faster than traditional concrete structures. Compared to similar reinforced concrete and steel buildings, CLT construction is 25% to 75% faster per square foot, reduces the overall project timeline by 20%, and requires 90% less construction traffic [56, 57]. For example, the Brock Commons Tallwood House was completed in just 70 days. This 53-meter-tall, 18-story structure demonstrates the efficiency of mass timber construction. In comparison, a concrete building of similar size would typically take much longer to complete due to longer concrete curing times [58, 59].

4.4. Preliminary conclusions

This section presents conclusions based on the results of the previous sections in this chapter. It is divided into three parts, each corresponding to a design aspect. At the end, the relevant subquestions are answered.

Dynamics behavior

Unwanted vibrations in the building, such as those caused by wind, can be a concern, especially in tall, light buildings with timber floors. The question is, to what extent are tall hybrid concrete-timber buildings susceptible to these vibrations?

Environmental performance

The ECI value per floor area provides a good indication of sustainability. It is crucial to consider which scenarios and stages are included for each material to ensure comparability in a variant study. This helps assess the sustainability of different building designs more accurately.

Construction cost

Direct construction costs for the structural system and foundation account for only 30% of the total direct construction cost, and therefore, these can serve as an indicator of the total construction cost. However, these costs are highly dependent on various factors, including the chosen construction method and the building's location. According to literature, the construction cost of a structural system and foundation increases gradually with building height.

Sub-question 2:
What modelling technique is used to analyze the dynamic behavior and obtain the natural frequencies of tall hybrid concrete-timber buildings?

Answer:
A tall building can be modeled as a multi-degree-of-freedom system, with the masses concentrated at the floor levels. To determine the first natural frequency, a simplified approach such as the Rayleigh method can be applied.

Sub-question 3:
How do concrete and timber floor types differ in environmental performance when considering production and end-of-life scenarios?

Answer:
Concrete floors are typically recycled and used as a substrate for road construction. However, their production generates significantly more CO2 than timber floors. Timber floors, in contrast, have lower embodied carbon due to the carbon stored in the material. At the end of their life cycle, timber floors are primarily incinerated.

Sub-question 4:
What factors must be included to accurately estimate the building cost of tall hybrid concrete-timber buildings in the early design stage?

Answer:
An accurate cost estimation must include:

- Material costs – covering the expenses of concrete, timber, and other structural components.
- Labour costs – influenced by the complexity and duration of construction.
- Construction equipment costs – depending on the chosen construction method.

The latter two factors are closely linked to the construction method, affecting both cost and feasibility.

Part III

Variant study

5

Design of building variants

This section outlines the steps involved in designing the building variants. First, the workflow for the design process is discussed. Following that, details are provided about the case study building, the Cooltoren, and the parameters used. The design process is divided into three steps: the floor design, the development of floor plans, and the design of the concrete core and foundation.

5.1. Design setup

The design setup outlines the steps involved in the design process, as visualized in Figure 5.1. The process begins with the floor design. The first stage of the floor design involves developing various floor plans. For each combination of floor plan and floor type, the dimensions of the floors and beams are determined using the Calculatis software from Stora Enso. Separately, the other structural elements, including columns and the foundation plate, are also dimensioned. The next stage focuses on designing the concrete core and foundation. A Grasshopper model is developed for this purpose, which utilizes the output from the floor design step to calculate the dimensions of the concrete core and the required number of foundation piles. Finally, the results from the first two steps are used to generate input for the models representing the design aspects. In this stage, the input is organized and allocated to the respective models required for each design aspect.

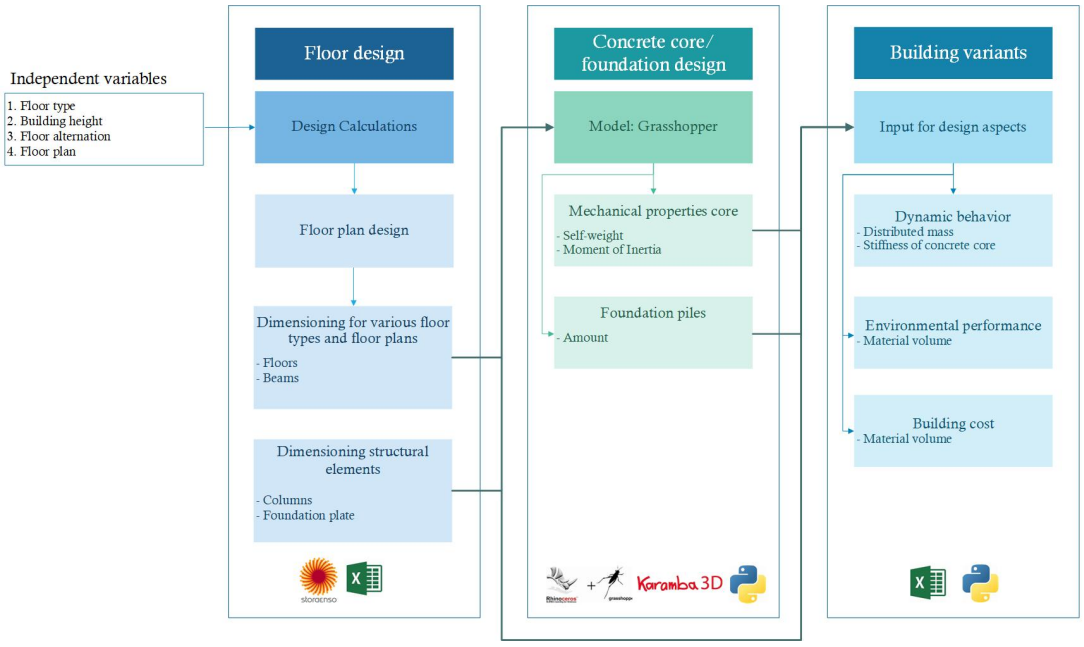

Figure 5.1: Design method

5.2. Case study building: Cooltoren

The building that is used for the case study is the Cooltoren in Rotterdam as shown in Figure 5.3. This building is located at Baan 38 as shown in Figure 5.2. The residential building has 50 storey and a total height of 150 m. Van Rossum Raadgevende Ingenieurs B.V. is responsible for the structural design of the building. In this chapter the the building characteristics are given that are used as starting point for the design of the building variants.

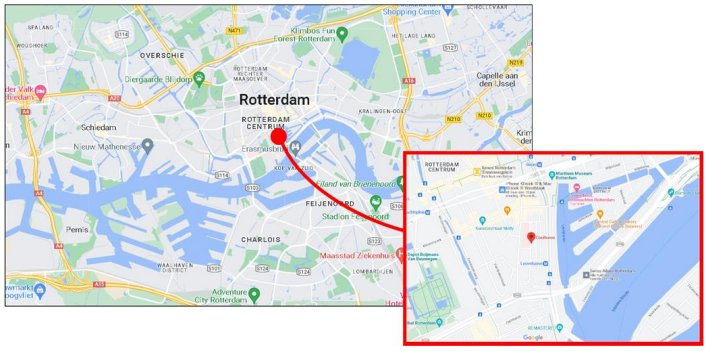

Figure 5.2: Location of Cooltoren

Figure 5.3: Cooltoren Ⓒ Ossip van Duivenbode

5.2.1 Geometry

The floor plan as shown in Figure 5.4 is based on the floor plan of an average storey with concrete balconies. For the case study, it is assumed that the floor plan remains consistent across all storeys. This means that the steel roof construction, the floors with steel balconies and wider plint at the bottom of the building are excluded from this altered design. There are concrete walls that act as outriggers that are situated between floors 16 and 19 and 32 and 35.

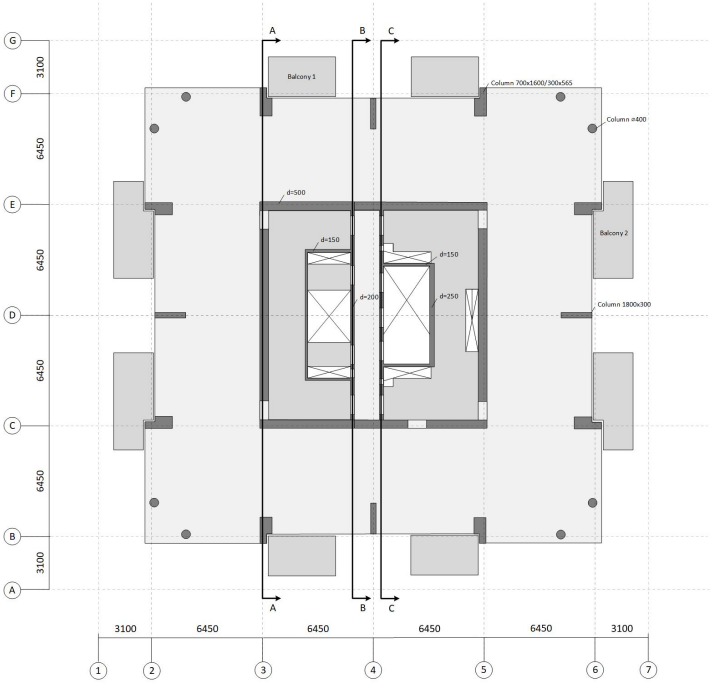

Figure 5.4: Floor plan Cooltoren

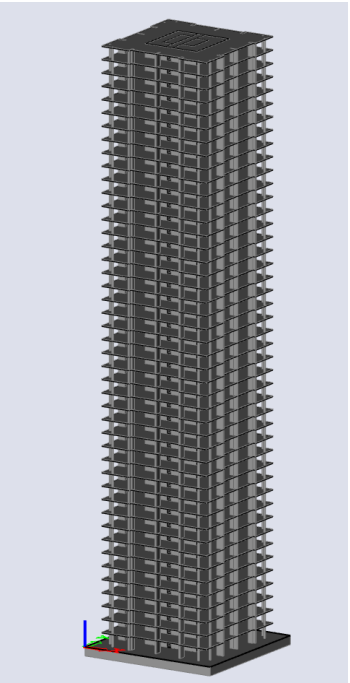

Figure 5.5: 3D view Cooltoren

5.3. Parameters

This section provides information on the parameters which are the base for the design of the building variants. These parameters will be used to analyse the results from the models of the design aspects.

5.3.1 Floor type

The parameter 'Floor type' is used for the type of floor that is used in the structural system of the building. It is related to the floor type of the individual floors in the building. The vertical loads are transferred through the beams to the columns and the horizontal loads are transferred through the beams to the concrete core. This parameter is selected because different floor types can be used in tall concrete-timber buildings, each affecting design aspects differently. For instance, one floor type might improve dynamic response but have a worse environmental impact or higher cost. Distinct floor types have been chosen for this study, each offering unique mechanical properties and structural advantages. Further details on these floor types are provided in Section 3.3. The floor types included in the research are:

- Concrete floors.
- CLT floors.
- TCC floors.
- CLT rib panel floors.

5.3.2 Building height

The parameter 'Building height' refers to the total height of the building. Since the floor height is constant, the building height corresponds to the number of floors. This variable is chosen because building height influences the design aspects. Based on the Cooltoren a structural system with one core is used as stability system with floors that are connected using pinned connections. The width of the building and width of the core dimensions are limited to have satisfactory gross net area ratio. Also the Dutch regulations on maximum distance for daylight intrusion(reference) limit the building width. These boundaries limit to building height of this structural system. Further information on this building system that will be used in this research is given in Section 3.2. The building heights that are investigated in this research are:

- 70 m
- 90 m
- 110 m

5.3.3 Floor alternation

The parameter 'Floor alternation' refers to how different types of floors are arranged within a building. A building may utilize various floor types across its different levels. For instance, in a 7-floor building, concrete floors may be used on levels 1, 4, and 7, while timber floors are used on levels 2, 3, 5, and 6. Employing a non-conventional floor alternation, where different floor types are used throughout the building, can offer advantages and disadvantages for certain design aspects. For consistency in comparison and to streamline workflow, each floor alternation in this study comprises a combination of concrete and timber floors. This allows for direct comparison with buildings that have solely timber or concrete floors and simplifies the analysis process. The floor alternations that evaluated are more clearly visualised in Figure 5.6. The floor alternations can are:

- All concrete floors.
- All timber floors.
- Alternating 1 concrete floor and 1 timber floor.
- Alternating 1 concrete floor and 2 timber floors.
- Alternating 1 concrete floor and 4 timber floor.

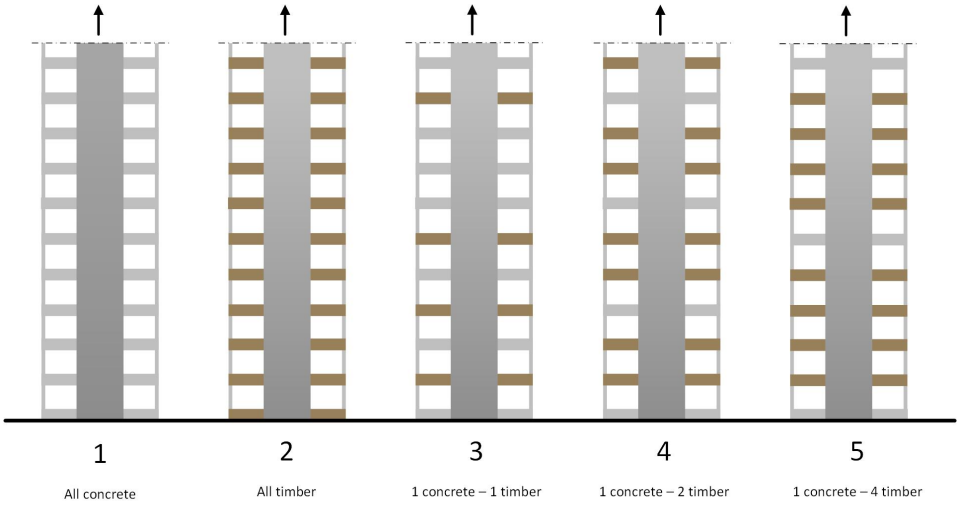

Figure 5.6: Floor alternations

5.3.4 Floor plan

The 'Floor plan' refers to the arrangement and orientation of the beams and floors in a floor system. The starting point for the floor plan variants is the floor design of the Cooltoren. To transform this building into a hybrid structure with timber floors, it is inadequate to merely replace the concrete floors with timber floors. The floor spans in the original design are large, resulting possible overdimensioning of the elements. This would skew the outcomes of the timber building variants in later analyses, potentially disadvantaging these variants and leading to unrealistic building designs. In total six variants are generated, from which three variants are selected to be incorporated in the generation of the building variants. The selection plans are given in Table 5.1 including the floor and beam span. In Figures L.4 to L.6 in Appendix L the six floor plans are shown.

Table 5.1: Floor layout variants

Variant	Name	Floor span (m)	Beam span (m)
1.	4.3 span	4.30	4.30
2.	3.2 span – variant 1	3.23	6.45
3.	3.2 span – variant 2 (beams other direction)	6.45	3.23

5.4. Floor and floor plan design

Initially, a realistic floor build-up is selected for each floor type. Next, various floor and beam plans with different spans are generated. For each floor plan variant, the thickness of the floors and beams is calculated. This allows the selection of the best layout variants, based on the floor-to-floor height and the total mass of the floors. The calculations for the floor and floor plan design can be found in Appendix E.

5.4.1 Floor design

This subsection explores realistic floor build-ups for the different floor types, drawing inspiration from current mid-rise and high-rise apartment buildings that use concrete and timber floors, as well as manufacturing guidelines. The 'floor build-up' refers to the combined layers of materials that make up a floor structure, from the bottom top to bottom. Each floor type in a tall building has unique requirements for various functional and safety standards. For every floor type, a realistic floor build-up is chosen, based on acoustic and fire safety requirements. An example of a floor build-up for a concrete floor is given in Table 5.2. The floor build-ups of the other materials are given in Table E.1 to E.4 in Appendix E. For the materials and thicknesses for the floor build-up several references are used [60, 61, 62].

Table 5.2: Concrete floor

Material	Thickness (mm)	Density (kg/m³)	Load (kN/m²)	
Cement screed	50	2000	1.0	
PE foil	0	1000	0.0	
Insulation	20	35	0.0	
Concrete floor	tbd	2500		+
Dead load			1.0	

In addition to the floor build-up, six floor plans have been designed, as outlined in Table 5.3.

Table 5.3: Floor layout variants

Variant	Name	Floor span (m)	Beam span (m)
1.	6.5 span – variant 1	6.45	6.45
2.	6.5 span – variant 2 (extra columns)	6.45	4.45
3.	5.0 span (cantilever beam)	6.45	5+1.45
4.	4.3 span	4.30	4.30
5.	3.2 span – variant 1	3.23	6.45
6.	3.2 span – variant 2 (beams other direction)	6.45	3.23

5.4.2 Floor dimensioning

The dimensioning of the floors uses several inputs that are divided into assumptions, materials, loads, load cases, and requirements. These are all given in Section E.2 of Appendix E, together with the resulting dimensions of the floors and beams of the different floor types and floor plans.

Results

In Tables 5.4 and 5.5 the stack height and the floor-to-floor height for all layout variants and floor types are summarized. The red values indicate the layout variants that do not meet requirement for maximum floor-to-floor height of 3.1 m. The results show that there is a big difference in stack height and floor-to-floor height for the various variants.

Table 5.4: Floor stack height for floor layout variants

Floor layout	**Floor stack height (mm)**			
Variant	Concrete	CLT	TCC	CLT rib
1	630	695	725	736
2	465	575	685	696
3	490	615	645	736
4	425	535	565	596
5	550	595	645	656
6	365	485	605	615

Table 5.5: Floor-to-Floor height for floor layout variants

Floor layout	**Floor-to-floor height (m)**			
Variant	Concrete	CLT	TCC	CLT rib
1	3.03	3.10	3.13	3.14
2	2.87	2.98	3.09	3.10
3	2.89	3.02	3.05	3.14
4	2.83	2.94	2.97	3.00
5	2.95	3.00	3.05	3.06
6	2.77	2.89	3.01	3.02

The mass of the floor layouts per floor type are visualized in Table 5.6 and in Figure 5.7. The floor masses are estimations as the total volume of the floors and the beams are separately calculated, so not accounted for the beam incorporated in the floor slabs.

Table 5.6: Mass of floor plan variants per floor type

Floor plan	**Floor type** (10^3 kg)			
Variant	Concrete	CLT	TCC	CLT rib
1	527	167	250	142
2	436	159	236	125
3	454	161	242	140
4	420	128	170	125
5	436	124	172	121
6	418	161	229	133

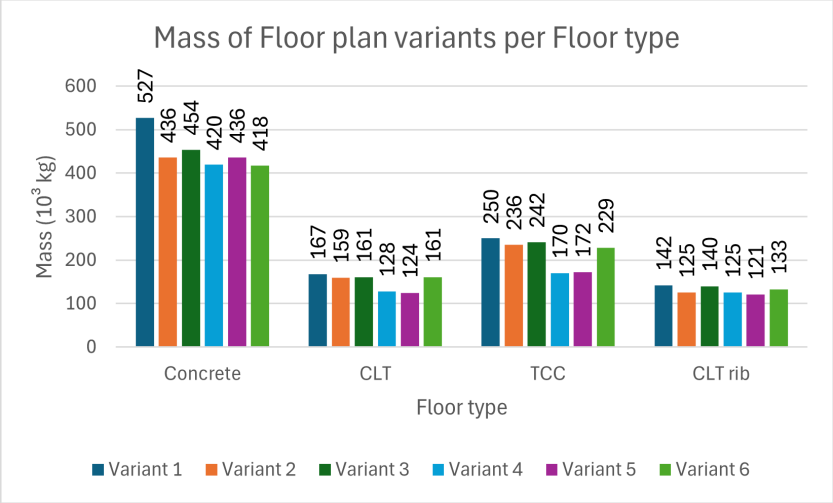

Figure 5.7: Mass of floor plan variants per floor type

5.4.3 Discussion of results

Table 5.5 indicates that floor layout variants 4 to 6 have the lowest floor-to-floor height for most floor types. Figure 5.7 shows that variants 4 and 5 have the lowest mass across all floor types. From a mass standpoint, for concrete floors, there is a preference for floor plans with either equal floor and beam spans or large floor spans with short beams, such as floor plans 4 and 6. For light timber floors like CLT and CLT rib panel floors, equal floor and beam spans or short floors with large beams, like floor plans 4 and 5, are favorable and show no visible difference in mass. For TCC floors, floor plans 4 and 5 are preferable with equal floor and beam lengths or large floor spans with short beams. Based on the concluding results, floor layouts 4 to 6 are used as a separate parameter in further analysis, based on their limited floor-to-floor height and mass.

5.5. Concrete core and foundation design

Next, the concrete core is designed together with the foundation. The goal of this modelling the concrete core is to dimension the concrete core for all building variants. General information about the Cooltoren case study building is provided in Appendix D. The alterations to the original design of the building, the assumptions, the load cases and the modelling of the core and foundation design can be found in Appendix F.

This input is incorporated in the model by using the software 'Grasshopper'. The analysis is divided into three main parts. The first part focuses on verifying the strength of the foundation piles, the second part examines the strength of the concrete core, and the third part evaluates the deformation of the building under various load conditions.

5.5.1 Results

The results in Table 5.7, show that the building height is the only factor affecting the core wall thickness and the number of foundation piles. In taller buildings, deformations are the governing factor, which is controlled by the rotational stiffness provided by the number of piles. Therefor, tall buildings with light timber floors need the same number of foundation piles. In shorter buildings, the governing factor is the maximum wind load on the piles.

Table 5.7: Results dimensioning concrete core and foundation, no floor alternation, floor plan 1

Building height (m)	Floor type	Thickness core (m)	Number of foundation piles	Unity check value	Governing unity check
70	Concrete	0.25	64	0.88	C: pile max Qwind
90	Concrete	0.25	81	0.93	F: core deformation
110	Concrete	0.40	169	1.00	F: core deformation
70	CLT	0.25	49	0.89	C: pile max Qwind
90	CLT	0.25	81	0.92	F: core deformation
110	CLT	0.40	169	0.99	F: core deformation

Floor plan

With the resulting dimensions of the structural elements, the total mass of the building variants can be established. Figure 5.8 shows the total mass per floor type and floor plan for a building height of 90 m with no floor alterations. The difference in mass between the floor types can be attributed to the mass difference of the floor systems. The variation in the mass of building with different floor plans within the timber floor systems correlates with the floor masses of variants 4 to 6, as shown in Figure 5.7.

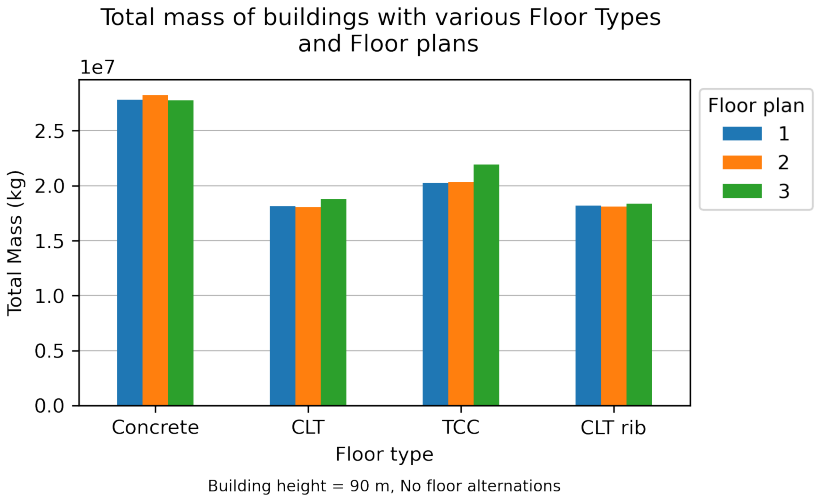

Figure 5.8: Mass of building for various floor types and floor plan

Material mass

Figure 5.9 presents the material mass distribution for floor plan 1 without floor alternation, distinguishing between materials in the building and the foundation. The graph indicates that concrete contributes between 85% and 95% of the total mass. Comparing different floor types reveals that the mass contribution of concrete floors significantly outweighs that of the timber floor types. The mass of the foundation piles remains constant for all floor types of the same height, except for buildings with a height of 70 m and concrete floors. This variant requires additional piles to support the extra floor mass. The contribution of the foundation becomes relatively smaller in 90 m buildings compared to 70 m buildings. In taller buildings (90 m and up), the governing requirement is deformation, necessitating a minimal number of piles to provide the required rotational stiffness.

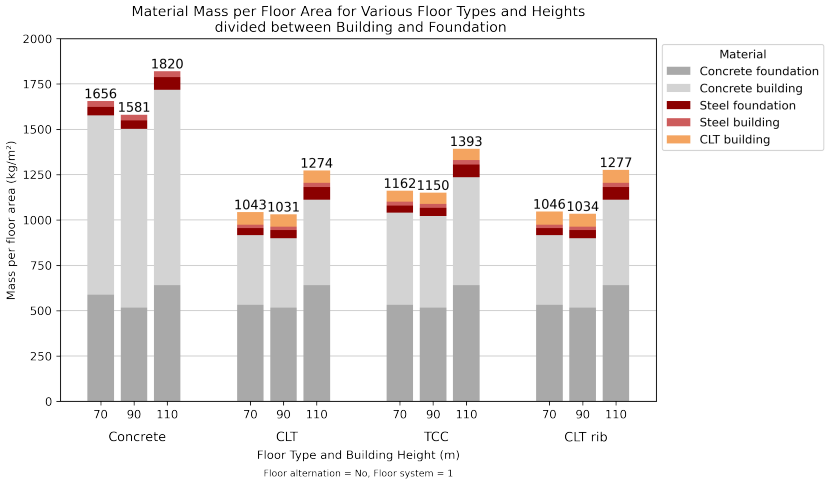

Figure 5.9: Material contribution to total mass by building height and floor type

Figure 5.10 illustrates the material mass for a building height of 90 m and floor plan 1. This figure highlights the increase in concrete mass and total mass with an increase in concrete floors. A linear increase in mass per floor area, proportional to the percentage of concrete floors, is more clearly depicted in Figure 5.11.

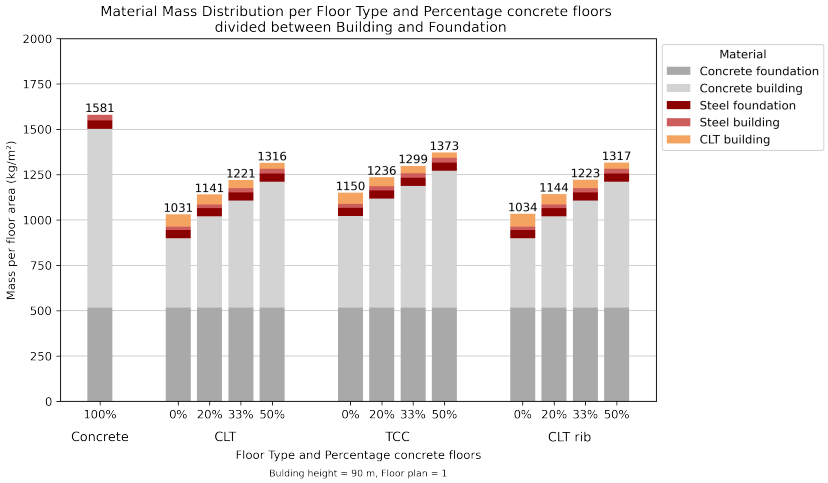

Figure 5.10: Material contribution to total building mass by concrete floor percentage and floor type

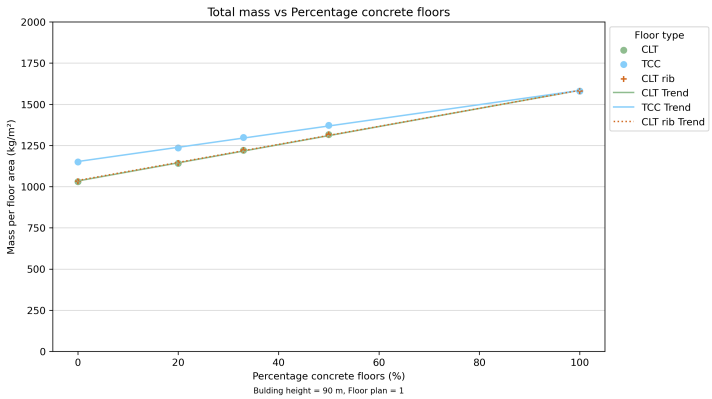

Figure 5.11: Total building mass against percentage concrete floors

Structural subsystems

The total mass of the building variants can be divided among various structural subsystems. As shown in Figure 5.12, the total mass is divided into the foundation system, the floor system, and others, which include the concrete core, columns, and facade. The figure illustrates the mass of building variants with different floor types and proportions of concrete floors. The timber floor systems (CLT, TCC, and CLT rib) all demonstrate that as the proportion of concrete floors increases, the contribution of the floor system to the mass and the total mass also increases. For timber floor types, the floor system contributes between 14% and 47% of the total building mass, while in buildings with concrete floors, the floors account for 46% of the total mass. Additionally, the foundation's contribution ranges from 35% to 56% in timber-based structures, compared to 36% in buildings with only concrete floors.

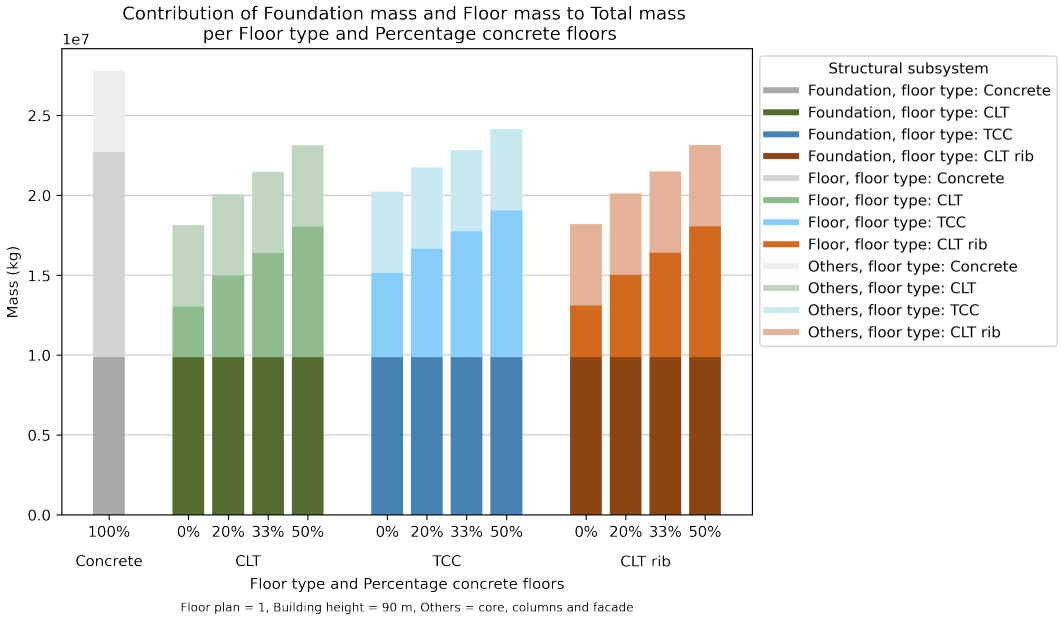

Figure 5.12: Contribution of subsystems to total mass

5.5.2 Discussion of results

First the results in Table 5.7 are discussed. The height of the building is the primary factor influencing the core wall thickness and the number of foundation. Variations in building mass due to changing floor type do not impact these variables significantly. This can be explained by the composition of the floors, where concrete accounts for 60% of the total floor mass in heavy concrete building variants and up to 80% in light building variants. Additionally, the concrete core contributes substantially to the overall

mass of the building. This is supported with the results that a lighter building requires the same amount of foundation piles. The reduction in mass only results in a decrease of the utilization factor of less than 0.01.

In shorter buildings, the governing factor is the maximum wind load on the piles, which leads to the assumption that fewer piles would be needed for a lighter load. This assumption holds true, but a minimum number of foundation piles is required, as 70 m tall buildings are governed by the maximum pile load resulting from the combination of self-weight and wind load. A shift to a higher number of piles occurs at 33% concrete floors. For buildings with CLT and CLT rib panels, 49 piles are required, whereas TCC (Timber-Concrete Composite) floors require 64 piles for the 2 timber floors and 1 concrete floor alternation.

Buildings from 90 m and above are more susceptible to wind loads, meaning that the rotational stiffness becomes the governing factor for determining the number of foundation piles, rather than the vertical load from self-weight and wind. Figure 5.9 illustrates this by showing that the foundation mass does not increase linearly with height.

5.6. Preliminary conclusions

In this section the conclusions are given based on the results of the previous sections in this chapter. It is divided into two parts, the floor design and the design of the concrete core and foundation.

Optimal floor systems for timber floors typically have short, even lengths for both floor spans and beam spans, or short beams with long floor spans of up to 6.5 meters. Long beams (6.5 meters) with short floor spans are also feasible. However, cantilevering timber beams are not ideal, as the connections become challenging. This contrasts with concrete floors, which can support floor spans of up to 12 meters. In timber floors, large spans result in larger beam dimensions, which lead to an increased stack height and greater floor-to-floor height. These changes have implications such as an expanded façade surface, adding to the building's overall complexity and cost.

Building height is the primary factor influencing core wall thickness and the number of foundation piles. However, these two dependent variables do not increase linearly with height. This is due to specific assumptions and boundary conditions defined beforehand and the governing load cases. Variations in building mass due to different floor types only affect the number of foundation piles. However, the number of foundation piles does not increase linearly with the addition of more concrete floors, as a minimum number of piles is required to resist wind loads. Together, the foundation and floor system account for 70-80% of the building's total mass.

Sub-question 5:
What is the relation between the mass of the floor type and the concrete core thickness and the number of foundation piles?

Answer:
Lighter timber floors result in fewer foundation piles for buildings up to 70 m. Above this height, however, the core wall thickness and the number of foundation piles become independent of the floor type mass and are instead governed by wind loads.

6

Dynamic behavior modelling and analysis

The natural frequencies of the building variants are determined through a series of steps. A comprehensive explanation of these steps, including the assumptions, input data, and the modeling approach, can be found in Appendix G.

6.1. Goal

This chapter aims to provide insights into the dynamic behavior of tall concrete-timber hybrid buildings by calculating the first natural frequencies and accelerations of the building variants. The analysis results are then used to explore how variations in the parameters influence the dynamic behavior of the building variants.

6.2. Model

To calculate the first natural frequency two different models are used, a simplified version of a continuous model and a single-degree-of-freedom (SDOF) model.

6.2.1 Raleigh's method

The Raleigh's method is a simplified method that is based on a continuous model. The natural frequency is calculated using the formula from Raleigh's method given in Equation 6.1 [63]. The background of this method is provided in Appendix G.

$$\omega_n = \kappa_n^2 \sqrt{\frac{EIg}{\gamma S}} \tag{6.1}$$

With;
$\kappa_1 l$ = 1.875 for first natural frequency
EI = bending stiffness (N/m²)
γ = density (kg/m³)
S = area (m²)

To calculate the natural frequency of a tall building using Raleigh's method, specific assumptions are made for the input parameters. The density γ is taken as the total building mass divided over the total volume of the building, while for the area S, the area of the core is assumed.

6.2.2 Single-degree-of-freedom model

An SDOF model is also created for the building to compare with the Rayleigh method. The reason for this comparison is to assess the sensitivity of both models and to better understand the assumptions

made in the Rayleigh method. This model simplifies the building to a single mass and stiffness, from which the first natural frequency is derived using Equation 6.2. The background of this model is provided in Section 4.1.

$$\omega_1 = \sqrt{\frac{k}{m}} \tag{6.2}$$

6.2.3 Model setup

The model setup outlines the steps involved in the modeling process, as shown in Figure 6.1. The process starts with input collected from the designs of the building variants, including the distributed mass of the building and the stiffness of the concrete core. A continuous model serves as the basis for calculting the natural frequency of the building variants. This model is developed using a Python script provided in Section K.

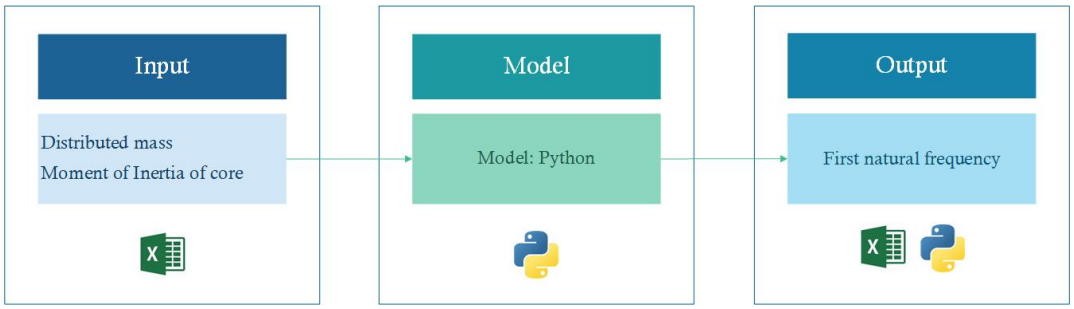

Figure 6.1: Dynamic model setup

6.3. Results

This section gives the results of the dynamic model. First, the first natural frequency is compared to the wind spectrum. Next, the first natural frequency is plotted for different percentages of concrete floors. Following this, the results for different building heights are presented. Subsequently, different calculation methods are compared and finally, the along-wind accelerations are evaluated.

Figure 6.2 shows the minimum and maximum first natural frequencies of all building variants within the Von Kármán wind spectrum. This spectrum is a mathematical model illustrating how wind turbulence energy varies with frequency [64, 65]. The highest frequency corresponds to the building variant with only CLT rib floors and a height of 70 m, while the lowest frequency is associated with the building variant featuring concrete floors and a height of 110 m.

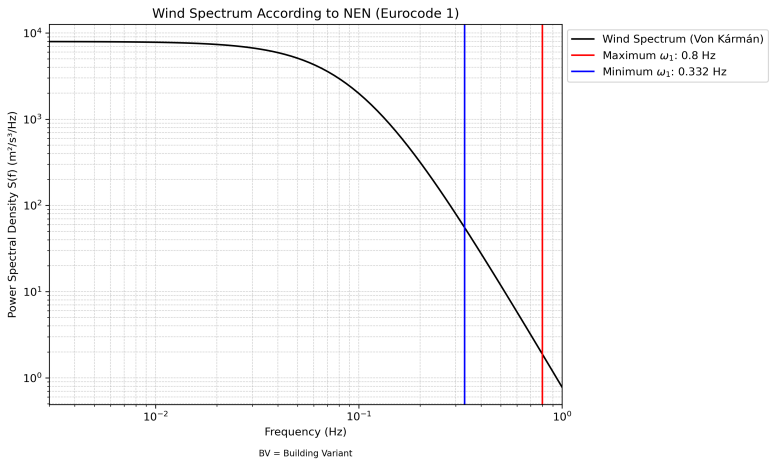

Figure 6.2: Minimum and maximum first natural frequency in wind spectrum

Figure 6.3 illustrates the first natural frequency calculated using Rayleigh's method for various floor types and concrete floor percentages. The results show that the natural frequency of buildings with only CLT floors is 18% lower than that of buildings with only concrete floors. Additionally, the first natural frequency decreases as the percentage of concrete floors increases. However, the variation in frequency between different floor types is minimal, and the decrease becomes less pronounced as the percentage of concrete floors rises. This is further supported by the observation that the impact of heavier TCC floors on the natural frequency is relatively small compared to the lighter CLT timber floors.

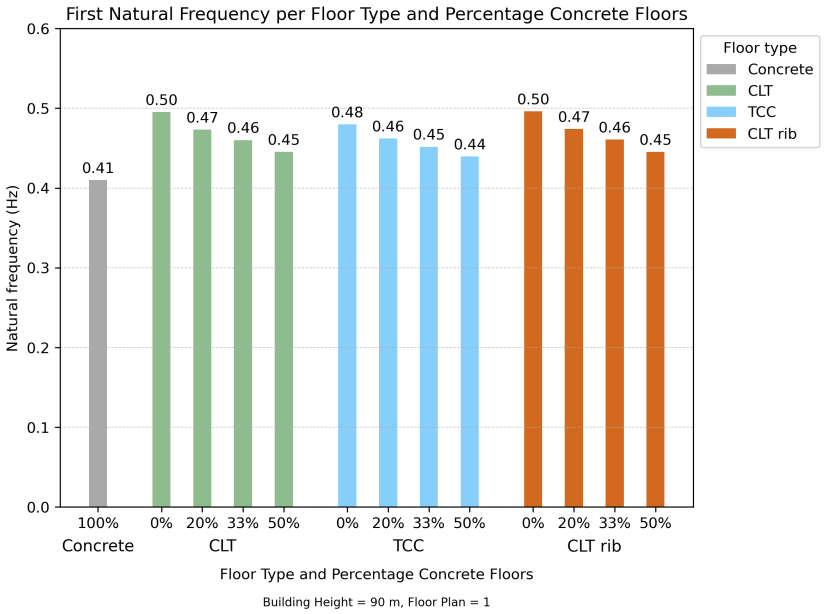

Figure 6.3: Natural frequency per floor type and percentage concrete floors

Figure 6.4 illustrates the first natural frequency for different floor types across varying building heights, calculated using the Rayleigh method. The results show that the natural frequency decreases with increasing building height, though the rate of decrease lessens at greater heights. The figure also reveals that buildings with timber floors have similar natural frequencies, whereas those with concrete floors exhibit lower values.

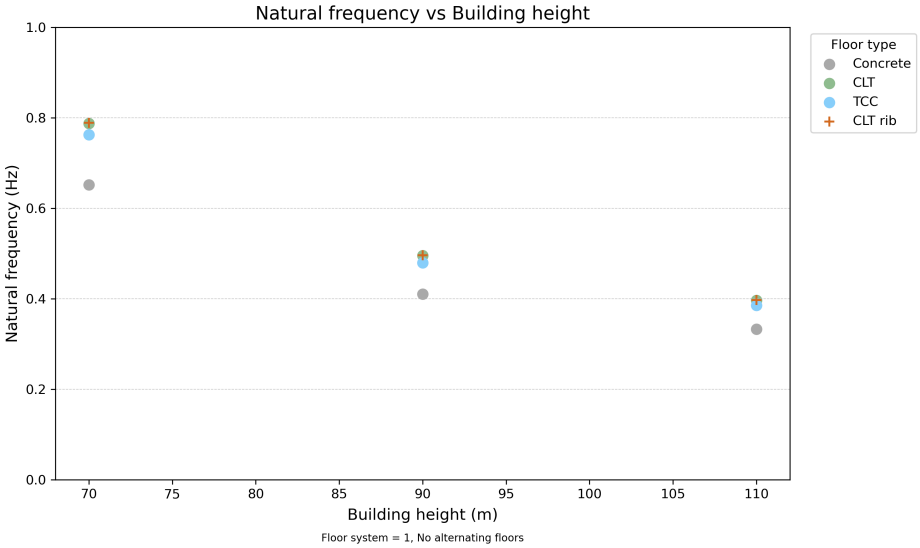

Figure 6.4: Variation of natural frequency with building height

Figure 6.5 compares the first natural frequency calculated using Rayleigh's method and the NEN 1991-1-4 procedure for varying percentages of concrete floors and building heights. The figure shows that the natural frequency determined by the NEN 1991-1-4 procedure depends solely on building height, as described by Equation G.15 in Appendix G. In contrast, the natural frequency derived from Rayleigh's method is influenced by both the building's mass and height, resulting in a decrease in frequency as the percentage of concrete floors—and consequently the total mass—increases.

The empirical formula in NEN 1991-1-4 is based on data from buildings, primarily concrete and steel structures taller than 70 m. This empirical formula has a correlation coefficient of $r = 0.8828$ and provides an approximation for the first natural frequency of a building [66]. The graph shows that the natural frequency calculated using the Rayleigh method is close to the natural frequency predicted by the empirical formula. The maximum deviation for each building height ranges from 20% to 22%, with the difference decreasing as the building height increases. Based on these results, it can be concluded that the empirical formula serves as a reliable estimation for concrete-timber buildings of similar heights.

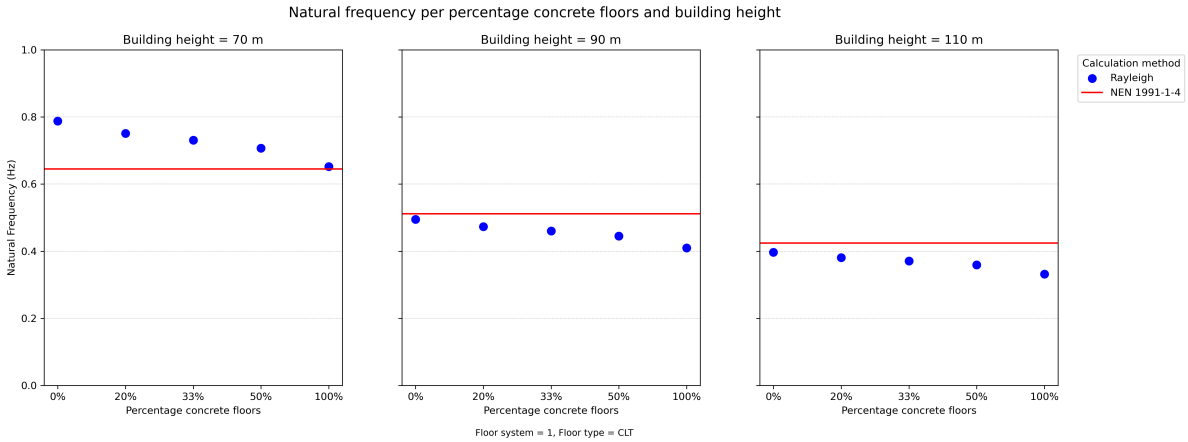

Figure 6.5: Variation of natural frequency with building height and percentage concrete floors

Figure 6.6 presents the combination value of the along-wind, across-wind and torsional accelerations calculated using the EN-NEN 1991-1-4 Appendix G procedure, with the first natural frequency obtained via Rayleigh's method as input for the along-wind and across-wind acceleraton. For the torsional acceleration, the first natural frequency is multiplied by 1.3 to account for the higher tiorsional stiffness of the structure. For these calculations, a damping ratio of 0.1, wind area category 2, and terrain category 4 are assumed. The graph also includes the maximum allowable accelerations specified by NEN and ISO standards for comfort criteria. The results indicate that the accelerations for all building variants remain below the thresholds for both residential and office buildings. This is only a modelled value which can deviate from the actual accelarations in the building. The graph further demonstrates that accelerations increase as floor mass decreases as shown by the red arrow and that the acceleration increases as building height increases, shown by the blue arrow.

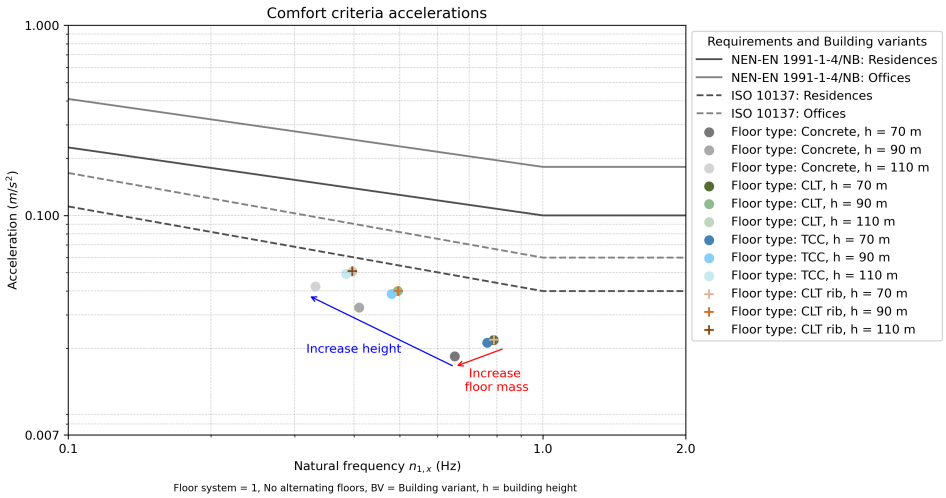

Figure 6.6: Variation of acceleration with natural frequency

6.4. Discussion of results

This section analyses the results to gain a deeper understanding of the relationships between the dependent variable, the first natural frequency, and the parameters. First, the first natural frequency is compared to the wind spectrum. Next, the relationship between the first natural frequency and the percentage of concrete floors is examined. Following this, the relationship between the first natural frequency and the building height is derived.

6.4.1 von Kármán wind spectrum

Figure 6.2 shows that the building's natural frequencies overlap with the typical range of the von Kármán wind spectrum, suggesting that there could be some interaction with wind-induced vibrations. However, since the first natural frequency is located in the tail of the wind spectrum, the interaction is likely to be relatively small. Whether this leads to significant resonance or discomfort will depend on factors such as the specific wind conditions, the damping characteristics of the building, and the proximity of the building's natural frequencies to those of the wind spectrum.

6.4.2 Relation first natural frequency and percentage concrete floors

To find the relation between the natural frequency and the percentage of concrete floors, first the relation with the total mass must be derived. Using the Rayleigh formula, the relationship between the total mass and the natural frequency can be expressed as shown in Equation 6.3.

$$\omega_1 \propto \frac{1}{\sqrt{m}} \tag{6.3}$$

The relationship between the total mass and the percentage of concrete floors is linear, as shown in Equation 6.4.

$$m = m_0 + a * p_{concrete floors} \tag{6.4}$$

With;
m_0 = mass of building with no concrete floors
a = increase of mass per percentage concrete floors
$p_{concrete floors}$ = percentage concrete floors

Substituting this relationship into the expression for the natural frequency yields the relationship between the first natural frequency and the percentage of concrete floors, as shown in Equation 6.5.

$$\omega_1 \propto \frac{1}{\sqrt{m_0 + a * p_{concrete floors}}} \tag{6.5}$$

6.4.3 Relation first natural frequency and building height

The relationship between the natural frequency and the building height is derived using the Rayleigh formula, as shown in Equation 6.6.

$$\omega_1 \propto \frac{\sqrt{l}}{l^2} \tag{6.6}$$

The buildings analyzed in this study can be categorized as squat, with a maximum slenderness ratio of 4.2 at a height of 110 m. The results in Figure 6.5 suggest that the limited slenderness may explain why the natural frequencies of the buildings remain between 0.3 and 1.0 Hz, rather than approaching the lower limit of 0.1 Hz.

6.5. Preliminary conclusions

The results indicate that the first natural frequency decreases as the percentage of concrete floors increases. However, the variation in frequency between different floor types is minimal, and the decrease becomes less significant as the percentage of concrete floors increases. This is also supported by Formula 6.5.

As building height increases, the natural frequencies of buildings with different masses converge, suggesting that mass has less influence at greater heights. This implies that height and stiffness are more important factors than the mass of the floors at greater heights.

For all building types, acceleration values remain well below the thresholds, indicating that all building variants meet the serviceability criteria. It should be noted that these values are calculated based on simplified models of buildings with several assumptions, and actual accelerations may deviate from these estimates.

Sub-question 6:
How do floor type and floor alternations influence the dynamic behavior of these buildings?

Answer:
Buildings with timber floor types exhibit higher first natural frequencies due to the reduced total mass compared to buildings with concrete floor types. A less significant influence is observed with the percentage of concrete floors. As the percentage of concrete floors increases, the first natural frequency decreases substantially, indicating that the mass of the floor system contributes significantly to the total building mass.

7

Environmental performance modelling and analysis

Several steps are taken to obtain the Environmental Cost Index (ECI) for all building variants. Detailed explanations are provided for each step to clarify the assumptions, the input data and the model used. To obtain the ECI value for the building variants, the described LCA method is followed. Detailed explanations are provided for each step to clarify the processes and calculations involved.

7.1. Goal

The objective of conducting a Life Cycle Analysis (LCA) is to determine the ECI value for various building variants. This ECI value serves as a reference point for comparing the environmental performance of these variants. The analysis explores how changes in parameters affect the environmental impact of building variants. In addition, it examines potential correlations between the environmental performance of a building and other design aspects. Since the building variants are based on early design assumptions, the ECI value provides a broad estimation of their environmental performance.

7.2. Scope

The scope outlines the boundary conditions and assumptions used in the LCA, structured across several subsections. First, the functional unit is discussed, followed by the lifespan.

7.2.1 Functional unit

The building variants are based on a case study building, the Cooltoren in Rotterdam. The height of the variants ranges between 70 and 110 m and can therefore be defined as high-rise buildings. All variants have the same function, a residential building. For the LCA only the main load-bearing structure is evaluated. The load bearing structure consists of:

- Floors
- Beams
- Columns
- Core
- Foundation plate
- Foundation piles

Other building elements are out of the scope. Elements that are not included are the facade, installations and partition walls. The materials that are used for all structural elements are divided per element. The building variants use different floor types. This means that several materials are used for the floor and beams of different building variants. The material choice per building element is given in Table 7.1.

Table 7.1: Materials of elements

Element	Material		
Floor	Concrete C30/37	Reinforment steel F500	CLT gl24
Beam	Concrete C30/37	Reinforment steel F500	Glulam gl28h
Column	Concrete C70/85	Reinforment steel F500	
Core	Concrete C55/67	Reinforment steel F500	
Foundation plate	Concrete C30/37	Reinforment steel F500	
Foundation pile	Concrete C30/37	Reinforment steel F500	Steel S355

7.2.2 Life span
The lifespan of the building variants is 50 years, which aligns with the design of other high-rise buildings. In this research, the Life Cycle Assessment focuses only on the load-bearing structure, which is assumed to require no maintenance, repair, or replacement. Typically, tall buildings of this height are not demolished before their lifespan ends and often they stand much longer. A 50-year lifespan is enough for CO2 storage and therefor permits the inclusion of specific scenarios in modules C and D of the LCA. All Environmental Product Declarations (EPDs) for the materials used have a lifespan equal to or longer than that of the building, and for this research, this assumption is considered acceptable.

7.3. System boundaries
The life cycle stages of products that are included are: 'Cradle-to-Gate principle with modules C3-4 and D'. The steps per life cycle stage are further elaborated.

7.3.1 Production stage
The production stage includes phases A1-A3, which cover raw material extraction, transportation, and manufacturing. The production processes for the primary materials used in the structural elements are desribed in Section H.2 in Appendix H.

7.3.2 Construction stage
The construction stage includes material transportation (A4) and on-site construction processes (A5). Although these stages can contribute significantly to the environmental impact of building projects, they are excluded from the scope of this research and the LCA calculations, as there is a lack of detailed, reliable data for the materials of the building variants. Transportation (A4) involves the delivery of materials to the construction site, with emissions depending on transport modes (e.g., truck, rail, ship) and distances. Construction processes (A5) include energy use by machinery, waste generation, and emissions related to on-site assembly. The environmental impact of this stage is influenced by:

- Construction methods
- Machinery and equipment
- Site-specific conditions

These factors are material- and project-specific, making it challenging to generalize the environmental impact of the construction stage across all building variants. For instance, although timber is lighter and allows for shorter construction times, integrating it with concrete in a hybrid system necessitates specialized connections and handling techniques, which may offset these advantages.

7.3.3 Use stage
In the use stage (B) of a building, the focus is directed towards environmental of the building's operations and usage. This stage covers the entire period during which the building is in service, including energy demands, water supply, maintenance measures and other activities that contribute to its environmental footprint.

It is assumed that there is not much impact on environmental impact of main load-bearing structure during this stage, because the energy consumption and maintenance during this stage have no significant impact on the foundation and structural system. It is also assumed that there is no significant

difference in between building with timber or concrete structural elements. Therefore the use stage is not included in the LCA [67].

7.3.4 End-of-life stage

The end-of-life stage (C1-4) consist of demolition, transport to waste processing, waste processing and disposal of building elements. This stage is essential for recycling and reusing of building materials in stage D. The way in which the different building materials are demolished and how the waste is processed depend on the chosen scenario, which can be linked to stage D. In this thesis, the stages waste processing (C3) and disposal (C4) are included. Thes stages demolition (C1) and transport (C2) are excluded from the calculatesion as these two stages largely depend on the material and external factors, making it challenging to generalize the environ- mental impact of these stage across all building variants.

7.3.5 Benefits and loads beyond the system boundary

In a Life Cycle Assessment, Stage D represents the benefits and loads beyond the system boundary. This stage accounts for the environmental benefits and burdens associated with the product's recycling, reuse, or recovery after its end-of-life (EoL). Two main types of benefits can be identified:

- Energy recovery: product waste can be used as biomass for energy generation, reducing the demand for fossil fuels and decreasing greenhouse gas emissions from conventional energy production. Material waste is incinerated and generates energy, which reduced the demand for fossil fuels.
- Avoided emissions: material reused and recycled in other construction projects, reducing the need for new raw materials and saving energy in the production of virgin products.

Tall buildings are seldom demolished due to their high initial investment. A disadvantage of this is that structural elements and materials cannot be reused or recycled. However, reusing the building as a whole is more feasible, which extends the lifespan of the structural system and eliminates the need for demolition and replacement. Extending the lifespan of a building can be achieved by upgrading and retrofitting, thereby reducing the embodied carbon over its lifespan. In this thesis is assumed that the building is demolished after 50 years.

7.3.6 EoL Scenarios

For each structural element and material, two End-of-Life (EoL) scenarios are established for stages C and D. These are presented in Table H.1 in Appendix H, along with an explanation of the choices made for specific scenarios. The first scenario represents an end-of-life approach that is currently standard for these materials, while the second scenario outlines a future approach envisioned within a circular economy. The outcomes are heavily influenced by the chosen scenarios and the fact that all material scenarios are combined. This means that the outcome does not necessarily represent the upper and lower boundaries of the ECI value but rather provides a comparison between the current approach and the future approach for calculating the ECI value of buildings.

7.4. LCA methodology

The environmental aspects are divided into categories, with one indicator selected for each category to serve as a reference point for weighting the other compounds within that category. Subsequently, the impact categories are weighted against each other to obtain the total ECI score. The 13 environmental impact categories used are those previously mentioned in Chapter 4.2 and are chosen because they are required for the Environmental Product Declarations (EPD) of the products used in this research.

7.4.1 LCI data

The Life Cycle Inventory (LCI) data of products are based on Environmental Product Declarations (EPD) available from various sources in Europe. LCI data is selected based on third party verification, ensuring that the data quality is assumed to be sufficient. Information on the used EPDs is given in Table H.3 in Appendix H together with an explanation on the choice for the specific EPDs. This and the individual EPDs are given in Section H.5.

7.4.2 Method of quantification
The environmental performance of the building variants is quantified using the ECI value. In the ECI calculation, the environmental impacts of materials and processes are monetized according to ISO 14040 standards. The weighting factors for environmental impact categories are included in Table H.16 in Appendix H. Although there are tools available to calculate the ECI of buildings, they are not utilized in this case because the building variants incorporate combinations of concrete and timber, which are not typically supported by these tools.

7.4.3 Life Cycle Inventory
The building materials are included in the LCA through spreadsheets extracted from the design of the floor systems and the design of the concrete core and foundation, provided in Appendices E and F. The data from the EPD's is gathered in spreadsheets and included in the python script that is used for the LCA. The life cycle stages that are included in the LCA are stages A1-3, C3-4 and D. Transport from and to the building site is excluded.

7.4.4 Life Cycle Impact Assessment
The Life Cycle Impact Assessment (LCIA) uses the material quantities and emissions data as input for various impact categories in the LCA. After analysing these factors, relative weights are assigned to each impact category. Based on this, the Environmental Cost Indicator for the building is calculated. The results are shown in Table H.4 in Appendix H.

7.4.5 Life Cycle Interpretation
In this step the output from the assessment is interpretated. This step discusses the results of the LCI and LCIA steps. The sensitivity and limitations are discussed and finally conclusions and recommendations are given.

7.5. Model setup
The design setup outlines the steps involved in the modeling process, as shown in Figure 7.1. The process begins with input gathered from the designs of the building variants, including the material volumes. For each structural component, two end-of-life scenarios are developed. External information on the emissions of the structural elements is obtained from EPD data. In the LCA model, the volumes of the structural elements are linked to the corresponding EPD data. By combining the emissions and multiplying by a weighted factor, the ECI value is calculated.

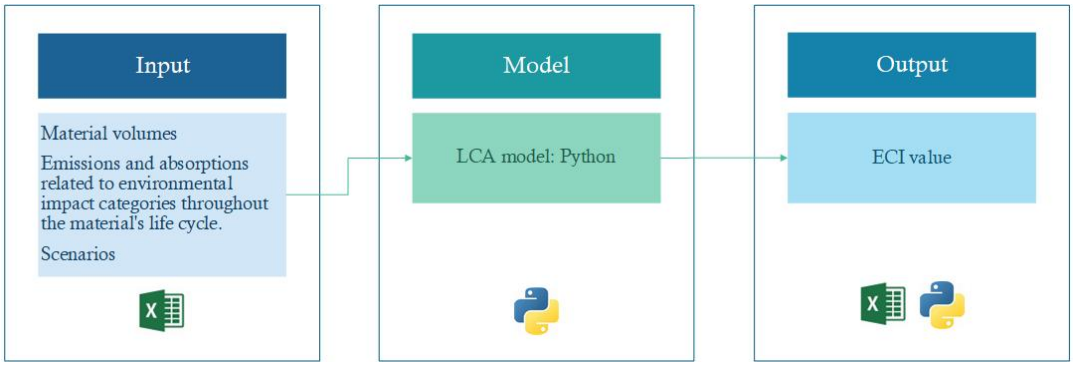

Figure 7.1: LCA model setup

7.6. Results
This section presents the LCA results. First, the environmental impacts of various building variants are shown for both scenarios. Next, the ECI results are provided for different percentages of concrete floors, followed by the ECI values for varying building heights. Finally, the ECI value is plotted against the floor plan.

The ECI values for specific building variants are visualized to show the contribution of different environmental impact categories and stages. The abbreviations used in the graph are explained in Table H.16. Figure 7.2 presents this for a concrete building, comparing scenarios 1 and 2. Both figures show that the largest contribution to the ECI value for stages A and D comes from GWP – fossil, mainly due to CO2 emissions in the production processes of concrete and steel. The contribution from stage C is small across all environmental impact categories, as the recycling of concrete and steel has a relatively minor impact compared to their production processes.

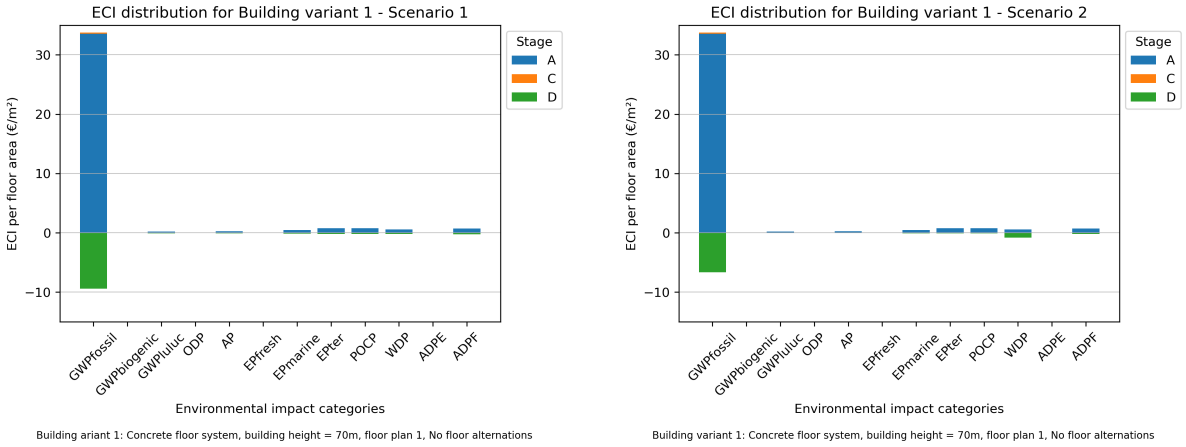

(a) Building variant 1: Concrete floor type for Scenario 1

(b) Building variant 1: Concrete floor type for Scenario 2

Figure 7.2: ECI value per environmental impact category - Building with concrete floors

Figure 7.3 illustrates the contribution of various environmental impact categories to the ECI value for a building variant with CLT floors. The GWP-Fossil contribution in Stage A primarily stems from the production of concrete and steel used in structural elements such as columns, the core, and the foundation. There is a significant contribution from the waste processing stage of CLT floors in both scenarios. This impact arises due to the biogenic carbon content being released back into the atmosphere.

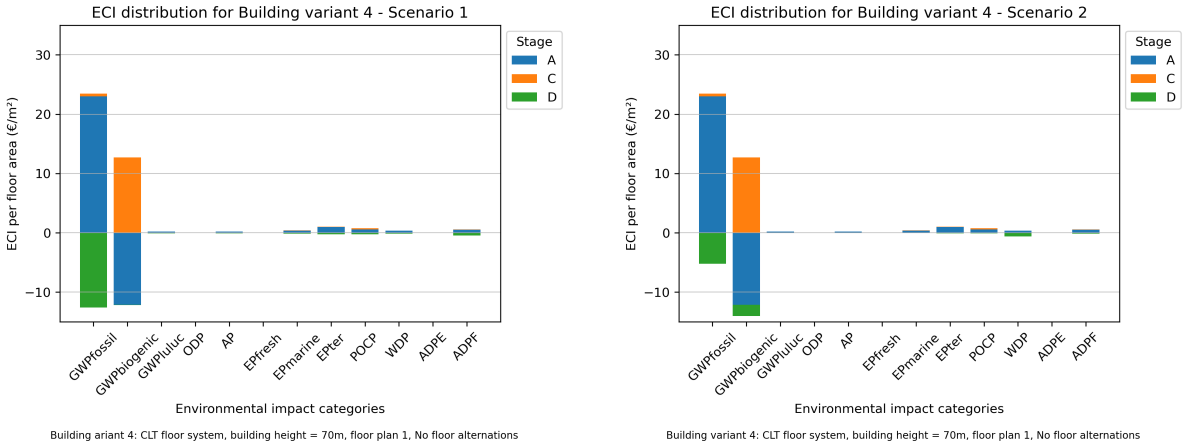

(a) Building variant 3: clt for Scenario 1

(b) Building variant clt for Scenario 2

Figure 7.3: ECI value per environmental impact category - Building with CLT floors

Figure 7.4 presents the total ECI value for different building variants, categorized by the percentage of concrete floors and floor type. The graph illustrates the division of the ECI value between the foundation and the building itself for the two scenarios. The results in the graph show that the ECI value increases with the percentage of concrete floors. While the ECI values for TCC floors are slightly higher than those for CLT and CLT rib panel floors, they remain significantly lower than for buildings with 100% concrete

floors. The foundation's ECI value is independent of the percentage of concrete floors and floor type, as it corresponds directly to the material quantities used. The foundation contributes substantially to the total ECI of the building, with the contribution being largest for timber buildings.

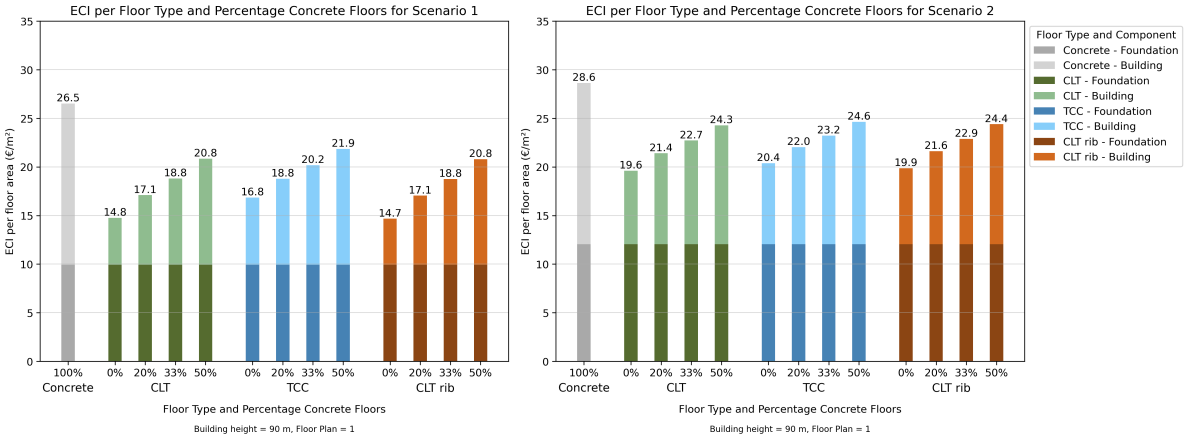

Figure 7.4: ECI variation across different floor types and concrete floor percentages

Figure 7.5 shows the ECI value for different building heights across both scenarios. The ECI value increases with height for timber floor types. For concrete buildings, the ECI value decreases between 70 m and 90 m but rises again at 110 m. In this case, for concrete buildings, the ECI value of the 70 m building is relatively higher than that of the 90 m building. This is because the 70 m building requires a minimal number of foundation piles as another load case is governing and it needs the same core thickness to meet minimum structural requirements.

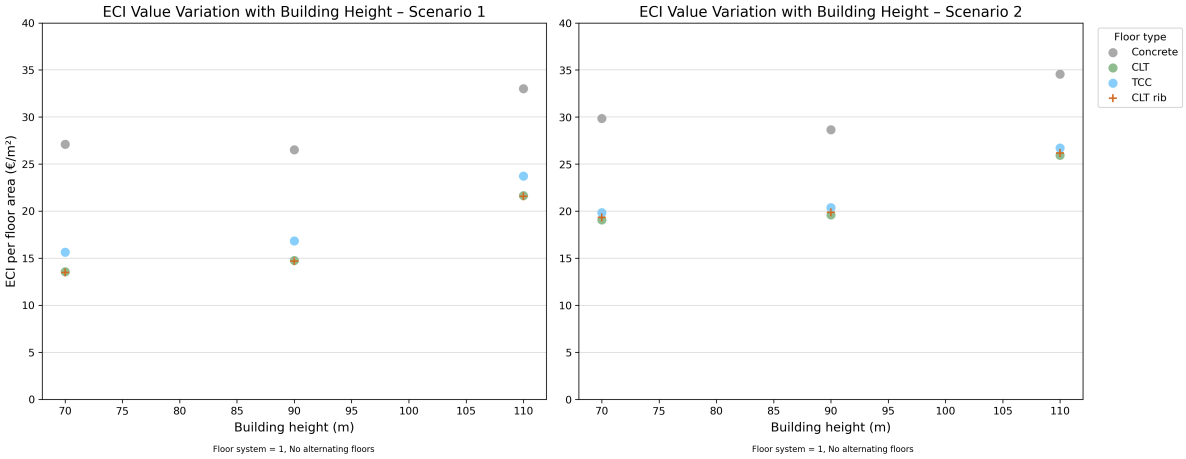

Figure 7.5: ECI in relation to building height

Figure 7.6 presents the ECI values of the building variants per floor type and floor plan for the two scenarios. Both graphs show a significant difference in ECI values between concrete and timber floor types, while the variations among the timber floor systems are relatively small. In Scenario 1, the building variant with CLT floors and floor plan 3 exhibits a lower ECI value, as its total timber mass is larger—unlike the variant with CLT rib panels. The building variant with TCC floors has the highest ECI value due to the thicker concrete topping used in this floor system. Among the timber floor variants, floor plan 2 consistently results in the lowest ECI values, followed by floor plans 1 and 3. The graph also highlights the clear difference between the two scenarios, with Scenario 2 showing higher ECI values across all floor types. This trend is further reflected in Figures 7.4 and 7.5.

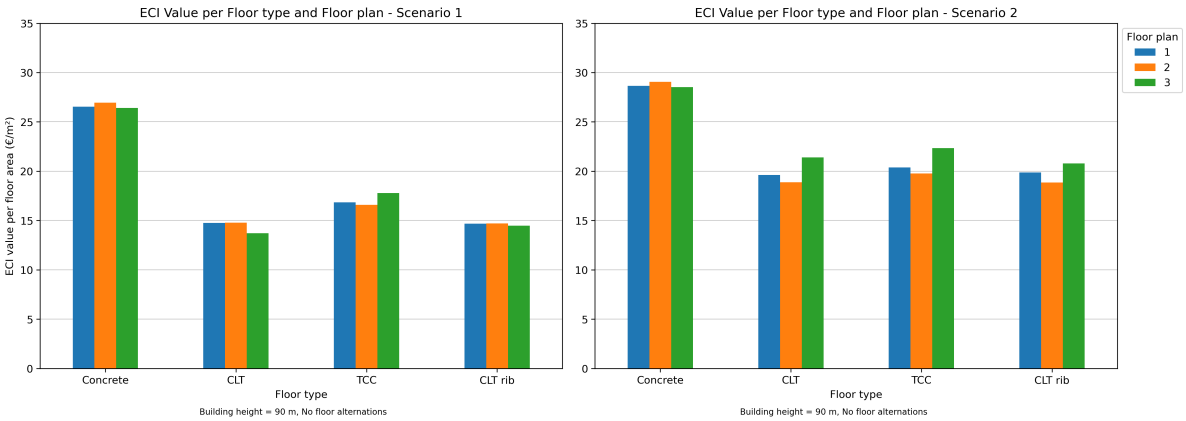

Figure 7.6: ECI value across different floor plans

7.7. Discussion of results

This section analyzes the results to gain a deeper understanding of the relationships between the dependent variable—the environmental cost index per floor area—and the various parameters. First, the chosen scenarios are discussed. Next, the contribution of each environmental impact category to the total ECI value is examined. The influence of the different scenarios on the ECI value is then explored. Finally, the differences between the ECI values for different floor plans are discussed.

7.7.1 Chosen EoL scenarios

Before analyzing the results, the chosen End-of-Life (EOL) scenarios are first discussed. The selected scenario for each structural element has a significant impact on the resulting ECI. To account for this, two scenarios are chosen to illustrate the effect of different choices on the ECI value. Particular attention should be given to scenario 2 for the foundation. This scenario assumes that the foundation piles and plate are recycled as substrate for road construction. While the foundation plate can indeed be recycled, it is unlikely that foundation piles will be extracted from the soil and recycled in the future, primarily due to their weight and size. This assumption has implications for the ECI value of the concrete and steel in this structural element. A more realistic alternative scenario for the foundation piles would be to attribute them to landfill and not attempt extraction or recycling, while still recycling the foundation plate.

7.7.2 Effect of environmental impact categories on ECI value

To analyze the effect of environmental impact categories on the ECI values, the results are examined separately for buildings with concrete floors and CLT floors. For buildings with concrete floors, the primary difference between Scenario 1 and Scenario 2 is the lower benefits in Stage D for Scenario 2 concerning GWP – fossil, as shown in Figure 7.2. This difference is mainly due to the foundation: Scenario 1 assumes the reuse of concrete and steel, which provides greater benefits compared to the recycling approach in Scenario 2. Since the scenarios for the other structural elements remain the same, the foundation plays a key role in the observed variation.

In addition, Scenario 2 shows a slight increase in benefits for WDP, which is linked to the recycling of steel. The benefits of steel recycling are substantial enough to outweigh emissions in Stages A and C, resulting in a net benefit, as indicated in the EPD of steel S355 (Table H.6). However, the reasoning behind this net benefit is not explained in the EPD. Interestingly, the recycling scenario for steel shows a greater benefit for this environmental impact category than the reuse scenario, which seems counterintuitive. This suggests that the data in the EPD for steel recycling is not directly comparable to the assumptions made for steel reuse.

For building with CLT floors for which the results are shown in Figure 7.3. In Scenario 1, the increase in GWP-Fossil during Stage D is attributed to incineration of timber product, which reduces the demand for fossil fuels. In Scenario 2, the benefit to GWP-Fossil is due to the reduced need for fossil fuels linked to the production of steel and concrete, while the benefits in GWP-Biogenic is linked to the recycling of CLT and glulam, which reduces the reliance on virgin materials.

7.8. Preliminary conclusions

Buildings with timber floor types demonstrate lower ECI values per floor area, resulting in better environmental performance compared to buildings with concrete floors. This advantage primarily stems from the embodied carbon storage in timber and the reduction in carbon emissions associated with fossil fuels. A linear relationship is observed between the percentage of concrete floors and the ECI value per floor area. Since ECI is strongly correlated with material mass, this serves as a reliable indicator of a building's ECI value. The ECI per floor area increases with height for buildings with timber floors, but this relationship is non-linear. This non-linearity arises from the fact that building height has a no-nlinear relationship with the required material quantities, such as the number of foundation piles and the thickness of the core walls. Besides, the influence of the floor system on the ECI value is largly dependent on the chosen scenario. From this can be concluded that no optimal floor type can be chosen based on the ECI value.

Sub-question 7:
What impact do the parameters: floor type, floor alternations and building height have on a building's environmental performance?

Answer:
Buildings with timber floor types demonstrate lower ECI values per floor area, resulting in better environmental performance compared to buildings with concrete floors. A linear relationship is observed between the percentage of concrete floors and the ECI value per floor area. Since ECI is strongly correlated with material mass, this serves as a reliable indicator of a building's ECI value. A non-linear relationship exists between the ECI per floor area and the height of the building.

8

Construction cost performance modeling and analysis

The construction cost for all variants of the building is determined through a series of steps. Each step is explained in detail to provide clarity on the assumptions, input data, and the model used. By the end of this chapter, the results from the model are presented and discussed, serving as the foundation for the conclusions.

8.1. Goal

The objective of this chapter is to clearly highlight the differences in construction costs across the building variants. These variants are based on early-stage design assumptions, and the construction costs serve as an indicative measure of total construction costs. The analysis investigates how variations in design parameters influence the construction costs of the different building variants.

8.2. Scope

The scope defines the boundary conditions, assumptions, and data collection methods employed in calculating building costs. It acknowledges that the total construction costs depend on numerous aspects and that the obtained values may not accurately represent all building variants. Other construction components that are out of scope are assumed to be similar in all building variants.

8.2.1 Functional unit

The two parts of the construction that are included in the building cost are the foundation and the structural system. Only these elements are considered, as these are the only components specifically designed for the building variants. These elements are:

Foundation

- Foundation piles
- Foundation plate

Structural system

- Floors
- Beams
- Columns
- Core

The materials that are used for all structural elements are divided per element. Additional information on the materials properties of these structural elements is provided in Section 7.2.1.

8.2.2 Construction process

The construction process can be divided into a number of sub-processes and it is limited to the structural elements. For each element, a separate sub-process has been developed. These sub-processes are outlined below and elaborated on in Section I.2 in Appendix I.

- Setup construction site
- Excavate foundation pit
- Construct foundation piles
- Construct foundation plate
- Construct concrete core
- Construct concrete column
- Construct concrete beams and floor
- Construct CLT floor and glulam beams
- Construct TCC floor and glulam beams
- Construct CLT rib panel floor and glulam beams
- Dismantling of the construction site

The sequence of these subprocesses partially overlaps. For building variants without floor alternations, the subprocesses can be followed in order as shown in Figure 8.1. However, when alternating between concrete and timber floors, the construction process differs. First, the concrete columns and floors are built, after which the timber beams and floors are placed in between as shown in Figure 8.2. The idea behind this construction sequence is to improve efficiency by first completing the concrete structure and then installing the timber elements. This can result in a faster construction process as the concrete curing process is quicker, and the concrete casting does not need to be repeatedly assembled and dismantled. This contrasts with a sequential floor-by-floor approach, where the concrete casting process would need to be interrupted multiple times.

When applying the second construction method for building variants with less concrete floors, such as a 2:1 ratio of timber to concrete floors, the concrete columns extend to 12.3 meters. To prevent buckling during construction, these taller columns must be increased in dimension. Only afterwards, columns be laterally supported by glulam beams. Another challenge arises when placing the glulam beams and CLT floors between the concrete floors. Since the space above is obstructed by the concrete floors, a crane cannot be used. The optimal construction sequence has not yet been thoroughly evaluated, as feasibility details remain unknown. Additionally, the specifics of this process are beyond the scope of this study.

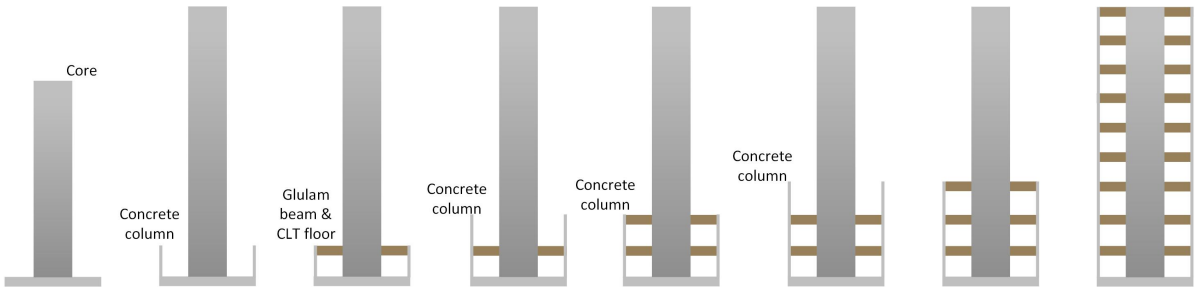

Figure 8.1: Construction sequency for building variants with no alternating floors

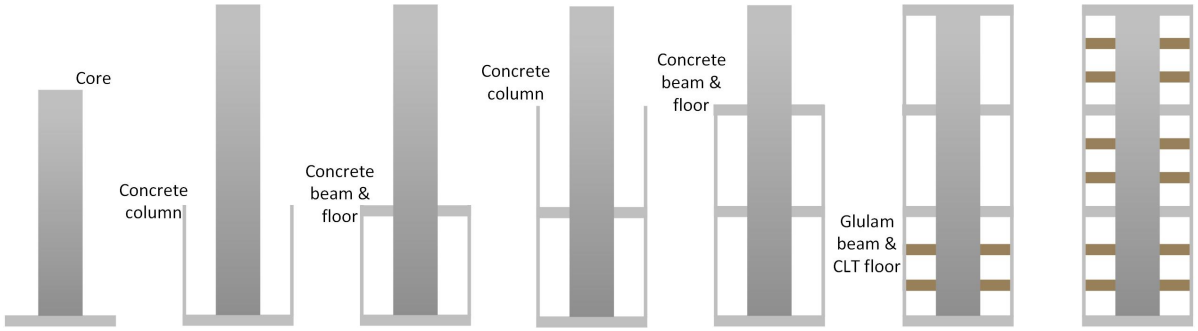

Figure 8.2: Construction sequency for building variants with alternating floors

8.2.3 System boundaries

In the preliminary design phase, the building variants are studied as part of the early design process. While the dimensions are not yet fully finalized, they are sufficiently detailed to allow for comparison between variants. However, it is impractical to calculate cost components, such as equipment costs, separately at this stage. For instance, equipment costs depend on rental prices and rental duration, which are influenced by the construction speed. Additionally, different subprocesses may require multiple types of equipment. Calculating costs at such a high level of detail increases complexity and the potential for errors, particularly when certain steps in the subprocesses are overlooked.

In the preliminary design phase, construction costs can deviate by up to 15% due to the preliminary nature of the design, as details about construction methods and techniques are not yet finalized. At this stage, it is more appropriate to estimate costs at a lower level of detail. For example, construction cost data for producing a concrete column per cubic meter includes an aggregated breakdown of material costs, transportation, framework assembly, reinforcement installation, concrete pouring, and framework removal.

8.3. Assumptions

For the construction of the foundation, several assumptions have been made, as outlined below. The data for the foundation slab is based on a basement floor with a thickness of 500 mm. Although a 2-meter-thick slab is used across the entire floor plan, high-rise buildings in the Netherlands more commonly use foundation beams and poers, with a thinner foundation plate on top. A thick foundation plate would require additional measures and lead to higher costs. For the foundation pit a sheet pile wall is constructed. For this steel sheet piles of type AZ 26 are used. Their weight and associated costs are accounted for in the calculations. The foundation pit is assumed to have dimensions of 35×35 m, providing an additional 1.5 m of space on both sides of the foundation slab.

8.4. Model setup

The construction cost model outlines the steps involved in the modeling process, as illustrated in Figure 8.3. The process begins with developing a database containing cost data for materials and construction activities. For this data the costs for materials, transportation, labor, and equipment are combined and assigned to each structural element. The material quantities are extracted from the designs of the building variants and integrated with the cost data. This approach aligns with standard practices for cost estimation during the preliminary design phase. The process ultimately calculates the total construction cost for each building variant.

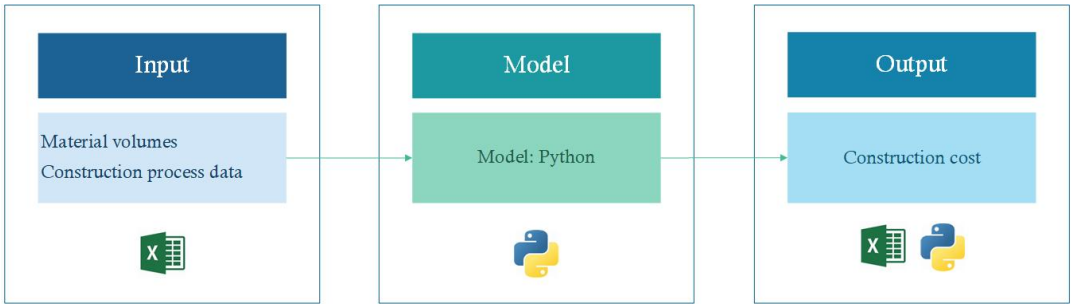

Figure 8.3: Construction cost model setup

8.4.1 Data resources

The data used as the basis for cost calculations are derived from multiple sources. The primary source is the data provided in the CME course Construction Technology. In addition, several data sources for the cost of CLT panels were compared. Since these sources showed significant variation in the costs of the CLT panel, an average value was selected. To reflect this variation, the minimum and maximum values were also calculated.

The cost data originates from estimates based on completed high-rise construction projects in the Netherlands. These estimates, used by a construction company, are applied in the preliminary design phase and include material, equipment, and labor costs for specific structural elements.

To ensure consistency, cost data from different sources has been harmonized by applying indexing. To compare cost data across different years, all values were adjusted to the most recent year, November 2024. This conversion is based on the construction material cost index for ‘nieuwbouw van woningen’, as provided by CBS [68].

The database with the building cost per structural element and the calculations are given in Section I.1 in Appendix I.

8.5. Results

This section presents the results of the construction cost model. First, construction costs are shown for different percentages and types of concrete floors, followed by the impact of CLT price variations on total cost. Next, the cost variations are presented for different building heights are presented. Subsequently, the costs are plotted against the floor plan, and finally, the contribution of structural elements to the total cost is given.

The construction costs of various building variants with different floor types and percentages of concrete floors are presented in Figure 8.4. For the CLT cost an average value is used. The figure distinguishes between the costs associated with the foundation and the structural system, labelled as ‘building´. The foundation costs include excavation, foundation piles, and the foundation plate. The costs are expressed per floor area or Gross Floor Area (GFA).

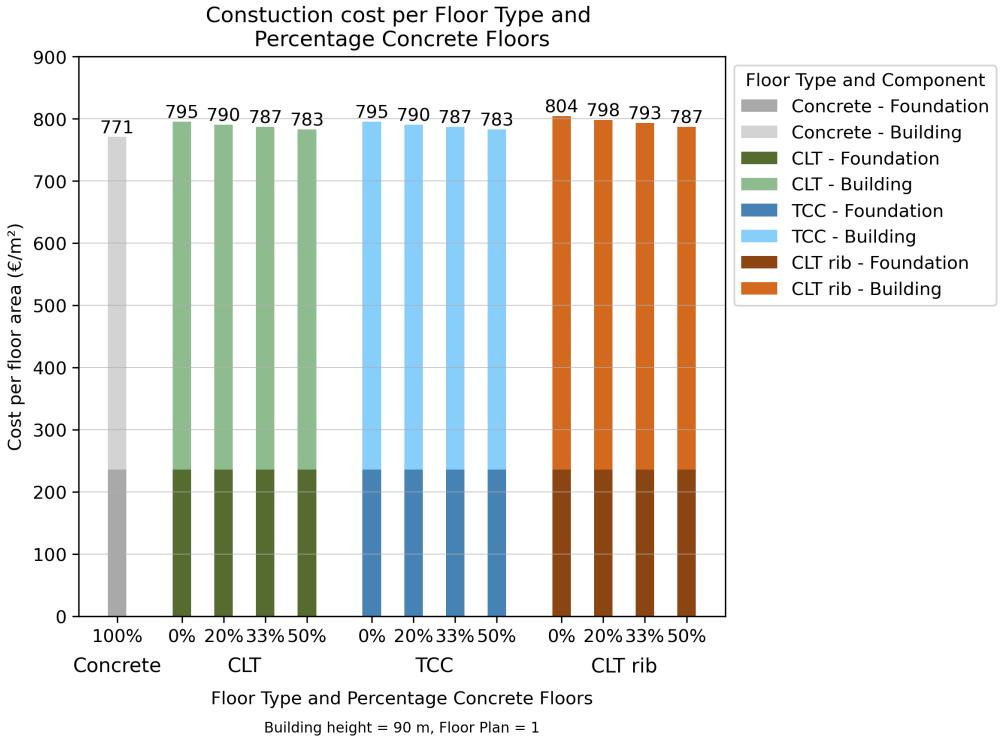

Figure 8.4: Construction cost based on percentage of concrete floors and floor type

Figure 8.5 illustrates the total construction cost per floor area for different floor types and percentages of concrete floors. The bar plot shows the minimum total cost, which corresponds to the lowest CLT price (mean -20%), as well as a variable range representing cost fluctuations due to a higher CLT price (mean +20%). This variation reflects the effect of CLT price fluctuations on the total cost. This variation is included to demonstrate the impact of CLT price changes on the total construction cost. The graph indicates that building variants with timber floors can result in either higher or lower total costs compared to buildings with concrete floors.

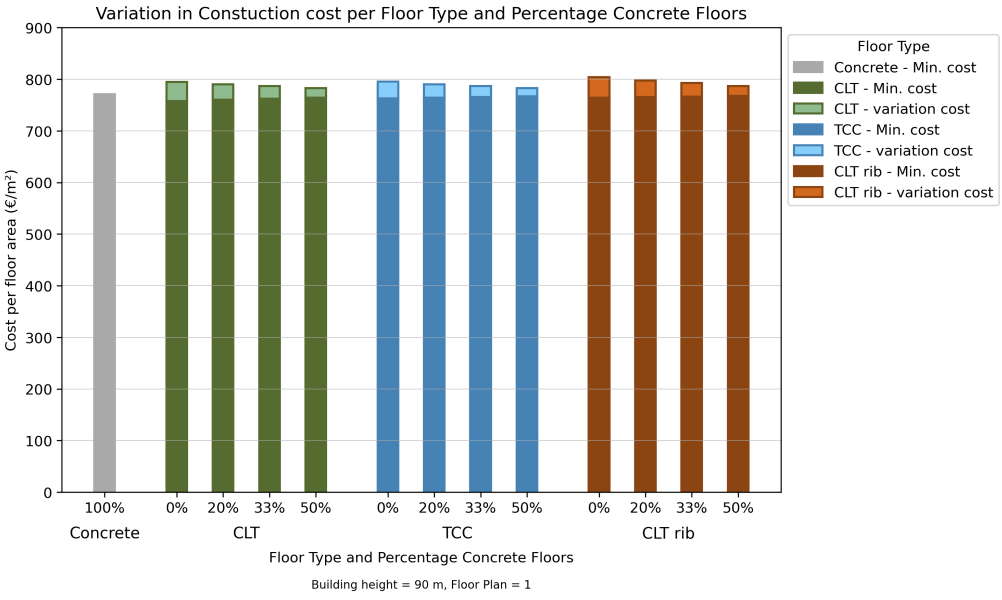

Figure 8.5: Construction cost variation depending on CLT price

The construction cost per floor area for different building heights and floor type is shown in Figure 8.6. In the graph a distinction is made between the contribution of the foundation and the structural system, labelled as 'building'. For buildings with timber floors, a nonlinear increase in cost with height is observed. In contrast, for buildings with concrete floors, the construction cost decreases between a building height of 70 and 90 m, and then increases again between 90 and 110 m. The graph shows that between 70 and 110 m, the cost of the structural system of the building variants with concrete floors decreases with height. For buildings with timber floors, the cost of the structural system decreases from 70 to 90 m, then slightly increases from 90 to 110 m. The cost of buildings with CLT and TCC floors is similar, while buildings with CLT rib panel floors have a slightly higher cost.

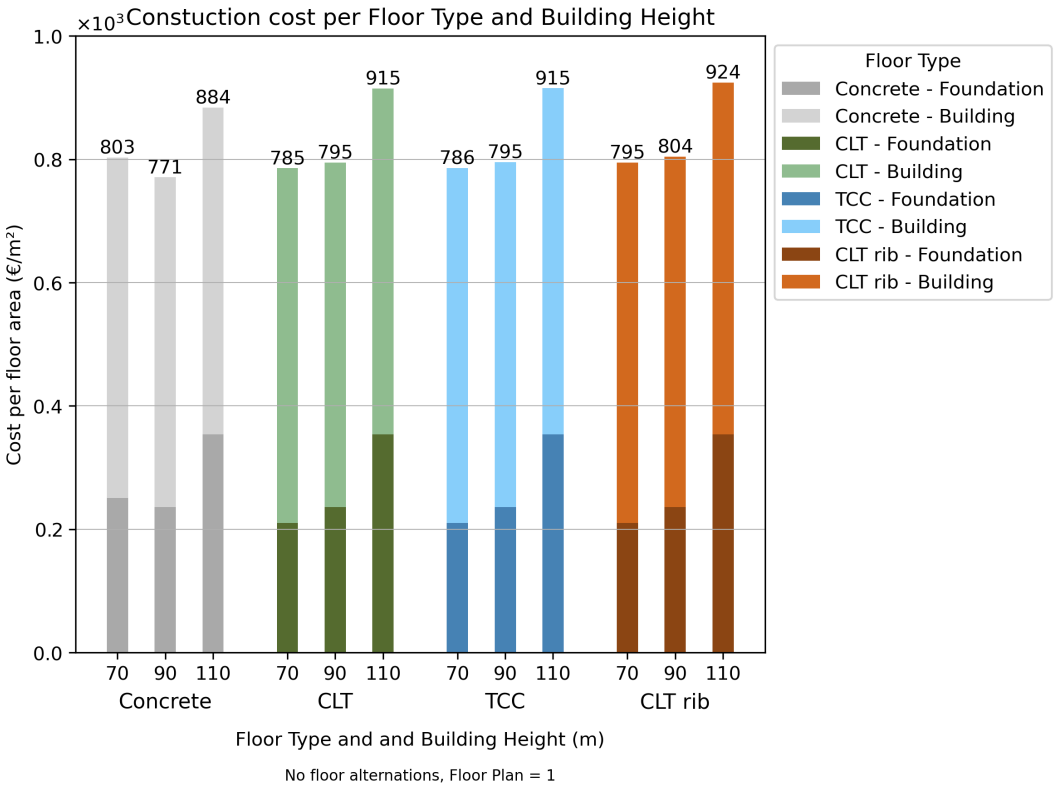

Figure 8.6: Construction cost of structural system over building height

Figure 8.7 presents the total construction cost for building variants with different floor types and floor plans. For all floor types, the reason for floor plan 1 being higher is the increased number of columns. For timber buildings, floor plan 3 generally has the highest cost. In general, floor plan 2 is the most cost-effective option for all floor types.

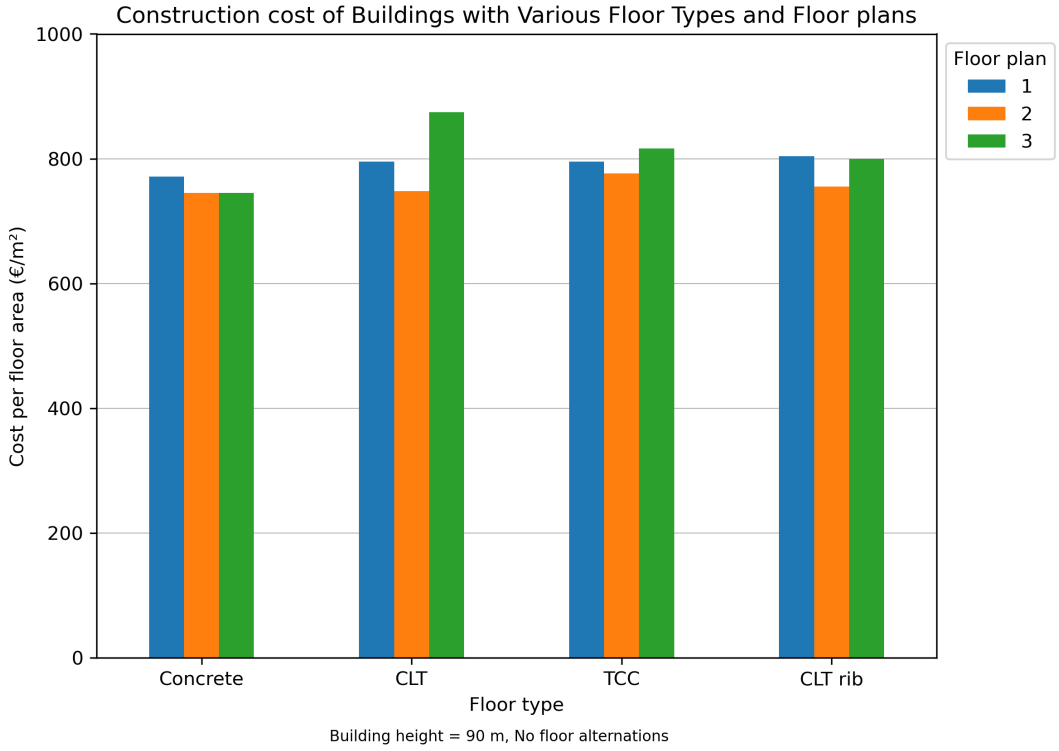

Figure 8.7: Construction cost based on floor plan

The share of various structural elements in the total construction cost of buildings with different floor types is illustrated in Figure 8.8. The graph shows that the main contributors to construction costs are floors, columns, core and foundation piles. The difference in contribution between buildings with concrete floors and timber floors is minimal, with slight percentage differences resulting from rounding.

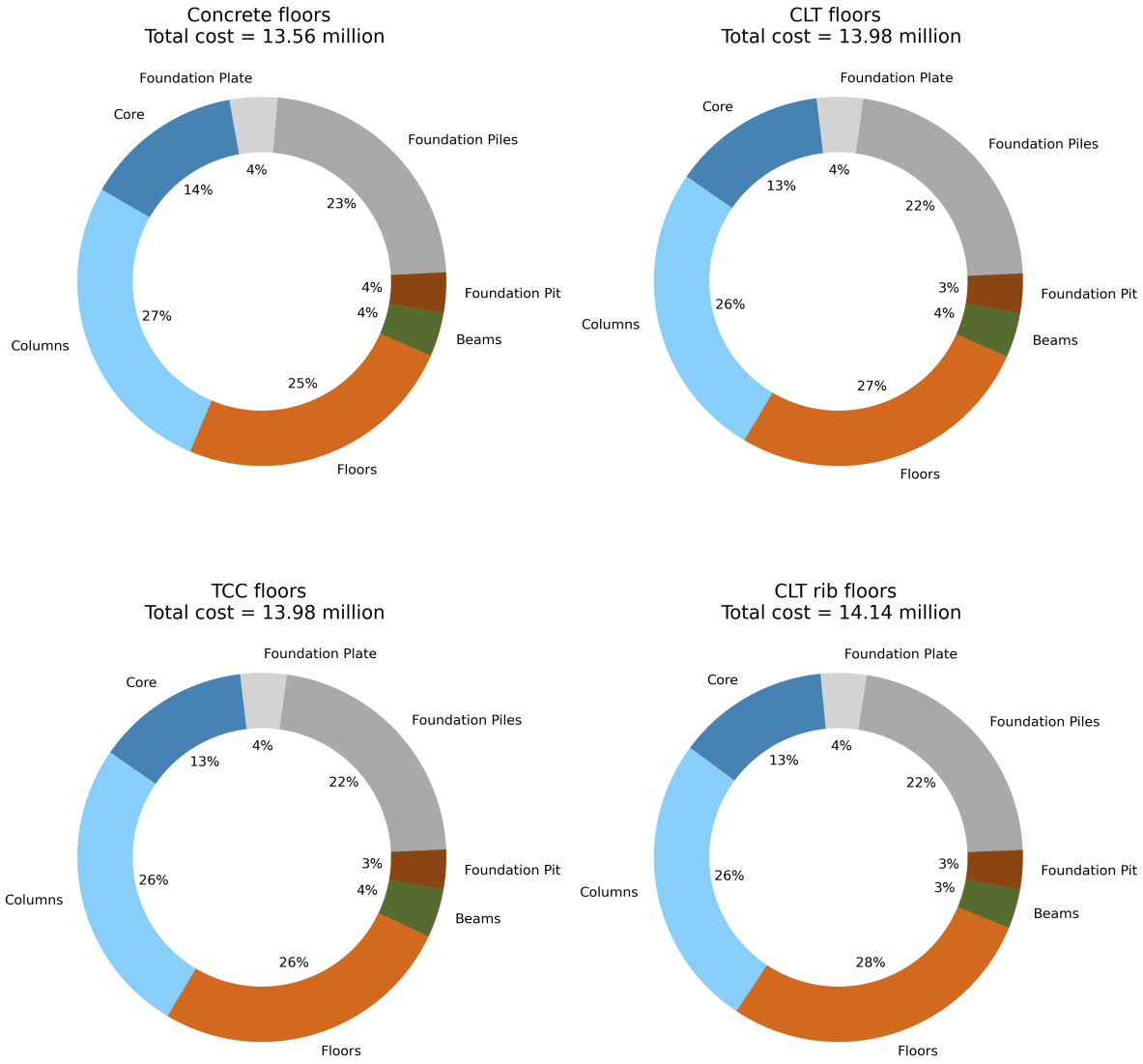

Figure 8.8: Construction cost breakdown by structural element

8.6. Discussion of results

This section analyzes the results to gain a deeper understanding of the relationship between the construction cost per floor area and the key parameters. First, the impact of the percentage of concrete floors and the floor type on the cost is examined, followed by an evaluation of how variable CLT prices affect the total construction cost. Next, the relationship between construction cost and building height is assessed. Subsequently, the construction cost is plotted against the floor plan, and finally, the contribution of structural elements to the total construction cost is analyzed.

8.6.1 Percentage concrete floors and floor types
Based on Figure 8.4, it can be observed that buildings with timber floor systems generally have slightly higher construction costs compared to fully concrete buildings. However, the cost differences between the various timber floor types are minimal. As the percentage of concrete floors increases, the overall construction cost decreases, eventually matching that of a 100% concrete building. The foundation construction cost accounts for 40% to 43% of the structural system cost. This indicates that the foundation's contribution remains consistent across all building variants, aligning with the material quantities discussed in Section 5.5.

8.6.2 Cost variation of CLT
The cost differences shown in Figure 8.5 arise from various factors, such as transportation, building height, and supplier pricing. The graph indicates that building variants with timber floors can result in either higher or lower total construction costs compared to buildings with concrete floors. This suggests that construction cost is not the determining factor in selecting a floor type for the building type.

8.6.3 Building height
Figure 8.6 aims to assess whether the construction cost of the structural system per floor area increases with height, as suggested by previous research. For all buildings, regardless of the floor type, the increase in construction cost with height is primarily driven by the rising cost of foundation piles. The figure shows that for buildings with concrete floors, the construction cost per floor area is lower at a height of 90 m compared to 70 m. This can be explained by fact that the 70 m concrete building requires more foundation piles than the 70 m timber building due to its higher floor mass.

When considering only the structural system, the cost increase between 90 m and 110 m in buildings with timber floors can be attributed to the need for substantially more reinforcement in the core of lighter buildings compared to those with concrete floors or 70 m tall buildings. Additionally, the higher costs of CLT rib floors compared to CLT and TCC floors result from the larger volume of CLT required in the floor system, while the reduction in glulam or beams does not sufficiently offset this increase.

From this graph, it can be concluded that the model aligns with the general statement that construction cost per floor area tends to increase with height, but contradicts the fact that the construction cost increases gradually with height. The data indicates that this trend is primarily driven by the contribution of foundation costs. However, the results also show that the cost of the structural system decreases between 70 m and 90 m. This contradicts previous research, which states that structural system costs should increase with height, as taller buildings typically require more material to transfer vertical loads [49, 69]. The discrepancy between the model results and existing research can be attributed to simplifications and assumptions made in the model, such as keeping the dimensions of the column and the core constant throughout the height of the building. As a result, the model does not fully capture the impact of height on the construction costs of the structural system.

8.6.4 Floor plan
Figure 8.7 shows that floor plan 2 is the most cost-effective. This is due to the greater floor panel height, which significantly increases the mass of CLT, outweighing the cost reduction from the smaller glulam beams. This aligns with the mass distribution shown in Figure 5.7. Overall, floor plan 2 is the most cost-effective option for all floor types. This is attributed to its smaller floor areas, longer beams, and fewer columns, resulting in a more efficient structural layout.

8.6.5 Contribution of structural elements
By analysing Figure 8.8 it can be suggested that absolute construction cost differences are more significant than the relative contributions of individual structural elements. The relative contribution of different structural elements is approximately the same for all floor types.

8.7. Preliminary conclusions
It should first be stated that the structural system and foundation account for only 20% of the total direct cost, and therefore, these results provide only an indication of the overall cost. Buildings with timber floor systems tend to have slightly higher costs compared to fully concrete buildings. However,

the cost differences between the various timber floor types are minimal. Variations in CLT prices lead to cost fluctuations of a similar magnitude to the difference in cost between buildings with only timber and concrete floors. The model cannot accurately predict the construction cost for increasing building height, as the results do not align with general established theory, which states that the cost of the structural system per floor area increases with building height.

Sub-question 8:
How do floor alternations affect the construction cost?

Answer:
The impact of alternating floors is small, as the cost values fall between those of 100% concrete and fully timber buildings, which themselves do not differ significantly.

9

Results and Discussion

This chapter combines the results from the individual models and analyzes the correlations between the design aspects. It then discusses the findings and evaluates the models.

9.1. Results

The results are divided into three subsections. First, the relationship between environmental performance and dynamic behavior is analyzed. Next, the correlation between dynamic behavior and building cost is examined. Finally, the relationship between environmental performance and building cost is discussed.

9.1.1 Relation between environmental and dynamic performance

This subsection explores the relationship between environmental performance and dynamic behavior. To achieve this, the results of the building variants for the two dependent variables are plotted against each other. To enhance clarity, the data is divided per parameter.

Figure 9.1 presents the ECI value plotted against the natural frequency, with building variants grouped by building height. The graph indicates a clear correlation between the ECI value and dynamic behavior across different building heights, supported by a high R^2-value. The R^2-value is the coefficient of determination derived from the Pearson correlation coefficient. The trend line suggests a linear relationship for between the ECI value and the first natural frequency for different building heights. The difference in natural frequency is more pronounced between 70 m and 90 m than between 90 m and 110 m. But the ECI value increases significantly for between 90 and 110 m compared to between 70 and 90 m. In general, as building height increases, natural frequency decreases, and the ECI value rises.

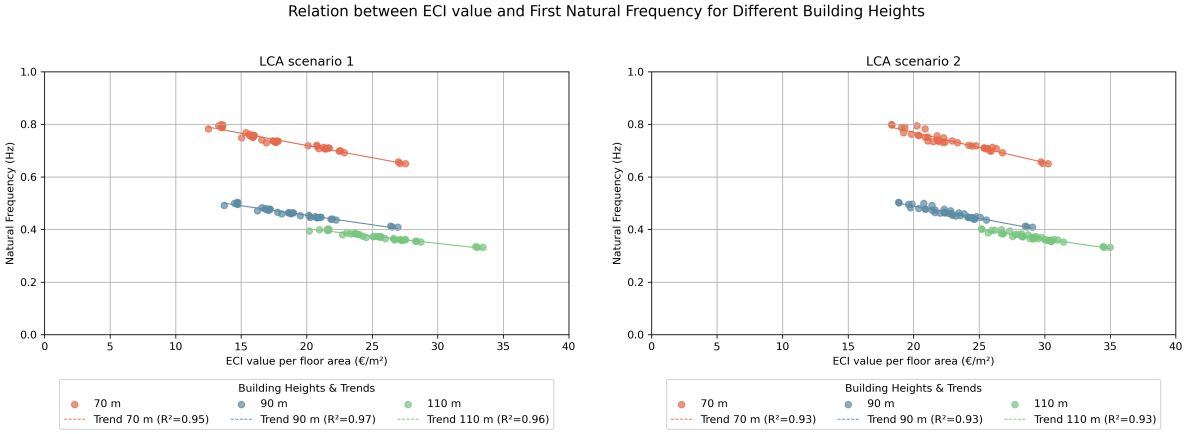

Figure 9.1: ECI and first natural frequency correlation across building height

Figure 9.2 presents the ECI value plotted against the natural frequency, with building variants grouped by percentage of concrete floors. When examining the data of building variants with similar building height, a gradual increase in the percentage of concrete floors is visible. This increase corresponds to a higher ECI value and a decrease in natural frequency. The increase in natural frequency and ECI gradually slows as the percentage of concrete floors increases.

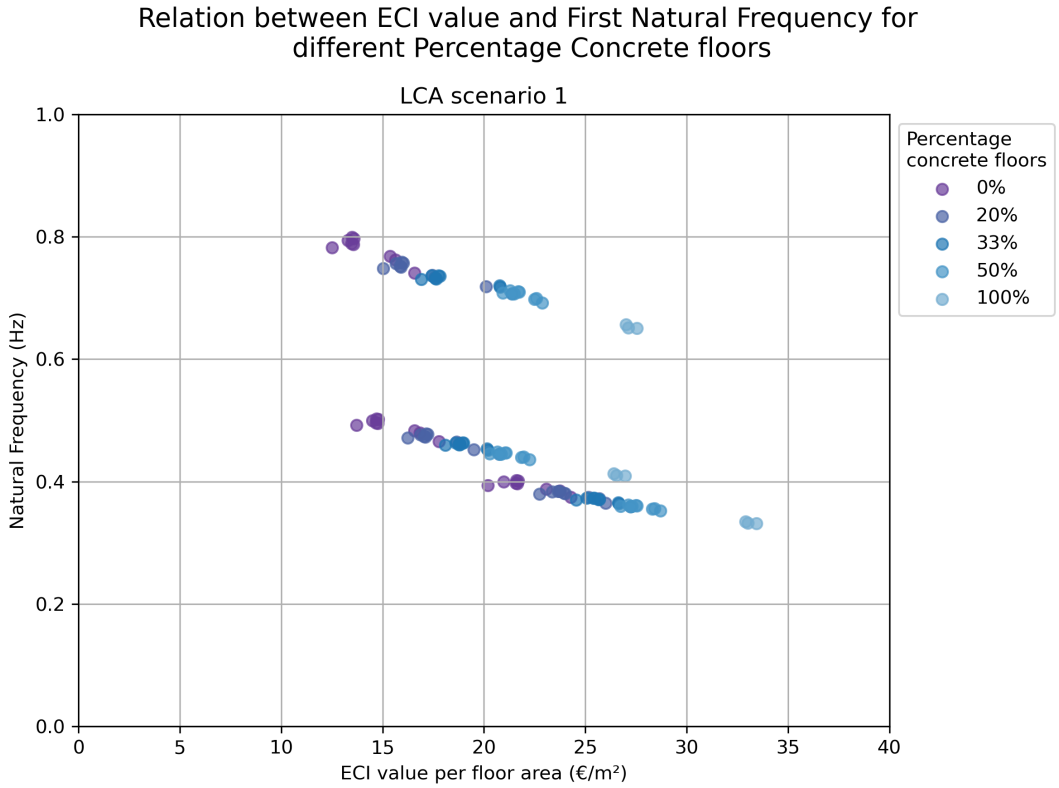

Figure 9.2: ECI and first natural frequency correlation across percentage concrete floors

Figure 9.3 builds on the results presented in Figure 9.2. The graphs show the normalized rate of change of natural frequency and Environmental Cost Indicator (ECI) per percentage of concrete floors. The results are presented for the three timber floor types and the three building heights used in the study. The dashed diagonal line represents the scenario where the normalized rate of change in natural frequency decreases proportionally to the increase in ECI.

- If a data point falls below the diagonal line, the rate of change in natural frequency is lower than the rate of change in ECI.
- If a data point is above the diagonal line, the ECI increases more significantly compared to the natural frequency.

This comparison helps to assess whether increasing the percentage of concrete floors leads to a balanced trade-off between improving structural dynamics and increasing environmental impact.

For example, in the top-left graph, the data point of 20% indicates that the normalized rate of change in natural frequency between 0 and 20% concrete floors is 0.4, while the rate of change for ECI is 1.0. Focusing on the top three graphs, which represent buildings with a height of 70 m, the variants with CLT and CLT rib floors show similar trends. For TCC floors, the rate of change in natural frequency is lower, while the range for ECI is larger. Additionally, the increase in ECI for 33% concrete floors is shifted to the right, meaning that a more significant increase in ECI occurs between 20% and 33% concrete floors compared to the other floor types.

For buildings with a height of 90 m, the graphs exhibit a similar pattern across all three floor types.

Compared to the 70 m buildings, the key differences are a lower rate of change for natural frequency across all variants and a shift in ECI values towards the 20% marker observed for the 70 m buildings. Additionally, the overall range of rate values is smaller for both ECI and natural frequency. For TCC floors, the rate of change is lower than that of CLT and CLT rib floors for both ECI and natural frequency.

In the case of 110 m buildings, the rate of change in natural frequency continues to decrease, though the reduction is smaller compared to the difference between 70 m and 90 m buildings. For ECI a shift occurs for 50% and 100% concrete floors, that move leftward, leading to lower values compared to 20% and 33% concrete floors. These graphs clearly show that the lower limit of the range for the natural frequency rate remains constant for building heights of 70 m and 90 m, while the upper limit continuously decreases. For ECI, both the upper and lower limits decrease with increasing building height. Additionally, the graphs indicate that for TCC floors, the limits deviate from the general trend.

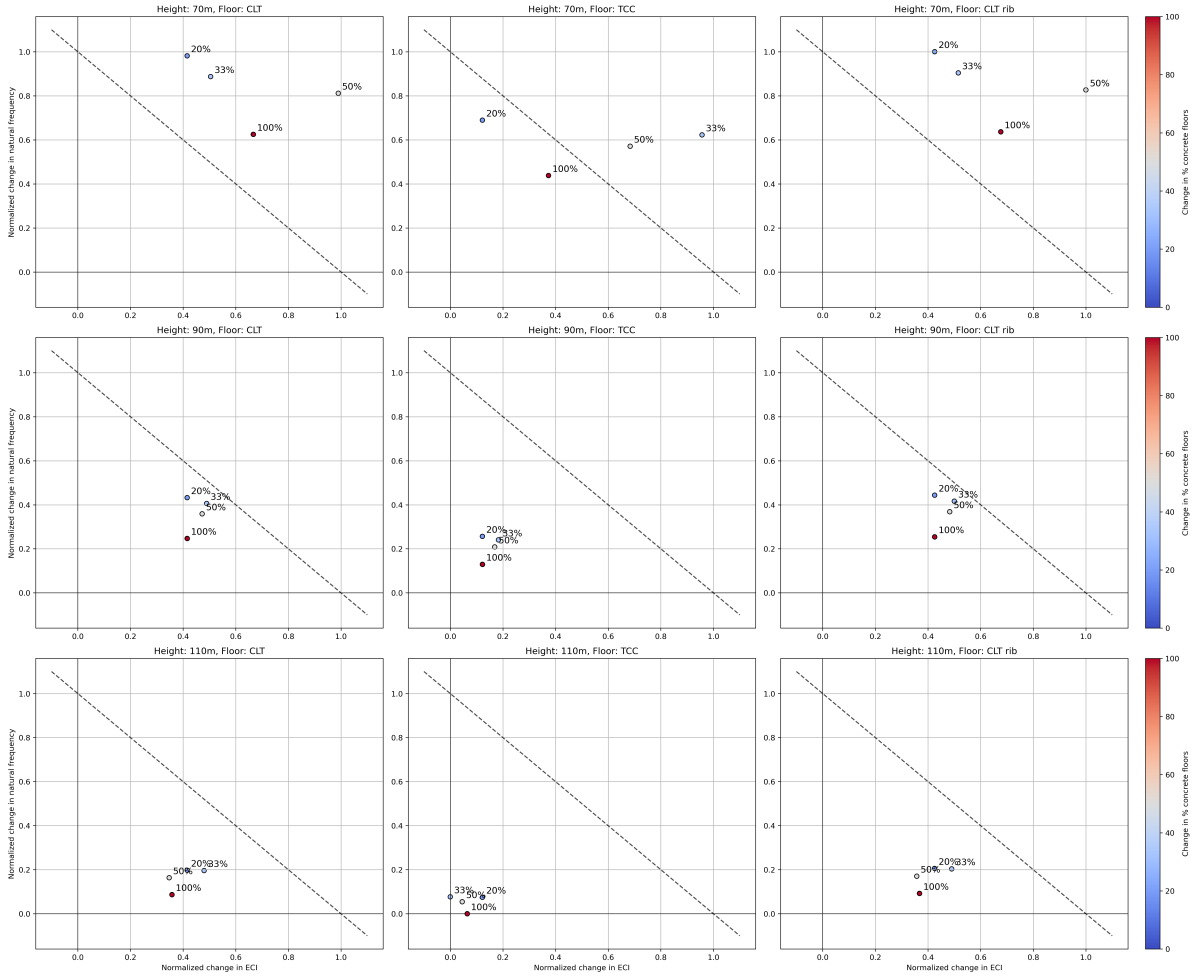

Figure 9.3: Normalized rate of change of natural frequency and ECI value with increasing percentage of concrete floors

9.1.2 Relation between dynamic performance and construction cost

This subsection examines the relationship between construction cost and dynamic behavior. To clarify this relationship, the results of the building variants for the two dependent variables are plotted against each other and categorized by parameter.

Figure 9.4 plots the construction cost against the natural frequency for various building variants grouped by height. The analysis reveals that the correlation between natural frequency and cost is negligible, with an R^2-value of approximately 0.1 across all height groups. For building variants between 70 and 90 m, the cost ranges from 735 to 875 €/m² without any clear distinction in natural frequency. In contrast, the 110 m tall buildings exhibit a broader cost range between 850 and 1000 €/m². These observations indicate that construction costs do not linearly increase with building height.

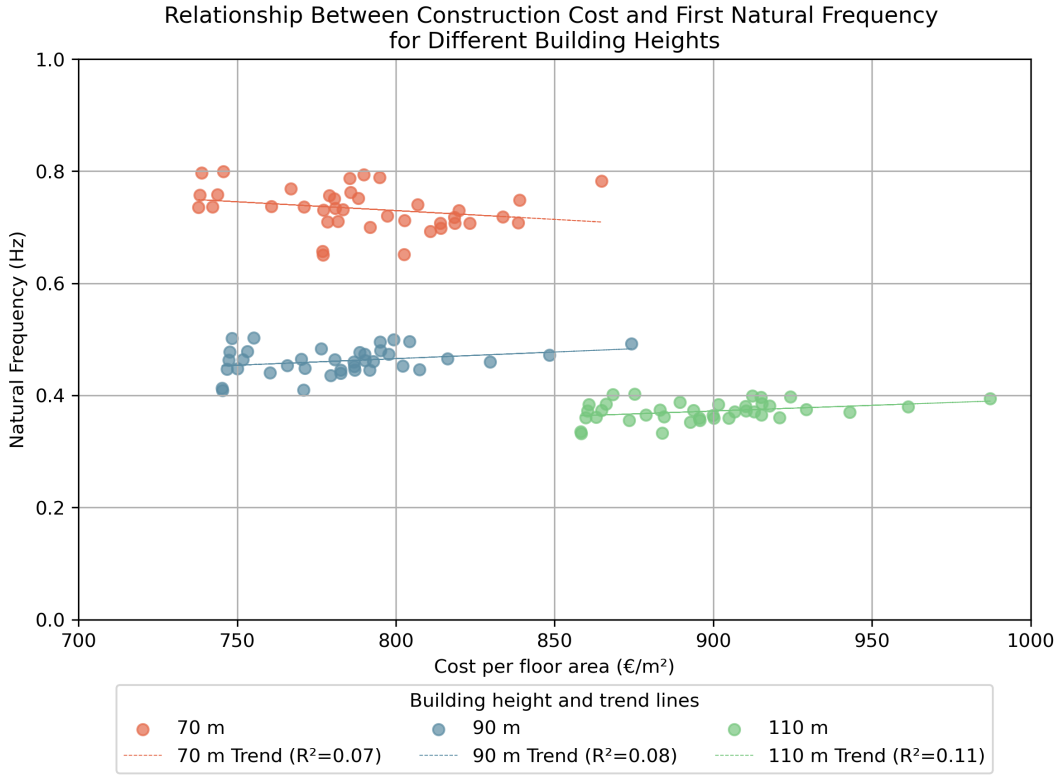

Figure 9.4: First natural frequency and construction cost correlation per building height

Figure 9.5 illustrates the relationship between construction cost and natural frequency for building variants, categorized by the percentage of concrete floors. For a fixed building height, an increasing percentage of concrete floors corresponds to a decrease in natural frequency, while the construction cost gradually converges toward that of a fully concrete building. In conclusion, the material composition—specifically, the share of concrete floors—significantly influences both the dynamic behavior and the cost profile of the building.

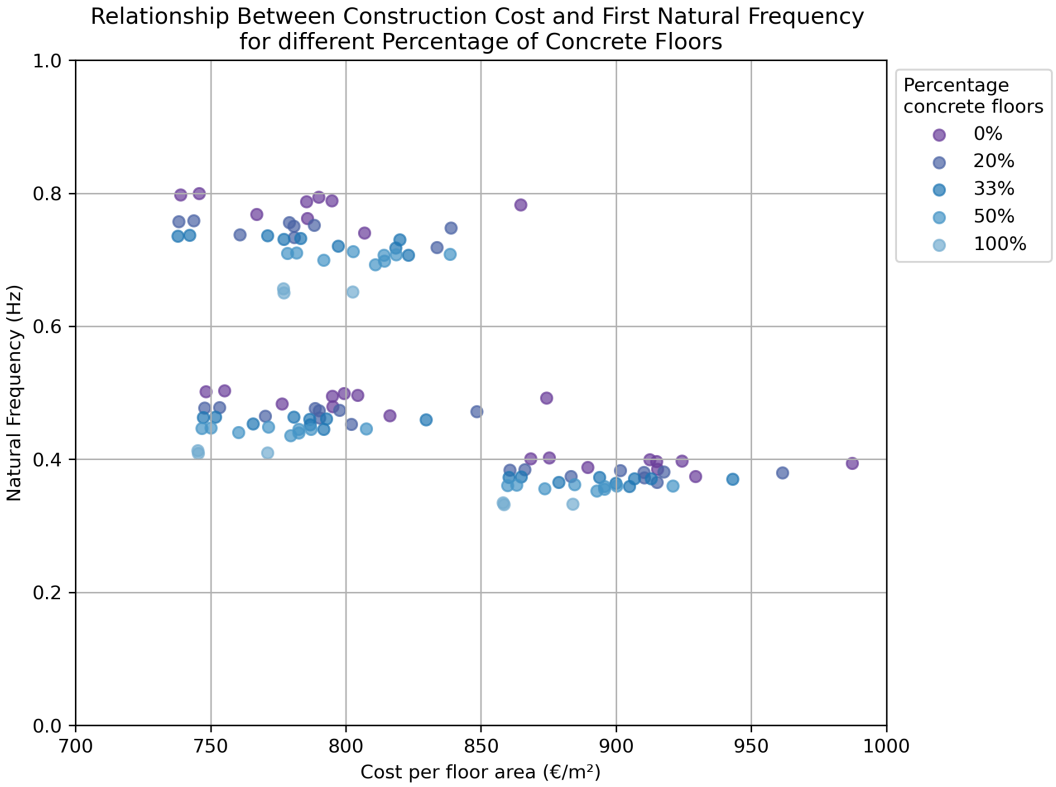

Figure 9.5: First natural frequency and construction cost correlation per percentage concrete floors

9.1.3 Relation between environmental performance and construction cost

This subsection explores the relationship between environmental performance and construction cost. To achieve this, the results of the building variants for the two dependent variables are plotted against each other. To enhance clarity, the data are divided per parameter.

Figure 9.6 displays the ECI value plotted against the construction cost, with building variants grouped by height. Although the graph includes a trend line, no clear correlation between ECI and cost is found based on the height of the building. Variants with heights of 70 m and 90 m fall within a similar range, while the 110 m building data is located in the top right corner, indicating that both cost and ECI are higher for these variants.

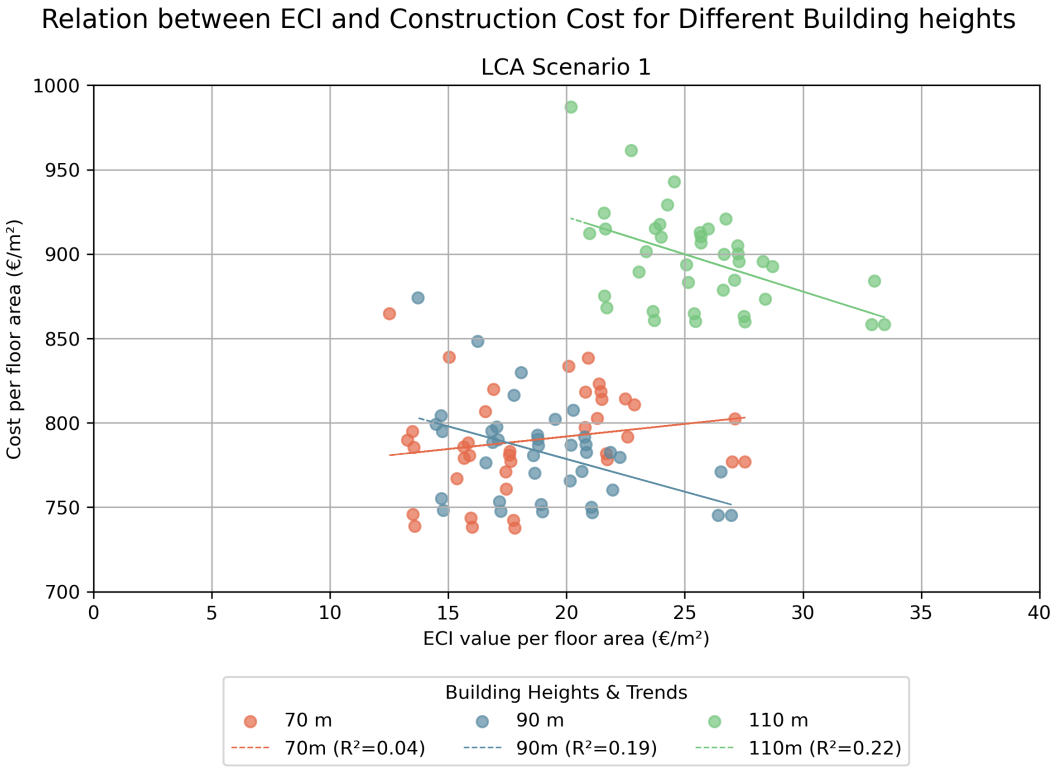

Figure 9.6: ECI and construction cost correlation per building height

Figure 9.7 presents the ECI value plotted against the construction cost, with building variants grouped by the percentage of concrete floors. The graph indicates that as the percentage of concrete floors increases, the ECI value converges towards a higher level, while the construction cost generally decreases for floor plans 1 and 3.

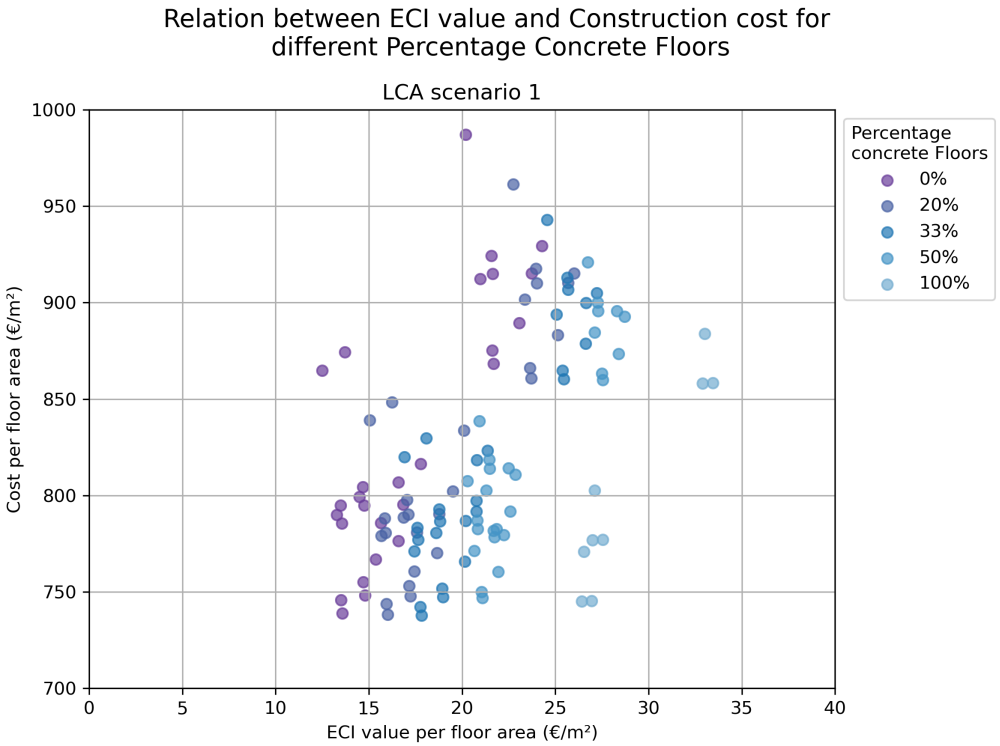

Figure 9.7: ECI and construction cost correlation per percentage concrete floors

Figure 9.8 presents the total life-cycle cost of the structural system and foundation, incorporating both construction cost and shadow cost. The figure indicates that, despite the lower shadow cost, the total life-cycle cost of building variants with timber floor types is higher than that of variants with concrete floors. Additionally, the graph shows that shadow cost represents only a minor portion of the total life-cycle cost. The highest total life-cycle cost is observed in buildings with CLT rib panel floors, followed by TCC floor panels and CLT floor panels.

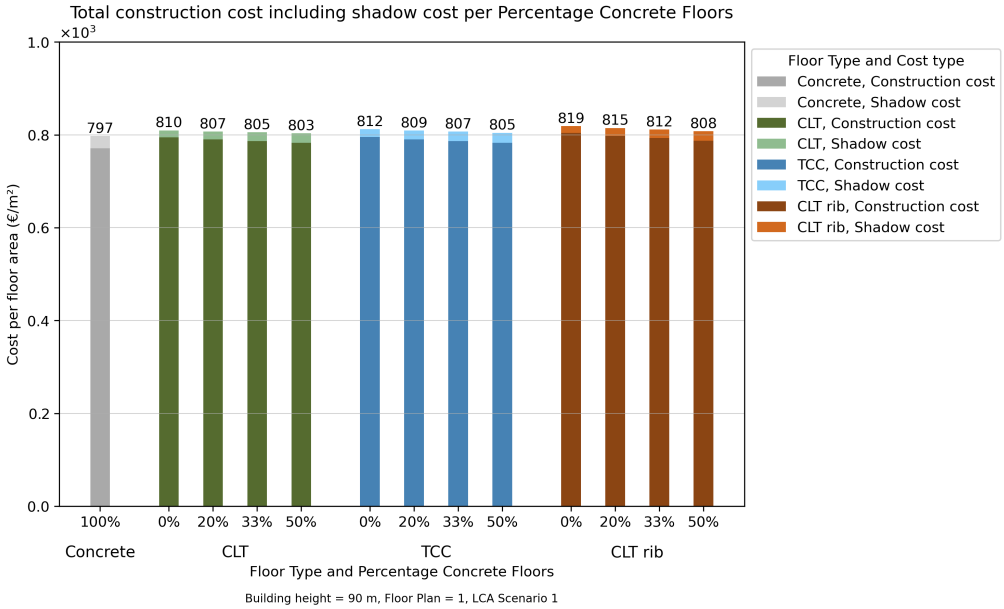

Figure 9.8: Total construction cost including shadow cost

9.2. Discussion

The discussion is divided into six parts. The first three sections analyze the relationships between ECI and natural frequency, construction cost and natural frequency, and ECI and construction cost. This is followed by a discussion of the outliers and the methodology that led to these results. Finally, it is discussed whether the implications of the findings, together with the earlier stated preliminary results, can support the hypotheses.

9.2.1 Relation between environmental and dynamic performance

First, it is crucial to draw conclusions from the results that support our hypotheses. Additionally, it is important to determine whether any correlations can be established between the design aspects or if other insights can be derived from the data.

In general, when plotting all data from the different building variants against each other for ECI and natural frequency which is shown in Figure 9.1 can be concluded that no overall correlation is apparent. This means that the ECI value cannot be accurately estimated based on the natural frequency, and vice versa. In the figure is also visible that the ECI value of 70 en 90 m buildings is in the same range and three distinct clusters of points can be identified.

A linear relationship is observed between natural frequency and the ECI value when considering a specific building height. This relationship is demonstrated by three separate trend lines, each corresponding to a different building height. The explanation for this is that taller buildings generally have lower natural frequencies, as the increasing height has a greater effect than the increase in stiffness or mass.

The influence of floor types and floor plans on the relationship between ECI and natural frequency is minimal, as shown by Figures J.1 and J.2 in Appendix J. Buildings with different timber floor types exhibit similar mass and, therefore, similar natural frequencies and ECI values. Since the mass of the floors is comparable and the materials are the same, there is no significant difference in the design of vertical elements, such as the core dimensions. Even for TCC floors, which use substantially more concrete, the ECI value deviates only slightly from the buildings with fully timber floor types.

Regarding floor plans, the variation in the layout does not have a significant effect on natural frequency or ECI because the overall structure remains largely the same. Variations in floor plan are smaller in magnitude than those caused by changes in the floor type, and as a result, they have minimal influence on the key parameters being analysed. While there may be an optimal floor plan, its impact on the natural frequency and ECI is much smaller compared to the influence of a chosen floor type.

In Figure 9.2, The results of the total concrete building appear to be quite far from the other results, but this is partly due to the choice of the percentage range for concrete floors, which goes from 0%, 20%, 33%, and 50%, and then jumps to 100%. These results show that as the percentage of concrete floors increases, both the ECI and natural frequency increase. The correlation across building heights can be explained by the fact that these two variables depend on the same parameter: the mass of concrete floors.

The explanation behind this is that the natural frequency depends on both stiffness and mass. As the percentage of concrete floors increases, the mass of the building increases while the stiffness remains the same, which results in a lower natural frequency. On the other hand, ECI depends on both the type and amount of material used. Buildings with a higher percentage of concrete floors have more concrete mass, leading to a higher ECI, as concrete has a greater impact on ECI compared to timber elements.

To further explore the effect of the percentage of concrete floors, the rate of change of the dependent variables, as shown in Figure 9.3, is analyzed per percentage of concrete. For the 70 m building height, the rate of change of natural frequency decreases with increasing building height. This is because, as the building height increases, the natural frequency becomes less dependent on the mass. Consequently, the difference in the rate of change between different percentages of concrete floors decreases with increasing building height.

For the 70 m building, the rate of change for ECI shows a wide range across different percentages of

concrete compared to data from the other building heights. For the 90 m and 110 m buildings, the rate of change for all percentages of concrete shifts towards the value associated with 20% concrete floors. The reason for the tightening of the range is discussed in Section 9.2.4.

9.2.2 Relation between dynamic performance and construction cost

To draw conclusions from the data and identify relationships between these two design aspects, the results are first discussed.

In graph 9.4, when considering all data points, no correlation is observed between natural frequency and construction cost. Therefore, natural frequency is not a reliable indicator of building cost, and vice versa. However, the graph reveals three distinct clusters of data points, corresponding to different building heights.

From the data can be observed that the statement that construction costs increase with building height is not necessarily correct [49]. The results indicate that building costs do not increase linearly with height. This is evident from the fact that the cost range for 70 and 90 m buildings is similar. The reasons for why the cost range for these two building heights remains the same are discussed in Section 9.2.4.

When considering a specific building height, no correlation is found between natural frequency and ECI. This raises the question: why is there a correlation between natural frequency and ECI, but not between natural frequency and construction cost? The explanation lies in the large variation in both natural frequency and construction cost due to differences in the percentage of concrete floors, as observed in the correlation between natural frequency and ECI. However, for construction cost, the variation is influenced not only by the percentage of concrete floors but also by other factors. One key reason is that the cost difference between concrete and timber is much smaller than the difference in ECI values between concrete and timber.

Based on Figures J.3 and J.4 in Appendix J, no correlation is found between natural frequency and construction cost for different floor types or floor plans. For floor types, a possible explanation is that there is not much difference in mass between the various floor types. Regarding floor plans, the reason is that a floor plan variation represents a change within the same floor type and therefore has an influence of one order of magnitude lower. Since floor type already shows no correlation, the impact of floor plan variations is even less significant.

Based on Figure 9.5, no correlation is found between natural frequency and construction cost for different percentages of concrete floors. However, when considering only a single building height, the cost moves closer to that of a fully concrete building as the percentage of concrete floors increases. At the same time, the natural frequency decreases.

The explanation for this is that as the percentage of concrete floors increases, the mass of the building increases, leading to a decrease in natural frequency. The same applies to construction cost. As the percentage of concrete floors increases, the building becomes more similar to a fully concrete building, resulting in construction costs that align more closely with those of a concrete structure.

9.2.3 Relation between environmental performance and construction cost

To draw conclusions from the data and identify relationships between these two design aspects, as well as to evaluate whether the hypothesis can be answered, the results are first discussed.

From Figure 9.6, it can be concluded that there is no correlation between ECI and construction cost, nor when considering different building heights. This may be due to the fact that both variables depend on many other factors that have a relatively strong influence. The building variants for 70 m and 90 m fall within the same range in the graph for both ECI and construction cost. The graphs show that for heights between 70 and 90 m, the data points overlap.

Similarly, when analyzing Figure J.5 and Figure J.6 in Appendix J, no correlation between ECI and construction cost is observed when the data are divided by floor type and floor plan.

From Figure 9.7, it can be concluded that there is no correlation between ECI and construction cost

for different percentages of concrete floors. However, when considering only a single building height, a band of data points appears for each percentage of concrete floors. As the percentage of concrete increases, the data converge towards the values of a fully concrete building. The explanation for this is that both the ECI and the construction cost converge towards the values of a concrete building as the mass and material composition of the variants become more similar to that of a fully concrete structure. The degree of convergence depends on the floor type and floor plan.

9.2.4 Explanation of deviations in results

The observations alone do not immediately lead to conclusions; first, the reliability of the results must be verified. To do this, the causes of deviations in the graphs are analyzed. The main deviations considered are the similar ECI and cost values for the 70 m and 90 m buildings and the rate of change of these variables, as these discrepancies are clearly visible in the graphs. Since the deviations in ECI and construction cost share the same underlying causes, they are examined together and categorized by building height.

The ECI and cost values for the 70 m and 90 m variants are in the same range due to two main factors: the contribution of foundation piles and the mass distribution of the structural system. First, as shown in Figure 5.9, the foundation piles have a relatively smaller impact on the ECI and the construction cost for the 90 m variant compared to the 70 m variant. The number of piles does not increase linearly with height but instead depends on the governing load case. For the 70 m variant, the number of piles is determined by a combination of vertical and wind loads, whereas for the 90 m variant, the governing factor is deformation due to wind.

Second, the mass per floor area of the structural system is slightly smaller for the 90 m building than for the 70 m building across all floor types. The increase in concrete mass per floor area is not driven by the floors, as these are proportional to the floor area. Instead, it is primarily influenced by the core thickness, which remains the same for both variants due to an assumed minimum core wall thickness. Additionally, in the model, the dimensions of the concrete core and columns do not increase further down the building, which affects the distribution of mass.

For the 110 m building variant, the core thickness increases, leading to a higher ECI and cost per floor area. Additionally, the number of foundation piles increases relatively more compared to the other building heights, further contributing to the rise in both values. In conclusion, the model does not fully capture the correct mass distribution for ECI and cost, leading to a misrepresentation of these values. This aligns with earlier findings discussed in the thesis.

In Figure 9.3, the rate of change of ECI shows a wide range for the 70 m building height. A sudden increase is observed at 50% and 100% concrete floors for all buildings with timber floors, as well as at 33% concrete floors for buildings with TCC floors. This marks a transition point where the additional mass from the increased percentage of concrete floors requires additional foundation piles. When no additional piles are required, the rate of change in cost remains constant, as seen in the 90 m variant.

The rate of change of ECI and construction cost shows a shift of data points for 50% and 100% concrete floors towards the left for the 110 m building height. This indicates a less positive rate of change for ECI. A similar trend is observed for TCC floors at 33% concrete. The reason for this shift is that these building variants use a smaller diameter for reinforcement steel, leading to a reduction in reinforcement volume and an increase in concrete volume in the core. A similar volume of reinforcement has a higher contribution to the total ECI value than concrete.

9.2.5 Method

The method defines building variants based on selected parameters and evaluates them against key design aspects to identify correlations. While effective, results are highly sensitive to variable choices and design assumptions, leading to discrete jumps. However, these jumps can be traced back to specific assumptions, unlike in self-learning models. The model is precise enough to capture global trends, the main objective of this research.

Parameters

The relationship between building height and design aspects is visually clear in the results. While additional intermediate heights could offer more insights, the chosen range is appropriate for this building

type.

The floor type has the most significant influence. CLT and CLT rib floors show no notable differences, as both require similar timber volumes when dimensioned. TCC floors introduce slight variations due to the added concrete mass. While other timber systems exist, the selected options effectively capture key differences relevant to high-rise applications. Comparing these timber floors with concrete floors provides a clear perspective on both extreme and intermediate cases. Variations in floor finish layers, which could impact ECI and construction cost, are not considered in this study.

A key focus of this thesis is the use of alternating floor systems. While incorporating more intermediate concrete floor percentages could refine trends and better define transition points, the current selection offers clear insights. However, practical feasibility remains a challenge. Discussions with structural engineers highlight why such systems are rarely implemented in practice.

The floor plan has a relatively minor impact compared to other parameters, as mass differences between variants are small. While factors such as floor dimensions, beam sizes, and column counts interact, the floor plan primarily influences spatial efficiency rather than structural performance.

Models

The design of the building variants begins with selecting the structural system, with the chosen building type imposing specific limitations, making the results particular to this configuration. Different structural designs may have varying proportions of vertical and horizontal elements, affecting the stiffness distribution. Therefore, the findings may not be directly applicable to buildings with significantly different structural layouts, but they provide estimates for buildings within this height range.

Several design aspects of the variants are discussed. Firstly, the reinforcement of the concrete core increases stepwise with height, with the minimum reinforcement at the base determined by structural requirements. Secondly, the dimensions of the columns and the concrete core do not increase further down the building. This explains why the mass per floor area does not increase with height, a characteristic common in such models and observable in reality. A key strength of the model is its inclusion of the foundation, which significantly impacts the results, as seen in the observed outliers. The model's sensitivity to foundation requirements leads to sudden jumps in results when additional piles are added, contributing to these outliers. Despite these limitations, general trends are still apparent.

The model used to analyze the dynamic behavior provides accurate results for the first natural frequency, effectively demonstrating the influence of various parameters. It offers a general understanding of the dynamics of the building and fulfills its intended purpose. A key question is whether the first natural frequency is truly representative of the dynamic behavior of these buildings. It is commonly used for this purpose, as seen in the Eurocode, where it helps determine building acceleration. Another consideration is how closely the calculated first natural frequency matches the actual frequency. The theory suggests that the modeled frequency can deviate by ±50% from reality, and improving this estimate is challenging due to the limited data in the preliminary design phase. Given these constraints, the first natural frequency calculated using the Rayleigh method is considered sufficient to represent its relationship with other design aspects.

The ECI value is used in the tendering process to assess the environmental performance of a building and is considered a representative parameter for evaluation. The calculated ECI covers only the structural system and foundation, representing a portion of the total ECI of the building. Using existing EPDs has proven to be effective in identifying trends and correlations. Although the choice of EPDs significantly impacts the absolute ECI value, it has little effect on overall trends and correlations, validating the method as a reliable approach to indicate relationships between design aspects and parameters. Including additional structural elements could alter the ECI value but may also introduce greater variability. For this study, the focus remained on the evaluation of the effects of specific parameters.

The results show that the material cost data significantly influences the analysis. In this study, the cost difference between timber and concrete buildings is relatively small. Additionally, the input for the cost model can skew the results, making a specific timber variant appear more favorable. Since construction costs in the preliminary design phase are approximate, they can vary by as much as ±15%. For these reasons, drawing definitive conclusions about construction costs based on this model is challenging.

9.2.6 Conclusions based on results

This section summarizes the conclusions based on the results and examines whether the hypotheses can be verified. First, the conclusions regarding the relationships between parameters and design aspects are presented, followed by the conclusions on the correlations between the design aspects.

The primary factor influencing design mass is building height, which determines the core wall thickness and the number of foundation piles. In terms of dynamics, the natural frequency decreases as the percentage of concrete floors increases. For environmental performance, material mass proves to be a reliable indicator of the environmental cost index (ECI) in hybrid buildings, as concrete has a substantially higher density and ECI contribution compared to timber. With regard to construction cost, the differences between concrete and timber buildings are relatively small and are highly dependent on material prices, making it difficult to conclude which option is the most cost-effective.

Examining the relationships between design aspects, a linear correlation is observed between ECI and natural frequency for a given building height, though no such correlation exists for floor type or floor plan. An increase in the percentage of concrete floors leads to a correlated increase in both ECI and natural frequency, as both variables are strongly influenced by concrete mass. However, with increasing height, the effect of mass on natural frequency diminishes, resulting in a decreasing rate of change. No correlation is found between natural frequency and construction cost for any parameter. While building height leads to an increase in cost, this result is not explicitly reflected in the model.

Overall, the building height has the most significant impact on design aspects, followed by the percentage of concrete floors, floor type, and floor plan. The model is particularly sensitive to specific load cases that increase the number of foundation piles, leading to significant jumps in data. The foundation contributes substantially to both ECI and construction cost, making them a critical factor in high-rise building design. Moreover, opting for a higher percentage of concrete floors can lead to an increased number of foundation piles, significantly raising both construction cost and ECI value.

To determine whether the hypotheses are supported by the results and conclusions, they are first explained in more detail. The hypotheses suggest a linear relationship between the dependent variables or an optimal percentage of concrete floors that balances the design aspects.

An inverse linear relationship is observed between dynamic behavior and environmental performance. However, no correlation is found between the other design aspects. Additionally, no optimal percentage of concrete floors is identified that minimizes both ECI and construction cost. Factors such as the number of foundation piles and the amount of reinforcement in the core play a critical role. Therefore, increasing the proportion of concrete floors may not always be advantageous, as it can lead to a significant rise in ECI and construction costs. This, however, remains highly case-dependent.

Part IV

Conclusions and Recommendations

10

Conclusions

The aim of this research is to establish correlations between building parameters and design aspects for tall concrete-timber buildings during the early design phase. This chapter presents the conclusions based on the research results. These results are used to either support or refute the hypotheses.

10.1. Hypotheses

The hypotheses formulated in the research framework are restated here to allow for reflection. They describe the three relationships between the key design aspects: dynamic behavior, environmental performance, and construction cost.

Environmental Performance – Dynamic Behaviour
There is an inverse linear relationship between the environmental cost index (ECI) and the first natural frequency as the percentage of concrete floors increases for a specific building height.

The hypothesis is supported by the results, which demonstrate an inverse linear relationship between the ECI and natural frequency. The R^2-values between the ECI and natural frequency range from 0.95 to 0.97 for different building heights. The cause of this linear relationship can be explained by the fact that these two variables depend on the same parameter: the mass of concrete floors. As the percentage of concrete floors increases, the mass of the building increases resulting in a lower natural frequency.

On the other hand, ECI is influenced by both the type and amount of material used, with buildings containing more concrete floors having a higher ECI, since concrete has a greater environmental impact than timber.

Dynamic Behaviour – Construction Cost
For a given building height, the relationship between the first natural frequency and the construction cost follows a linear trend with increasing percentage of concrete floors.

Based on the data, the hypothesis cannot be confirmed. While the natural frequency decreases as the percentage of concrete floors increases, the relationship between the first natural frequency and construction cost does not follow a linear trend. The construction cost shows significant variations and does not increase linearly with the percentage of concrete floors due to the strong influence of other parameters.

Environmental Performance – Construction Cost
A specific floor system with an optimal percentage of concrete floors achieves a balance between the ECI value and building cost.

Based on the data, the hypothesis is not correct. While the ECI value increases linearly with a rising percentage of concrete floors, the variation in construction cost is significant, and the impact of the percentage of concrete floors is just as large as that of other parameters. Considering these two factors together, no balance can be found between the ECI value and construction cost at a specific percentage of concrete floors for a given building height.

10.2. General conclusions

Besides reflecting on the hypotheses, several general conclusions can be drawn from this variant study.

- The building height has the most significant effect on the three dependent variables. The influence of the other parameters cannot be ranked further, as this depends on the specific design aspect.
- The effects of the three parameters—floor type, floor alternation, and floor plan—on construction cost are within the same range. This can be derived from the results, which show a scatter plot per building height with a low correlation.
- The acceleration due to wind in tall concrete-timber buildings, calculated using Rayleigh's model and the procedure provided in NEN-EN 1991-1-4, remains below the thresholds set by NEN-EN 1991-1-4 and ISO 10137 for both office and residential buildings.
- Including variations in foundation piles and concrete core dimensions is essential when comparing building variants for ECI and construction cost, as they significantly impact design aspects. The model incorporates assumptions and constraints, leading to discrete changes in pile count or core thickness due to increased mass (e.g., concrete floors). This aligns with real-world practice, where construction cost and ECI show discrete steps with increasing height or floor mass.
- The model is suitable for analysing the influence of a specific parameter on a design aspect by examining a subset of the data. It helps visualize and understand the relationships between parameters and a single design aspect.

11

Recommendations

Based on the results and conclusions of this thesis, several recommendations can be made. These are divided into practical advice for professionals in the construction industry and theoretical advice for further research in this field.

11.1. Practical advice

The following recommendations highlight key considerations for designing and analysing tall concrete-timber buildings.

- **Consider the impact of additional concrete floors on foundation design**
  Replacing timber floors with concrete floors in a building can result in the need for additional foundation piles, which can significantly increase both ECI and cost. While a limited number of concrete floors already provides substantial improvement in dynamic behavior, their effect on ECI remains limited. Therefore, a careful trade-off must be made when increasing the percentage of concrete floors.
- **Carefully plan the construction process for hybrid structures**
  The integration of concrete and timber floors within the same building requires a well-thought-out construction process. This thesis does not account for construction logistics, but these could have a major effect on construction cost. At the same time, efforts to simplify the construction process should not discourage the development of innovative construction techniques that optimize hybrid structures.
- **Ensure accurate EPDs for environmental impact comparison**
  For a reliable comparison of ECI values between concrete and timber building variants, it is essential to have accurate Environmental Product Declarations (EPDs) for both concrete and timber products. These should account for comparable end-of-life scenarios in the Netherlands to provide a realistic assessment of environmental performance.

11.2. Theoretical advice

During the research process, several assumptions had to be made due to data limitations or model constraints. These aspects offer opportunities for further research:

- **Investigate dynamic behavior through real-world measurements**
  Conducting acceleration measurements in newly built hybrid and timber buildings in the Netherlands would provide valuable insights into actual dynamic behavior and whether floor vibrations pose a real issue in design practice.
- **Develop a more precise building design model**
  When modeling material quantities for ECI or cost calculations, the building and foundation design should be less sensitive to assumptions. Further research could focus on:
  - More accurate foundation modeling to reduce sensitivity to load cases.

  - Including column and concrete core dimension increases over the building height.
  - Incorporating floor build-ups into the analysis for a more complete material quantity estimation.
  - Perform advanced modal analysis on concrete floor distribution.

- **Analyze the impact of vertical distribution of concrete floors on dynamic behavior**
  A dynamic multi-degree-of-freedom (MDOF) analysis on the vertical distribution of concrete floors could provide deeper insight into the effect of their position on dynamic behavior. This could help determine the optimal location of concrete floors in combination with their total percentage.
- **Refine ECI calculations with more detailed end-of-life scenarios**
  Further research should explore different combinations of end-of-life scenarios for timber and concrete buildings to establish a more accurate range for ECI values. This would improve the reliability of sustainability assessments for hybrid high-rise buildings.
- **Automated workflow for structural design and analysis**
  The research method utilizes Grasshopper to design the structural system of a building variant and export data for analysis using Python-based models. This approach ensures a clear and structured workflow with a short processing time.
- **Enhancing data visualization and interaction**
  An additional feature could be the development of a user interface to highlight data from the scatter plots and clearly display relationships between design aspects for specific parameters. Furthermore, incorporating visual representations would be beneficial for presenting results more effectively.

References

[1] Danan Gu, Kirill Andreev, and Matthew E. Dupre. “Major Trends in Population Growth Around the World”. In: *China CDC Weekly* 3.28 (2021), pp. 604–613. DOI: 10.46234/ccdcw2021.160.

[2] Doug Smith, Adam Scaife, and Ed Hawkins. “Predicted Chance That Global Warming Will Temporarily Exceed 1.5 °C”. In: *Geophysical Research Letters* 45 (Oct. 2018). DOI: 10.1029/2018GL079362.

[3] *Global Status Report for Buildings and Construction 2019*. https://www.iea.org/reports/global-status-report-for-buildings-and-construction-2019. Paris, 2019. URL: https://www.iea.org/reports/global-status-report-for-buildings-and-construction-2019.

[4] Ranjana Yadav and Jitendra Kumar. “Engineered Wood Products as a Sustainable Construction Material: A Review”. In: *Engineered wood products for construction*. IntechOpen, Sept. 2021. DOI: 10.5772/intechopen.99597.

[5] Abhijeet Mishra et al. “Land use change and carbon emissions of a transformation to timber cities”. In: *Nature Communications* 13.1 (2022), p. 4889. ISSN: 2041-1723. DOI: 10.1038/s41467-022-32244-w. URL: https://doi.org/10.1038/s41467-022-32244-w.

[6] *Canadian CLT Handbook*. https://web.fpinnovations.ca/wp-content/uploads/clt-handbook-complete-version-en-low.pdf. FPInnovations, 2019. URL: https://web.fpinnovations.ca/wp-content/uploads/clt-handbook-complete-version-en-low.pdf.

[7] Erik Nilsson et al. “Effects of building height on the sound transmission in cross-laminated timber buildings – Airborne sound insulation”. In: *Building and Environment* (2023). URL: https://api.semanticscholar.org/CorpusID:255671655.

[8] Gerhard Fink et al. “HOLISTIC DESIGN OF TALLER TIMBER BUILDINGS - COST ACTION HELEN (CA20139)”. In: *World Conference on Timber Engineering (WCTE 2023)*. WCTE. World Conference on Timber Engineering (WCTE 2023), 2023, pp. 1001–1008. DOI: 10.52202/069179-0137.

[9] Hüseyin Emre Ilgın. “Analysis of the Main Architectural and Structural Design Considerations in Tall Timber Buildings”. In: *Buildings* 14.1 (2024). ISSN: 2075-5309. DOI: 10.3390/buildings14010043. URL: https://www.mdpi.com/2075-5309/14/1/43.

[10] John A. Stark. “Parametric Study and Early-Stage Structural Design for Tall Timber Buildings”. MA thesis. Massachusetts Institute of Technology, 2023.

[11] Ebenezer Ussher, Angelo Aloisio, and Saaruja Rathy. “Effect of lateral resisting systems on the wind-induced serviceability response of tall timber buildings”. In: *Case Studies in Construction Materials* 19 (2023), e02540. ISSN: 2214-5095. DOI: 10.1016/j.cscm.2023.e02540. URL: https://www.sciencedirect.com/science/article/pii/S2214509523007209.

[12] Yuxin Pan et al. “Seismic performance of a proposed wood-concrete hybrid system for high-rise buildings”. In: *Engineering Structures* 238 (2021), p. 112194. ISSN: 0141-0296. DOI: https://doi.org/10.1016/j.engstruct.2021.112194. URL: https://www.sciencedirect.com/science/article/pii/S0141029621003448.

[13] Fabrizio Ascione et al. “Sustainable and Efficient Structural Systems for Tall Buildings: Exploring Timber and Steel–Timber Hybrids through a Case Study”. In: *Buildings* 14.2 (2024). ISSN: 2075-5309. DOI: 10.3390/buildings14020524. URL: https://www.mdpi.com/2075-5309/14/2/524.

[14] Pierre Landel. “Wind-induced vibrations in tall timber buildings - Design standards, experimental and numerical modal analyses”. PhD thesis. Linnéuniversitetet, June 2022.

[15] Daniel Safarik, Jake Elbrecht, and Will Miranda. “State of Tall Timber 2022”. In: *CTBUH Journal* (2022).

[16] Robert Foster, Michael Ramage, and Thomas Reynolds. “Rethinking CTBUH Height Criteria In the Context of Tall Timber”. In: *CTBUH Journal* (2017).

[17] Ivana Kuzmanovska et al. “Tall timber buildings: Emerging trends and typologies”. In: Aug. 2018.

[18] Erik A Poirier et al. *Design and construction of a 53-meter-tall timber building at the university of British Columbia*. TU Verlag Wien, 2016.

[19] Saule Tulebekova et al. “Modeling stiffness of connections and non-structural elements for dynamic response of taller glulam timber frame buildings”. In: *Engineering Structures* 261 (2022), p. 114209. ISSN: 0141-0296. DOI: 10.1016/j.engstruct.2022.114209. URL: https://www.sciencedirect.com/science/article/pii/S014102962200339X.

[20] H.R. Milner and A.C. Woodard. “Sustainability of engineered wood products”. In: *Sustainability of Construction Materials*. Elsevier, 2016, pp. 159–180. DOI: 10.1016/b978-0-08-100370-1.00008-1.

[21] *Germany: Wood products prices rising in April*. https://holz.ru/ru/germany-wood-products-prices-rising-in-april/. 2018.

[22] Hans Joachim Blass Carmen Sandhaas. *Timber engineering*. Karlsruher Institut für Technologie (KIT), 2017.

[23] *Designing Mass Timber Floor Assemblies for Acoustics*. https://www.woodworks.org/resources/designing-mass-timber-floor-assemblies-for-acoustics/. Woodworks Innovation Network, 2024. URL: https://www.woodworks.org/resources/designing-mass-timber-floor-assemblies-for-acoustics/.

[24] Anita Ogrin and Tomaž Hozjan. “Timber-Concrete Composite Structural Elements”. In: *Engineered Wood Products for Construction*. Ed. by Meng Gong. Rijeka: IntechOpen, 2021. Chap. 14. DOI: 10.5772/intechopen.99624. URL: https://doi.org/10.5772/intechopen.99624.

[25] A.J. Breunese. *Fire Safety Design CIE5131*. TU Delft. 2015.

[26] Dougal Drysdale. *An introduction to fire dynamics*. 3rd ed. Hoboken, N.J: Wiley, 2011. 11 pp. ISBN: 9781119976103.

[27] Rijksoverheid. *Bouwbesluit 2012 - Afdeling 2.2: Sterkte bij brand*. 2024. URL: https://rijksoverheid.bouwbesluit.com/Inhoud/docs/wet/bb2012/hfd2/afd2-2.

[28] Rijksoverheid. *Bouwbesluit 2012 - Artikel 4.17 (tijdsduur niet-bezwijken)*. 2024. URL: https://wetten.overheid.nl/BWBR0041297/2024-01-01#Hoofdstuk4_Afdeling4.2_Paragraaf4.2.8.

[29] Ruud van Herpen. “HANDREIKING BRANDVEILIGHEID HOGE GEBOUWEN”. In: *Stedebouw en Architectuur* 2 (Apr. 2015), pp. 23–25.

[30] Priyan Mendis et al. “Wind Loading on Tall Buildings”. In: *Electronic Journal of Structural Engineering* Volume 7 (Jan. 2007), pp. 41–54. DOI: 10.56748/ejse.641.

[31] Sigong Zhang, Jianhui Zhou, and Ying Hei Chui. “Deflection criteria for controlling timber floor vibrations: A 200-year evolution”. In: *Engineering Structures* 326 (2025), p. 119370. ISSN: 0141-0296. DOI: https://doi.org/10.1016/j.engstruct.2024.119370. URL: https://www.sciencedirect.com/science/article/pii/S0141029624019321.

[32] Y. Paauwe. “Obtaining Insight into the Influence of the Main Parametersin the Preliminary Structural Design on the Wind-Induced Dynamic Response Including Soil-Structure Interaction Effects of High-Rise Buildings in the Netherlands”. MA thesis. TU Delft, 2020.

[33] A. V. Metrikine. *Dynamics of Mechanical Systems and Slender Structures*. Tech. rep. TU Delft, 2005.

[34] J.M.J Spijkers, A.C.W.M. Vrouwenvelder, and E.C. Klaver. *Structural Dynamics, Part 1: Structural Vibrations. Lectures Notes CT4140*. Tech. rep. Faculty of Civil Engineering and Geosciences, 2005.

[35] R.L.J. van den Berg. “Investigation of damping in high-rise buildings”. MA thesis. Delft University of Technology, 2012.

[36] Junbo Jia. “Vibration of Multi-Degrees-of-Freedom Systems”. In: *Essentials of Applied Dynamic Analysis*. Berlin, Heidelberg: Springer Berlin Heidelberg, 2014, pp. 203–231. DOI: 10.1007/978-3-642-37003-8_13. URL: https://doi.org/10.1007/978-3-642-37003-8_13.

[37] J.D. Holmes. *Basic structural dynamics II: Wind loading and structural response - Lecture 11*. Louisiana State University. 2014. URL: https://www.svibs.com/technical-review/.

[38] Adnan Akay and Antonio Carcaterra. “Damping Mechanisms”. In: *Active and Passive Vibration Control of Structures*. Ed. by Peter Hagedorn and Gottfried Spelsberg-Korspeter. Vienna: Springer Vienna, 2014, pp. 259–299. DOI: 10.1007/978-3-7091-1821-4_6. URL: https://doi.org/10.1007/978-3-7091-1821-4_6.

[39] Yukio Tamura. “Amplitude dependency of damping in buildings and critical tip drift ratio”. In: *International Journal of High-Rise Buildings* 1 (Jan. 2012), pp. 1–13.

[40] Daryl W. Boggs and Jeff Dragovich. “The Nature of Wind Loads and Dynamic Response”. In: *SP-240: Performance-Based Design of Concrete Building for Wind Loads* (2006).

[41] Theodore Stathopoulos. “Introduction to Wind Engineering, Wind Structure, Wind-Building Interaction”. In: *Wind Effects on Buildings and Design of Wind-Sensitive Structures*. Ed. by Ted Stathopoulos and Charalambos C. Baniotopoulos. Vienna: Springer Vienna, 2007, pp. 1–30. DOI: 10.1007/978-3-211-73076-8_1. URL: https://doi.org/10.1007/978-3-211-73076-8_1.

[42] Nicholas Isyumov. “Alan G. Davenport’s mark on wind engineering”. In: *Journal of Wind Engineering and Industrial Aerodynamics* 104-106 (2012), pp. 12–24. ISSN: 0167-6105. DOI: 10.1016/j.jweia.2012.02.007. URL: https://www.sciencedirect.com/science/article/pii/S0167610512000311.

[43] G. Brundtland. *Report of the World Commission on Environment and Development: Our Common Future*. United Nations, Aug. 4, 1987.

[44] Henk M. Jonkers. *Reader Sustainability*. Tech. rep. TU Delft, 2018.

[45] Luc Hillege. *Milieukostenindicator (MKI) – Overzicht*. https://ecochain.com/nl/blog/milieukosten-indicator-mki/. Ecochain. URL: https://ecochain.com/nl/blog/milieukosten-indicator-mki/.

[46] Nederlands Normalisatie Instituut. *NEN-EN 15804 Duurzaamheid van bouwwerken - Milieuverklaringen van producten - Basisregels voor de productgroep bouwproducten*. Delft: Koninklijk Nederlands Normalisatie-instituut, 2019.

[47] European Committee for Standardization (CEN). *NEN 2699 Investerings- en exploitatiekosten van onroerende zaken - Begripsomschrijvingen en indeling*. CEN. 2017.

[48] C Gerritse. *Kosten en kwaliteit*. Delft University Press, 1999. ISBN: 9040719365.

[49] S. van Oss. “Onderzoek naar de invloed van de bouwhoogte opde investeringskosten van kantoorgebouwen in Nederland”. MA thesis. TU Delft, 2007.

[50] Peter Jong and Hans Wamelink. *HIGH RISE AND LAND COSTS; A THEORETICAL FRAMEWORK*. Jan. 2007.

[51] K. van Nieuwenhuisen. “Leidschenveen de lucht in”. MA thesis. TU Delft, 2005.

[52] Wytze Brandsma. *Bouwkostenmanagement*. AT Osborne, Feb. 1, 2024.

[53] Roy Smeets. “Bouwmethodiek voor high-rise woongebouwen”. MA thesis. TU Delft, 2009.

[54] Freek Schaap. *CME Construction Technology - formwork*. Dec. 5, 2024.

[55] Henk Oude Kempers. *Werkplan Schoonbeton*. Ed. by Cindy Vissering. Cement&Beton Centrum, Oct. 1, 2023.

[56] WoodWorks. *Construction Advantages Sell Hotel Developer on CLT. CLT builds faster and more safely with fewer workers*. 2016. URL: https://www.woodworks.org/wp-content/uploads/4-Story-CLT-Hotel-WoodWorks-Case-Study-Redstone-Arsenal-01-05-16.pdf.

[57] Augustus Raymond. *Cross-Laminated Timber - What is it and When Does it Make Sense?* Nov. 20, 2019. URL: https://www.cesolutionsinc.com/blog/2019/11/20-advantages-clt-concrete-steel-cpcd5?utm_source=chatgpt.com.

[58] Sheryl Staub-French et al. “Construction process innovation on Brock Commons Tallwood House”. English. In: *Construction Innovation* 22.1 (2022), pp. 1–22. ISSN: 14714175. DOI: 10.1108/CI-11-2019-0117.

[59] Mohamed Kasbar et al. “Construction productivity assessment on Brock Commons Tallwood House”. In: *Construction Innovation* 21.4 (Apr. 2021), pp. 951–968. ISSN: 1471-4175. DOI: 10.1108/ci-11-2019-0118.

[60] *CLT by Stora Enso Building physics*. Stora Enso Wood Products Building Solutions. June 2020.

[61] Sebastian Knoflach. *Das Holz-beton-verbundelement*. MMK Holz-Beton-Fertigteile GmbH. Kirchdorfer Platz 1, 2752 Wollersdorf, Austria, 2022.

[62] CLT by Stora Enso Building physics. *Soundproofing for CLT by Stora Enso*. Stora Enso Wood Products Building Solutions. 2020.

[63] William F. Stokey. “Chapter 7 Vibration of systems having distributed mass and elasticity”. In: *Harris’ Shock and Vibration Handbook*. 2001. Chap. 7. URL: https://api.semanticscholar.org/CorpusID:124423642.

[64] Theodore von Kármán. “Progress in the Statistical Theory of Turbulence”. In: *Proceedings of the National Academy of Sciences* 34.11 (Nov. 1, 1948), pp. 530–539. DOI: 10.1073/pnas.34.11.530. eprint: https://www.pnas.org/doi/pdf/10.1073/pnas.34.11.530. URL: https://www.pnas.org/doi/abs/10.1073/pnas.34.11.530.

[65] Nederlands Normalisatie Instituut. *NEN-EN 1991-1-4 Eurocode 1: Belastingen op constructies - Deel 1-4: Algemene belastingen - Windbelasting*. Delft: Stichting Koninklijk Nederlands Normalisatie Instituut, 2022.

[66] BR Ellis. “AN ASSESSSMENT OF THE ACCURACY OF PREDICTING THE FUNDAMENTAL NATURAL FREQUENCIES OF BUILDINGS AND THE IMPLICATIONS CONCERNING THE DYNAMIC ANALYSIS OF STRUCTURES.” In: *Proceedings of the Institution of Civil Engineers* 69.3 (1980), pp. 763–776.

[67] Kathrina Simonen. *Life Cycle Assessment of Buildings: A Practice Guide*. Life Cycle Lab, 2018.

[68] Centraal Bureau voor de Statistiek. *Nieuwbouwwoningen; inputprijsindex bouwkosten 2000=100, vanaf 1990*. 2025. URL: https://www.cbs.nl/nl-nl/cijfers/detail/80444ned#shortTableDescription (visited on 02/07/2025).

[69] David Picken and Benedict Ilozor. “The Relationship between Building Height and Construction Costs”. In: Mar. 2015, pp. 47–60. DOI: 10.1002/9781118944790.ch4. URL: https://doi.org/10.1002/9781118944790.ch4.

[70] Magne Bjertnæs and Kjell Arne Malo. “Wind-Induced Motion Of ’Treet’ - A 14-Storey Timber Residential Building in Norway”. In: *World Conference on Timber Engineering*. 2014.

[71] Angelique Pilon, Zahra Teshnizi, and Diana Lopez. “An overview of the construction of a tall wood building: Brock Commons Tallwood House”. In: *NZ Joernal of Forestry*. Vol. 63. 1. 2018. URL: https://api.semanticscholar.org/CorpusID:240158660.

[72] *Brock Commons Tallwood House: The advent of tall wood structures in Canada*. Tech. rep. University of British Colombia, 2018.

[73] Lin Hu and Samuel Cuerrier Auclair. *Advanced Wood-based Solutions for Mid-rise and High-rise Construction: In-Situ Testing of the Brock Commons 18- Storey Building for Vibration and Acoustic Performances*. Research rep. 2018.

[74] Alejandro Fernandez, Jordan Komp, and John Peronto. “Ascent - Challenges and Advances of Tall Mass Timber Construction”. In: *International Journal of High-Rise Buildings* 9.3 (2020), pp. 235–244.

[75] M. Mohammad. *Connections in CLT Assemblies*. https://wood-works.ca/wp-content/uploads/CLT-Connections.pdf. FPInnovations, Sept. 2011.

[76] Stefan Loebus, Philipp Dietsch, and Stefan Winter. “Two-way Spanning CLT-Concrete-Composite-Slabs”. In: Aug. 2017.

[77] David Barber et al. *Design Guide 37: Hybrid Steel Frames with Wood Floors*. AISC. 2022.

[78] *UV T TIMBER-TO-TIMBER DOVETAIL CONNECTOR*. https://www.rothoblaas.com/products/fastening/brackets-and-plates/concealed-connections/uv-t.

[79] Stora Enso. *Rib Panels*. https://www.storaenso.com/en/products/mass-timber-construction/building-products/rib-panels. Stora Enso. URL: https://www.storaenso.com/en/products/mass-timber-construction/building-products/rib-panels.

[80] Sadik Girgin, Ibrahim Misir, and Serap Kahraman. "Seismic Performance Factors for Precast Buildings with Hybrid Beam-Column Connections". In: *Procedia Engineering* 199 (Dec. 2017), pp. 3540–3545. DOI: 10.1016/j.proeng.2017.09.510.

[81] *ALUMEGA PINNED CONNECTION FOR POST AND BEAM*. https://www.rothoblaas.com/products/fastening/brackets-and-plates/concealed-connections/alumega.

[82] *Mass Timber*. https://www.woodworks.org/cad-revit/mass-timber/. Woodworks. URL: https://www.woodworks.org/cad-revit/mass-timber/.

[83] Bridget Fryer. "Wind Dynamics of the Next Generation of Tall Timber Buildings". PhD thesis. University of Cambridge, 2021. DOI: 10.17863/CAM.83500.

[84] Clara Youssef and Meriam Basilious. "Global Analysis of a Tall Timber- Concrete Hybrid Structure Subjected to Wind Load : A Parametric Study of Different Hybrid Solutions". MA thesis. KTH, Concrete Structures, 2022.

[85] Alex Sixie Cao and Haris Stamatopoulos. "A theoretical study of the dynamic response of planar timber frames with semi-rigid moment-resisting connections subjected to wind loads". In: *Engineering Structures* 240 (Aug. 1, 2021), p. 112367. ISSN: 0141-0296. DOI: 10.1016/j.engstruct.2021.112367. URL: https://www.sciencedirect.com/science/article/pii/S0141029621005174.

[86] Nederlands Normalisatie Instituut. *NEN-EN 14080 Houtconstructies - Gelijmd gelamineerd hout en gelijmd massief hout*. Delft: Nederlands Normalisatie-instituut, 2013.

[87] Nederlands Normalisatie Instituut. *NEN-EN 1991 Eurocode 1: Belastingen op constructies - Deel 1-2: Algemene belastingen - Belasting bij brand*. Delft: Koninklijk Nederlands Normalisatie-instituut, 2019.

[88] Nederlands Normalisatie Instituut. *NEN-EN 1990 Eurocode: Grondslagen van het constructief ontwerp*. Delft: Koninklijk Nederlands Normalisatie-instituut, 2019.

[89] C.R. Braam. *Constructieleer Gewapend Beton*. Aeneas, 2011.

[90] *Glued laminated timber*. HASSLACHER group. Austria.

[91] *De Cooltoren, een 150 meter hoog avontuur*. https://v8architects.nl/2365/. Rotterdam: V8 Architects. URL: https://v8architects.nl/2365/.

[92] P.H. Ham. *Structural calculations of High Rise Structures*. TU Delft, 2022.

[93] Cyril M. Harris, Charles E. Crede, and Horace M. Trent. "Shock and vibration handbook". In: 1976. URL: https://api.semanticscholar.org/CorpusID:110374775.

[94] Endrit Hoxha and Alexander Passer. "Biogenic carbon in buildings: a critical overview of LCA methods". In: *Buildings and Cities* (Aug. 2020). DOI: 10.5334/bc.46.

[95] C. E. Andersen et al. "Embodied GHG Emissions of Wooden Buildings—Challenges of Biogenic Carbon Accounting in Current LCA Methods". In: *Frontiers in Built Environment* 7 (2021). ISSN: 2297-3362. DOI: 10.3389/fbuil.2021.729096. URL: https://www.frontiersin.org/journals/built-environment/articles/10.3389/fbuil.2021.729096.

[96] O. Çopuroglu. *Lecture 08 Natural rocks and aggregates*. 2018. URL: https://brightspace.tudelft.nl/d2l/le/content/66337/viewContent/787800/View.

[97] O. Çopuroglu. *Lecture 10 Concrete*. 2018. URL: https://brightspace.tudelft.nl/d2l/le/content/66337/viewContent/794314/View.

[98] O. Çopuroglu. *Lecture 09 Portland Cement*. TU Delft, 2018. URL: https://brightspace.tudelft.nl/d2l/le/content/66337/viewContent/790844/View.

[99] *Structural hollow sections Environmental Product Declaration*. https://products.tatasteelnederland.com/sites/producttsn/files/Tata-Steel-Structural-Hollow-Sections-EPD-EN.pdf. 2022. URL: https://products.tatasteelnederland.com/sites/producttsn/files/Tata-Steel-Structural-Hollow-Sections-EPD-EN.pdf.

[100] Swerock AB. *Environmental Product Declaration – Ready mix concrete, Sweexp55 C30/37*. https://www.epd-norge.no/getfile.php/1344817-1695714904/EPDer/Byggevarer/Betongvarer/NEPD-5036-4376_Environmental-Product-Declaration-----Ready-mix-concrete--Sweexp55-C30-37.pdf. 2023. URL: %7Bhttps://www.epd-norge.no/getfile.php/1344817-1695714904/EPDer/Byggevarer/Betongvarer/NEPD-5036-4376_Environmental-Product-Declaration-----Ready-mix-concrete--Sweexp55-C30-37.pdf%7D.

[101] InformationsZentrum Beton GmbH. *EPD Beton der Druckfestigkeitsklasse C55/67*. https://www.beton.org/fileadmin/beton-org/media/Dokumente/PDF/Wissen/Beton-Bautechnik/Nachhaltigkeit/2023-10-20-EPD-C55-67.pdf. Oct. 20, 2023.

[102] BE Group Sverige AB. *Environmental Product Declaration - Reinforcing Steel Mesh*. https://api.environdec.com/api/v1/EPDLibrary/Files/89e98751-b41f-48bb-efdb-08d966bc9806/Data. 2021. URL: https://epd-online.com/EmbeddedEpdList/Detail?id=14448.

[103] Stora Enso. *Environmental Product Declaration CLT*. https://www.storaenso.com/-/media/documents/download-center/certificates/wood-products-approvals-and-certificates/epd/stora-enso-epd-clt---may-2024.pdf. 2023. URL: https://www.storaenso.com/-/media/documents/download-center/certificates/wood-products-approvals-and-certificates/epd/stora-enso-epd-clt---may-2024.pdf.

[104] *EPD Glulam construction wood products of spruce*. https://www.epddanmark.dk/media/demnkofe/md-22038-en.pdf. Lilleheden A/S, July 4, 2022.

A

Overview of constructed hybrid timber buildings

This appendix provides detailed information on constructed concrete-timber buildings, with a particular focus on their structural systems.

A.1. Constructed timber-concrete hybrid buildings

By analysing the architectural and structural design of three tall timber-concrete hybrid buildings built in recent years, important design parameters can be discovered and further insight can be gained into the design and construction of such structures. The first building is the Treet building which uses a post-beam system and the second and third building which are the Brock Commons and Ascent MKE both use a hybrid structure with a concrete core and CLT floors.

A.1.1 Treet

Treet is a 49m-high timber apartment building in Norway that was completed in 2015, shown in Figure A.1. The structural system consists of glulam trusses, additional concrete slabs and prefabricated modules which are visible in Figure A.2. The apartments are designed by stacking prefabricated modules on top of the concrete slabs at levels 5 and 10 and the concrete garage at the bottom of the building. The glulam trusses provide lateral stability and stiffness, while the concrete slabs transfer horizontal and vertical loads to the trusses and connect the trusses to each other to form a stability system. The additional CLT walls and core are not part of the lateral stability system. To increase the mass of the structure, concrete floors were added, thus improving the dynamic behavior of the building. To understand the dynamic behavior of the building, tests of the prefabricated modules were conducted and the results showed that the natural frequency of four stacked modules was much higher than the global response of the building. No additional connections were placed between the slabs and the modules, so the global natural frequency of the building would not change. To further decrease acceleration, an additional concrete slab was added on the roof to connect the trusses and increase the modal mass and natural frequency. A Finite Element Model (FEM) was generated using the test results to better understand the global response of the building [70].

Figure A.1: Exterior of Treet [70]

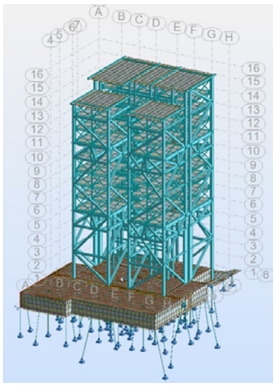

Figure A.2: Global FE model of Treet [70]

A.1.2 Brock Commons Tallwood House

Brock Commons Tallwood House is an 18-story hybrid apartment building in Canada, which combines concrete and timber elements. The structure consists of two concrete cores with glulam columns and CLT slabs with a concrete topping for improved sound insulation and global dynamic behavior, as seen in Figure A.3. Also, fire and water management are incorporated into the concrete topping. Plywood splines are nailed and screwed to connect the CLT floor panels to form a plate with diaphragm action, while steel drag straps are screwed to the CLT panels and bolted to the concrete core at each floor to transfer lateral load. Drag straps are 100mm wide steel plates welded to faceplates and anchored to core [71]. The two bottom floors are constructed with concrete. Dynamic analysis predicted a natural frequency of 0.5 Hz for the first mode, and the building was designed to limit the acceleration at the top floor to 15 milli-g [72]. A dynamic wind load analysis was performed according to the NBCC 2015, with analysis the sensitivity of the system to damping values between 1% and 3%. For a damping of 1.5%, the acceleration at the top floor met the design requirements. Accelerometers were placed in the building to monitor the acceleration and in-situ damping from ambient vibration testing when the building was almost complete. The results showed that the natural frequency of the first mode (translation short axis) was 1.0 Hz and 1.2 Hz for the torsional mode, with a modal damping ratio of 1.0% for both modes, which were lower than expected. The natural frequencies were in line with the estimations [71, 72, 73].

A.1.3 Ascent MKE

Ascent MKE, located in Milwaukee, Wisconsin, is the tallest timber building built as of 2022, with a height of 86.6 m, as shown in Figure A.4 The building is composed of a 7-story concrete parking garage and 18 stories of residential apartments made of glulam beams and columns and CLT slabs. A 50 mm gypsum-concrete topping is added for fire protection and acoustical separation. The tight column grid of the residential floor plan is incompatible with the large column spacing of the garage, so a transitions level was introduced with a concrete floor supported by post-tensioned transfer beams. Lateral stability is provided by two concrete cores that also serve as a means of egress. Dynamic analyses were likely conducted to ensure that accelerations are within limits, but no information is available on this topic [74].

Figure A.3: Structural system of Brock Commons Tallwood House [73]

Figure A.4: Structural system of Ascent MKE in Milwaukee. Courtesy: Thornton Tomasetti

A.2. hybrid timber high-rise buildings

In Table A.1 the hybrid timber high-rise buildings are shown with a height exceeding 49 m. The table includes the structural system including the vertical, lateral and flooring system.

Table A.1: Overview timber hybrid high-rise buildings

Building	Height (m)	Structural system		Flooring
		Vertical	Lateral	
Treet	49	GL columns, modules CLT/TF, RCGF	Bracing GL	TF, RC 5th & 10th floor & CLT slabs
Silva	50	GL columns + RC core	RC core	CLT slabs + Sc
Brock Commons	53	GL columns + RC cores, RCGF	2 RC cores	CLT slabs + Sc
Eunoia Junior College	56	RC columns + RC core & CLT walls	RC core	RC slabs with GL beams
Hypérion Wooden Tower	57	GL columns + RC core	RC core	CLT slabs & GL beams
Baufeld 1 Suurstoffi Abro	60	Steel columns + RC core	RC core	CLT slabs
36-52 Wellington Street	63	GL columns + RC core	RC core	CLT slabs
55 Southbank	70	RC & steel columns & CLT walls	RC & steel cores	CLT slabs & concrete slabs
De Karel Doorman	71	RC & steel columns + RC cores	2 RC cores	CLT slabs & steel beams
HAUT	73	GL columns + RC core, RCGF	RC core & shear walls CLT	TCC slabs & GL beams
Sara Kulturhus	73	GL columns + CLT cores	2 CLT cores & shear walls CLT	Prefab CLT modules & RC 19th & 20th floors
Hoho Vienna tower	84	GL columns + RC core & walls	RC core and shear walls	RC beams & TCC slabs
Mjøstårnet	85	GL columns	bracing GL	CLT slabs & RC slabs at top 7 floors
Ascent MKE	87	RC & GL columns + RC cores	2 RC cores	PT concrete slabs & CLT slabs & GL beams

RC: reinforced concrete, GL: glulam, CLT: Cross Laminated Timber, Sc: concrete screed, RCGF: reinforced concrete ground floor, TF: timber frame, PT: post-tensioned

B

Connections between structural elements

In this appendix the connections that are used to transfer the loads on the buildings are discussed. This appendix is divided into connections between floor panels, connections between the floor panels and beams, between beams and columns and between beams and the concrete core. All connections are hinged connections. The horizontal wind load is transferred from the facade to the floors. The floor transfer the lateral loads through diaphragm action in the panels and in the connections between the panels as described in Section 3.2. From the floor panels the loads are transferred to the beams and eventually to the core.

B.1. Connections between floor panels

B.1.1 Concrete floor type

The concrete floor is cast in situ as a monolithic slab with a reinforcement mesh, eliminating the need for special connections.

B.1.2 CLT panel floor type

In CLT panels and CLT rib panels, shear forces occur between the panels, which are absorbed by the joints connecting them. Various connection types can be employed to link adjacent CLT panels. One such type is the single surface spline joint, depicted in Figure B.1,a, which employs a jointing strip made of LVL and self-tapping screws to join two panels. Another type is the half-lapped joint, which utilizes screws or nails to connect two panels, as illustrated in Figure B.1,b.

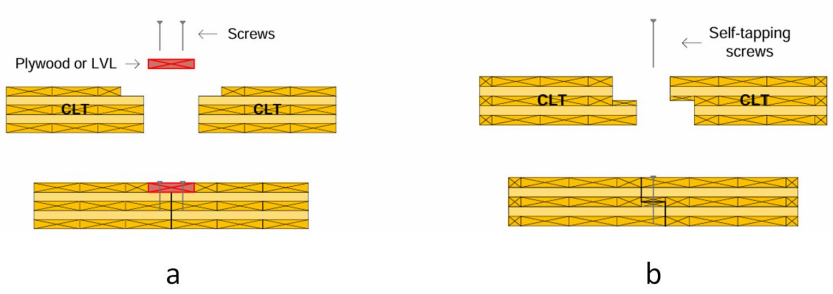

Figure B.1: Connection types between adjacent CLT panels [75]

B.1.3 TCC panel floor type

The CLT panels of Timber concrete composite panels can be connected the same way as normal CLT panels. Other options are using additional reinforced concrete or a steel profile within these connections as shown in Figures B.2 and B.3.

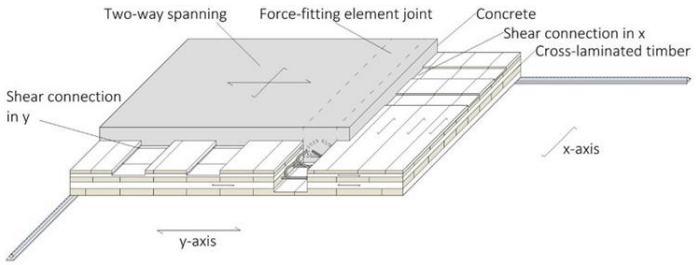

Figure B.2: TCC panel connection with steel reinforcement [76]

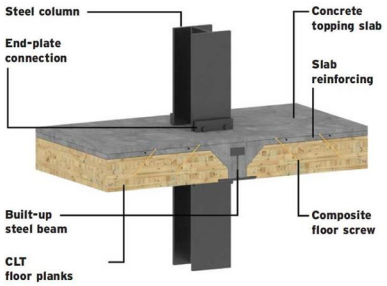

Figure B.3: TCC panel connection with steel profile [77]

B.2. Floor-beam connections

B.2.1 Concrete

When the concrete floor and beam are cast in-situ a monolithic connection can be made. The beam can be part of the lab as shown in Figure B.4.

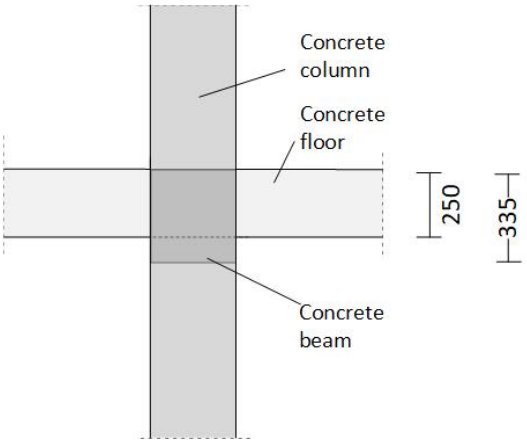

Figure B.4: Connection concrete floor and beam

B.2.2 CLT panel floor type

The connection between CLT panels and glulam beams can be achieved in two ways. One method involves placing the CLT panel on top of the beam, as shown in Figure B.5, where the panels are secured with self-tapping screws into the glulam beam. Alternatively, the CLT panel can rest on a bearing block attached to the beam or on a T-shaped beam. In this case, the CLT panel can be connected to the beam using self-tapping screws at a 45° angle or with a prefabricated connector, as illustrated in Figure B.6. This type of connection helps reduce the overall stack height.

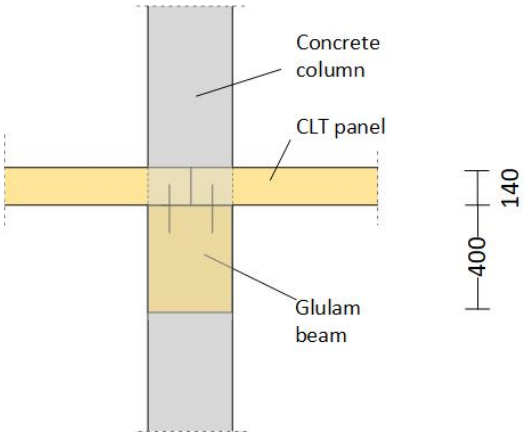

Figure B.5: Connection CLT panel floor and glulam beam

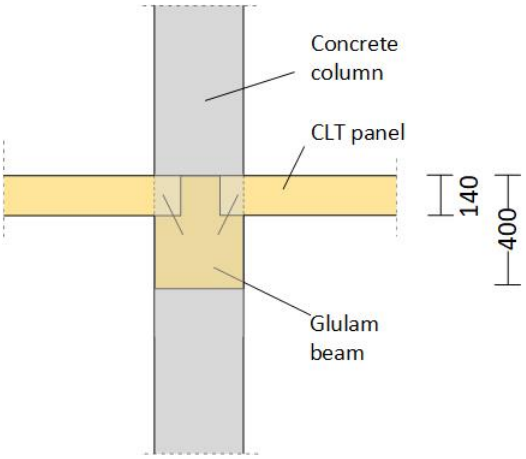

Figure B.6: Connection CLT panel floor and glulam beam on bearing block

B.2.3 TCC panel floor type

The CLT panels of TCC floor panels can be connected to the beams in the same way as the normal CLT panels. The concrete layer can be cast in-situ on top of the CLT panels.

B.2.4 CLT rib panel floor type

The ribs of the CLT rib panel can be connected to the side of the beam using steel connectors, as shown in Figure B.7. Another option is to connect them with steel screws, depicted in Figure B.8. Figure B.9 provides a view of the underside of a CLT rib panel floor, highlighting how the ribs are connected to the primary beam. Additionally, Figure B.10 presents a cross-section of a CLT rib panel floor with realistic dimensions for the structural elements.

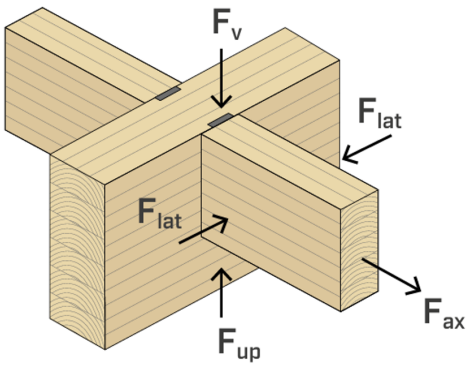

Figure B.7: Connection CLT ribs and glulam beam with steel connector [78]

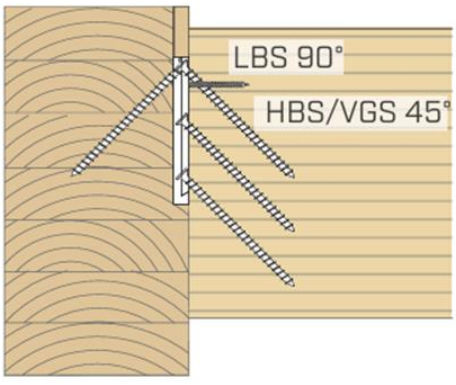

Figure B.8: Connection CLT ribs and glulam beam with screws [78]

Figure B.9: Underside of CLT rib panel and glulam beam [79]

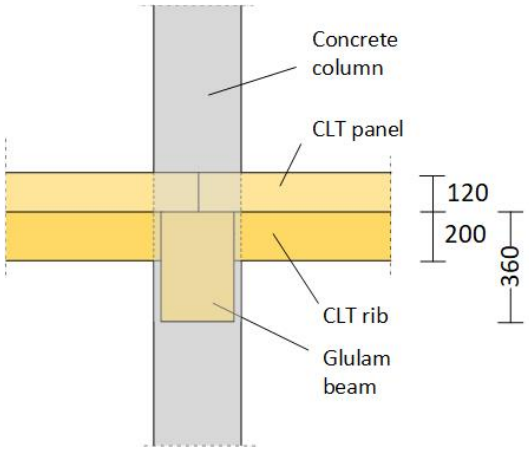

Figure B.10: Cross section of connection CLT rib panel floor and glulam beam

B.3. Beam-column connections

The beams are connected to the columns as the columns are assumed to be continuous. This is highlighted by the semi-transparant grey color in the figures.

Concrete beam – concrete column

Concrete beams can be connected to concrete columns using corbels as shown in Figure B.11. A solid in-situ connection is also feasible. Additionally, cantilevered beams can be incorporated in concrete structures.

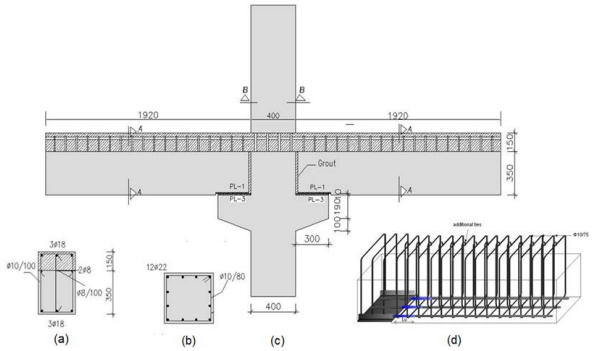

Figure B.11: Connection between concrete beam and column using a corbel [80]

Glulam beam – concrete column

Glulam beams can be connected to concrete columns with steel connectors as shown in Figure B.12.

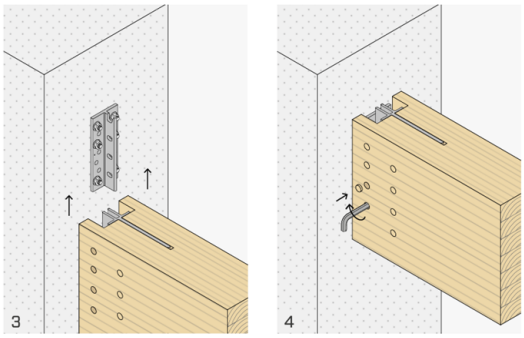

Figure B.12: Connection between glulam beam and concrete column using a hidden steel connector [81]

For large spans, where beams may become tall and wide, a double beam can be used as an alternative. To connect a double beam to a concrete column, steel plates can be used to attach the beams to the column as shown in Figures B.13 and B.14. It is essential to ensure that the column only transfers the floor loads to the beams, with no additional forces from the column acting on the beam. A double beam also allows for the possibility of a cantilever.

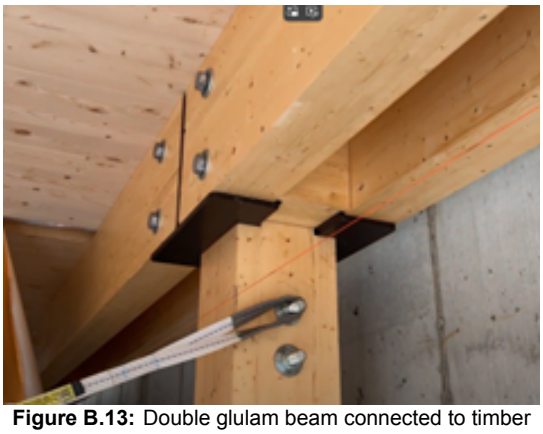

Figure B.13: Double glulam beam connected to timber column using steel corbel plates

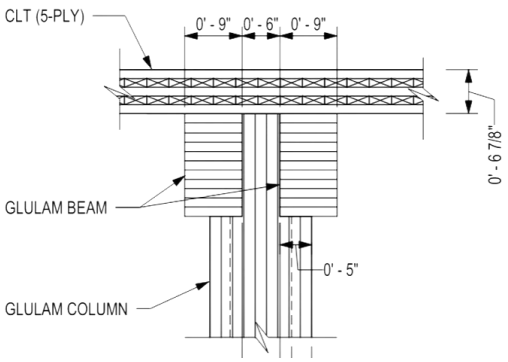

Figure B.14: Cross section of a double glulam beam connected to timber column

B.4. Beam-core connections

Glulam and concrete beams can be connected to concrete walls with corbels or recesses as shown in Figure B.15. Another connection type can be a steel head plate or steel shoe as shown in Figure B.16.

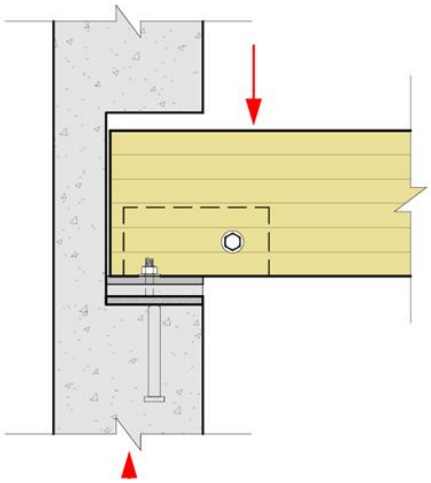

Figure B.15: Connection glulam beam in recess in concrete wall [82]

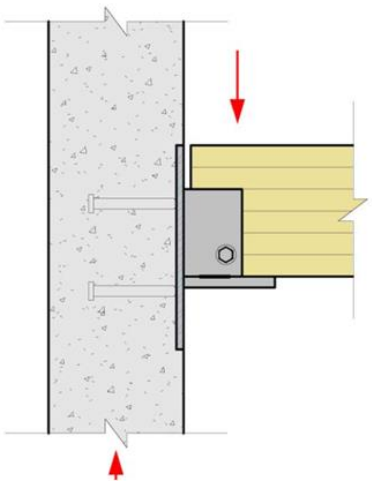

Figure B.16: Connection glulam beam to concrete wall with steel plate [82]

C

Influence of floor systems on dynamic behavior of tall buildings

In this appendix the current research regarding the building characteristics that influence the dynamic behavior of a tall building. The influence of reducing the floor loads by replacing concrete floors by CLT floor panels. Besides the influence of the distribution of CLT floor panels and concrete floors over the height of a building on the global dynamic behavior is discussed.

C.1. Mass

The effectiveness of reducing mass to control acceleration depends on the type of structural system in place. In a recent study, Fryer investigated the dynamic behavior of existing buildings where concrete floors were replaced with CLT floors [83]. The study examined four buildings with different structural systems: The Gherkin, The Shard, John Hancock, and 432 Park Avenue shown in Figure C.1. Results showed that, on average, the natural frequency of all buildings increased by 30% after the replacement, as shown in Figure C.2. The increase in natural frequency ranged from 8% to 86%. The variability in natural frequency is attributed to three factors:

- Mass of the original concrete floors compared to the CLT floors.
- Ratio of the floor mass to total building mass.
- Possible saving of structural material due to lower dead load.

Figure C.1: Studied buildings [83]

The study categorized the buildings based on their design approach, either strength-based or stiffness-based. The Gherkin and John Hancock were categorized as strength-based designs, while The Shard and 432 Park Avenue were categorized as stiffness-based designs. In the case of strength-based designs, the lighter timber floors result in a reduced dead load and hence, a reduced cross-section of the columns. The decrease in both modal stiffness and modal mass due to lighter floors counteract each other, leading to a smaller increase in natural frequency of 12% compared to stiffness-based

designs as shown in Figure C.3. The strength-based designs experience larger accelerations due to the material savings in the columns, resulting in an average increase in peak acceleration of 68%. In contrast, buildings with stiffness-based designs cannot save any material in the columns. Thus, the average increase in natural frequency of these buildings is 42%, and the average increase in peak acceleration is 33%.

Building	Floors	Height				Average
		304 - 436m	182 - 200m	~135m	~80m	(per building)
Gherkin	CLT + Screed		31%	30%	34%	32%
	CLT		68%	64%	67%	66%
Shard	CLT + Screed	13%	17%	22%	22%	18%
	CLT	19%	25%	31%	31%	27%
John Hancock	CLT + Screed	12%	27%	30%	34%	26%
	CLT	25%	62%	65%	80%	58%
432 Park Avenue	CLT + Screed	4%	15%	51%	54%	31%
	CLT	6%	23%	66%	70%	41%
Average	CLT + Screed	*10%*	*23%*	*33%*	*36%*	***26%***
(per height)	CLT	*17%*	*45%*	*56%*	*62%*	***47%***

Figure C.2: Natural frequency increase of buildings [83]

Building	Floors	Height				Average
		304 - 436m	182 - 200m	~135m	~80m	(per building)
Gherkin	CLT + Screed		9%	7%	9%	9%
	CLT		14%	14%	13%	14%
Shard	CLT + Screed	11%	17%	18%	25%	18%
	CLT	17%	24%	27%	36%	26%
John Hancock	CLT + Screed	13%	5%	4%	4%	6%
	CLT	28%	10%	10%	8%	14%
432 Park Avenue	CLT + Screed	20%	46%	56%	65%	47%
	CLT	26%	60%	74%	86%	62%
Average	CLT + Screed	*15%*	*19%*	*21%*	*26%*	***21%***
(per height)	CLT	*24%*	*27%*	*31%*	*36%*	***30%***

Figure C.3: Acceleration increase of buildings [83]

Buildings that use a concrete core for lateral stability experience a reduction in global stiffness due to a decrease in diaphragm action and the global stiffness of the floor plates when replacing concrete floors with CLT floors and glulam beams. The study concluded that accelerations increase due to a reduction in stiffness, a reduction in modal mass, more shear deflection, and a decrease in damping [83].

Youssef and Basilious conducted a study on modelling the Sara Kulturhus and replacing the concrete core and floors with CLT and cores, respectively [84]. During the early design stages, the design assumed concrete cores, which were later replaced by pretensioned CLT cores in the final design. The study analysed several combinations of the number and location of timber floors, as shown in Figure C.4, with Case C having seven alternative floor configurations and CLT cores. Table C.5 presents the resulting natural frequency, peak accelerations, utility u, and equivalent mass. The accelerations requirements of ISO10137 are adopted. Only the design with concrete cores and floors met the comfort criteria, while the design with a concrete core and timber floors was at the limit of the comfort criteria, as shown in Figure C.6. The graph provided in ISO10137 was used to evaluate the dynamic behavior of the designs.

Alternatives 4, 5, and 6, which have the same number of timber floors but at different positions, showed different accelerations and natural frequencies. Alternatives 1, 3, and 6, which respectively have an increasing number of concrete floors, showed similar dynamic behavior.

Alternatives A, 2, and 5, with an increasing number of concrete floors at the bottom of the building, exhibited the same dynamic behavior. Based on the quantitative results of this study, no definite conclusions can be drawn regarding the relationship between the number of concrete and timber floors. However, the study showed that positioning concrete floors at the top of the building has a positive influence on the dynamic response compared to buildings with only timber floors [84].

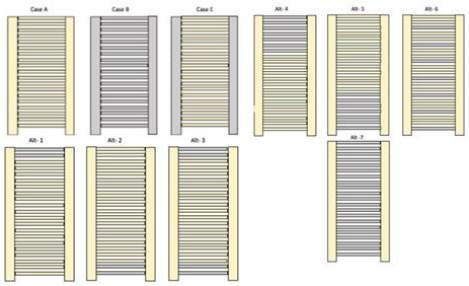

Figure C.4: Building configurations [84]

	Concrete floors	Core material	f_n [Hz]	a_{peak} [m/s^2]	u [-]	m_e [tonne/m]
Case A	0	Timber	0.822	0.153	3.51	44.63
Case B	21	Concrete	0.608	0.055	1.10	184.30
Case C-alt. 1	2	Timber	0.725	0.122	2.64	66.09
Case C-alt. 2	2	Timber	0.832	0.151	3.48	44.64
Case C-alt. 3	4	Timber	0.736	0.120	2.62	66.11
Case C-alt. 4	7	Timber	0.620	0.103	2.08	95.36
Case C-alt. 5	7	Timber	0.845	0.146	3.39	45.55
Case C-alt. 6	7	Timber	0.740	0.128	2.80	61.63
Case C-alt. 7	21	Timber	0.619	0.091	1.84	108.20
Case E	0	Concrete	0.707	0.072	1.54	120.70

Figure C.5: Dynamic properties of building configurations [84]

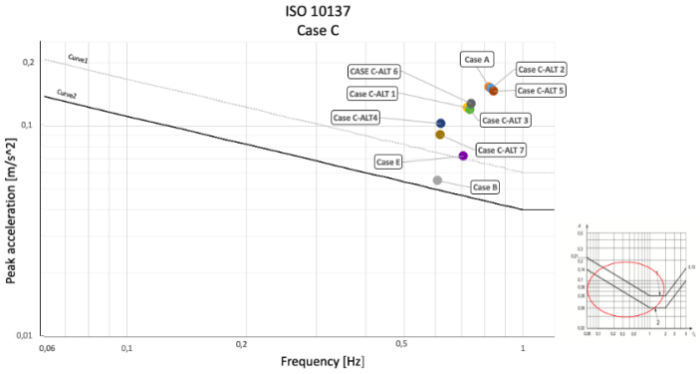

Figure C.6: Evaluation of accelerations of building configurations [84]

C.2. Mass distribution

The effect of mass distribution over the height of the building is researched by modelling a moment resisting timber frames with semi-rigid connections or mid-rise buildings. The building consists of continuous glulam columns and composite floors connected to columns with semi-rigid connections. Connection is screwed-in threaded rods. Accelerations reduced more by increase in stiffness than reduction mass. Interaction between mass and stiffness. The buildings are modelled as a system of continuous columns with beams connected by rotational springs. In Figure C.7 is accelerations are shown for different mass factor n_m and height of added mass n_h. n_m is defined as a factor of the lowest mass and n_h is defines as the floor at which the additional mass is added. For example n_h = 10/10 means mass is added at the top floor. The results shown that adding mass at the top has the largest contribution of acceleration reduction. In Figure C.8 is visible that adding mass at the top replaces the location of the maximal acceleration. Additional mass can be added at new mode shape maxima to further reduce accelerations [85].

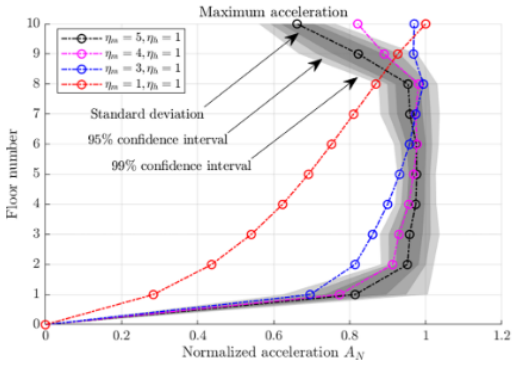

Figure C.7: Normalized accelerations with respect to floor number with additional mass for generalized wind load [85]

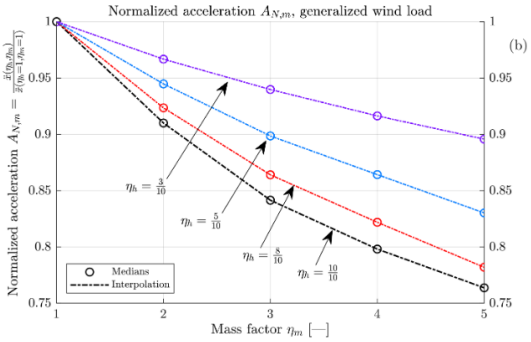

Figure C.8: Normalized acceleration with respect to the mass factor for a non-uniform mass distribution for the generalized wind load [85]

Pan et al. investigated the effects of alternating concrete and timber floors on the seismic performance of tall structures. The proposed system consists of two components: a concrete coupled core with concrete flat slabs placed every third floor as the main structure, and prefabricated wood modules serving as substructures as shown in Figure C.9. The findings indicate that by strategically alternating between concrete and timber floors, the building's natural frequency can be adjusted, which helps control the seismic acceleration experienced by each floor as shown in Figure C.10. Concrete floors provide stability and rigidity, while timber floors contribute to overall lightness, reducing inertia forces. This alternation improves the structure's dynamic behavior, potentially enhancing resilience under seismic loads [12].

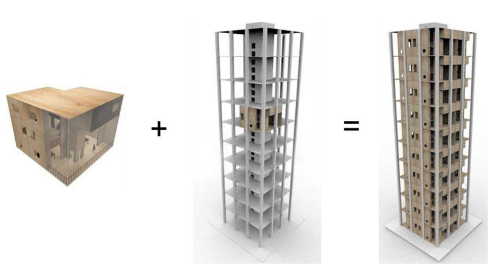

Figure C.9: Concrete coupled core with concrete flat slabs at every third floor as a main structure, and the prefabricated wood modules as substructures [12]

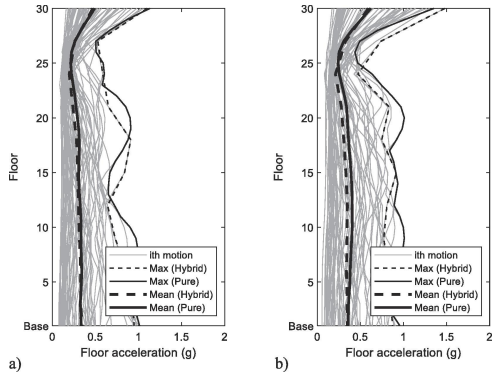

Figure C.10: Comparison of peak floor accelerations: (a) coupling direction, (b) cantilever direction [12]

D

Structural details of the case study building

This appendix provides additional structural information on the case study building, the Cooltoren. It includes details on the dimensions of structural elements, the materials used, and the foundation design.

D.1. Dimensions

The dimensions of the storeys are 26.6 by 26.6 m and the storey height is 2.95 m. Figure D.2 shows vertical cross sections of the concrete core showing the recesses in the core. The positions of these vertical cross sections are shown in Figure D.1 and the height of the recesses is 2.5 m.

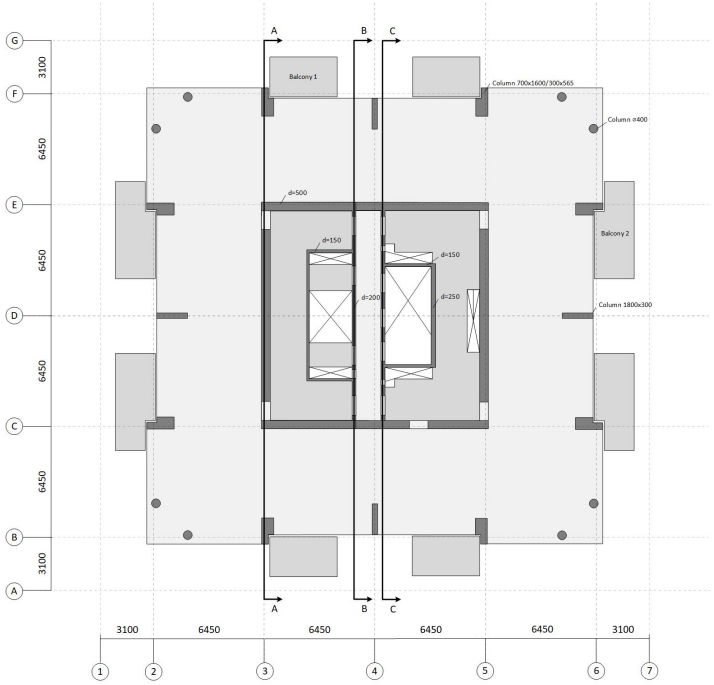

Figure D.1: Floor plan Cooltoren

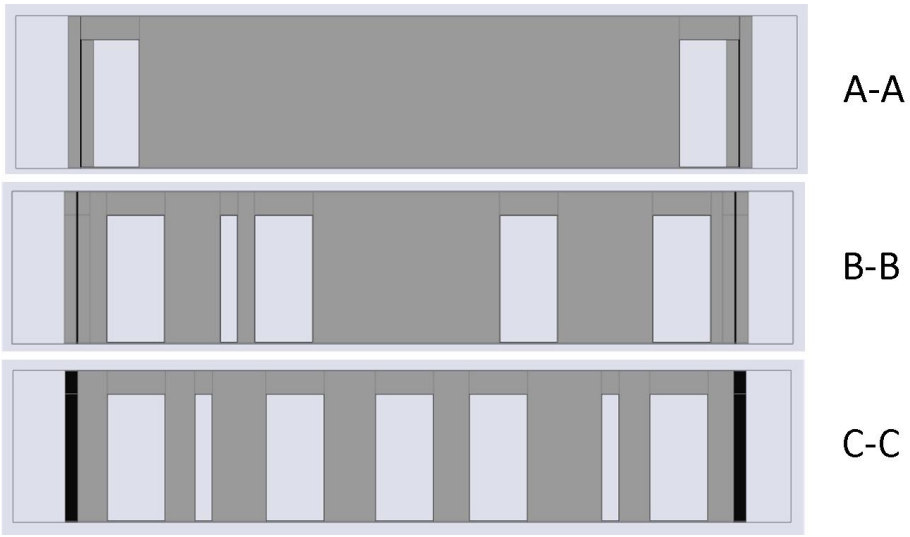

Figure D.2: Cross sections concrete core

The dimensions of the columns that are used in the original design become smaller in the top of the building. In Table D.1 the dimensions of three column types are given. The building has concrete floors with a thickness of 250 mm.

Table D.1: Column dimensions

Column type	Height (mm)	Width (mm)
Round	400	400
L-shape	1600/565	700/300
Rectangular	1800	300

D.2. Materials

The Cooltoren mainly uses concrete as its structural material. In Table D.2 the material properties of the structural elements are given.

Table D.2: Material properties

Structural element	Concrete class	E-modulus (N/mm^2)
Foundation floor	C45/55	10 000
Core walls	C55/67	15 000
Floors	C30/37	5 000
Columns	C70/85	15 000

D.3. Foundation

The foundation of the building consist of a foundation floor and foundation piles. The dimensions of the foundation floor are 32 m by 32 m and the distance between the foundation piles is 2.5 m. This results in a total of 169 piles. The foundation plan is shown in Figure D.3. The foundation piles are Tubex grout injection piles with dimensions ∅720 × 8.0 / 940 mm. Depth of the bottom of the foundation piles is -56.5 m NAP. The bottom of the foundation is situated at -1.45 m NAP.

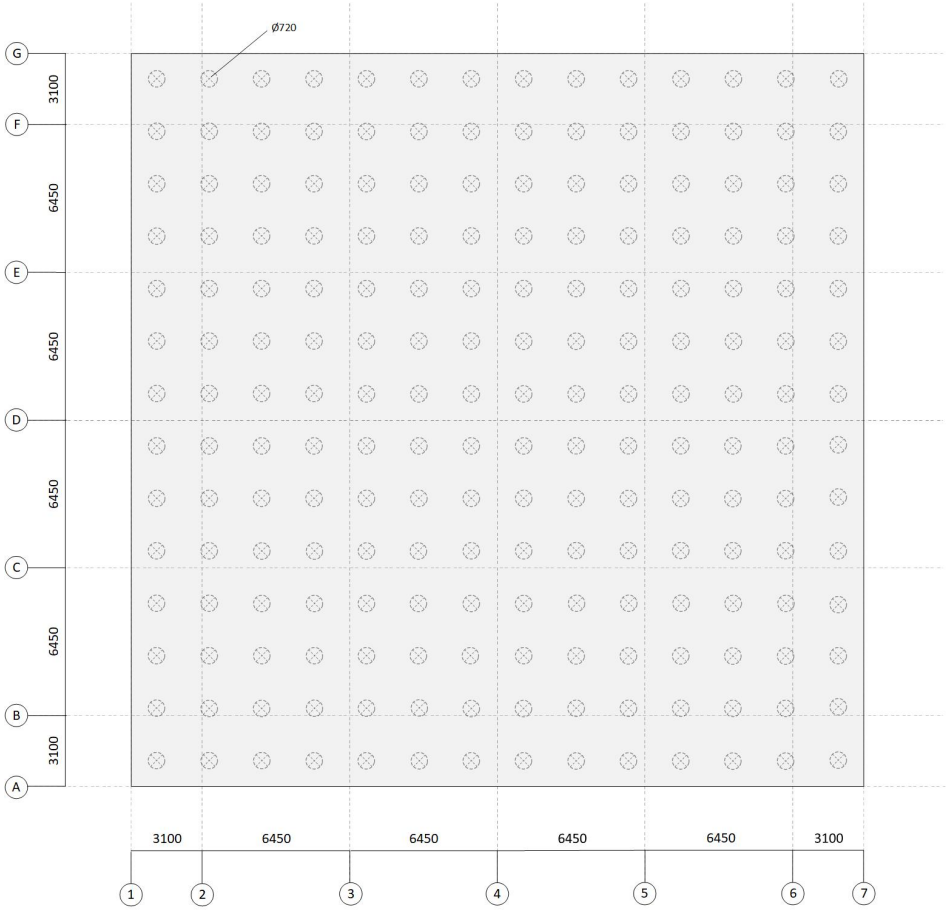

Figure D.3: Foundation plan

E

Design process of floor types variants

This appendix includes the design process of the floor types variants. The first step of the design process is to select a realistic floor buildup for each floor type. Next, various floor and beam layouts with different spans are generated, followed by the selection of the layout variants that will be used as parameter.

E.1. Floor design

For every floor type a realistic floor build up is chosen, based on acoustic and fire safety requirements. These are given in Table E.1 to E.4.For the materials and thicknesses for the floor build-ups several references are used [60, 61, 62]. To maintain uniformity, each floor type incorporates a 25 mm plasterboard layer at the bottom, providing 120 minutes of fire resistance. The exceptions are the concrete floor, which does not require any fire-proofing material, and the CLT rib panel floor, which uses a 36 mm plasterboard layer for fire protection.

Table E.1: Concrete floor

Material	Thickness (mm)	Density (kg/m3)	Load (kN/m2)	
Cement screed	50	2000	1.0	
PE foil	0	1000	0.0	
Insulation	20	35	0.0	
Concrete floor	tbd	2500		+
Dead load			1.0	

Table E.2: CLT floor

Material	Thickness (mm)	Density (kg/m3)	Load (kN/m2)	
Cement screed	50	2000	1.0	
Insulation	30	35	0.0	
Gravel fill	30	1800	0.5	
CLT panel	tbd	2500		
Plasterboard	25	800	0.2	+
Dead load			1.7	

Table E.3: TCC floor

Material	Thickness (mm)	Density (kg/m3)	Load (kN/m2)	
Cement screed	50	2000	1.0	
Insulation	30	35	0.0	
Concrete floor	tbd	2400		
CLT panel	tbd	2500		
Plasterboard	25	800	0.2	+
Dead load			1.2	

Table E.4: CLT rib floor

Material	Thickness (mm)	Density (kg/m3)	Load (kN/m2)	
Dry screed	20	2000	0.4	
Insulation	10	35	0.0	
Gravel(backfill)	50	1800	0.9	
CLT panel	tbd	500		
CLT ribs	tbd	500		
Plasterboard	36	800	0.3	+
Dead load			1.6	

E.2. Floor dimensioning

In this section, the design process for each floor type is outlined. First, several design assumptions are established, followed by a presentation of the geometry and material properties of the elements. Next, the applied loads on the floors are described, along with the relevant load cases and requirements. Afterward, the calculations are performed, leading to the determination of the dimensions. Finally, the floor layouts are selected.

E.2.1 Assumptions

The basic principles and assumptions are the same for all different types of floors. This has been done to simplify and standardize the calculation. The following assumptions apply to all floor types:

- The floor is a 1-way slab supported by two beams.
- The beams are assumed simply supported.
- The floors are designed for one governing floor length for each floor layout.
- The free height between the top of the floor and the ceiling is 2.4 m.

E.2.2 Geometry

The length of the floor slabs and the position of the girders is given in Table 5.3 and shown in the floor plans in Figure L.1 to L.6 in Appendix L.

E.2.3 Materials

Several materials are used for the floors and beams of the floor types. The floor types that are the base for building variants are discussed in Section 3.3. The material properties of GL24h are given in Table E.5 and the materials properties of the concrete class C20/25 and steel grade F500 for reinforcement are given in Tables E.6 and E.7.

Table E.5: Characteristic mechanical properties GL24h according to NEN-EN 14080 [86]

Mechanical properties		Value	Unit
Bending strength	$f_{m,k}$	24	N/mm^2
Compression strength parallel to grain	$f_{c,0,k}$	24	N/mm^2
Compression strength perpendicular to grain	$f_{c,90,k}$	2.5	N/mm^2
Tension strength parallel to grain	$f_{t,0,k}$	19.2	N/mm^2
Tension strength perpendicular to grain	$f_{t,90,k}$	0.5	N/mm^2
Shear strength	$f_{v,k}$	2.7	N/mm^2
Rolling shear strength	$f_{r,k}$	1.5	N/mm^2
Modulus of elasticity parallel to grain	$E_{0,mean}$	12000	N/mm^2
Modulus of elasticity perpendicular to grain	$E_{90,mean}$	370	N/mm^2
Shear modulus parallel to grain	$G_{0,mean}$	250	N/mm^2
Rolling shear modulus	G_r	50	N/mm^2
Density	ρ_k	400	kg/m^3
Poisson ratio	ν	0.3	-

Table E.6: Characteristic mechanical properties concrete class C20/25

Mechanical properties		Value	Unit
Characteristic cylinder compressive strength	f_{ck}	20	N/mm^2
Design compressive strength	f_{cd}	13.33	N/mm^2
Elastic modulus	E_{cm}	29 962	N/mm^2
Density	ρ_k	2500	kg/m^3

Table E.7: Characteristic mechanical properties steel grade F500

Mechanical properties		Value	Unit
Design yield strength	f_{yd}	435	N/mm^2
Modulus of elasticity	E	210 000	N/mm^2
Density	ρ_k	7850	kg/m^3

E.2.4 Loads

The loads acting on the building can be categorized in permanent and variable loads. The permanent load includes the self-weight of the floor and the additional dead load which differs per floor type. Table E.8 shows the variable load that are include, which are the 'Residential area' and partition walls [87].

Table E.8: Variable loads on floors

Variable loads	Unit (kN/m2)
Partition walls	0.8
Residential area (cat A – Woon- en verblijfsruimtes)	1.75

E.2.5 Load cases

Building above 70m have consequence class CC3, corresponding to a high consequence for loss of human life or financial damage. The fundamental load combinations for safety of the construction, the Ultimate Limit State (ULS) and the characteristic load combination for the Serviceability Limit State (SLS) are derived from Eurocode 0 Table NB.5 [88]. The equations that are used as shown below in Formula E.1 to E.3, assuming that the unfavourable situation is governing.

$$ULS_{6.10a} : 1.5 \sum_{j \geq 1} G_{k,j} + 1.65 \sum_{i>1} \varphi_{0,i} Q_{k,i} \tag{E.1}$$

$$ULS_{6.10b} : 1.3 \sum_{j \geq 1} G_{k,j} + 1.5 Q_{k,1} + 1.5 \sum_{i>1} \varphi_{0,i} Q_{k,i} \tag{E.2}$$

$$SLS : 1.0 \sum_{j \geq 1} G_{k,j} + 1.0 Q_{k,1} + 1.0 \sum_{i>1} \varphi_{0,i} Q_{k,i} \tag{E.3}$$

E.2.6 Requirements

The requirements for the dimensioning of the floors depend on the strength (ULS) and stiffness (SLS) requirements given in the Eurocode [87]. Below the requirements that are used are stated for both concrete and timber. Besides the structural requirements the floors must also meet the fire resistance requirements of 120 min.

Concrete

For the Ulimtate Limit State (ULS) it is assumed that the steel reinforcements yield. The acoustic and fire safety requirements are not verified and assumed to be met because of the inherent properties of concrete and the resulting thickness of the elements after the designing procedure. For the Serviceability Limit State (SLS), a maximum deformation is allowed. The following validations for both ULS and SLS are:

- ULS: steel strength: σ_s < f_{yd}
- SLS: deformation: w < $\frac{l}{250}$

Timber

For the Ultimate Limit State (ULS), several verifications are conducted, including checks for flexural strength, shear strength, and rolling shear. Acoustic requirements are critical for timber elements, as their low density and stiffness make them more susceptible to vibrations. Fire safety requirements are also verified. The following validations are carried out for both the ULS and Serviceability Limit State (SLS):

- ULS:
  - flexural strength: $\sigma_{m,y,d}$ < $f_{m,k}$
  - shear strength: $\tau_{v,d}$ < $f_{v,k}$
  - rolling shear: $\tau_{r,d}$ < $f_{r,k}$
- SLS: deformation: w < $\frac{l}{250}$
- Acoustics: natural frequency > 8 Hz

Additional criteria

Additional criteria are set for selecting the floor layouts that shall be used as parameters in further analysis. For each floor type, the maximum floor-to-floor height is 3.1 meters, and the floor layouts with the lowest total mass are chosen.

E.2.7 Calculations

This section gives the calculation procedure for the design of the floor types. First the calculations are given for the concrete floor type, followed by the CLT, TCC and CLT rib floor type. The calculation procedure gives the resulting dimensions of the floors and beams.

Concrete floor and beam

The floor dimensions are obtained using the calculations provided in the Book 'Constructieleer Gewapend Beton' C.R. Braam [89]. The requirements for the floors are for the longitudinal reinforcement percentage between 0.15 and 1.85% and the total reinforcement must be below 0.41% of the total cross section to fulfil the deformation requirements.

Besides a concrete cover of 40 mm is assumed to fulfil fire safety requirements for R120. A minimum thickness of 250 mm is required, otherwise additional acoustic measures are needed like lowered

ceiling with additional insulation. This is not wanted, therefor this requirement is stated. In Table E.9, the loads on the concrete floor are given. The variable loads are combined into one variable load.

Table E.9: Loads on concrete floor

Loads	Unit (kN/m2)
Permanent load	
Self-weight concrete	tbd
Dead load (screed + insulation)	1
Variable loads	2.55

Results
The resulting concrete floor height for the floor layout variants are given in Table E.10.

Table E.10: Floor dimensions - Concrete floor type

Variant	Floor span (m)	Floor height (mm)
1	6.45	270
2	6.45	270
3	6.45	270
4	4.30	250
5	3.23	250
6	6.45	270

It is assumed that the beam is integrated into the concrete floor, as depicted in Figure B.4 in Appendix B, resulting in a shallow beam. For all dimension calculations, a beam width of 400 mm is assumed as this is also the width of the columns. This is also done to easily compare the different beam heights. The resulting beam height for the floor layout variants are given in Table E.11.

Table E.11: Beam dimensions - Concrete floor type

Variant	Beam span (m)	Beam width (mm)	Beam height (mm)
1	6.45	400	550
2	4.45	400	385
3	5.00	400	410
4	4.30	400	335
5	6.45	400	400
6	3.23	400	285

The total floor stack height for all variants is given in Table E.12. The beams are partially integrated into the thickness of the floors.

Table E.12: Floor stack height (mm) - Concrete floor type

Variant	**1**	**2**	**3**	4	5	6	
Finish	80	80	80	80	80	80	
Structure	270	270	270	250	250	270	
Ceiling	0	0	0	0	0	0	+
Beam	550	385	410	335	470	285	
Total stack	630	465	490	415	550	365	
Free height	2400	2400	2400	2400	2400	2400	+
Floor-to-floor height (m)	3.0	2.9	2.9	2.8	2.9	2.8	

Example calculation total stack height = 80+550+0 = 630 mm

CLT floor panel and glulam beam

The thickness of the panels and beams are calculated using the software Calculatis. Table E.13 gives the loads on the CLT floor.

Table E.13: Floor on CLT floor

Loads	Unit (kN/m2)
Permanent load	
Self-weight concrete	tbd
Dead load (screed + insulation)	1.7
Variable loads	2.55

The material properties of CLT panels are not identical to the material GL24h, therefor the material properties of CLT are given in Table E.14 together with the properties of GL28h which is the strength class used for the glulam beams.

Table E.14: Mechanical properties C24 and GL28h

Material	Class	Flexural strength fm,k (N/mm2)	Shear strength fv,k (N/mm2)	Rolling shear strength fr,k (N/mm2)
CLT	C24 spuce ETA	24	4	1.25
Glulam	GL28h	28	3.5	

Results

The resulting clt panel height for the floor layout variants are given in Table E.15.

Table E.15: Floor dimensions - CLT floor type

Variant	Floor span (m)	Floor height (mm)
1	6.45	240
2	6.45	240
3	6.45	240
4	4.30	140
5	3.23	120
6	6.45	240

For the calculations the standard beam dimensions of Hasslacher Glulam are used [90]. In several cases a double beam is needed. A 1:2 ratio for the width and height of the beams is aimed for Table E.16 shows the beam dimensions of the glulam beam for each floor layout variant.

Table E.16: Beam dimensions - CLT floor type

Variant	Beam span (m)	Beam width (mm)	Beam height (mm)
1	6.45	(2x160) 320	560
2	4.45	240	440
3	5.00	260	480
4	4.30	200	400
5	6.45	220	460
6	3.23	210	350

It is assumed that the beams have a bearing block on which the floors rest as shown in Figure B.5. The floor height is therefor reduced. In Table E.17 the height of the floor elements are given together with the total floor stack height and the floor-to-floor height.

Table E.17: Floor stack height (mm) - CLT floor type

Variant	**1**	**2**	**3**	**4**	**5**	**6**	
Finish	110	110	110	110	110	110	
Floor	240	240	240	140	120	240	
Ceiling	25	25	25	25	25	25	+
	365	365	365	265	245	365	
Beam	560	440	480	400	460	350	
Total stack	695	575	615	535	595	485	
Free height	2400	2400	2400	2400	2400	2400	+
Floor-to-floor height (m)	3.1	3.0	3.0	2.9	3.0	2.9	

TCC floor panel and glulam beam

The thickness of the panels and beams are calculated using the software Calculatis. The software does not have fire safety calculations for TCC panels, so it is possible that several variants have a floor height that do not meet fire safety requirements. For this a minimum required CLT floor thickness of 120mm is assumed. Additional calculations are done for a normal CLT panel with the additional concrete layer for which fire safety calculations are available. These result in higher thicknesses for the CLT panel for all spans. The floor loads on the TCC floor panels is given in Table E.18.

Table E.18: Loads on TCC floor

Loads	Unit (kN/m²)
Permanent load	
Self-weight concrete	tbd
Dead load (screed + insulation)	1.2
Variable loads	2.55

For materials that are used for the TCC floor are simular to the CLT floors. Concrete class C20/25 is used and the contribution of reinforcement steel is not included in the strength calculations.

Results

In Table E.19 the resulting floor dimensions of the TCC floor type are given.

Table E.19: Floor dimensions - TCC floor type

Variant	Floor span (m)	Floor height (mm)	
		CLT	Concrete
1	6.45	160	100
2	6.45	160	100
3	6.45	160	100
4	4.30	120(80)	60
5	3.23	120(60)	60
6	6.45	160	100

In several cases a double beam is needed. A 1:2 ratio for the width and height of the beams is aimed for. Table E.20 gives the resulting beam dimensions of the glulam beams for the TCC floor type.

Table E.20: Beam dimensions - TCC floor type

Variant	Beam span (m)	Beam width (mm)	Beam height (mm)
1	6.45	480(2x240)	520
2	4.45	260	480
3	5.00	400(2x200)	440
4	4.30	220	400
5	6.45	240	480
6	3.23	240	400

It is assumed that the beams have a bearing block on which the CLT rests. The concrete layer is poured on top of this and the floor height is reduced in this way. Table E.21 shows the stack height and the floor-to-floor height for the TCC floor type.

Table E.21: Floor stack height (mm) - TCC floor type

Variant	**1**	**2**	**3**	**4**	**5**	**6**	
Finish	80	80	80	80	80	80	
Concrete	100	100	100	60	60	100	
CLT	160	160	160	120	120	160	
Ceiling	25	25	25	25	25	25	+
	365	365	365	225	285	365	
Beam	520	480	440	400	480	400	
Total stack	725	685	645	565	645	605	
Free height	2400	2400	2400	2400	2400	2400	+
Floor-to-floor height (m)	3.1	3.1	3.0	3.0	3.0	3.0	

CLT rib panel floor and glulam beam

The thickness of the panels and beams are calculated using the software Calculatis. The distance between the ribs is 800mm. The rib width of CLT rib panels cannot be too small for fire safety. Table E.22 shows the loads on the CLT rib panel floor.

Table E.22: Loads on CLT rib panel floor type

Loads	**Unit (kN/m²)**
Permanent load	
Self-weight concrete	tbd
Dead load (screed + insulation)	1.6
Variable loads	2.55

Results

Table E.23 shows the floor dimension of the CLT rib panel floor type.

Table E.23: Floor dimensions - CLT rib panel floor type

Variant	**Floor span (m)**	**Floor height (mm)**		
		CLT	**Rib height (mm)**	**Rib width (mm)**
1	6.45	140	240	140
2	6.45	140	240	140
3	6.45	140	240	140
4	4.30	120	200	120
5	3.23	100	160	120
6	6.45	140	240	140

The beam dimensions of the glulam beams are given in Table E.24. It is assumed that the ribs are connected to the side of the primary beams as shown in Figure B.4,a in Appendix B and the CLT panel rests on the primary beams. The floor height is in this way reduced. Table E.25 shows the stack height and the floor-to-floor height for the CLT rib panel floor type.

Table E.24: Beam dimensions - CLT rib panel floor type

Variant	**Beam span (m)**	**Beam width (mm)**	**Beam height (mm)**
1	6.45	(2x200)400	480
2	4.45	220	440
3	5.00	220	480
4	4.30	200	360
5	6.45	240	440
6	3.23	180	360

Table E.25: Floor stack height (mm) - CLT rib panel floor type

Variant	**1**	**2**	**3**	**4**	**5**	**6**	
Finish	80	80	80	80	80	80	
Structure	380	380	380	320	260	380	
Ceiling	36	36	36	36	36	35	+
Beam	480	440	480	360	440	360	
Total stack	736	696	736	596	656	615	
Free height	2400	2400	2400	2400	2400	2400	+
Floor-to-floor height (m)	3.1	3.1	3.1	3.0	3.1	3.0	

E.3. Design variants

Figure E.1 shows the building variants that are used as input in the models.

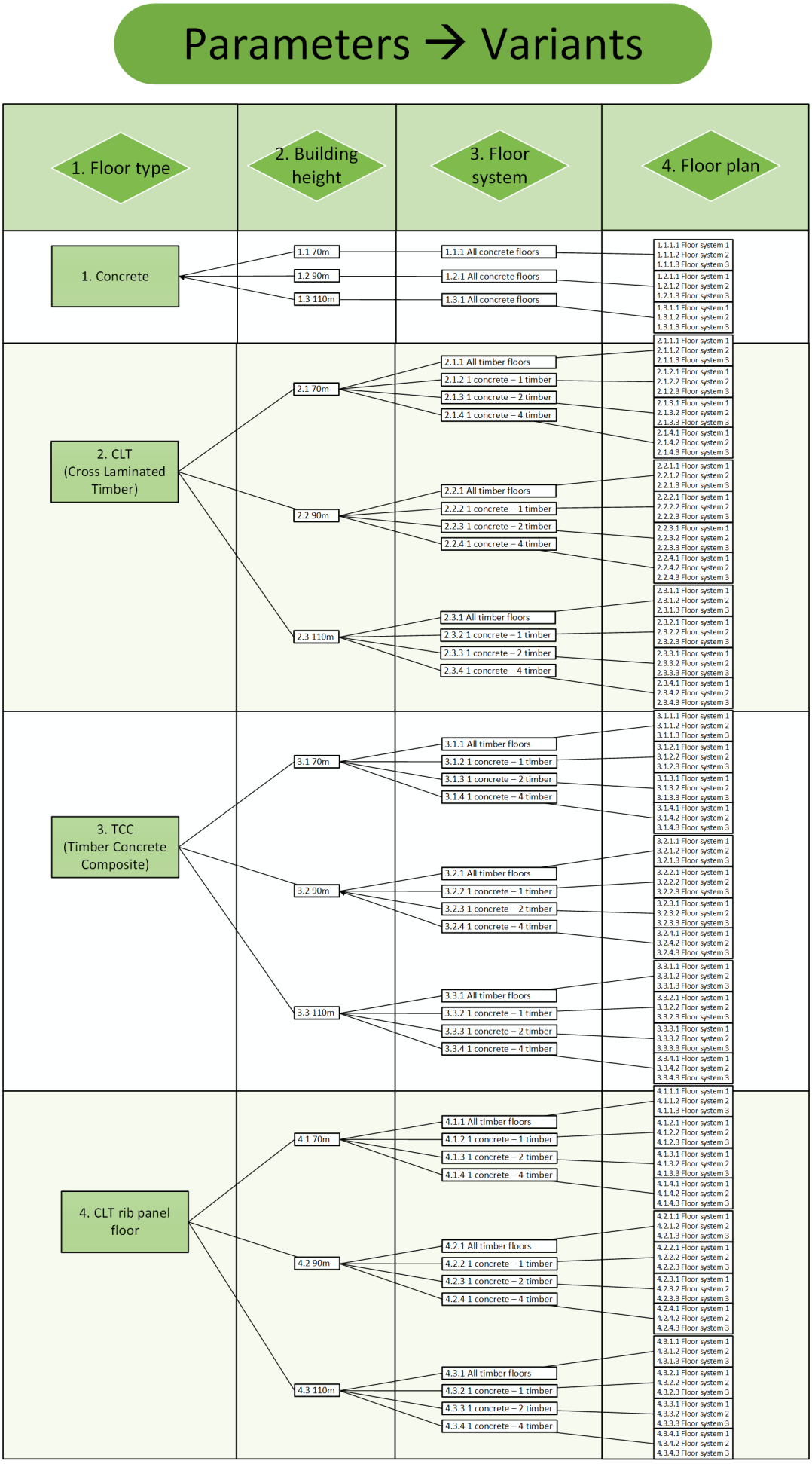

Figure E.1: Building variants

F

Design process of building variants

This section discusses the alterations to the original design of the building, the assumptions, the modelling and the resulting core dimensions for the building variants.

F.1. Alternations

Below the alternations to the structural elements of the Cooltoren are discussed. These include the core, the floors, the outriggers, the columns, the balconies, the facade and the foundation. Additional information on dimensions and amount of reinforcment of each structural element is given in Table F.1.

F.1.1 Concrete core

The original design of the concrete core has dimensions of 13 by 13 m and a thickness of 0.5 m. In the development of the building variants the dimensions can change based on the parameters. This means that the lettable floor space of the building can change, but this is not further discussed in the thesis. The design of the concrete core is depending on these parameters by the self-weight acting on the mass and the wind load that depends on the height of the building. For the concrete core of the building, there are several functional requirements, which result in minimum requirements for the size of the concrete core. These can be divided into requirements for the elevator and the staircases. Fire safety requirements for elevators and staircases are provided in Section F.1.8. In the core several functions are situated. The dimensions of these functions remain unchanged as these are essential parts of a functional and safe tall building. The elements include the elevators shaft with dimensions of 2.7 m by 5.7 m and a wall thickness of 150 mm, the staircase with dimensions 3 m by 2.5 m, surrounded by a wall with a thickness of 150 mm. The dimensions of the corridors between the elevators and the staircases are 1.5 m in width [49].

F.1.2 Floors

The floor system in the Cooltoren consists of concrete floors cast in-situ with steel tensile reinforcement, and no beams are used in the tower's floor systems. However, in the case study, the floor system includes both floors and beams made of either concrete or timber. This approach is chosen to facilitate a uniform comparison between the building variants, as timber floor panels are typically used with timber beams.

F.1.3 Outriggers

In the Cooltoren, outriggers are situated between floors 16 and 19 and between floors 32 and 35. These outriggers are excluded in the design to create more general building variants, as they were specifically used in the Cooltoren to increase the total building height. Since the goal of this thesis is not to focus on having a very tall building, the comparison is made with other concrete-timber hybrid buildings and concrete buildings that have the same structural system with a central core.

F.1.4 Columns
In the original design of the Cooltoren, the dimensions of the concrete columns decrease towards the top of the building, and different shapes are used for different columns. However, for this case study, one column size and shape is selected and rotated based on the position of the column. This is considered acceptable because the concrete columns have a minor influence on the dynamic analysis, as the connections are hinged. For the environmental and cost analyses, it is assumed that the columns constitute a minor part of the total concrete volume. Therefore, it is permissible to keep all columns the same size, even though this does not fully mimic reality. This decision is also based on the goal of generalizing the design of building variants, as columns are not the main focus of the thesis.

F.1.5 Balconies
The original design includes concrete and steel balconies attached to the concrete floors. Although it is acknowledged that most residential buildings have balconies and that they are an essential part of the design, for simplicity, these are excluded in the design of the building variants. This is allowed as they are not part of the main structural system.

F.1.6 Façade
The Cooltoren features façade elements that are attached to the concrete floors. However, in the case study buildings, the façade is excluded from the design of the floor systems and the analysis. This exclusion is justified as the thesis focuses solely on the structural system, which does not include the façade.

F.1.7 Foundation
The foundation design of the Cooltoren serves as the basis for designing the foundations of the building variants. The foundation stiffness is included in the dimensioning of the concrete core as it has big influence on the deformation of the building. Including it will give a more accurate representation of the actual deformation. The number of foundation piles varies across different building variants, depending on whether they are lighter or heavier. The Tubex piles are equipped with load-transfer reinforcement steel at the top, consisting of six 16 mm diameter bars with a length of 3 meters.

Table F.1: Dimensions and reinforcement of structrual elements

Structural element	Dimensions (m)	Reinforcement steel (kg/m^3)
Foundation plate	32x32x2	80
Column	0,7x0,4	80
Concrete floor	tbd	50
Beams	tbd	100

F.1.8 Fire safety design
Reasons for not including fire safety design measures in the thesis is: these elements are out of the scope of the thesis and it is assumed that the measures minorly influence the results of the design aspects as the measures are the same for all building variants. The sprinkler system that is required is not included in the research of the building variants. The stairwell in the Cooltoren has fire locks with over pressure. The Cooltoren has two fire elevators within one shaft [91]. Uniform fire safety design for all floor types. In the thesis a fire proofing material is used on the ceiling of the timber floors. For the concrete floors no additional fire proofing is used. In the design for the concrete floors the required minimal coverage of the reinforcement for R120 is used.

- Separation walls sufficient for fire compartmentation. Also not further incorporated in design except as permanent load.
- Openings and fire protection of these openings not taken into account.

F.2. Design assumptions

To find the dimensions of the concrete core for the building variants a distinction is made between fixed input parameters and variable parameters. The justification for the which parameters are chosen and their value if they are fixed.

The fixed parameters are applicable to all building variants. The reason for choosing several fixed parameters is to simplify the design process and not to end up in an iterative design process with several variables.

Starting with the dimensions of the concrete core, the thickness of the core is chosen as a variable to facilitate the strength and stiffness of the concrete core for different building heights and mass. For this variable boundaries are chosen. A minimal thickness of 0.25 m to facilitate fire safety design and an upper limit of 0.4 m which is common in concrete core buildings of this height. The fixed measurements are the outer perimeter of the core, because the floors and beams of the building variants are dimensioned beforehand. Besides minimal inner measurements in the core must be available for general services, which are staircases, lift shafts and evacuation routes through corridors and other services like MEP and HVAC. These two limitations results in decreasing apartment size when the core thickness is increased.

The material properties of the concrete core are constant for all building variants. The foundation plate has constant dimensions for all building variants. The foundation plate is assumed to be infinity stiff and able to redistribute the forces and moment to the foundation piles.

F.3. Design strategy

For the design strategy is chosen to optimize the core size for a maximal rentable space and a minimal number of foundation piles. These variables are contradicting as with more foundation piles a smaller core thickness is possible and vice versa. The goal is to minimize both parameters.

F.4. Modelling

The modelling of the concrete core is done using the plugin Karamba3D in grasshopper and Rhino. The modelling needs several inputs which are provided with Python and Excel spreadsheets. Below the inputs, the model and the outputs are discussed.

F.4.1 Input

An overview of the input for the model is shown in Figure F.1 and includes the loads(orange bottom), the cross section of the concrete core(grey), the material(orange top) and the foundation(orange middle).

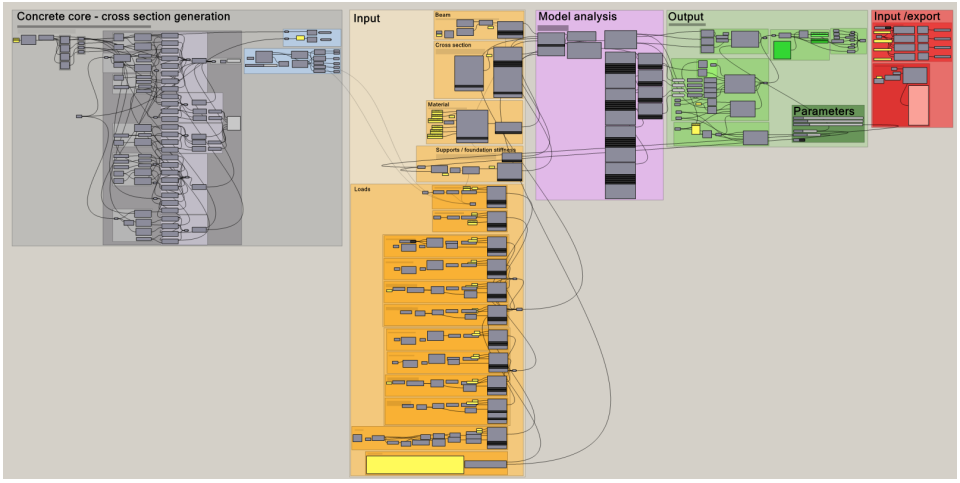

Figure F.1: Grasshopper script overview

Beam
The building is modelled in grasshopper as a beam with a specific height, which is the height of the building.

Cross section
The cross section of the concrete core is based on the core dimensions of the Cooltoren. This cross section serves as the basis for calculating the dimensional properties of the concrete core. To account for openings within the core, a 30% reduction is applied to the moment of inertia. Figure F.2 shows a Rhino visualization of the concrete core's cross section, where the thickness of the outer perimeter is variable. The dimensional properties of this cross section are integrated into the 'Modify Cross Section' component, which includes the correct deformation and resistance properties.

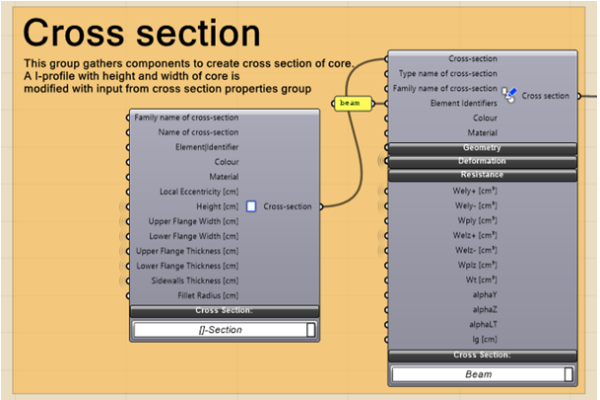

Figure F.2: Grasshopper script: Cross section

Material
The core is constructed from reinforced concrete with a strength class of C55/67, similar to what was used in the Cooltoren for the full height of the building. Table F.2 provides the material properties. A 50% reduction in the E-modulus of the concrete is applied for Serviceability Limit State calculations to account for cracking in the concrete.

Table F.2: Material properties Concrete class C55/67

C55/67	Value	Unit
E modulus (reduced 50%)	1910	N/cm2
Density	25	kN/m3
f_{ct}	0.197	kN/cm2
f_{cd}	3.667	kN/cm2

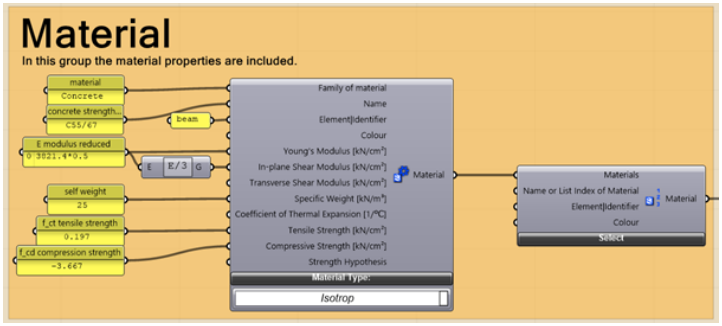

Figure F.3: Grasshopper script: Material

Foundation stiffness
The rotational stiffness of the foundation is included in the script. For this a Python script is produced that calculated the rotational stiffness of the foundation based on the number of foundation piles [92] that contribute to the resisting bending moment. It is assumed that bending moment is resisted by the concrete core and transferred to foundation piles under and surrounding the core. Together these foundation piles therefor also provide the rotational stiffness. Further information on how the number of contributing foundation piles is determined is provided in Section F.6.1. The pile stiffness is based on the static pile stiffness calculated for the Cooltoren, which is 239000 kN/m. This is a conservative value as for dynamic wind load a higher stiffness can be assumed. Incorporated in model through python code as shown in Figure F.4. The python script is proved in Figure K.5 in Appendix K.

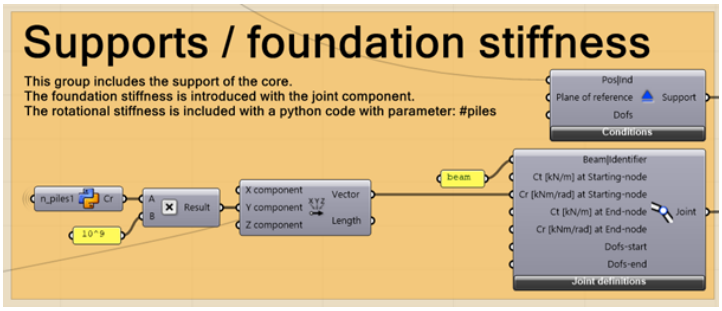

Figure F.4: Grasshopper script: Foundation stiffness

Loads
The loads on the concrete core can be divided into permanent loads which are the self-weight of the concrete core, self-weight of the foundation plate and the self-weight of the floors and the variable loads which are the imposed weight of the floors and the wind load.

Self-weight of the core
The self-weight of the concrete core is determined by its size and material properties. The weight is calculated based on the core's volume and the density of the concrete. Figure F.5 illustrates the component group used to calculate the permanent load of the concrete core. A distributed vertical load along the height of the building is assumed for these calculations.

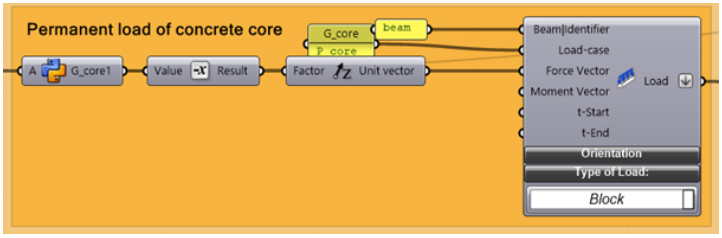

Figure F.5: Grasshopper script: Permanent load of concrete core

Self-weight of the foundation plate
The self-weight of the concrete core is influenced by the size of the foundation plate and the material properties. The weight of the foundation plate is calculated based on its volume and density. The dimensions of the original foundation plate from the Cooltoren are used, which measure 32 by 32 meters with a thickness of 2 meters. These dimensions and thickness justify the assumption of a stiff foundation plate for further calculations. Figure F.6 shows the component group used to calculate the permanent load of the foundation plate, where a concentrated vertical load at the base of the building is assumed.

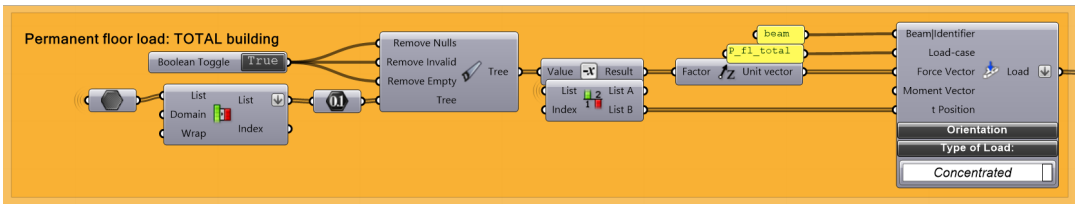

Figure F.7: Grasshopper script: Total permanent floor load

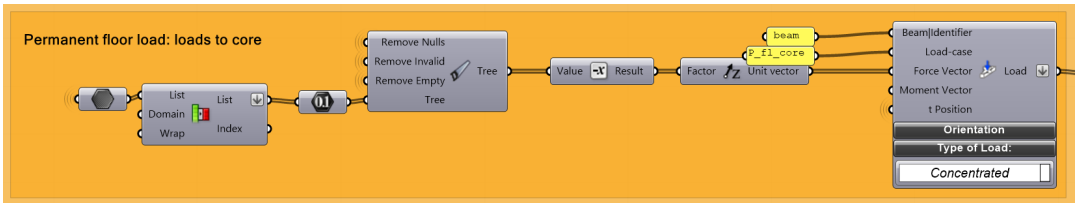

Figure F.8: Grasshopper script: Permanent floor load to core

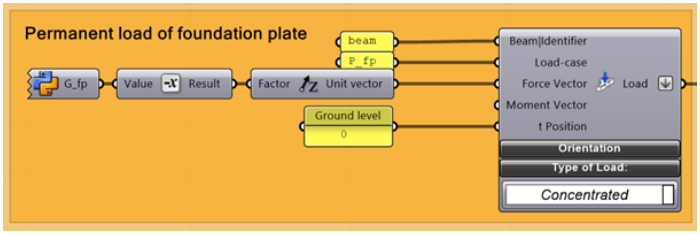

Figure F.6: Grasshopper script: Permanent load of foundation plate

Self-weight of the floor loads

The self-weight of the storeys consists of two parts: the self-weight transferred to the concrete core and the total self-weight acting on the foundation. For calculating the self-weight of the storeys, the output from the dimensioning of beam and floor elements is used. The total self-weight also includes additional loads from the façade, floors inside the core, and columns. For the concrete floors within the core, a thickness of 250 mm is assumed, with the floor area estimated based on the core's area. While this area is considered independent of the core's thickness—an approximation—it is acceptable for the design of the concrete core. For the façade load, an estimate is made using calculations from the original Cooltoren design, with a self-weight of 2.88 kN/m² assumed. The relevant calculations are provided in Appendix K, Figures K.1 to K.4. The combined data is imported via an Excel sheet into the Grasshopper script, with these loads concentrated at the vertical position of each floor. Figures F.7 and F.8 illustrate the Grasshopper components used for calculating the total permanent loads on a floor and the permanent loads transferred to the core.

Variable floor loads

For the variable floor loads, the output from the dimensioning calculations of the floor elements is used. A distinction is made between the variable loads acting on the entire floor and the loads transferred to the core. Figures F.9 and F.10 show the Grasshopper components used to calculate the total variable loads on a floor and the variable loads transferred to the core for each floor.

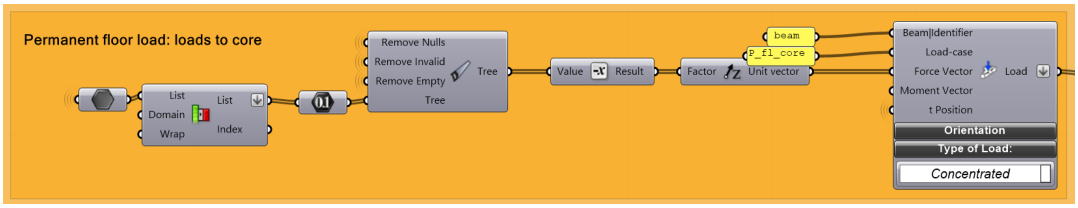

Figure F.9: Grasshopper script: Total variable floor load

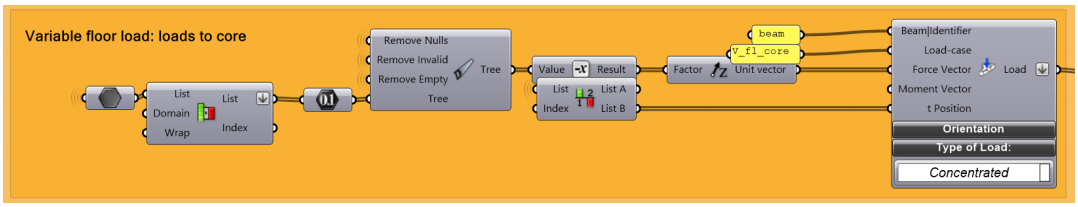

Figure F.10: Grasshopper script: Variable floor load to core

Wind load

The wind load on the building is transferred from the façade to the core. The wind load on the building is calculated using the EN1991-1-1-4 procedure [65]. For this a python script is used as shown in Figure K.6 in Appendix K. Figure F.12 shows the resulting wind load over the height of the building.

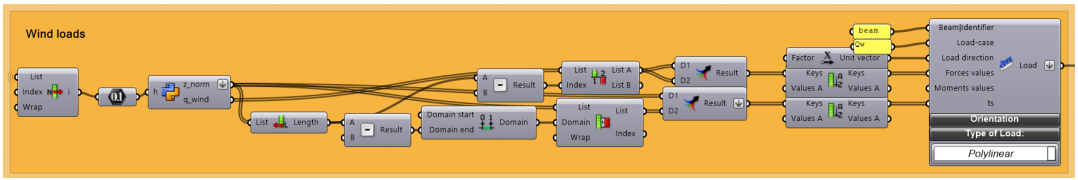

Figure F.11: Grasshopper script: Wind loads

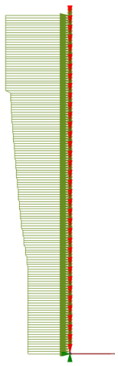

Figure F.12: Wind load distributed over height of building

F.5. Load combinations

The load combinations are determined based on the extreme loads acting on the concrete core and foundation piles, as well as the maximum deformation of the building. Further details on the load combinations are provided in Section F.6. In Table F.3 the combination factors for the load combinations are given. The load combinations are incorporated in the grasshopper scripts using a 'load case combinator' component as shown in Figure F.13.

Table F.3: Load factors and combination factors for permanent (G) and variable (Q) loads in load combinations

Load combination	G	Q	Combination factor Q floor	Combination factor Q wind
A_pile_max_G	1.5	1.65	0.5	0.0
B_pile_max_Qfl	1.3	1.65	1.0 (2 extreme floors), 0.5 (other floors)	0.0
C_pile_max_Qwind	1.3	1.65	0.5	1.0
D_pile_tension	0.9	0.0	0.0	1.0
E_pile_horizontal	0.0	0.0	0.0	1.0
F_core_deformation	0.0	1.0	0.5	1.0
G_core_max_G	1.5	1.65	0.5	0.0
H_core_max_Qfl	1.3	1.65	1.0 (2 extreme floors), 0.5 (other floors)	0.0
I_core_max_Qwind	1.3	1.65	0.5	1.0
J_core_tension	0.9	0.0 .0	0.0	1.0

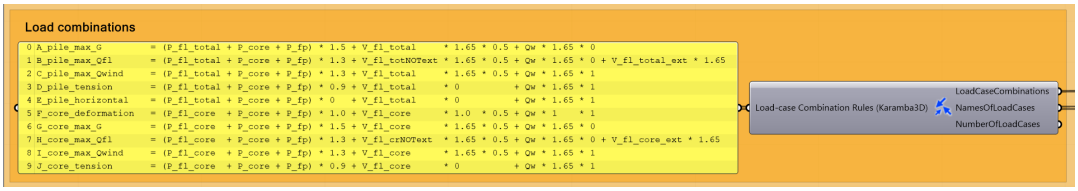

Figure F.13: Load combinator component

F.6. Model

The analysis is divided into three main parts. The first part focuses on verifying the strength of the foundation piles, the second part examines the strength of the concrete core, and the third part evaluates the deformation of the building under various load conditions.

F.6.1 Load combinations for pile loads

This section verifies the total forces acting on the foundation piles using a 'First-order analysis' component. The relevant load combinations A to E for foundation design are assessed through a Python script, as shown in the Grasshopper group in Figure F.16. The calculation of the governing foundation pile force is based on the normal force and bending moment at the base of the building, as detailed in Figure K.7 in Appendix K.

The 2-meter-thick foundation plate serves as a load redistributor, as depicted in Figure F.15. Assuming infinite stiffness for the foundation plate, this approximation is considered reasonable given the variability in the building designs. The normal forces are evenly distributed across the foundation piles, while the bending moment—primarily caused by wind loads—is assumed to be fully transferred to the building's concrete core. It is further assumed that the piles directly beneath and surrounding the core resist this moment, as shown in Figure F.14. To estimate the number of foundation piles contributing to the bending moment resistance, an additional distance of four times the raft thickness, plus the width of the concrete core, is considered.

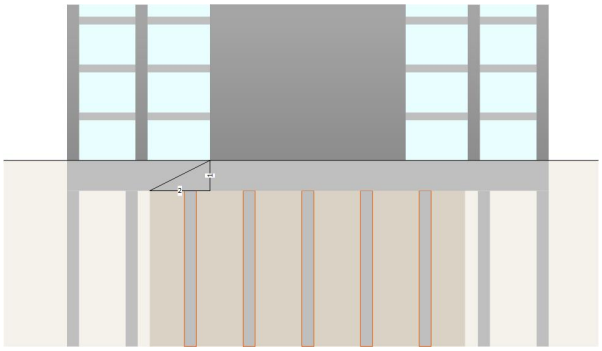

Figure F.14: Piles that contribute to resisting bending moment

The bending moment induces a linear stress distribution in the foundation plate, following Euler-Bernoulli beam theory. These stresses result in forces on the foundation piles around the core as shown in Figure F.15. The pile furthest from the core resists the highest load due to the bending moment and is thus considered the governing pile.

Load combinations A to C focus on the maximum vertical load on a foundation pile, accounting for normal force and bending moment under conditions of maximum self-weight, variable floor load, and wind load, respectively. These loads are evaluated against the maximum design load on foundation pile. This design load is reduced by 20% as a safety measure in this early design model. Load combination D addresses tension in the foundation pile, which is not permissible given the soft soil conditions in Rotterdam. Load combination E examines the horizontal load on the foundation pile due to wind, which is verified against the pile's horizontal characteristic strength.

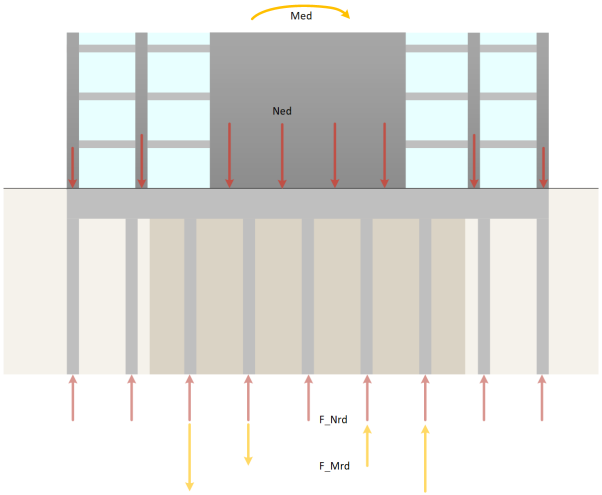

Figure F.15: Normal loads and bending moment on building and resulting loads in foundation piles

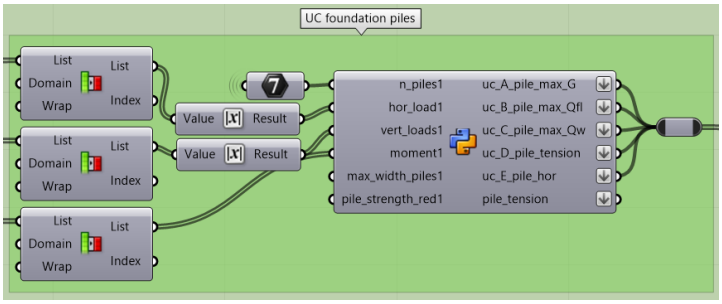

Figure F.16: Grasshopper script: Load combination A - E

F.6.2 Load combinations for concrete core

Load combinations G to J focus on the stress conditions at the base of the concrete core. Maximum and minimum stresses are calculated using the 'Beam view' component, with unity checks performed using a Python script that incorporates the strengths of both concrete and steel (Figure F.17).

Load combinations G to I address compressive stresses due to the normal force and bending moment under conditions of maximum core self-weight, variable floor load on the core, and wind load, respectively. The verification results are shown in Appendix K. Load combination J focuses on tensile stresses, which are resisted by the steel reinforcement. For all building variants, a double mesh configuration ⌀16/100 is assumed for the steel reinforcement. The normal force is evenly distributed across the cross-section of the concrete core, while the lever arm for the bending moment is defined as the distance between the centerlines of the core's walls, with the assumption that all walls contribute due to their significant cross-sectional area. The tensile stress is verified over a 1-meter width of the core, with results provided in Appendix K.

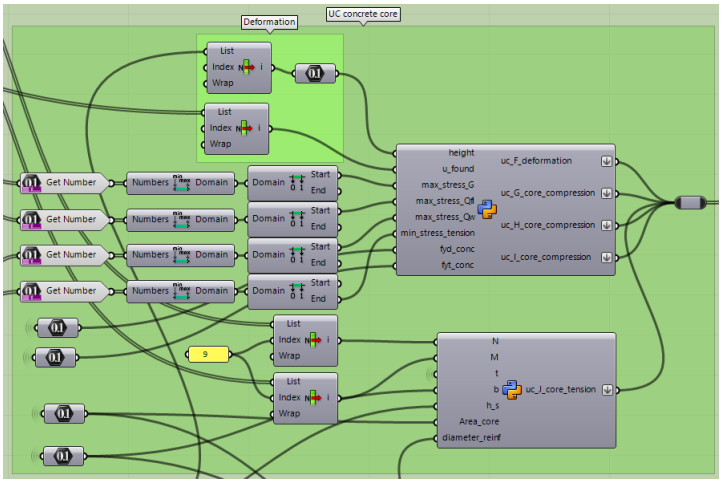

Figure F.17: Grasshopper script: Load combination F - J

F.6.3 Load combination for deformation of building

The third part of the analysis focuses on the deformation at the top of the building, using a 'Second-order analysis' component. The maximum deformation for load combination F is calculated and verified using the 'Python' component, as shown in Figure K.9.

F.6.4 Mass reinforced concrete core

Once the governing load combination is identified, the mass of concrete and reinforcement in the core is calculated. The required reinforcement decreases with height, so the concrete core is divided into four sections, each with its own reinforcement diameter. Table F.4 outlines the diameter and spacing of the reinforcement for each section. These quantities of reinforcement are verified for the heaviest and tallest building designs. Additionally, the internal walls of the concrete core are assumed to have the same reinforcement configuration as the outer walls. The python script for these calculations is given in Figure K.10 in Appendix K.

Table F.4: Diameter reinforcement for height range in core

Height range	Diameter (mm)	Spacing (mm)
0 - h/4	16/20	100
h/4 - h/2	12	100
h/2 - 3h/4	10	150
3h/4 - h	8	150

The results of the model are checked by hand calculations and with the software 'MartrixFrame'. The

total normal force, shear force and bending moment and the deformation at the top is verified. When no foundation stiffness was applied the difference in deformation output was 1%. The order of magnitude for the stresses is also checked.

F.6.5 Discussion

The influence of model inputs on the output is significant, especially due to the strict assumptions within the model. One example is the number of foundation piles, which resist the bending moment and provide rotational stiffness. This has a major impact on the required number of piles. The position of these piles must be strictly within predefined boundaries—if a pile is placed even 0.5 meters outside this boundary, it is modeled as not contributing to the bending moment. However, this assumption does not reflect reality, where piles outside the boundary would still provide some contribution to the structural behavior.

The boundary for pile placement is intentionally relaxed to some extent, as a stricter boundary would necessitate significantly more piles. This is because, in stricter conditions, the next set of piles would still fall outside the boundary, and the structural requirements would not be met until even more piles are added. To prevent this issue, the boundary has been expanded by 0 to 2 meter for each building height. This adjustment is applied consistently across all variants with the same height, ensuring fairness in the modeling process.

Additionally, the number of piles increases quadratically because the foundation plan must be symmetrical — another key modeling assumption. The grid layout for the piles remains unchanged, and the total distance between the piles increases as more piles are added. This symmetry constraint was an initial modeling choice, and no alterations to the grid can be made. The constant total distance means that as the number of piles increases, the spacing between them decreases.

G

Dyncamic model

Several steps are taken to obtain the natural frequencies and mode shapes of all building variants. Detailed explanations are provided for each step to clarify the assumptions, input data, and the model used.

G.1. Scope

The scope defines the structural elements and assumptions for the modelling of the dynamic behavior.

G.1.1 Structural elements

The structural elements are the base for the intermediate variables, mass and stiffness that are used in the model. The structural elements that are included are:

- Floors
- Beams
- Columns
- Core
- Façade

G.1.2 Assumptions

This section outlines the assumptions made to model a tall building using a mass-spring system. The assumptions are organized into three categories: general assumptions, assumptions related to mass, and assumptions related to stiffness.

General Assumptions:

- Damping: The damping value is assumed to be zero. Since damping is not required for determining the natural frequency, it is excluded from the analysis.
- Foundation: The foundation is assumed to be clamped, meaning it is fixed at the base with no rotation or translation. This assumption simplifies the modelling by neglecting soil-structure interaction, which is allowed for modelling in early design phase. However, for the case study building, the Cooltoren in Rotterdam, which is situated on soft soil, this assumption may lead to an unsafe design, as it does not accurately capture potential foundation movements.
- Torsional effects: Torsional effects are neglected, and only translational displacements are considered. This is based on the assumption that the building is symmetrical, which applies to the case study building.

Mass assumptions:

- The masses are concentrated at each floors to create a model with discrete masses.
- Rigid floors: floors are assumed as rigid body in their plane, which means they do not deform horizontally when moved horizontally. This reduces the number of degrees of freedom to lateral displacement and rotation of each floor.

Stiffness assumptions:

- A single stiffness parameter is assumed for the whole building, which is only depending on the stiffness of the concrete core.

G.2. Model

To calculate the first natural frequency two different models are used, a continuous model and a Single-degree of freedom model.

G.2.1 Continuous model

First, the derivation of the solution to the equation of motion for a bending beam is presented. For this the Euler-Bernoulli model which use Newton's second law along with the kinematic and constitutive relations. As a result, the equation of motion is given in Formula G.1.

$$EI\frac{\delta^4 u(z,t)}{\delta z^4} + \rho A\frac{\delta^2 u(z,t)}{\delta t^2} = f(z,t) \tag{G.1}$$

To derive the natural frequency of the system, the free vibration model is used. From this, the eigenvalue problem is obtained and presented in Formula G.2.

$$\frac{d^4 u(z)}{d^4 z} - \beta^4 u(z) = 0 \tag{G.2}$$

With;
$\beta^4 = \frac{\rho A \omega^2}{EI}$

A solution for the eigenvalue problem can be written as $u(z) = e^{\lambda z}$. Substituting this into the characteristic equation, the solution is obtained and given in Formula G.3.

$$u(z) = A\cosh(\beta z) + B\sinh(\beta z) + C\cos(\beta Z) + Dsin(\beta z) \tag{G.3}$$

The four constants A to D depend on the boundary conditions of the cantilever beam. For a clamped cantilever beam, the boundary conditions are:

$$\begin{aligned} z = 0: \quad & u = 0, & & \frac{du}{dz} = 0 \\ z = h: \quad & -EI\frac{d^2 u}{dz^2} = 0, & & -EI\frac{d^3 u}{dz^3} = 0 \end{aligned}$$

Substituting these boundary conditions into the homogeneous equation results in a system of algebraic equations. A non-trivial solution exists when the determinant of the system is set to zero, resulting in Formula G.4.

$$\cos\beta h = \frac{-1}{\cosh\beta h} \tag{G.4}$$

Solving this equation yields infinitely many solutions. With the obtained values of β, the eigenfrequencies of the system can be determined. Using one of the system's functions, the corresponding eigenfunctions can then be derived [32, 33].

Continuous model for equally distributed load

For equally distributed loads on a continuous model, the first natural frequency can be calculated using Raleigh's method. The natural frequency is calculated using the formula from Raleigh's method given in Formula G.5 [63].

$$\omega_n = \kappa_n^2 \sqrt{\frac{EIg}{\gamma S}} \tag{G.5}$$

With;
$\kappa_1 l$ = 1.875 for first natural frequency
EI = bending stiffness (N/m²)
γ = density (kg/m³)
S = area (m²)

To calculate the natural frequency of a tall building using Raleigh's method, specific assumptions are made for the input parameters. The density γ is taken as the total building mass divided over the total volume of the building, while for the area S, the area of the core is assumed.

The Rayleigh formula presented in Formula G.5 is derived under the assumptions that the material is homogeneous, isotropic, and follows Hooke's law, and that the beam is straight with a uniform cross-section, as shown in Figure G.1. This model is ideal for tall buildings with distributed loads and stiffness, as its continuous nature allows for a precise estimation of the first natural frequency. This is especially crucial for higher-order structures, which are difficult to accurately represent using a single lumped mass. Compared to an SDOF model, which assumes a single rigid mode of deformation, this model provides greater flexibility and accuracy [33].

Formula G.6 relates the curvature of the beam to the bending moment at each section. This formula is valid only for small deflections and for beams that are long compared to their cross-sectional dimensions, as the effects of shear deflection are neglected [93].

$$EI\frac{d^2y}{dx^2} = M \tag{G.6}$$

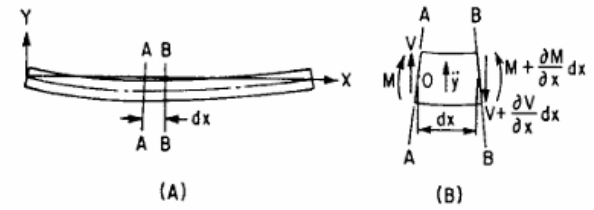

Figure G.1: A. Beam executing lateral vibration. B. Element of beam showing shear forces and bending moments [93]

The sum of the vertical forces action on the element in Figure G.1 must be equal to the mass of the element times the acceleration as given by Newton's law and given in Formula G.7.

$$\frac{\delta V}{\delta x} = -\frac{\gamma S}{g}\frac{\delta^2 t}{\delta t^2} \tag{G.7}$$

Substitute Formula G.7 in Formula G.6 gives Formula G.8.

$$-\frac{\delta^2}{\delta x^2}\left(EI\frac{\delta^2 y}{\delta x^2}\right) = \frac{\gamma S}{g}\frac{\delta^2 y}{\delta t^2} \tag{G.8}$$

The solution of this equation for constant EI is given in Formula G.9.

$$y = X(x)[cos(\omega_n t + \phi] \tag{G.9}$$

Substituting Formula G.10 in Formula G.9 and dividing by $cos(\omega_n t + \phi)$ gives Formula G.11.

$$\kappa^4 = \frac{\omega_n^2 \gamma S}{EIg} \tag{G.10}$$

$$\frac{d^4 X}{dx^4} = \kappa^4 X \tag{G.11}$$

The function X in Formula G.12 must satisfy the required conditions, providing the solution to the equation. An alternative way to express this equation is shown in Formula G.13.

$$X = A_1 sin(\kappa x) + A_2 cos(\kappa x) + A_3 sinh(\kappa x) + A_4 cosh(\kappa x) \tag{G.12}$$

$$X = A(cos(\kappa x) + cosh(\kappa x)) + B(cos(\kappa x) - cosh(\kappa x)) + C(sin(\kappa x) + sinh(\kappa x)) + D(sin(\kappa x) - sinh(\kappa x)) \tag{G.13}$$

The derivatives can be derived from Formula G.13. By applying the boundary conditions, Formula G.12 can then be solved. The boundary conditions for a cantilever beam are:

$$For x = 0 : X = 0, X' = 0$$
$$For x = l : X'' = 0, X''' = 0$$

G.2.2 SDOF

Treating a distributed system as an SDOF model oversimplifies the problem by assuming the mass is concentrated at a single point and that the structure deforms in a single mode. Additionally, modifications to the building's mass and height are required to fit the SDOF model, unlike the Rayleigh method, which directly uses the structure's original mass and stiffness distribution.

To calculate the natural frequency of a tall building using an SDOF system, specific assumptions are made for the input parameters. The mass m is typically taken as the top half of the building's total mass, while for the stiffness k, 3/4th of the building's total height is used.

G.3. Input

The input data for both models depend on the characteristics of each building variant, which are the total mass of the building and the bending stiffness EI.

G.3.1 Mass

The total mass is derived from a combination of permanent and variable loads. For permanent loads, the masses of structural elements are used. The variable load is a distributed load on the floors, specified for residential areas (category A – "Woon- en verblijfsruimtes"). For dynamic analysis, the semi-permanent load combination is applied in accordance with Eurocode standards, as shown in Formula G.14.

$$LC_{semi-permanent} = 1.0G + 1.0\psi_2 Q \tag{G.14}$$

G.3.2 Stiffness

OnlThe bending stiffness EI is used in the two models. It is assumed that a tall building can be approximated as a bending cantilever with one fixed end and one free end. The total building stiffness is based on the stiffness of the concrete core, which is used to simplify the dynamic analysis by applying static stiffness rather than dynamic stiffness. The bending stiffness EI consists of the modulus of elasticity E and the moment of inertia I. The moment of inertia I depends on the core geometry, with a 30% reduction applied to account for openings in the core. The modulus of elasticity E is assumed to be $38.2 * 10^{12}$ N/m^2, corresponding to uncracked concrete of C55/67, which is suitable for wind load in Serviceability Limit State.

G.4. Validation

The calculated natural frequency is validated against the first natural frequency calculated with the a method proved in NEN-EN 1991-1-4. This standardized approach provides an reference point, as it is based on Dutch national standards for structural design and is widely accepted for similar types of high-rise buildings. In the Eurocode the first natural frequency is estimated using Formula G.15, with h the height of the building.

$$f = 46/h \tag{G.15}$$

G.5. Output

This section presents the natural frequencies obtained for the analyzed buildings. Table G.1 summarizes the first natural frequencies for buildings with either exclusively concrete or CLT floors across various heights. These frequencies were determined using Rayleigh's method, the approach outlined in NEN 1991-1-4, and an SDOF-based method. The results from all three methods are consistent and fall within a comparable range.

Table G.1: Natural frequency calculated with different methods

Building height (m)	**Floor type**	n_{x1} **(Hz) Rayleigh's method**	n_{x1} **(Hz) SDOF method**	n_{x1} **(Hz) NEN 1991-1-4**
70	Concrete	0.652	0.699	0.645
90	Concrete	0.410	0.440	0.512
110	Concrete	0.332	0.357	0.424
70	CLT	0.788	0.845	0.645
90	CLT	0.495	0.531	0.512
110	CLT	0.397	0.425	0.424

H

Environmental performance

This appendix includes both theoretical and practical information related to the environmental performance of concrete and timber elements.

H.1. Carbon storage and emissions

H.1.1 Biogenic carbon storage and biogenic carbon content and GWP – Biogenic

Biogenic carbon storage refers to the carbon absorbed and temporarily stored in biomass during its lifecycle. It is crucial to quantify how much carbon is stored in the product and for how long. This carbon sequestration is accounted for in Stage A1: Raw Material Supply within the GWP – biogenic category as a negative emission since it temporarily removes CO2 from the atmosphere. The carbon emission is reported in Stage C3: Recycling under the same category as a positive value when the material is reused, recycled or incinerated. To calculate biogenic carbon storage, the biogenic carbon content of the material must be determined. Biogenic carbon content represents the total carbon present in a biomass-based material. It is the inherent carbon within the material, irrespective of the product's lifespan. It is typically expressed in kilograms of carbon (kg C) per unit defined [94, 95].

H.1.2 GWP – Fossil

The GWP – Fossil category includes the greenhouse gas emissions from the combustion of fossil fuels, which are released when coal, oil, natural gas, and fuels like diesel or gasoline are burned for energy production, transportation, or manufacturing. This category also encompasses emissions from fossil-based electricity and heat generation, as well as the production of fossil-derived materials. Additionally, it covers the extraction and refining processes associated with fossil fuels. When biobased products, such as wood or biomass, are incinerated, CO2 is released back into the atmosphere. However, in Stage D, energy recovery from these biobased materials can result in a benefit for GWP – Fossil, as the energy generated can displace the need for fossil fuels, thereby avoiding the CO2 emissions that would have been produced by burning fossil fuels for energy. This leads to a reduction in the overall carbon footprint and a positive contribution to Stage D by avoiding fossil fuel emissions [46].

H.2. Production stage

The production stage includes phases A1-A3, which cover raw material extraction, transportation, and manufacturing. The following describes the production processes for the primary materials used in the structural elements: concrete, CLT, and steel.

H.2.1 Concrete

The production of concrete consists of multiple stages, each contributing to its environmental impact as assessed through a Life Cycle Assessment. These stages are outlined below.

H.2.2 Stage A1: Raw material extraction

Cement production involves the mining and crushing of limestone, which is the primary raw material. Additional materials, such as clay, bauxite, and iron ore, are also be extracted for use in the cement manufacturing process. Aggregates like sand, gravel, and crushed stone are mined from quarries or riverbeds.Water is typically sourced locally to the concrete plant. Optional chemical admixtures are sourced from specialized suppliers. These can include materials like plasticizers, accelerators, or retarders.

H.2.3 Stage A2: Transport to manufacturing site

The raw materials for cement production are typically transported to the cement plant by road, rail, or ship. Once produced, the cement is transported to the concrete plant, usually by road. Aggregates and chemical admixtures used in concrete manufacturing are transported to the concrete plant via road, rail, or ship. Water can be sourced locally or transported to the concrete plant [96].

H.2.4 Stage A3: Manufacturing process

Two different manufacturing processes can be defined, the cement and concrete production. The cement manufacturing process involves clinker production, where raw materials are heated in a kiln. This process is highly energy-intensive and generates significant CO2 emissions due to the combustion of fossil fuels and the chemical transformation of limestone into lime. The resulting clinker is then ground with gypsum to produce cement powder. Concrete production involves proportioning the cement, aggregates, water, and optional admixtures according to the desired mix design. The raw materials are then combined in a concrete mixer to create a uniform concrete mix [97].

H.2.5 Types of cement

The type of cement used in concrete production has a significant impact on the environmental footprint, particularly in terms of CO2 emissions. Three different types of cement are available, CEMI, CEMII and CEMIII.

CEM I is composed almost entirely of clinker (95%). It has a high carbon footprint due to the energy-intensive process of clinker production, making it the least sustainable option for concrete production.

CEM II is a blend of clinker and supplementary materials such as fly ash or slag. This reduces the clinker content, resulting in lower CO2 emissions compared to CEM I. CEM II is a more sustainable choice for many construction applications, offering improved environmental performance while still maintaining adequate strength and durability.

CEM III contains a higher proportion of blast furnace slag, significantly reducing the amount of clinker required. As a result, it has the lowest carbon footprint of the three types of cement and is particularly beneficial in reducing CO2 emissions. It is often used in projects requiring high durability, such as in environments exposed to aggressive conditions division between three concrete classes C30/37, C55/67 and C70/85 for the different elements [98].

For a high-rise building utilizing C30/37 concrete for the floors and foundation, C55/67 for the walls, and C70/85 for the columns, the selection of cement should align with the necessary strength and durability while also emphasizing sustainability. CEM II or CEM III are preferable options due to their greater environmental sustainability, all the while providing sufficient strength. Although CEM I remains the conventional choice for high-strength requirements, CEM III can serve as a more sustainable alternative that still meets the strength demands of these structural elements.

H.2.6 Steel

Two different steel grades, S355 and F500, are used for the steel tubes in Tubex piles and steel reinforcement respectively. The production process of these materials involve the extraction and processing of raw materials and alloying and forming of steel products. The production stages are outlined below.

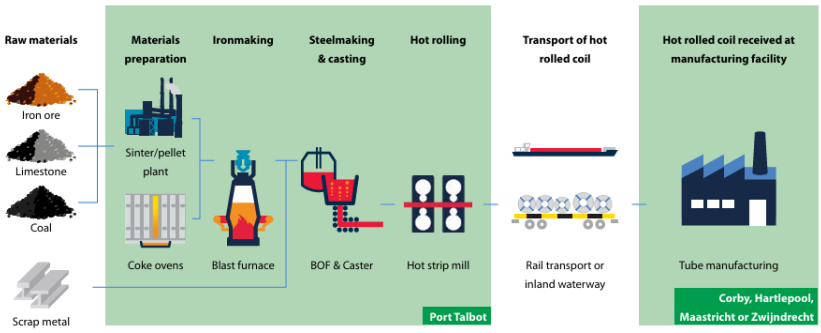

Figure H.1: Steel manufactoring process [99]

H.2.7 Stage A1: Raw material supply

Both steel grades primarily consist of iron and alloys such as carbon, manganese and silicon. The extraction and processing of these raw materials involve activities such as mining, beneficiation, and the production of alloying elements.

H.2.8 Stage A2: Transport to manufacturing site

The transport phase includes the movement of iron ore, scrap steel and alloying materials to steel mills. Typically, these materials for steel production are transported via ships, trains, or trucks.

H.2.9 Stage A3: Manufacturing

Both grades can be produced using blast furnace-basic oxygen furnace (BF-BOF) or electric arc furnace (EAF) routesIn the Netherlands, the primary method used for steel production is the blast furnace–basic oxygen furnace (BF-BOF) route, as illustrated in Figure H.1. The production of steel tubes with strength class S355 includes rolling and welding and surface treatment. The production of F500 steel requires additional alloying and heat treatment to achieve its higher yield strength [99].

H.2.10 CLT

The construction phase in the Life Cycle Assessment for CLT covers the extraction of raw materials, transportation and manufacturing of CLT panels and glulam beams.

H.2.11 Stage A1: Raw material supply

The production of CLT begins with the extraction of timber, typically sourced from sustainably managed forests. In addition to timber, adhesives are used in the manufacturing of CLT panels. Phenol-Resorcinol Formaldehyde (PRF) is a common adhesive in CLT production. The key raw materials for PRF are phenol, resorcinol, and formaldehyde, which are derived through petrochemical processes.

H.2.12 Stage A2: Transport to manufacturing site

This stage involves the transportation of timber logs and adhesives to the manufacturing site. The materials are typically transported by trucks, ships, or rail, depending on the location and infrastructure.

H.2.13 Stage A3: Manufactoring

The manufacturing process begins with sawmilling, where timber logs are processed into smaller components. For CLT production, the individual wood pieces are planed and dried. CLT panels are then created by gluing layers of wood together in perpendicular directions, forming a cross-laminated structure. In contrast, glulam beams are made by gluing lamellas together in parallel arrangements, with all layers running in the same direction.

To bond the layers together, structural adhesives such as Phenol-Resorcinol Formaldehyde or Melamine-Urea Formaldehyde (MUF) are used. For PRF production, phenol, resorcinol, and formaldehyde are combined under controlled heat and pressure in a polymerization reaction. The resin is then blended with other chemicals such as hardeners and stabilizers to improve its performance. The mixture is then heated to a curing temperature, allowing the adhesive to bond securely and ensure the durability of the

panels.

Once the layers are bonded, the CLT panels and glulam beams are pressed and cured. They are then cut to precise sizes for final installation, ensuring accuracy and strength in the finished product [22, 6].

H.3. Scenarios

In Table H.1, for each structural element and material two scenarios are given for stages C and D. The EPDs that are used per structural material are given in Table H.3.

Table H.1: Scenarios for Stage C and D for each material

Concrete C30/37 Floor system	**Scenario 1**	**Scenario 2**
Description	Concrete is recycled as a substrate in road costruction.	50% reused in new concrete applications, 50% reuse as substrate in road construction.
Stage C3	Crushing and sorting.	Crushing, sorting, washing, grading.
Stage D	Avoiding impact of production of road substrate from virgin material.	Avoiding impact of production of road substrate and concrete aggregates from virgin material.
Concrete C30/37 Foundation	**Scenario 1**	**Scenario 2**
Description	Assumed to be reused in new building at the same location	Foundation piles recycled as substrate in road construction.
Stage C3	X	Crushing and sorting.
Stage D	Avoiding impact of production of concrete from virgin material.	Avoiding impact of production of road substrate from virgin material.
Concrete C55/67 & C70/85 Columns and core	**Scenario 1**	**Scenario 2**
Description	Concrete is 100% reused as a substrate in road costruction.	50% recycled in new concrete applications, 50% recycled as a substrate in road construction.
Stage C3	Crushing and sorting.	Crushing, sorting, washing, grading.
Stage D	Avoiding impact of production of road substrate from virgin material.	Avoiding impact of production of road substrate and agrregates for concrete from virgin material.
Steel S355 Foundation	**Scenario 1**	**Scenario 2**
Description	Assumed to be be reused in new building.	100% recycle of steel of foundation plate and foundation piles.
Stage C3	X	Crushing and sorting.
Stage D	Avoided impact of production of steel tubes from virgin material	Avoiding impact of production of steel from virgin material.

Steel F500 Floor system, columns, core	**Scenario 1**	**Scenario 2**
Description	100% recycle of steel	100% recycle of steel
Stage C3	Crushing and sorting.	Crushing and sorting.
Stage D	Avoiding impact of production of steel from virgin material.	Avoiding impact of production of steel from virgin material.

Steel F500 Foundation	**Scenario 1**	**Scenario 2**
Description	Assumed to be reused in new building.	100% recycle of steel of foundation plate and foundation piles.
Stage C3	X	Crushing and sorting.
Stage D	Avoiding impact of production of steel from virgin material.	Avoiding impact of production of steel from virgin material.

CLT & glulam Floor system	**Scenario 1**	**Scenario 2**
Description	100% incineration with energy recovery	100% recycle to be used in particle board.
Stage C3	Crushing and sorting followed by wood combustion, during which biogenic carbon is released back into the atmosphere. This process generates thermal and electrical energy.	Sorting and preparing for recycling. Biogenic carbon is released back into the atmosphere.
Stage D	Avoided impacts include replacing natural gas for thermal energy and electric energy from European average grid mix.	Avoiding impact of production of particle boards from virgin wood.

TCC Floor system	**Scenario 1**	**Scenario 2**
Description	Concrete is 100% reused as a substrate in road construction and 100% of the CLT and Glulam is incinerated with energy recovery.	100% of the concrete is reused as a substrate in road construction, 75% of the CLT and 100% of the Glulam recycled into particle boards, and 25% of CLT is incinerated.
Stage C3	Crushing and sorting followed by wood combustion, during which biogenic carbon is released back into the atmosphere. This process generates thermal and electrical energy.	The process involves separating concrete and CLT, crushing the concrete, preparing CLT and Glulam for recycling. Biogenic carbon is released back into the atmosphere.
Stage D	Avoided impacts include replacing natural gas for thermal energy and electric energy.	Avoiding impact of production of virgin material for particle boards and road construction and incineration generates thermal and electrical energy.

H.3.1 Explanation of scenarios

Here further explanation is given on the chosen scenarios for the various materials. Recycling concrete for use as aggregates in new concrete requires an additional step: sifting the aggregates. It is assumed that 50% of the concrete is suitable for reuse in new concrete, while the remaining 50% is used as a substrate for road construction. Since information on stages C and D for recycling concrete into new concrete is not available, the data for recycling into road substrate is applied instead. This approach results in identical input data for both recycling pathways.

It is assumed that Tubex piles can be extracted from the soil and recycled. Although this practice is not currently implemented, nor is theoretical information available, it is envisioned as a future scenario within a circular economy. For the reuse of foundations in new buildings, it is assumed that 50% of the emissions in stage A can be allocated to stage D. Further details on this assumption are provided in Section H.5.

For CLT rib panels, the same EPD as for CLT panels is used. However, this is not entirely accurate, as the values for stages A, C, and D do not align between these two elements. In the EPD for CLT rib panels, it is assumed that the ribs are made of glulam beams, and that the panel recycling scenario involves wood chips rather than particle boards. When using the EPD for CLT rib panels, this would results in significantly higher ECI values compared to CLT and TCC panels. This is primarily due to differences in biogenic carbon emissions in Stages A and C, which are much smaller for CLT and TCC. Additionally, in Stage D, CLT rib panels contribute less to fossil emissions than the other two floor types. As a result, CLT rib panels lead to higher ECI values in both Scenario 1 and Scenario 2.

For CLT and Glulam, it has been decided to recycle these materials into particle boards rather than reuse them as structural elements. This choice was made because the emissions and benefits for stage C and D related to the reuse of Glulam are not available. For the recycling process of CLT and Glulam from TCC floors, it is assumed that 25% of the material is unsuitable for recycling due to contamination and will be incinerated. The emissions and benefits for stages C and D from both recycling and incineration are combined and weighted accordingly. Energy produced through incineration replaces natural gas for thermal energy and electric energy from European average grid mix.

H.4. Output

This section presents the Environmental Cost Index (ECI) per floor area of the analyzed buildings. Table H.2 summarizes the ECI values for various building variants. The table indicates that the ECI generally increases with building height, except for buildings with concrete floors. For all building variants, the ECI rises significantly when the building height reaches 110 meters, with this increase being more pronounced than the jump between 70 and 90 meters. Additionally, the ECI of buildings with concrete floors is consistently higher than that of buildings with timber floors.

Table H.2: Environmental Cost Index (ECI) per floor area for various Building variants

Building height (m)	Floor type	ECI (€/m^2) Scenario 1	ECI (€/m^2) Scenario 2
70	Concrete	27.1	29.8
90	Concrete	26.5	28.6
110	Concrete	33.0	34.5
70	CLT	13.5	19.1
90	CLT	14.8	19.6
110	CLT	21.6	25.9

H.5. LCA input data

In this section the Environmental Product Declarations (EPD) are given that are used in the LCA and the weight factors for calculating the ECI.

Table H.3: Environmental Product Declaration information

Structural element	Material	Nr.	Scenario	Stages	Company	Valid until	Location	Reference
Foundation piles	Concrete C30/37 CEMII	1	Reuse	A1-3, D	Swerock	25-9-2028	Norway	[100]
Foundation plate	Concrete C30/37 CEMII	1	Reuse	A1-3, D	Swerock	25-9-2028	Norway	[100]
Foundation piles	Concrete C30/37 CEMII	2	Recycle	A1-3, C3, D	Swerock	25-9-2028	Norway	[100]
Foundation plate	Concrete C30/37 CEMII	2	Recycle	A1-3, C3, D	Swerock	25-9-2028	Norway	[100]
Columns and core	Concrete C55/67 CEMI	1	Recycle	A1-3, C3, D	InformationsZentrum Beton GmbH	19-10-2028	Germany	[101]
Columns and core	Concrete C55/67 CEMI	2	Recycle	A1-3, C3, D	InformationsZentrum Beton GmbH	19-10-2028	Germany	[101]
Foundation piles	Steel tubes S355	1	Reuse	A1-3, D	Tata Steel	7-6-2027	Netherlands	[99]
Foundation piles	Steel tubes S355	2	Recycle	A1-3, C3, D	Tata Steel	7-6-2027	Netherlands	[99]
Foundation piles	Steel reinforcement F500	1	Reuse	A1-3, D	BE Group Sverige AB	7-6-2027	Sweden	[102]
Foundation plate	Steel reinforcement F500	2	Recycle	A1-3, C3, D	BE Group Sverige AB	7-6-2027	Sweden	[102]
Floor system	Steel reinforcement F500	1	Recycle	A1-3, C3, D	BE Group Sverige AB	7-6-2027	Sweden	[102]
Floor system	Steel reinforcement F500	2	Recycle	A1-3, C3, D	BE Group Sverige AB	7-6-2027	Sweden	[102]
Columns and core	Steel reinforcement F500	1	Recycle	A1-3, C3, D	BE Group Sverige AB	7-6-2027	Sweden	[102]
Columns and core	Steel reinforcement F500	2	Recycle	A1-3, C3, D	BE Group Sverige AB	7-6-2027	Sweden	[102]
Floor system	CLT - gl24	1	Incineration	A1-3, C3, D	Stora enso	10-6-2028	Austria	[103]
Floor system	CLT - gl24	2	Recycle	A1-3, C3, D	Stora enso	10-6-2028	Austria	[103]
Floor system	Glulam - gl28h	1	Incineration	A1-3, C3, D	Lilleheden A/S	2-8-2026	Austria	[104]
Floor system	Glulam - gl28h	2	Recycle	A1-3, C3, D	Lilleheden A/S	2-8-2026	Austria	[104]
Floor system	TCC - CLT gl24	1	Incineration	A1-3, C3, D	Stora enso	10-6-2028	Austria	[103]
Floor system	TCC - CLT gl24	2	Recycle	A1-3, C3, D	Stora enso	10-6-2028	Austria	[103]
Floor system	TCC - Concrete C30/37 CEMII	1	Recycle	A1-3, C3, D	Swerock	25-9-2028	Norway	[100]
Floor system	TCC - Concrete C30/37 CEMII	2	Recycle	A1-3, C3, D	Swerock	25-9-2028	Norway	[100]
Floor system	Concrete C30/37 CEMII	1	Recycle	A1-3, C3, D	Swerock	25-9-2028	Norway	[100]
Floor system	ConcreteC30/37 CEMII	2	Recycle	A1-3, C3, D	Swerock	25-9-2028	Norway	[100]

H.5.1 Explanation choice EPDs

Here an explanation is given on the specific EPDs chosen for the structural elements per scenario.

Concrete foundation

In Scenario 1, it is assumed that the concrete used in the foundation plate and piles will be reused in a new building. The foundation has an estimated lifespan of 100 years, while the building is demolished after 50 years. Based on this, half of the emissions from Stage A1-3 can be attributed to Stage D. The remaining lifespan of the foundation relative to its initial design lifespan is assessed, and the benefit in Stage D is calculated as the avoided impacts of producing a new foundation for the subsequent building. It is not accounted for that the lifespan of the new building might exceed the remaining lifespan of the reused foundation.

Concrete class C55/67

For concrete classes C55/67 and C70/85, the same EPD for C55/67 is used due to the absence of specific data for C70/85. This practical solution is allowed as both are high-strength concrete classes used in similar structural elements that provide vertical load resistance and have the same durability class. The cement composition for both classes is assumed to be approximately equivalent.

TCC floor panels

No EPD data is available for TCC floors that combine concrete and CLT. For Scenario 1, it is assumed that the two materials can be separated, and the CLT is incinerated. For this potential contamination is not considered an issue. In Scenario 2, it is assumed that the CLT is recycled, with 75% suitable for recycling and 25% incinerated. The data for Stages C and D are adjusted accordingly to reflect a balanced combination of these two end-of-life scenarios.

In the tables below the EPDs are given that ar used as input for the LCA.

Table H.4: EPD Concrete C30/37 foundation piles - Scenario 1 [100]

Environmental impact category	**Unit**	**A1-3**	**C3**	**C4**	**D**
GWPtotal	kg CO2 eq	2,51E+02	0,00E+00	0,00E+00	-1,26E+02
GWPfossil	kg CO2 eq	2,51E+02	0,00E+00	0,00E+00	-1,26E+02
GWPbiogenic	kg CO2 eq	2,00E-01	0,00E+00	0,00E+00	-1,00E-01
GWPluluc	kg CO2 eq	2,00E-01	0,00E+00	0,00E+00	-1,00E-01
ODP	kg CFC11 eq	3,04E-06	0,00E+00	0,00E+00	-1,52E-06
AP	mol H+ eq	4,35E-01	0,00E+00	0,00E+00	-2,18E-01
EPfresh	kg P eq	1,51E-02	0,00E+00	0,00E+00	-7,55E-03
EPmarine	kg N eq	4,75E-02	0,00E+00	0,00E+00	-2,38E-02
EPter	mol N eq	1,69E+00	0,00E+00	0,00E+00	-8,45E-01
POCP	kg NMVOC eq	4,08E-01	0,00E+00	0,00E+00	-2,04E-01
WDP	m3	1,32E+02	0,00E+00	0,00E+00	-6,60E+01
ADPE	kg Sb eq	5,50E-05	0,00E+00	0,00E+00	-2,75E-05
ADPF	MJ	9,47E+02	0,00E+00	0,00E+00	-4,74E+02
Company	Swerock				
Unit	m3				
Density	kg/m3	2332			

Table H.5: EPD Concrete C55/67 columns and core - Scenario 1 and 2 [101]

Environmental impact category	Unit	A1-3	C3	C4	D
GWPtotal	kg CO2 eq	2,86E+02	5,05E+00	0,00E+00	-1,21E+01
GWPfossil	kg CO2 eq	2,86E+02	4,99E+00	0,00E+00	-1,20E+01
GWPbiogenic	kg CO2 eq	4,61E-01	5,05E-02	0,00E+00	-1,06E-01
GWPluluc	kg CO2 eq	8,40E-02	1,14E-02	0,00E+00	-2,02E-02
ODP	kg CFC11 eq	7,19E-08	7,61E-11	0,00E+00	1,50E-10
AP	mol H+ eq	4,61E-01	1,67E-02	0,00E+00	-2,90E-02
EPfresh	kg P eq	3,28E-04	1,91E-05	0,00E+00	-4,02E-05
EPmarine	kg N eq	1,42E-01	7,44E-03	0,00E+00	-1,11E-02
EPter	mol N eq	1,63E+00	8,14E-02	0,00E+00	-1,25E-01
POCP	kg NMVOC eq	3,86E-01	2,04E-02	0,00E+00	-2,69E-02
WDP	m3	5,17E+00	7,30E-03	0,00E+00	-2,94E+00
ADPE	kg Sb eq	2,33E-05	1,85E-06	0,00E+00	-3,67E-06
ADPF	MJ	1,46E+03	6,53E+01	0,00E+00	-1,56E+02
Name Company	InformationsZentrum Beton GmbH				
Unit	m3				
Density	kg/m3	2400			

Table H.6: EPD Steel tubes S355 foundation - Scenario 1 [99]

Environmental impact category	Unit	A1-3	C3	C4	D
GWPtotal	kg CO2 eq	2,59E+03	0,00E+00	0,00E+00	-1,30E+03
GWPfossil	kg CO2 eq	2,59E+03	0,00E+00	0,00E+00	-1,30E+03
GWPbiogenic	kg CO2 eq	2,23E+00	0,00E+00	0,00E+00	-1,12E+00
GWPluluc	kg CO2 eq	5,21E+01	0,00E+00	0,00E+00	-2,61E+01
ODP	kg CFC11 eq	7,30E-10	0,00E+00	0,00E+00	-3,65E-10
AP	mol H+ eq	7,33E+00	0,00E+00	0,00E+00	-3,67E+00
EPfresh	kg P eq	6,57E-04	0,00E+00	0,00E+00	-3,29E-04
EPmarine	kg N eq	1,67E+00	0,00E+00	0,00E+00	-8,35E-01
EPter	mol N eq	1,76E+01	0,00E+00	0,00E+00	-8,80E+00
POCP	kg NMVOC eq	5,92E+00	0,00E+00	0,00E+00	-2,96E+00
WDP	m3	5,69E+02	0,00E+00	0,00E+00	-2,85E+02
ADPE	kg Sb eq	2,51E-04	0,00E+00	0,00E+00	-1,26E-04
ADPF	MJ	2,65E+04	0,00E+00	0,00E+00	-1,33E+04
Company	Tata Steel				
Unit	kg	1000			
Density	kg/m3	7850			

Table H.7: EPD Steel reinforcement F500 foundation - Scenario 1 [102]

Environmental impact category	Unit	A1-3	C3	C4	D
GWPtotal	kg CO2 eq	5,63E-01	0,00E+00	0,00E+00	-2,82E-01
GWPfossil	kg CO2 eq	5,53E-01	0,00E+00	0,00E+00	-2,77E-01
GWPbiogenic	kg CO2 eq	1,01E-02	0,00E+00	0,00E+00	-5,05E-03
GWPluluc	kg CO2 eq	6,72E-04	0,00E+00	0,00E+00	-3,36E-04
ODP	kg CFC11 eq	6,75E-08	0,00E+00	0,00E+00	-3,38E-08
AP	mol H+ eq	3,41E-03	0,00E+00	0,00E+00	-1,71E-03
EPfresh	kg P eq	3,53E-05	0,00E+00	0,00E+00	-1,77E-05
EPmarine	kg N eq	8,31E-04	0,00E+00	0,00E+00	-4,16E-04
EPter	mol N eq	9,45E-03	0,00E+00	0,00E+00	-4,73E-03
POCP	kg NMVOC eq	3,04E-03	0,00E+00	0,00E+00	-1,52E-03
WDP	m3	4,28E-01	0,00E+00	0,00E+00	-2,14E-01
ADPE	kg Sb eq	4,43E-06	0,00E+00	0,00E+00	-2,22E-06
ADPF	MJ	1,14E+01	0,00E+00	0,00E+00	-5,70E+00
Company	BE Group Sverige AB				
Unit	kg				
Density	kg/m3	7850			

Table H.8: EPD Steel reinforcement F500 floors, columns and core - Scenario 1 and 2, foundation piles and plate - Scenario 2 [102]

Environmental impact category	Unit	A1-3	C3	C4	D
GWPtotal	kg CO2 eq	5,63E-01	2,21E-02	2,64E-04	7,17E-02
GWPfossil	kg CO2 eq	5,53E-01	2,34E-02	2,63E-04	7,22E-02
GWPbiogenic	kg CO2 eq	1,01E-02	-1,34E-03	5,22E-07	-5,36E-04
GWPluluc	kg CO2 eq	6,72E-04	2,66E-05	7,82E-08	-2,00E-06
ODP	kg CFC11 eq	6,75E-08	3,37E-09	1,08E-10	1,92E-09
AP	mol H+ eq	3,41E-03	2,84E-04	2,50E-06	2,79E-04
EPfresh	kg P eq	3,53E-05	1,62E-06	3,18E-09	2,90E-06
EPmarine	kg N eq	8,31E-04	6,27E-05	8,61E-07	5,48E-05
EPter	mol N eq	9,45E-03	7,28E-04	9,48E-06	5,80E-04
POCP	kg NMVOC eq	3,04E-03	1,99E-04	2,75E-06	3,79E-04
WDP	m3	4,28E-01	4,61E-03	3,40E-04	1,03E-02
ADPE	kg Sb eq	4,43E-06	1,30E-06	2,41E-09	7,17E-08
ADPF	MJ	1,14E+01	3,25E-01	7,36E-03	5,33E-01
Company	BE Group Sverige AB				
Unit	kg				
Density	kg/m3	7850			

Table H.9: EPD CLT - Scenario, TCC - CLT - Scenario 1 [79]

Environmental impact category	Unit	A1-3	C3	C4	D
GWPtotal	kg CO2 eq	-7,08E+02	7,82E+02	0,00E+00	-2,68E+02
GWPfossil	kg CO2 eq	5,26E+01	2,02E+01	0,00E+00	-2,67E+02
GWPbiogenic	kg CO2 eq	-7,26E+02	7,62E+02	0,00E+00	-7,51E-01
GWPluluc	kg CO2 eq	8,78E-01	2,27E-03	0,00E+00	-2,77E-01
ODP	kg CFC11 eq	9,15E-06	2,26E-07	0,00E+00	-2,86E-05
AP	mol H+ eq	3,11E-01	1,75E-06	0,00E+00	-7,43E-01
EPfresh	kg P eq	6,35E-03	2,04E-01	0,00E+00	-1,25E-02
EPmarine	kg N eq	9,19E-02	1,01E-04	0,00E+00	-1,17E-01
EPter	mol N eq	1,06E+01	9,41E-02	0,00E+00	-1,32E+00
POCP	kg NMVOC eq	4,65E-01	1,07E+00	0,00E+00	-3,90E-01
WDP	m3	2,09E+01	1,21E+00	0,00E+00	2,79E+01
ADPE	kg Sb eq	2,21E-04	2,00E-04	0,00E+00	-1,40E-04
ADPF	MJ	8,16E+02	1,21E+02	0,00E+00	-5,07E+03
Company	Stora enso				
Unit	m3				
Density	kg/m3	470			

Table H.10: EPD Glulam - Scenario 1 [104]

Environmental impact category	Unit	A1-3	C3	C4	D
GWPtotal	kg CO2 eq	-5,56E+02	6,91E+02	0,00E+00	-3,57E+02
GWPfossil	kg CO2 eq	1,22E+02	1,24E+01	0,00E+00	-3,57E+02
GWPbiogenic	kg CO2 eq	-6,78E+02	6,78E+02	0,00E+00	-3,23E-01
GWPluluc	kg CO2 eq	5,27E-01	1,04E-02	0,00E+00	-1,78E-01
ODP	kg CFC11 eq	1,10E-05	1,08E-13	0,00E+00	-2,34E-12
AP	mol H+ eq	7,34E-01	1,41E-01	0,00E+00	-2,75E-01
EPfresh	kg P eq	1,56E-02	2,29E-05	0,00E+00	-4,47E-04
EPmarine	kg N eq	2,59E-01	3,55E-02	0,00E+00	-1,07E-01
EPter	mol N eq	2,92E+00	6,06E-01	0,00E+00	-1,13E+00
POCP	kg NMVOC eq	7,22E-01	9,42E-02	0,00E+00	-2,90E-01
WDP	m3	5,05E+01	7,66E+01	0,00E+00	-6,81E+00
ADPE	kg Sb eq	1,62E-03	1,68E-06	0,00E+00	-3,72E-05
ADPF	MJ	2,13E+03	1,56E+02	0,00E+00	-5,64E+03
Company	Lilleheden A/S				
Unit	m3				
Density	kg/m3	470			

Table H.11: EPD Concrete C30/37 floors - Scenario 1 and 2, foundation piles and plate - Scenario 1 [100]

Environmental impact category	Unit	A1-3	C3	C4	D
GWPtotal	kg CO2 eq	2,51E+02	1,50E+00	0,00E+00	-3,40E+00
GWPfossil	kg CO2 eq	2,51E+02	1,40E+00	0,00E+00	-3,30E+00
GWPbiogenic	kg CO2 eq	2,00E-01	0,00E+00	0,00E+00	0,00E+00
GWPluluc	kg CO2 eq	2,00E-01	0,00E+00	0,00E+00	0,00E+00
ODP	kg CFC11 eq	3,04E-06	1,86E-16	0,00E+00	-1,01E-14
AP	mol H+ eq	4,35E-01	8,40E-03	0,00E+00	-1,83E-02
EPfresh	kg P eq	1,51E-02	4,33E-06	0,00E+00	-2,50E-05
EPmarine	kg N eq	4,75E-02	4,11E-03	0,00E+00	-8,72E-03
EPter	mol N eq	1,69E+00	4,55E-02	0,00E+00	-9,42E-02
POCP	kg NMVOC eq	4,08E-01	7,92E-03	0,00E+00	-1,70E-02
WDP	m3	1,32E+02	1,27E-02	0,00E+00	-3,10E+01
ADPE	kg Sb eq	5,50E-05	1,11E-07	0,00E+00	-5,92E-07
ADPF	MJ	9,47E+02	1,94E+01	0,00E+00	-7,84E+01
Company	Swerock				
Unit	m3				
Density	kg/m3	2332			

Table H.12: EPD Steel tubes S355 foundation - Scenario 2 [99]

Environmental impact category	Unit	A1-3	C3	C4	D
GWPtotal	kg CO2 eq	2,59E+03	1,02E+00	1,45E-01	-1,61E+03
GWPfossil	kg CO2 eq	2,59E+03	1,02E+00	1,49E-01	-1,61E+03
GWPbiogenic	kg CO2 eq	2,23E+00	4,75E-03	-4,42E-03	-9,84E-01
GWPluluc	kg CO2 eq	5,21E+01	5,92E-05	2,75E-04	-6,22E-02
ODP	kg CFC11 eq	7,30E-10	5,05E-12	3,51E-13	-5,36E-11
AP	mol H+ eq	7,33E+00	1,43E-03	1,06E-03	-3,02E+00
EPfresh	kg P eq	6,57E-04	1,05E-06	2,53E-07	-3,56E-04
EPmarine	kg N eq	1,67E+00	4,39E-04	2,71E-04	-5,99E-01
EPter	mol N eq	1,76E+01	4,77E-03	2,97E-03	-6,09E+00
POCP	kg NMVOC eq	5,92E+00	1,38E-03	8,22E-04	-2,58E+00
WDP	m3	5,69E+02	4,33E-02	1,64E-02	-4,02E+03
ADPE	kg Sb eq	2,51E-04	1,05E-07	1,53E-08	-3,65E-03
ADPF	MJ	2,65E+04	1,51E+01	1,95E+00	-1,59E+04
Company	Tata Steel				
Unit	kg	1000			
Density	kg/m3	7850			

Table H.13: EPD CLT - Scenario 2 [79]

Environmental impact category	Unit	A1-3	C3	C4	D
GWPtotal	kg CO2 eq	-7,08E+02	7,68E+02	0,00E+00	-1,62E+01
GWPfossil	kg CO2 eq	5,26E+01	5,52E+00	0,00E+00	-1,59E+01
GWPbiogenic	kg CO2 eq	-7,26E+02	7,62E+02	0,00E+00	-1,63E-01
GWPluluc	kg CO2 eq	8,78E-01	5,51E-04	0,00E+00	-1,81E-01
ODP	kg CFC11 eq	9,15E-06	1,18E-06	0,00E+00	-1,12E-06
AP	mol H+ eq	3,11E-01	5,73E-02	0,00E+00	-1,33E-01
EPfresh	kg P eq	6,35E-03	1,83E-05	0,00E+00	-2,34E-03
EPmarine	kg N eq	9,19E-02	2,54E-02	0,00E+00	-3,45E-02
EPter	mol N eq	1,06E+01	2,78E-01	0,00E+00	-4,02E-01
POCP	kg NMVOC eq	4,65E-01	7,65E-02	0,00E+00	-1,35E-01
WDP	m3	2,09E+01	1,08E-01	0,00E+00	-2,01E+01
ADPE	kg Sb eq	2,21E-04	2,84E-06	0,00E+00	-1,55E-04
ADPF	MJ	8,16E+02	7,57E+01	0,00E+00	-3,37E+02
Company	Stora Enso				
Unit	m3				
Density	kg/m3	470			

Table H.14: EPD Glulam - Scenario 2 [104]

Environmental impact category	Unit	A1-3	C3	C4	D
GWPtotal	kg CO2 eq	-5,56E+02	6,82E+02	0,00E+00	-7,24E+02
GWPfossil	kg CO2 eq	1,22E+02	2,11E+00	0,00E+00	4,11E+01
GWPbiogenic	kg CO2 eq	-6,78E+02	6,80E+02	0,00E+00	-6,80E+02
GWPluluc	kg CO2 eq	5,27E-01	5,15E-03	0,00E+00	-2,40E-01
ODP	kg CFC11 eq	1,10E-05	6,89E-14	0,00E+00	-2,91E-06
AP	mol H+ eq	7,34E-01	3,68E-03	0,00E+00	-2,64E-01
EPfresh	kg P eq	1,56E-02	1,31E-05	0,00E+00	-1,65E-02
EPmarine	kg N eq	2,59E-01	1,24E-03	0,00E+00	7,45E-02
EPter	mol N eq	2,92E+00	1,21E-02	0,00E+00	-8,02E-01
POCP	kg NMVOC eq	7,22E-01	2,98E-03	0,00E+00	-2,33E-01
WDP	m3	5,05E+01	1,99E-01	0,00E+00	-1,05E+01
ADPE	kg Sb eq	1,62E-03	1,05E-06	0,00E+00	-9,25E-05
ADPF	MJ	2,13E+03	2,55E+01	0,00E+00	-6,60E+02
Company	Lilleheden A/S				
Unit	m3				
Density	kg/m3	470			

Table H.15: EPD TCC - CLT - Scenario 2 [79]

Environmental impact category	Unit	A1-3	C3	C4	D
GWPtotal	kg CO2 eq	-7,08E+02	7,72E+02	0,00E+00	-7,92E+01
GWPfossil	kg CO2 eq	5,26E+01	9,19E+00	0,00E+00	-7,87E+01
GWPbiogenic	kg CO2 eq	-7,26E+02	7,62E+02	0,00E+00	-3,10E-01
GWPluluc	kg CO2 eq	8,78E-01	9,81E-04	0,00E+00	-2,05E-01
ODP	kg CFC11 eq	9,15E-06	9,42E-07	0,00E+00	-7,99E-06
AP	mol H+ eq	3,11E-01	4,30E-02	0,00E+00	-2,86E-01
EPfresh	kg P eq	6,35E-03	5,10E-02	0,00E+00	-4,88E-03
EPmarine	kg N eq	9,19E-02	1,91E-02	0,00E+00	-5,51E-02
EPter	mol N eq	1,06E+01	2,32E-01	0,00E+00	-6,32E-01
POCP	kg NMVOC eq	4,65E-01	3,25E-01	0,00E+00	-1,99E-01
WDP	m3	2,09E+01	3,84E-01	0,00E+00	-8,10E+00
ADPE	kg Sb eq	2,21E-04	5,21E-05	0,00E+00	-1,51E-04
ADPF	MJ	8,16E+02	8,70E+01	0,00E+00	-1,52E+03
Company	Stora Enso				
Unit	m3				
Density	kg/m3	470			

Table H.16: Weight factor environmental impact categories

Impact categorie	Abriviation	Value (€)
Global Warming Potential total	GWPtotal	0,116
Global Warming Potential fossil fuels	GWPfossil	0,116
Global Warming Potential biogenic	FWPbiogenic	0,116
Global Warming Potential luluc	GWPluluc	0,116
Depletion potential of the stratospheric ozone layer	ODP	32
Acidification potential of land and water	AP	0,39
Eutrophication potential aquatic freshwater	Epfresh	1,96
Eutrophication potential aquatic marine (EPmarine)	EPmarine	3,28
Eutrophication potential terrestrial (EPterrestrial)	EPter	0,36
Formation potential of tropospheric ozone photochemical oxidants	POCP	1,22
Water use	WDP	0,00506
Abiotic depletion potential for non fossil resources	ADPE	0,3
Abiotic depletion potential for fossil resources	ADPF	0,00033

I

Building cost

This appendix includes both theoretical and practical information related to the material cost and construction process of tall concrete-timber buildings.

I.1. Material cost data

I.2. Construction process

The construction process is divided into subprocesses. Per subprocess there are several steps. In I.1 these steps are followed with the corresponding material and, equipemeent and type of workers.

Table I.1: Construction processes

Process	Step	Description
Construction site	1	Installing a construction fence
	2	Applying foundation layer
	3	Installing steel road plate
	4	Cleaning up soil
	5	Placing prefabricated cabin
	6	Laying temporary pipes
	7	Installing a temporary energy supply
	8	Assembling distribution and storage facility
	9	Assembling construction crane
Foundation pit/ Foundation piles	10	Installing sheet piles
	11	Installing piles formed in the ground
	11	welding pipe parts
	12	bentonite injection, grout injection
	13	Install reinforcement
	14	Pouring cast-in-place reinforced concrete.
	15	Excavate construction pits
	16	Installing pump installation
	17	Install steel stuts
Foundation plate	18	Formwork for foundation plate
	19	Install reinforcement
	20	Pouring cast-in-place reinforced concrete
Concrete core	21	Install climbing formwork
	22	Install reinforcement
	23	Pouring cast-in-place reinforced concrete.
	24	raise formwork.
	25	De-install climbing formwork
Concrete column	25	Install reinforcement
	27	Make and install framework column.
	28	Pouring cast-in-place reinforced concrete.
	29	Remove formwork
Concrete floor and beams	30	Make and install formwork floor
	30	Make and install formwork beam
	31	Install reinforcement
	32	Pouring cast-in-place reinforced concrete
	33	Remove formwork floor and beam
CLT floor and beams	34	Applying beam layer to the floor
	35	Installing a CLT panel.
TCC floor and beams	36	Applying beam layer to the floor
	37	Installing a CLT panel
	38	Install reinforcement
	39	Pouring cast-in-place reinforced concrete layer
CLT rib panel floor and beams	40	Applying beam layer to the floor
	41	Installing a CLT rib panel floor
Demolishing construction site	42	Removing storage facility
	43	Removing temporary pipes
	44	Removing prefabricated cabin
	45	Remove crane
	46	Deinstalling steel road plate
	47	Deinstalling a construction fence

Figure I.1: Set up construction site

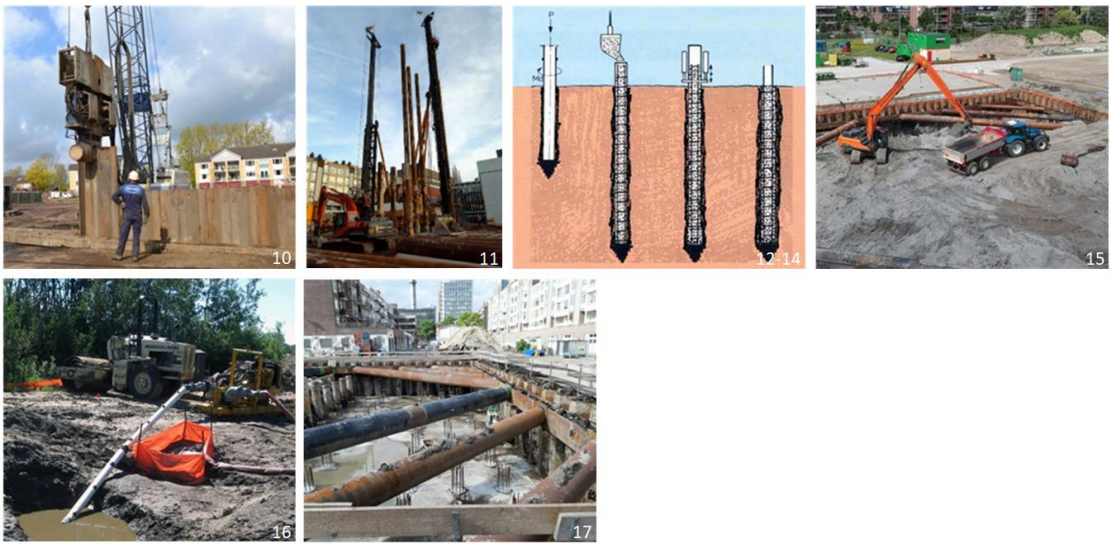

Figure I.2: Excavate foundation pit and foundation piles

Figure I.3: Construct foundation plate

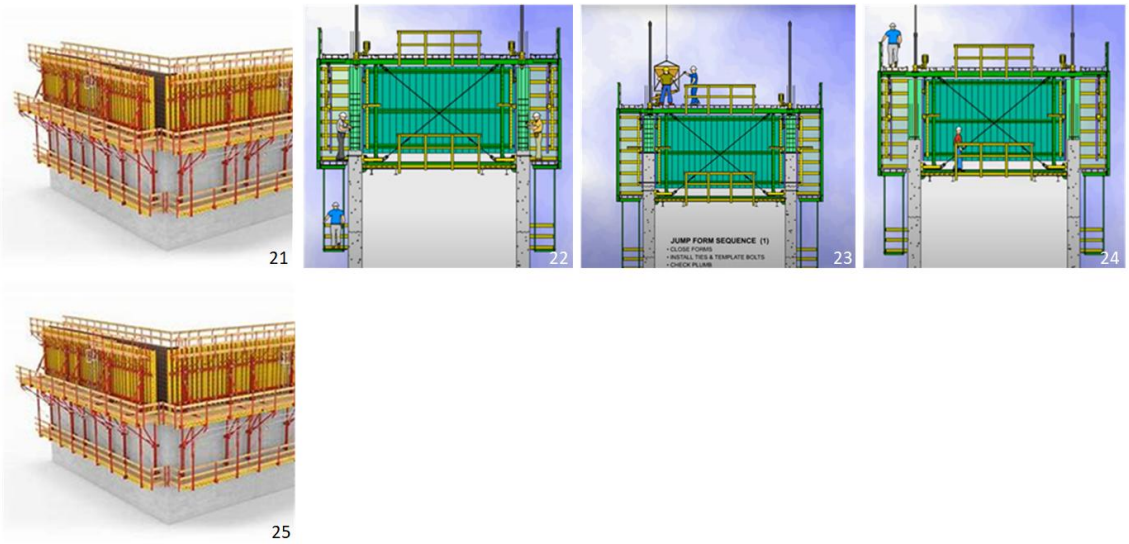

Figure I.4: Construct concrete core

Figure I.5: Construct concrete column

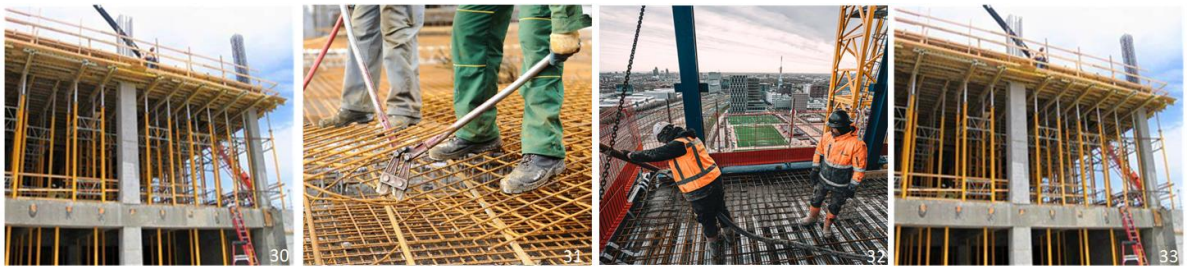

Figure I.6: Concrete floor

Figure I.7: Construct CLT floor

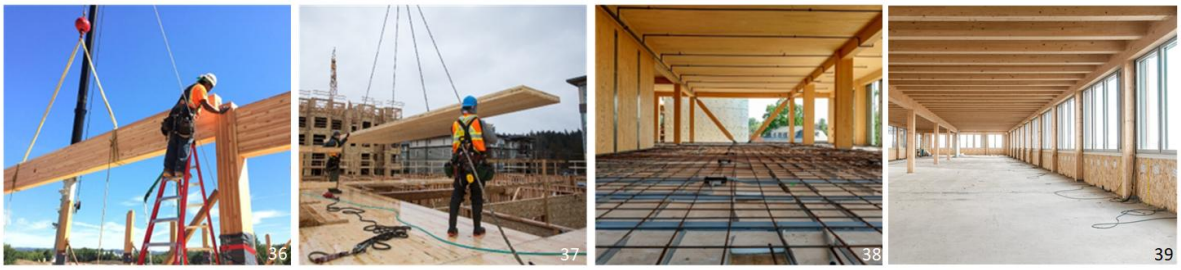

Figure I.8: Construct TCC floor

Figure I.9: Construct CLT rib panel floor

I.3. Cost data and calculations

Figure I.10 shows the cost data and the calculations based on the dimensions of the structural elements.

structural element/process	**value**	**unit**	**cost per unit**		**cost**
excavation and removal groundwork					
volume pit	1225	m3			
excavation depth	2	m			
excavation (excavator)	61,25	uur	€ 104,85		€ 6.421,79
removal transport	153	trucks	€ 85,19		€ 13.044,26
dumping costs	1225	m3	€ 4,59		€ 5.619,07
total cost excavation	1225	m3	€ 20,48		**€ 25.085,12**
steel sheet pile AZ 26 - temporary					
area	2520	m2			
scheet length	140	m			
pile length	18	m			
rent sheet pile	155	kg/m2			
total rent sheet pile	390600	kg	€ 0,52		€ 204.763,42
loss/cleaning	2520	m2	€ 7,86		€ 19.815,81
vibrating/dimensioning	2520	m2	€ 27,52		€ 69.355,35
pulling sheet pile	2520	m2	€ 23,59		€ 59.447,44
total cost sheet piles	2520	m2	€ 140,23		**€ 353.382,03**
steel tube prop frame					
steel tube	280	kg/m			
area	2040	m2			
corners	12	m			
tube length	170	m			
auxiliary posts	2040	m2			
rent tube profile	47,6	ton	€ 589,76		€ 28.072,40
application incl. cutting/welding	16	pc	€ 1.113,98		€ 17.823,75
head plates	32	pc	€ 85,19		€ 2.725,99
disassembly	16	m2	€ 294,88		€ 4.718,05
transport costs	47,6	m2	€ 32,76		€ 1.559,58
assembly	470	m	€ 72,08		€ 33.878,23
auxiliary posts	9	pc	€ 1.179,51		€ 10.615,62
various, loss	1024	m2	€ 7,86		€ 8.052,14
total cost steel tube prop frame	2040	m2	€ 52,67		**€ 107.445,75**
tubex palen					
diameter	720	mm			
pile length	55	m			
total cost per pile	55	m	€ 694,60		**€ 38.203,11**
foundation plate					
area	1024	m2			
thickness	2	m			
reinforcement foundation plateamount	80	kg/m3			
leveling sand	1024	m2	€ 3,93		€ 4.026,07
labour floor	1024	m2	€ 11,80		€ 12.078,21
miscellaneous	128	m	€ 23,59		€ 3.019,55
concrete delivery foundation	2048	m3	€ 115,33		€ 236.196,12
concrete pouring	2048	m3	€ 23,59		€ 48.312,84
reinforcement	163840	kg	€ 1,44		€ 236.196,12
crane costs, pump costs	2048	m3	€ 11,80		€ 24.156,42
miscellaneous	1024	m2	€ 3,93		€ 4.026,07
total cost foundation plate	1024	m2	**€ 554,70**		**€ 568.011,42**

structural element/process	value	unit	cost per unit		cost
concrete core wall					
m1 core wall horizontal	97	m			
formwork insert wall + floor core	628	m2	€ 1.729,95		€ 1.085.655,65
labor formwork + pouring core	627,564	m2	€ 49,80		€ 31.253,72
concrete delivery core	1	m3	€ 133,68		€ 133,68
reinforcement core	1	kg	€ 1,57		€ 1,57
pumping costs core	1	m3	€ 34,07		€ 34,07
miscellaneous core	627,564	m2	€ 7,86		€ 4.934,80
concrete column					
area column	0,28	m2			
reinforcement column amount	80	kg/m3			
height column	3,1	m			
formwork column	6,82	m2/pc	€ 419,38		€ 2.860,19
labour formwork column	1	pc	€ 176,93		€ 176,93
concrete material	0,868	m3	€ 133,68		€ 116,03
pour concrete	0,868	m3	€ 45,87		€ 39,82
reinforcement concrete	69,44	kg	€ 1,44		€ 100,11
miscellaneous	1	pc	€ 19,66		€ 19,66
total per column	1	pc			**€ 3.312,73**
in-situ concrete beam					
reinforcement beam amount	100	kg/m3			
formwork material incl edge form	1	m2	€ 36,70		€ 36,70
setting, demoulding	1	m2	€ 76,01		€ 76,01
concrete delivery	1	m3	€ 133,68		€ 133,68
pour concrete beam	1	m3	€ 36,70		€ 36,70
reinforcement concrete beam	1	kg	€ 1,44		€ 1,44
in-situ concrete floor					
reinforcement floor amount	50	kg/m3			
install concrete floor	1	m3	€ 786,34		€ 786,34
reinforcement floor	1	kg	€ 1,44		€ 1,44
CLT (rib) floor					
CLT floor installation	1	m3	€ 1.400,00		€ 1.400,00
TCC floor					
CLT floor installation 2	1	m3	€ 1.400,00		€ 1.400,00
concrete top layer	1	m3	€ 400,00		€ 400,00
glulam beam					
install glulam beam	1	m3	€ 1.400,00		€ 1.400,00

Figure I.10: Construction cost data

J

Additional results

This appendix presents additional results that are not included in Chapter 9 due to their limited impact on the conclusions. Additionally, these results are discussed.

J.1. Relation between environmental and dynamic performance

Figure J.1 presents the environmental cost index (ECI) value plotted against the natural frequency, with building variants grouped by floor type. In the graph for scenario 1, a clear grouping of dots is visible, while in scenario 2, the results for the floor types appear more scattered.

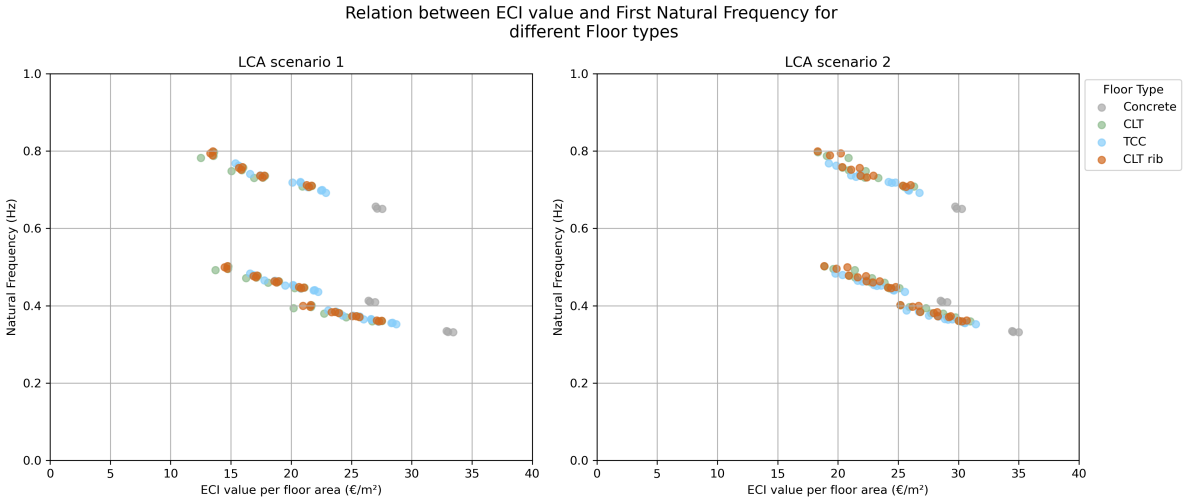

Figure J.1: ECI and first natural frequency correlation across floor type

Figure J.2 presents the ECI value plotted against the natural frequency, with building variants grouped by floor plan. The graph shows an even distribution of building variants within each floor plan. This suggests that the influence of floor plan on the relationship between ECI and dynamic behavior is minimal.

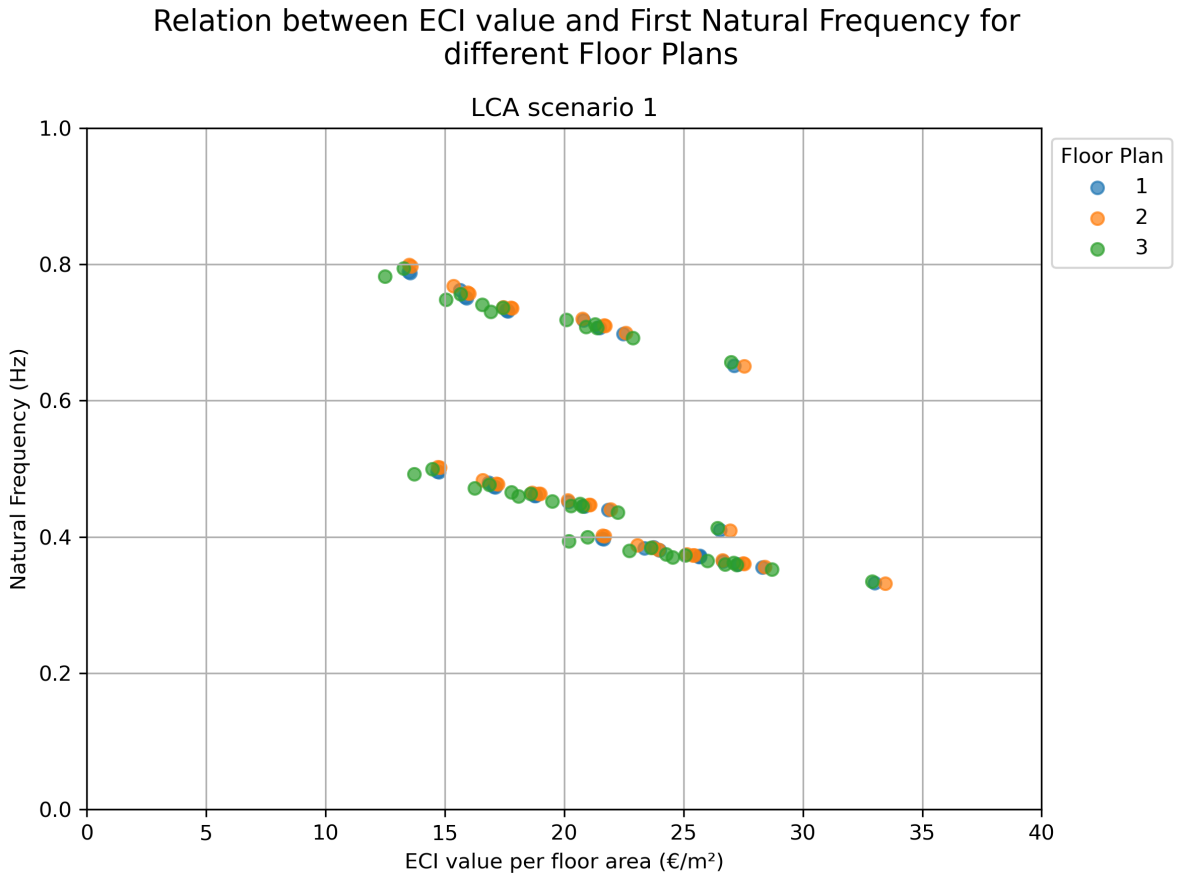

Figure J.2: ECI and first natural frequency correlation across floor plan

J.2. Relation between dynamic performance and construction cost

Figure J.3 presents the construction cost plotted against the natural frequency, with building variants grouped by floor type. The graph shows a wide range of costs for different floor types, indicating significant variability. No clear correlation between construction cost and natural frequency is observed.

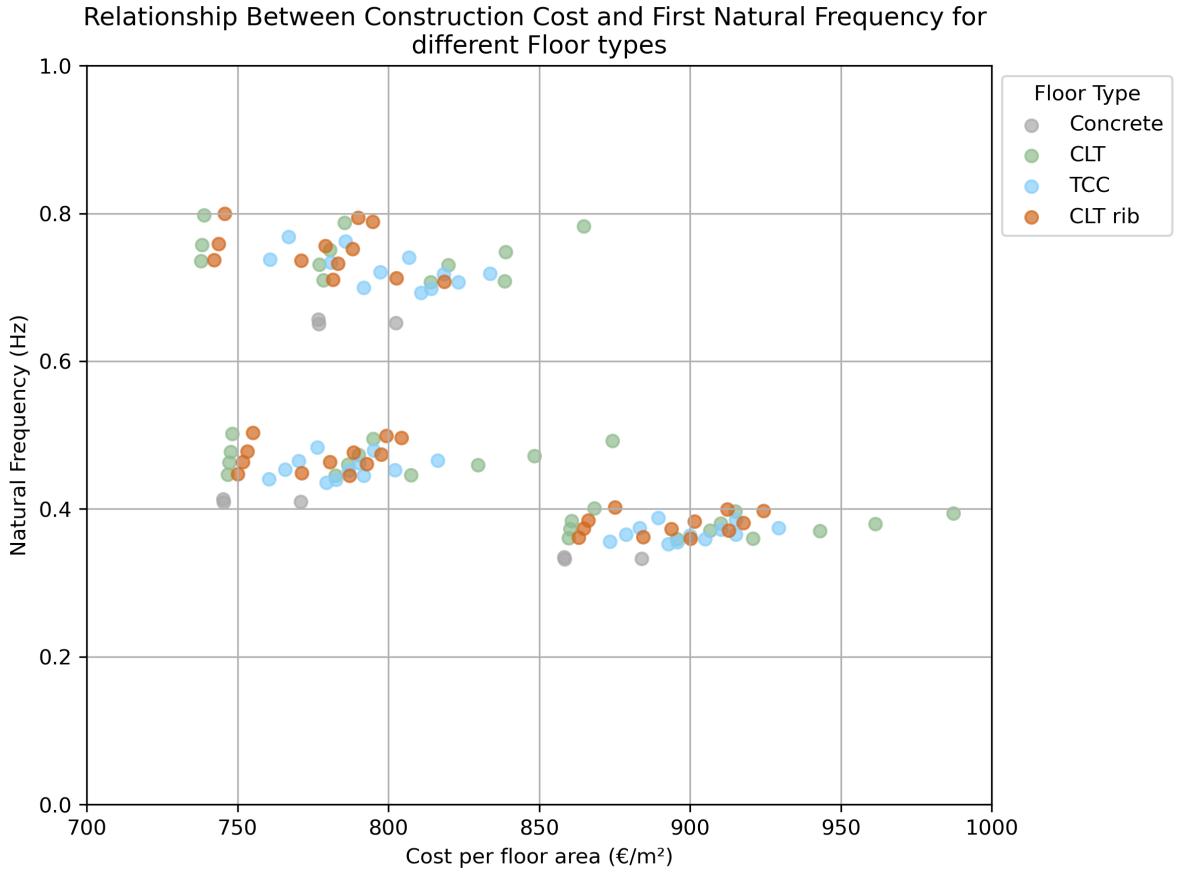

Figure J.3: First natural frequency and construction cost correlation per floor type

Figure J.4 presents the construction cost plotted against the natural frequency, with building variants grouped by floor plan. The graph shows that, across all building variants, floor plan 2 is beneficial in achieving lower construction costs for all building heights. Additionally, the natural frequency remains relatively constant despite variations in the floor plan.

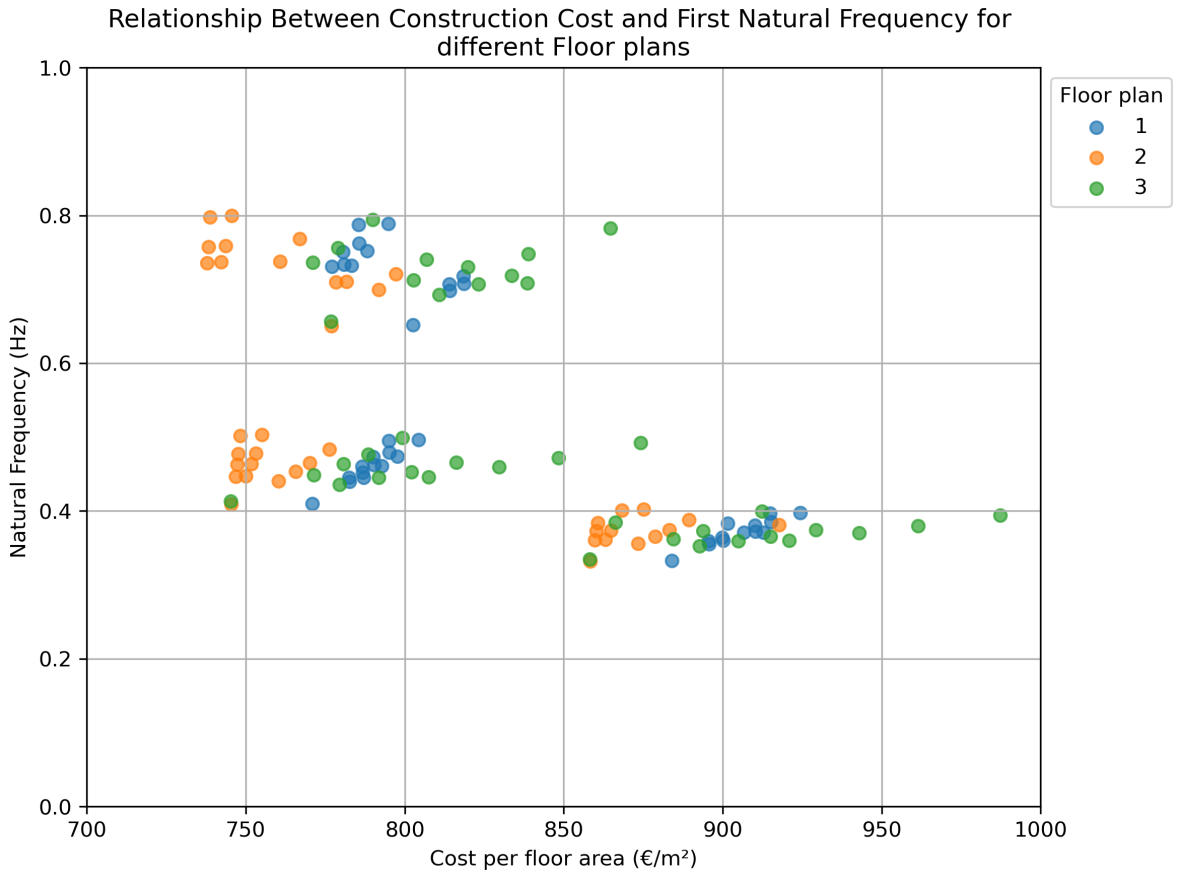

Figure J.4: First natural frequency and construction cost correlation per floor plan

J.3. Relation between environmental performance and construction cost

Figure J.5 illustrates the relationship between the ECI value and construction cost for building variants categorized by floor type. Timber-based floor types generally display a similar range of cost and ECI values, although variants with CLT floors can have higher costs. In contrast, concrete buildings exhibit noticeably higher ECI values while maintaining a comparable construction cost.

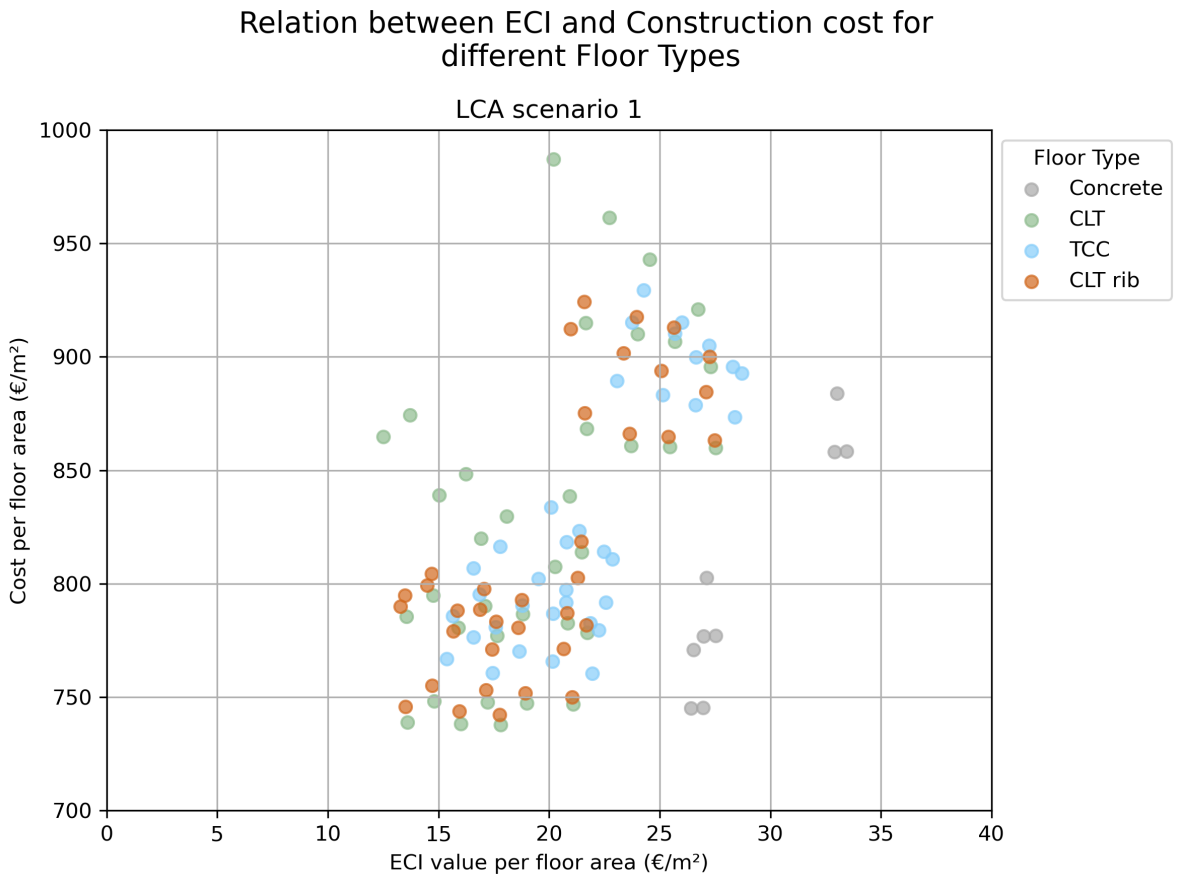

Figure J.5: ECI and construction cost correlation per floor type

Figure J.6 presents the ECI value plotted against the construction cost, with building variants grouped by floor plan. The graph highlights differences in construction cost between floor plans, while the ECI values remain relatively similar across them. A distinct clustering of floor plans is observed, with a noticeable trend of convergence towards the characteristics of concrete buildings.

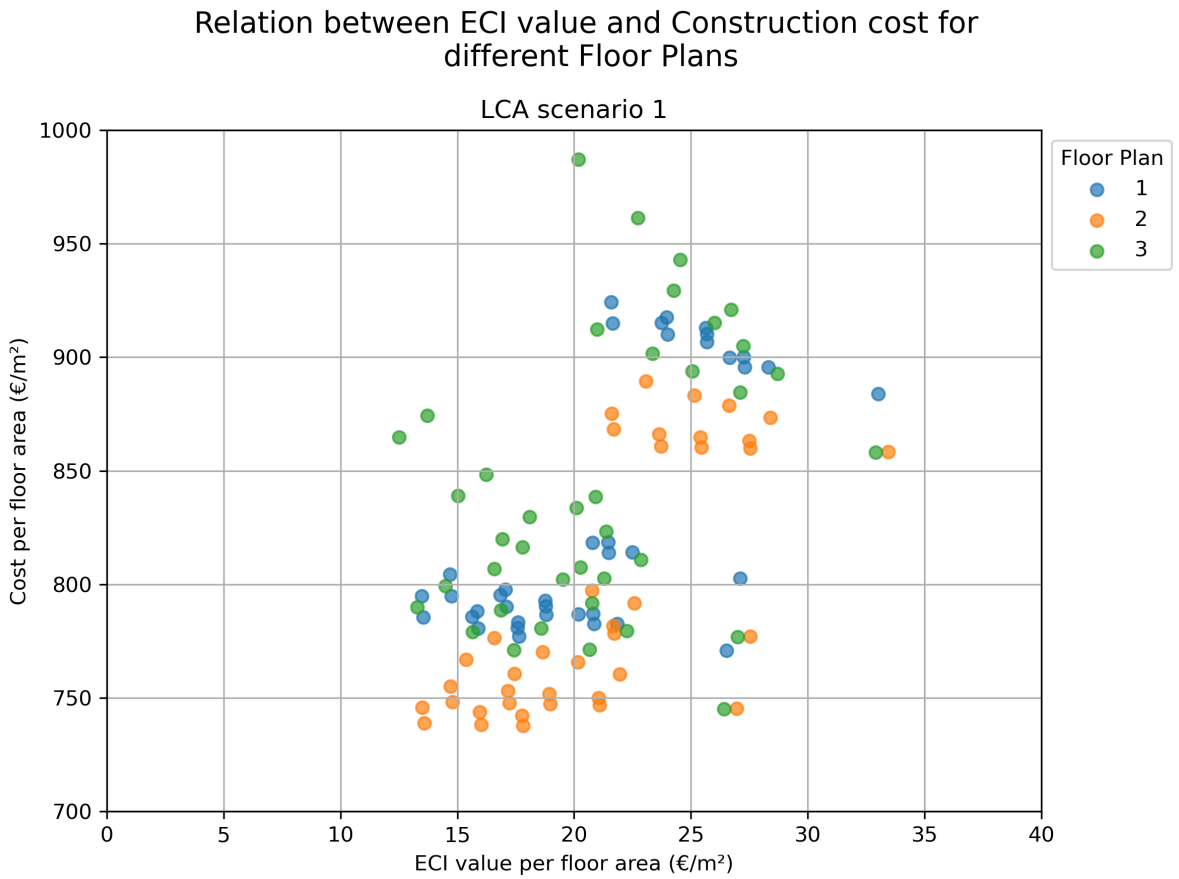

Figure J.6: ECI and construction cost correlation per floor plan

Figure J.7 presents the same graph as shown in Figure 9.7, alongside a version highlighting the data points for floor plan 3 and floor type CLT. This visualization aims to emphasize the insights and relationships that can be extracted from these graphs. When considering all data points together, no clear correlations between the dependent variables are apparent. However, when focusing on the relationship between the ECI value and the construction cost for a specific parameter, meaningful patterns can be identified. The left graph illustrates a distinct inverse linear relationship between the ECI value and the construction cost for specific parameters.

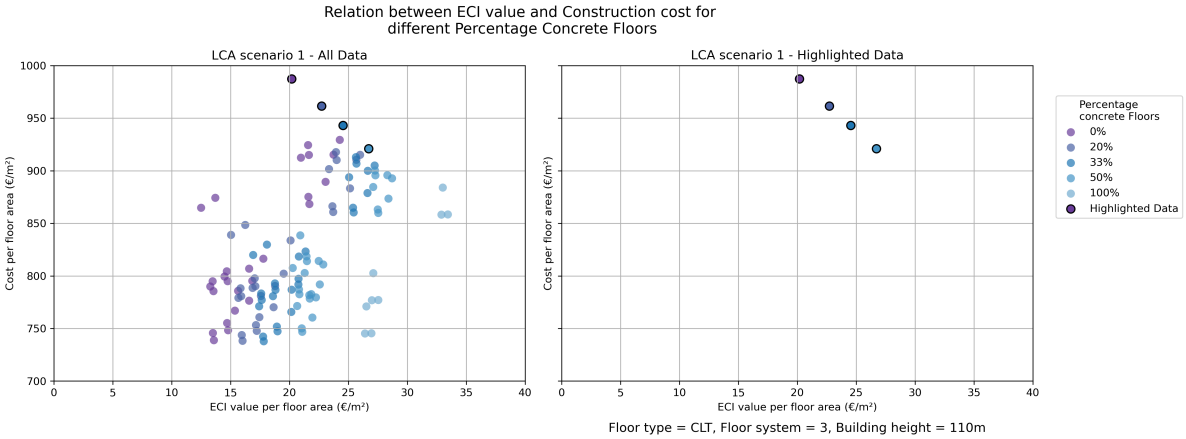

Figure J.7: Highlighted data from ECI and construction cost correlation

K

Calculation sheets and Python script

This appendix includes Excel sheets and Python scripts developed for designing the building variants.

K.1. Floor design

Concrete floor	Variant 4		Variant 5		Variant 6		Inside core	
Material properties								
Concrete	C20/25							
Self weight	2500	kg/m3						
Dimensions floor			**Dimensions floor**		**Dimensions floor**		**Dimensions floor**	
Height	250	mm	Height	250 mm	Height	270 mm	Height	250 mm
Width	1000	mm	Width	1000 mm	Width	1000 mm	Area	106311700 mm2
Length	4300	mm	Length	3230 mm	Length	6450 mm	Area	106,3 m2
Loads floor			**Loads floor**		**Loads floor**		**Loads floor**	
Permanent load			*Permanent load*		*Permanent load*		*Permanent load*	
dead load(ceiling + finishing floor)	1,0	kN/m2	dead load(ceiling + finishing floor)	1,0 kN/m2	dead load(ceiling + finishing floor)	1,0 kN/m2	dead load(ceiling + finishing floor)	1,0 kN/m2
self weight floor	6,13	kN/m2	self weight floor	6,13 kN/m2	self weight floor	6,62 kN/m2	self weight floor	6,13 kN/m2
self weight seperation walls	0,80	kN/m2	self weight seperation walls	0,80 kN/m2	self weight seperation walls	0,80 kN/m2	self weight seperation walls	0,80 kN/m2
Total permanent load	7,93	kN/m2	Total permanent load	7,93 kN/m2	Total permanent load	8,42 kN/m2	Total permanent load	7,93 kN/m2
Category A: domestic, residential areas			*Variable load*		*Variable load*		*Variable load*	
Category A: domestic, residential areas	1,75	kN/m2	Category A: domestic, residential areas	1,75 kN/m2	Category A: domestic, residential areas	1,75 kN/m2	Category A: domestic, residential areas	1,75 kN/m2
Floor area	500	m2	**Floor area**	500,00	**Floor area**	500,00 m2	**Floor area**	106,3 m2
Permanent floor load	3966	kN	Permanent floor load	3966 kN	Permanent floor load	4211 kN	Permanent floor load	843 kN
Variable floor load	875	kN	Variable floor load	875 kN	Variable floor load	875 kN	Variable floor load	186 kN
Dimensions beam			**Dimensions beam**		**Dimensions beam**			
Height	335	mm	Height	400 mm	Height	285 mm		
Width	400	mm	Width	400 mm	Width	400 mm		
Length	4300	mm	Length	6450 mm	Length	3230 mm		
n beams	39		n beams	28	n beams	32		
Volume	22,47	m3	Volume	28,90 m3	Volume	11,78 m3		
Loads beams			**Loads beams**		**Loads beams**			
Permanent load - self weight beam	14	kN	Permanent load - self weight beam	25 kN	Permanent load - self weight beam	9 kN		
Permanent beam load	551	kN	Permanent beam load	709 kN	Permanent beam load	289 kN		
Dimensions column			**Dimensions column**		**Dimensions column**			
Height	700	mm	Height	700 mm	Height	700 mm		
Width	400	mm	Width	400 mm	Width	400 mm		
Length	3100	mm	Length	3100 mm	Length	3100 mm		
Volume	0,87	m3	Volume	0,87 m3	Volume	0,87 m3		
n columns per floor	38		n columns per floor	32	n columns per floor	32		
Loads columns			**Loads columns**		**Loads columns**			
Permanent load - self weight column	21	kN	*Permanent load - self weight column*	21 kN	*Permanent load - self weight column*	21 kN		
Permanent column load	809	kN	Permanent column load	681 kN	Permanent column load	681 kN		
Dimensions facade			**Dimensions facade**		**Dimensions facade**			
Height storey	3,1	m	Height storey	3,1 m	Height storey	3,1 m		
Width building	26	m	Width building	26 m	Width building	26 m		
Area facade per floor	322,40	m2	Area facade per floor	322,40 m2	Area facade per floor	322,40 m2		
Loads facade			**Loads facade**		**Loads facade**			
Permanent load - self weight column	2,88	kN/m2	*Permanent load - self weight column*	2,88 kN/m2	*Permanent load - self weight column*	2,88 kN/m2		
Permanent facade load	929	kN	Permanent facade load	929 kN	Permanent facade load	929 kN		
Total load floors + beams + columns + facade			**Total load floors + beams + columns + facade**		**Total load floors + beams + columns + facade**			
Permanent	6254	kN	Permanent	6284 kN	Permanent	6110 kN		
Variable	875	kN	Variable	875 kN	Variable	875 kN		
TOTAL PERM LOAD (storey + inside core)	7097	kN	TOTAL PERM LOAD (storey + inside core)	7127 kN	TOTAL PERM LOAD (storey + inside core)	6953 kN		
TOTAL VAR LOAD (storey + inside core)	1061	kN	TOTAL VAR LOAD (storey + inside core)	1061 kN	TOTAL VAR LOAD (storey + inside core)	1061 kN		

Figure K.1: Excel sheet calculations: Concrete floor type

CLT	variant 4		variant 5			variant 6		
Material properties								
CLT	GL24							
selfweight	500	kg/m3						
Glulam	GL28h							
selfweight	460	kg/m3						
Dimensions floor			**Dimensions floor**			**Dimensions floor**		
Height	140	mm	Height	120	mm	Height	240	mm
Width	1000	mm	Width	1000	mm	Width	1000	mm
Length	4300	mm	Length	3230	mm	Length	6450	mm
Loads			**Loads**			**Loads**		
Permanent load			*Permanent load*			*Permanent load*		
dead load	1,7	kN/m2	dead load	1,7	kN/m2	dead load	1,7	kN/m2
self weight floor	0,69	kN/m2	self weight floor	0,59	kN/m2	self weight floor	1,18	kN/m2
self weight seperation walls	0,80	kN/m2	self weight seperation walls	0,80	kN/m2	self weight seperation walls	0,80	kN/m2
Total permanent load	3,19	kN/m2	Total permanent load	3,09	kN/m2	Total permanent load	3,68	kN/m2
Variable load			*Variable load*			*Variable load*		
Category A: domestic, residential areas	1,75	kN/m2	Category A: domestic, residential areas	1,75	kN/m2	Category A: domestic, residential areas	1,75	kN/m2
Floor area	500	m2	**Floor area**	500		**Floor area**	500	m2
Permanent floor load	1593	kN	Permanent floor load	1544	kN	Permanent floor load	1839	kN
Variable floor load	875	kN	Variable floor load	875	kN	Variable floor load	875	kN
Dimensions beam			**Dimensions beam**			**Dimensions beam**		
Height	400	mm	Height	460	mm	Height	350	mm
Width	200	mm	Width	220	mm	Width	210	mm
Length	4300	mm	Length	6450	mm	Length	3230	mm
n beams	39		n beams	28		n beams	32	
Volume	13,42	m3	Volume	18,28	m3	Volume	7,60	m3
Loads			**Loads**			**Loads**		
Permanent load - self weight beam	1,6	kN	Permanent load - self weight beam	2,9	kN	Permanent load - self weight beam	1,1	kN
Permanent beam load	60,5	kN	Permanent beam load	82,5	kN	Permanent beam load	34,3	kN
Dimensions column			**Dimensions column**			**Dimensions column**		
Height	700	mm	Height	700	mm	Height	700	mm
Width	400	mm	Width	400	mm	Width	400	mm
Length	3100	mm	Length	3100	mm	Length	3100	mm
Volume	0,87	m3	Volume	0,87	m3	Volume	0,87	m3
n columns per floor	38		n columns per floor	32		n columns per floor	32	
Loads columns			**Loads columns**			**Loads columns**		
Permanent load - self weight column	809	kN	*Permanent load - self weight column*	681	kN	*Permanent load - self weight column*	681	kN
Permanent column load	809	kN	Permanent column load	681	kN	Permanent column load	681	kN
Dimensions facade			**Dimensions facade**			**Dimensions facade**		
Height storey	3,1	m	Height storey	3,1	m	Height storey	3,1	m
Width building	26	m	Width building	26	m	Width building	26	m
Area facade per floor	322,40	m2	Area facade per floor	322,40	m2	Area facade per floor	322,40	m2
Loads facade			**Loads facade**			**Loads facade**		
Permanent load - self weight column	2,88	kN/m2	*Permanent load - self weight column*	2,88	kN/m2	*Permanent load - self weight column*	2,88	kN/m2
Permanent facade load	929	kN	Permanent facade load	929	kN	Permanent facade load	929	kN
Total load floors + beams + columns + facade			**Total load floors + beams + columns + facade**			**Total load floors + beams + columns + facade**		
Permanent	3391	kN	Permanent	3236	kN	Permanent	3483	kN
Variable	875	kN	Variable	875	kN	Variable	875	kN
TOTAL PERM LOAD (storey + inside core)	4235	kN	TOTAL PERM LOAD (storey + inside core)	4080	kN	TOTAL PERM LOAD (storey + inside core)	4326	kN
TOTAL VAR LOAD (storey + inside core)	1061	kN	TOTAL VAR LOAD (storey + inside core)	1061	kN	TOTAL VAR LOAD (storey + inside core)	1061	kN

Figure K.2: Excel sheet calculations: CLT floor type

TCC	variant 4		variant 5			variant 6		
Material properties								
CLT	GL24							
self weight	500	kg/m3						
Glulam	GL28h							
selfweight	460	kg/m3						
concrete	C20/25							
selfweight	2400	kg/m3						
Dimensions floor			**Dimensions floor**			**Dimensions floor**		
Total height	180	mm	Total height	180	mm	Total height	260	mm
Height concrete	60	mm	Height concrete	60	mm	Height concrete	100	mm
Height CLT	120	mm	Height CLT	120	mm	Height CLT	160	mm
Width	1000	mm	Width	1000	mm	Width	1000	mm
Length	4300	mm	Length	3230	mm	Length	6450	mm
Loads			**Loads**			**Loads**		
Permanent load			*Permanent load*			*Permanent load*		
dead load	1,2	kN/m2	dead load	1,2	kN/m2	dead load	1,2	kN/m2
self weight floor	2,00	kN/m2	self weight floor	2,00	kN/m2	self weight floor	3,14	kN/m2
self weight seperation walls	0,80	kN/m2	self weight seperation walls	0,80	kN/m2	self weight seperation walls	0,80	kN/m2
Total permanent load	4,00	kN/m2	Total permanent load	4,00	kN/m2	Total permanent load	5,14	kN/m2
Variable load			*Variable load*			*Variable load*		
Category A: domestic, residential areas	1,75	kN/m2	Category A: domestic, residential areas	1,75	kN/m2	Category A: domestic, residential areas	1,75	kN/m2
Floor area	500	m2	**Floor area**	500	m2	**Floor area**	500	m2
Permanent floor load	2001	kN	Permanent floor load	2001	kN	Permanent floor load	2570	kN
Variable floor load	875	kN	Variable floor load	875	kN	Variable floor load	875	kN
Dimensions beam			**Dimensions beam**			**Dimensions beam**		
Height	400	mm	Height	480	mm	Height	400	mm
Width	220	mm	Width	240	mm	Width	240	mm
Length	4300	mm	Length	6450	mm	Length	3230	mm
n beams	39		n beams	28		n beams	32	
Volume	14,76		Volume	20,81		Volume	9,92	
Loads			**Loads**			**Loads**		
Permanent load - self weight beam	1,71	kN	Permanent load - self weight beam	3,35	kN	Permanent load - self weight beam	1,40	kN
Permanent beam load	67	kN	Permanent beam load	94	kN	Permanent beam load	45	kN
Dimensions column			**Dimensions column**			**Dimensions column**		
Height	700	mm	Height	700	mm	Height	700	mm
Width	400	mm	Width	400	mm	Width	400	mm
Length	3100	mm	Length	3100	mm	Length	3100	mm
Volume	0,87	m3	Volume	0,87	m3	Volume	0,87	m3
n columns per floor	38		n columns per floor	32		n columns per floor	32	
Loads columns			**Loads columns**			**Loads columns**		
Permanent load - self weight column	21	kN	*Permanent load - self weight column*	21	kN	*Permanent load - self weight column*	21	kN
Permanent column load	809	kN	Permanent column load	681	kN	Permanent column load	681	kN
Dimensions facade			**Dimensions facade**			**Dimensions facade**		
Height storey	3,1	m	Height storey	3,1	m	Height storey	3,1	m
Width building	26	m	Width building	26	m	Width building	26	m
Area facade per floor	322,40	m2	Area facade per floor	322,40	m2	Area facade per floor	322,40	m2
Loads facade			**Loads facade**			**Loads facade**		
Permanent load - self weight column	2,88	kN/m2	*Permanent load - self weight column*	2,88	kN/m2	*Permanent load - self weight column*	2,88	kN/m2
Permanent facade load	929	kN	Permanent facade load	929	kN	Permanent facade load	929	kN
Total load floors + beams + columns + facade			**Total load floors + beams + columns + facade**			**Total load floors + beams + columns + facade**		
Permanent	3805	kN	Permanent	3704	kN	Permanent	4224	kN
Variable	875	kN	Variable	875	kN	Variable	875	kN
TOTAL PERM LOAD (storey + inside core)	4648	kN	TOTAL PERM LOAD (storey + inside core)	4547	kN	TOTAL PERM LOAD (storey + inside core)	5067	kN
TOTAL VAR LOAD (storey + inside core)	1061	kN	TOTAL VAR LOAD (storey + inside core)	1061	kN	TOTAL VAR LOAD (storey + inside core)	1061	kN

Figure K.3: Excel sheet calculations: TCC floor type

CLT rib	variant 4		variant 5			variant 6		
Material properties								
CLT	GL24							
self weight	500	kg/m3						
Glulam	GL28h							
self weight	460	kg/m3						
Concrete	C20/25							
self weight	2400	kg/m3						
Dimensions floor			**Dimensions floor**			**Dimensions floor**		
Total height	320	mm	Total height	260	mm	Total height	380	mm
Height CLT	120	mm	Height CLT	100	mm	Height CLT	140	mm
Height rib	200	mm	Height rib	160	mm	Height rib	240	mm
Width rib	120	mm	Width rib	120	mm	Width rib	140	mm
Width floor	1000	mm	Width floor	1000	mm	Width floor	1000	mm
Length	4300	mm	Length	3230	mm	Length	6450	mm
Loads			**Loads**			**Loads**		
Permanent load			*Permanent load*			*Permanent load*		
dead load	1,6	kN/m2	dead load	1,6	kN/m2	dead load	1,6	kN/m2
self weight floor	0,75	kN/m2	self weight floor	0,62	kN/m2	self weight floor	0,91	kN/m2
self weight seperation walls	0,80	kN/m2	self weight seperation walls	0,80	kN/m2	self weight seperation walls	0,80	kN/m2
Total permanent load	3,15	kN/m2	Total permanent load	3,02	kN/m2	Total permanent load	3,31	kN/m2
Variable load			*Variable load*			*Variable load*		
Category A: domestic, residential areas	1,75	kN/m2	Category A: domestic, residential areas	1,75	kN/m2	Category A: domestic, residential areas	1,75	kN/m2
Floor area	500	m2	**Floor area**	500	m2	**Floor area**	500	m2
Permanent floor load	1575	kN	Permanent floor load	1510	kN	Permanent floor load	1655	kN
Variable floor load	875	kN	Variable floor load	875	kN	Variable floor load	875	kN
Dimensions beam			**Dimensions beam**			**Dimensions beam**		
Height	360	mm	Height	440	mm	Height	360	mm
Width	200	mm	Width	240	mm	Width	180	mm
Length	4300	mm	Length	6450	mm	Length	3230	mm
n beams	39		n beams	28		n beams	32	
Volume	12,07	m3	Volume	19,07	m3	Volume	6,70	
Loads			**Loads**			**Loads**		
Permanent load - self weight beam	1,40	kN	Permanent load - self weight beam	3,07	kN	Permanent load - self weight beam	0,94	kN
Permanent beam load	54	kN	Permanent beam load	86	kN	Permanent beam load	30	kN
Dimensions column			**Dimensions column**			**Dimensions column**		
Height	700	mm	Height	700	mm	Height	700	mm
Width	400	mm	Width	400	mm	Width	400	mm
Length	3100	mm	Length	3100	mm	Length	3100	mm
Volume	0,87	m3	Volume	0,87	m3	Volume	0,87	m3
n columns per floor	38		n columns per floor	32		n columns per floor	32	
Loads columns			**Loads columns**			**Loads columns**		
Permanent load - self weight column	21	kN	*Permanent load - self weight column*	21	kN	*Permanent load - self weight column*	21	kN
Permanent column load	809	kN	Permanent column load	681	kN	Permanent column load	681	kN
Dimensions facade			**Dimensions facade**			**Dimensions facade**		
Height storey	3,1	m	Height storey	3,1	m	Height storey	3,1	m
Width building	26	m	Width building	26	m	Width building	26	m
Area facade per floor	322,40	m2	Area facade per floor	322,40	m2	Area facade per floor	322,40	m2
Loads facade			**Loads facade**			**Loads facade**		
Permanent load - self weight column	2,88	kN/m2	*Permanent load - self weight column*	2,88	kN/m2	*Permanent load - self weight column*	2,88	kN/m2
Permanent facade load	929	kN	Permanent facade load	929	kN	Permanent facade load	929	kN
Total load floors + beams + columns + facade			**Total load floors + beams + columns + facade**			**Total load floors + beams + columns + facade**		
Permanent	3367	kN	Permanent	3206	kN	Permanent	3295	kN
Variable	875	kN	Variable	875	kN	Variable	875	kN
TOTAL PERM LOAD (storey + inside core)	4210	kN	TOTAL PERM LOAD (storey + inside core)	4049	kN	TOTAL PERM LOAD (storey + inside core)	4138	kN
TOTAL VAR LOAD (storey + inside core)	1061	kN	TOTAL VAR LOAD (storey + inside core)	1061	kN	TOTAL VAR LOAD (storey + inside core)	1061	kN

Figure K.4: Excel sheet calculations: CLT rib panel floor type

K.2. Concrete core design

K.2.1 Foundation stiffness

```python
## Calculate foundation stiffness(C_rotation) based on number of #piles
def foundation_stiffness(n_piles, max_width_piles):
    # Distance between center line and first pile next to center line
    hoh = max_width_piles / (n_piles - 1)
    
    # Number of piles on left side of center line
    if n_piles % 2 != 0:
        distance1 = hoh
        n = list(range(n_piles // 2))
    else:
        distance1 = hoh / 2
        n = list(range(n_piles // 2))
        
    Ip  = []
    # Distance of piles n from center line
    for i in n:
        a_i_value = i * hoh + distance1             # Distance of pile to center line (m)
        Ip_value =  a_i_value **2 * 2 * n_piles     # Inertia value of a pile row(vertical) with same distance to centre line (m2)
        Ip.append(Ip_value)
        
    Ip_sum = sum(Ip)                                # Inertia of piles (m2)

    # Calculate foundation stiffness
    EI_p = 239000                                   # Stiffness of foundation piles (kN/m)
    rot_stiffness = (Ip_sum * EI_p) / (10 ** 9)     # Foundation stiffness (kNm/rad)
    return rot_stiffness
    
Cr = foundation_stiffness(n_piles1, max_width_piles1)
```

Figure K.5: Python script in grasshopper: Foundation stiffness

K.2.2 Wind load

```python
## Wind load and position for load distribution
import math
# List with vertical position of floors
def frange(start, stop, step):
    while start < stop:
        yield round(start, 2)
        start += step

h_storey= 3.1 # Height of storey (m)
b = 26        # width of building (m)
·
z = [round(x, 2) for x in frange(0, h + 1, h_storey)]  # h = height of building (m)

# List with normalized vertical position of floors
z_norm = [0.0] * len(z)  # 1D array filled with zeros

for i in range(len(z)):
    z_norm[i] = z[i]/h

# Eurocode calculatin wind load
def wind_load(z):
    k_l = 1  # turbulence intensity
    z_min = 7
    z0 = 0.5
    z02 = 0.05
    
    c0_z = 1
    c_dir = 1
    c_season = 1
    
    # Turbulence intensity
    Iv_z = k_l / (c0_z * math.log(z_min / z0)) if z < z_min else k_l / (c0_z * math.log(z / z0))

    # Terrain factor
    k_r = 0.19 * (z0 / z02) ** 0.07
    cr_z = k_r * math.log(z_min / z0) if z <= z_min else k_r * math.log(z / z0)

    # Wind probability
    n = 0.5
    K = 0.234
    p = 1 / 50
    c_prob = ((1 * K * math.log(-math.log(1 - p))) / (1 * K * math.log(-math.log(0.98)))) ** n
    
    vb0 = 27
    vb = c_dir * c_season * c_prob * vb0
    vm_z = cr_z * c0_z * vb

    # Wind pressure calculation
    rho = 1.25
    qp_z = (1 + 7 * Iv_z) * 0.5 * rho * vm_z ** 2 / 1000
    
    # Wind load
    cf = 0.85 * (0.8 + 0.7)
    cs_cd = 1.15  # assumption for safety
    qw = qp_z * cs_cd * cf * b * 1 # Distributed wind load on building at certian point (kN/m)
    return round(qw)
    
# Wind load on vertical positions of floors
def load_range():
    qw = [0.0] * len(z)
    
    for i in range(len(z)):
        if z[i] < b:
            qw[i] = wind_load(z = b)
        elif z[i] > h-b:
            qw[i] = wind_load(z = h)
        else:
            qw[i] = wind_load(z = z[i])
    return qw

q_wind = load_range()
```

Figure K.6: Python script in Grasshopper: Wind loads

K.2.3 Verification load combinations

```python
## Unity checks for foundation piles,  load case A - E

def foundation_analysis(n_piles, moment, vert_load, hor_load, max_width_piles, strength_red):
    # Material properties
    rho_conc = 2500                                 # Density of reinforced concrete (kg/m3)
    max_rw_pile_load = 7800 * strength_red          # Maximum design load on pile (kN)
    max_rw_pile_hor = 125                           # Horizontal characteristic strength (kN)

    # Distance between center line and first pile next to center line
    hoh = max_width_piles / (n_piles - 1)

    # Number of piles on one side of center line
    if n_piles % 2 != 0:
        distance1 = hoh
        n = list(range(n_piles // 2))
    else:
        distance1 = hoh / 2
        n = list(range(n_piles // 2))

    # Calculate moment of inertia for distances between piles a_i
    M = []
    a_i = []
    a_i_midden =[]
    length_moment_area = (13/2 + 2 * 2 / 1) + 1                         # Width concrete core + 2 * thickness foundation plate

    for i in n:
        a_i_value = i * hoh + distance1                                 # Distance of pile to center line
        a_i.append(a_i_value)
        if a_i_value < (length_moment_area):                            # Piles only contribute to Mtot if they are close to core: within certain distance.
            a_i_midden.append(a_i_value)

    if n_piles % 2 == 0:                                                # Number of piles on a row that attribute to moment resistance
        n_piles_moment = len(a_i_midden) * 2
    else: n_piles_moment = len(a_i_midden) * 2 + 1

    for i in a_i_midden:
        M_value = (i / a_i_midden[-1])  * (i * 2) * n_piles_moment      # percentage from f0 * (a_i * 2) * n_piles_moment. Multiplication factor for pile:
        M.append(M_value)                                               # M = F * a, F = f0 *factor(0-1), a = a_i * 2(total arm), f0 = unknown


#    n_piles_moment = 2 * len(M)                                        # Number of piles on a row that attribute to moment resistance
    Mtot = sum(M)                                                       # M_ed = f0* Mtot, f0 unkown

    # Calculate loads on piles for Load cases
    F_tot_maxv = []
    F_tot_minv = []
    F_horv = []
    N_pile = []
    M_pile = []

    for i in range(len(moment)):
        # Calculate load due to normal force and moment and shear force
        Tot_vert_load = vert_load[i]
        F_pile_N = Tot_vert_load / (n_piles ** 2)       # Vertical load per pile
        F_pile_M = moment[i] / Mtot                     # f0 = M_ed / Mtot: Load on outer pile that contributes to reisistance of moment of wind load
        F_hor = hor_load[i] / (n_piles ** 2)            # Horizontal load on foundation pile due to wind

        # Combine load due to normal force and moment
        F_tot_max = F_pile_N + F_pile_M                 # Maximum load on foundation pile
        F_tot_min = F_pile_N - F_pile_M                 # Minimum load on foundation pile

        # Assign load to list
        F_tot_maxv.append(F_tot_max)
        F_tot_minv.append(F_tot_min)
        F_horv.append(F_hor)
        N_pile.append(F_pile_N)
        M_pile.append(F_pile_M)

    # Unity checks for load cases
    uc_A_pile_max_G   = F_tot_maxv[0] / max_rw_pile_load # Unity check for max vertical load (G governing)
    uc_B_pile_max_Qfl = F_tot_maxv[1] / max_rw_pile_load # Unity check for max vertical load (Qfloor governing)
    uc_C_pile_max_Qw  = F_tot_maxv[2] / max_rw_pile_load # Unity check for max vertical load (Qw governing)

    if F_tot_minv[3] <= 0:                          # Unity check for tension(not allowed)
        uc_D_pile_tension = 1
    else: uc_D_pile_tension = F_tot_minv[3]  / max_rw_pile_load
    pile_tension = F_tot_minv[3]

    uc_E_pile_hor = F_horv[4] / max_rw_pile_hor     # Unity check for horizontal load

    return uc_A_pile_max_G, uc_B_pile_max_Qfl, uc_C_pile_max_Qw, uc_D_pile_tension, uc_E_pile_hor, pile_tension

# Grasshopper output
uc_A_pile_max_G, uc_B_pile_max_Qfl, uc_C_pile_max_Qw, uc_D_pile_tension, uc_E_pile_hor, pile_tension = foundation_analysis(n_piles1, moment1, vert_loads1, hor_load1, max_width_piles1, pile_strength_red1)
```

Figure K.7: Python script in grasshopper: Calculation and verification of load combinations A - E

```python
## Unity check load case F-I

#Load case F
u_max = height/750                                  # maxamimum allowed deformation (m)
uc_F_deformation = (u_found/100)/ u_max             # Unity check deformation top building

#Load case G
uc_G_core_compression = max_stress_G/fyd_conc       # Unity check concrete compression, governing load: G

#Load case H
uc_H_core_compression = max_stress_Qfl/fyd_conc     # Unity check concrete compression, governing load: V_floor

#Load case I
uc_I_core_compression = max_stress_Qw/fyd_conc      # Unity check concrete compression, governing load: V_wind
```

Figure K.8: Python script in grasshopper: Verification of load combinations G - I

```python
## Load case J: unity check

import math
# Calculate force due to induced normal force and moment
N_m = N / Area_core * t  # Normal force in core per meter (F/m)
F_M = M / (b - t) / b    # Tensile force in core due to moment per meter (F/m) assumption lever arm = (b-t)

F_tension_steel = N_m + F_M # Total tensile force per meter (kN / m)
print(F_tension_steel)

# Calculate resisting force from reinforcement steel
steel_d = diameter_reinf / 1000                # Diameter steel reinforcement (m)
n_steel = (1000 / 100) * 2                     # Number of steel bars per meter, distance between bars 100mm, 2 meshes (-)
A_s = (0.25 * math.pi * steel_d **2) * n_steel # Area reinforcement steel per meter (m2 / m)
fyd = 435000                                   # Steel design strength (kN/m2)
F_res = A_s * fyd                              # Tensile resistance per meter (kN / m)

uc_J_core_tension = F_tension_steel / F_res
```

Figure K.9: Python script in grasshopper: Calculation and verification of load combincation J

K.2.4 Calculation mass reinforced concrete of core

```python
## Calculate mass reinforcement steel and concrete in core
import math

# Define steel area for various rebar diameter
d = [diameter_reinf, 12, 10, 8]
A_steel = []

for i in range(len(d)):
    if d[i] > 10:                                          # Above d = 10 distance between bars = 100mm, below distance = 150mm
        A_s = 0.25 * math.pi * (d[i]/1000) ** 2 * (1000/100) * 2     # Area reinforcement steel per meter (m2 / m)
    else: A_s = 0.25 * math.pi * (d[i]/1000) ** 2 * (1000/150) * 2   # Area reinforcement steel per meter (m2 / m)
    A_steel.append(A_s)

# Calculate mass steel reinforcement core (direction 1&2)
V_s = []
height_section = height_building / len(d)        # heigth of building is equally divided into 4 parts for each reinforcement diameter

for i in range(len(A_steel)):
    A_s = A_steel[i] * ((4 * b) + (2 * (b - 2 * t)) + length_innerwalls) # Total area rebar = Area / m * (perimeter + reinforcement in walls inside core) (m2)

    V_s_value = A_s * height_section             # Total Volume rebar = Area * height section
    V_s.append(V_s_value)
    
V_s_TOTAL = sum(V_s) * 2                         # 2 directions

# Calculate mass reinforcement
density_steel = 7850                             # Density steel (kg/m3 )
mass_rs = V_s_TOTAL * density_steel              # Mass reinforcement (kg)

# Calculate mass concrete core
V_total = Area_core * height_building            # Volume core (m3)
V_concrete = V_total - V_s_TOTAL                 # Volume concrete in core (m3)

density_concrete = 24000 / 9.81                  # Density concrete (without reinforcement) (kg/m3)
mass_concrete = V_concrete * density_concrete    # Mass concrete in core (kg)
```

Figure K.10: Python script in grasshopper: Calculations of mass of concrete and reinforcement steel of core

L

Floor plans

This appendix includes the floor plans of the six floor systems that are evaluated in Section 5.4.

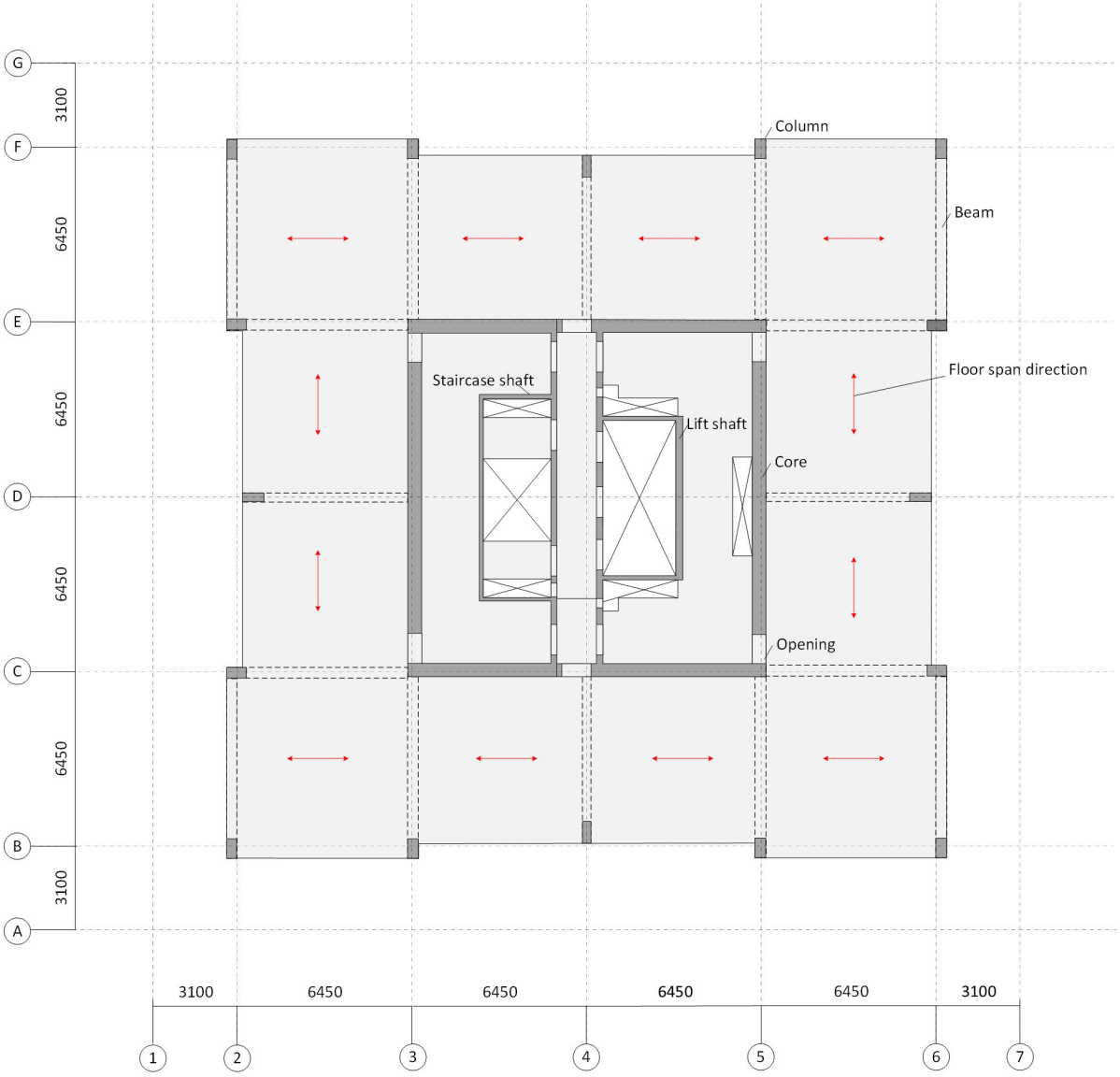

Figure L.1: Variant 1: 6.5 span - variant 1

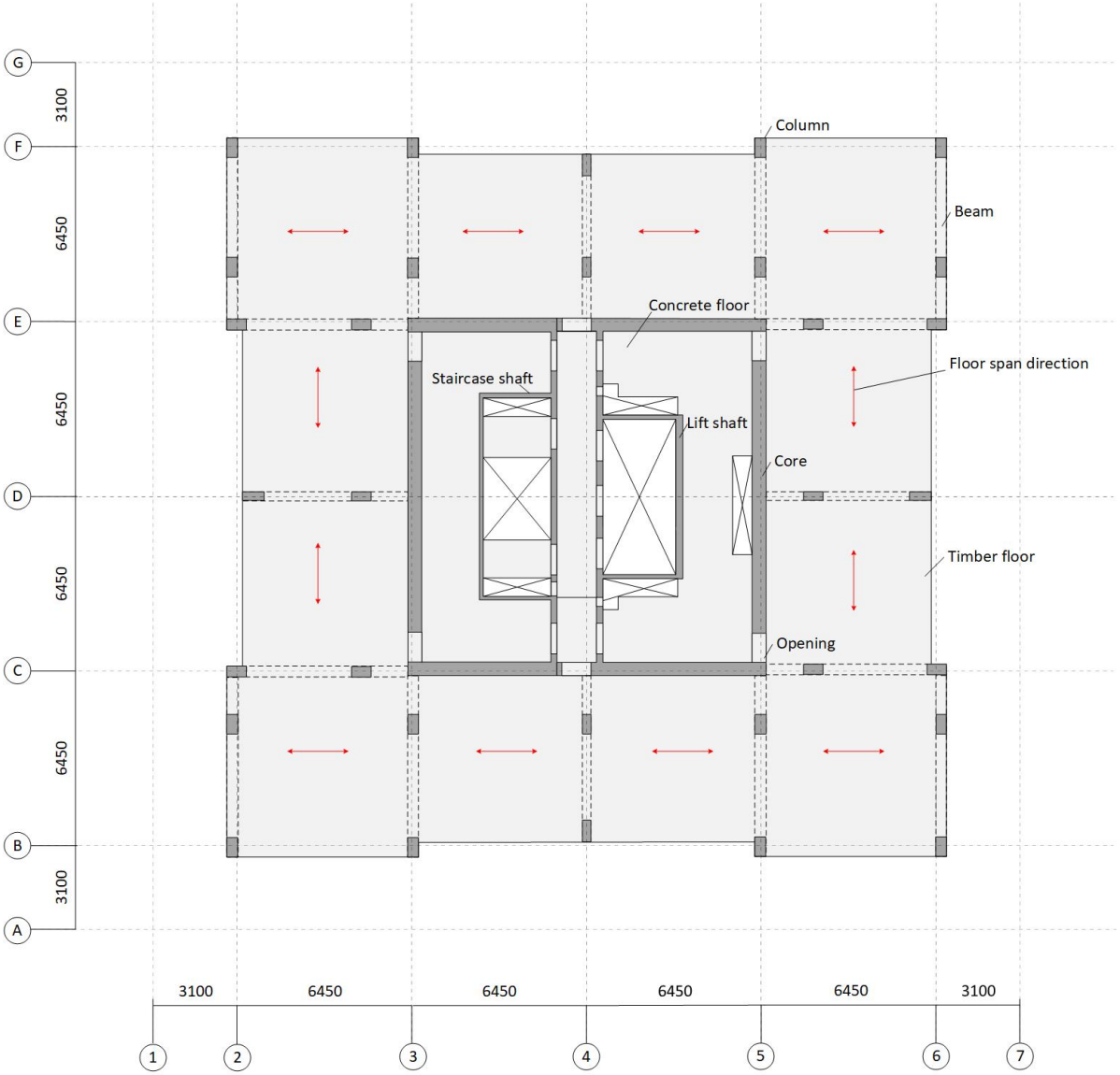

Figure L.2: Variant 2: 6.5 span - variant 2

Figure L.3: Variant 3: 5.0 span (cantilever beam)

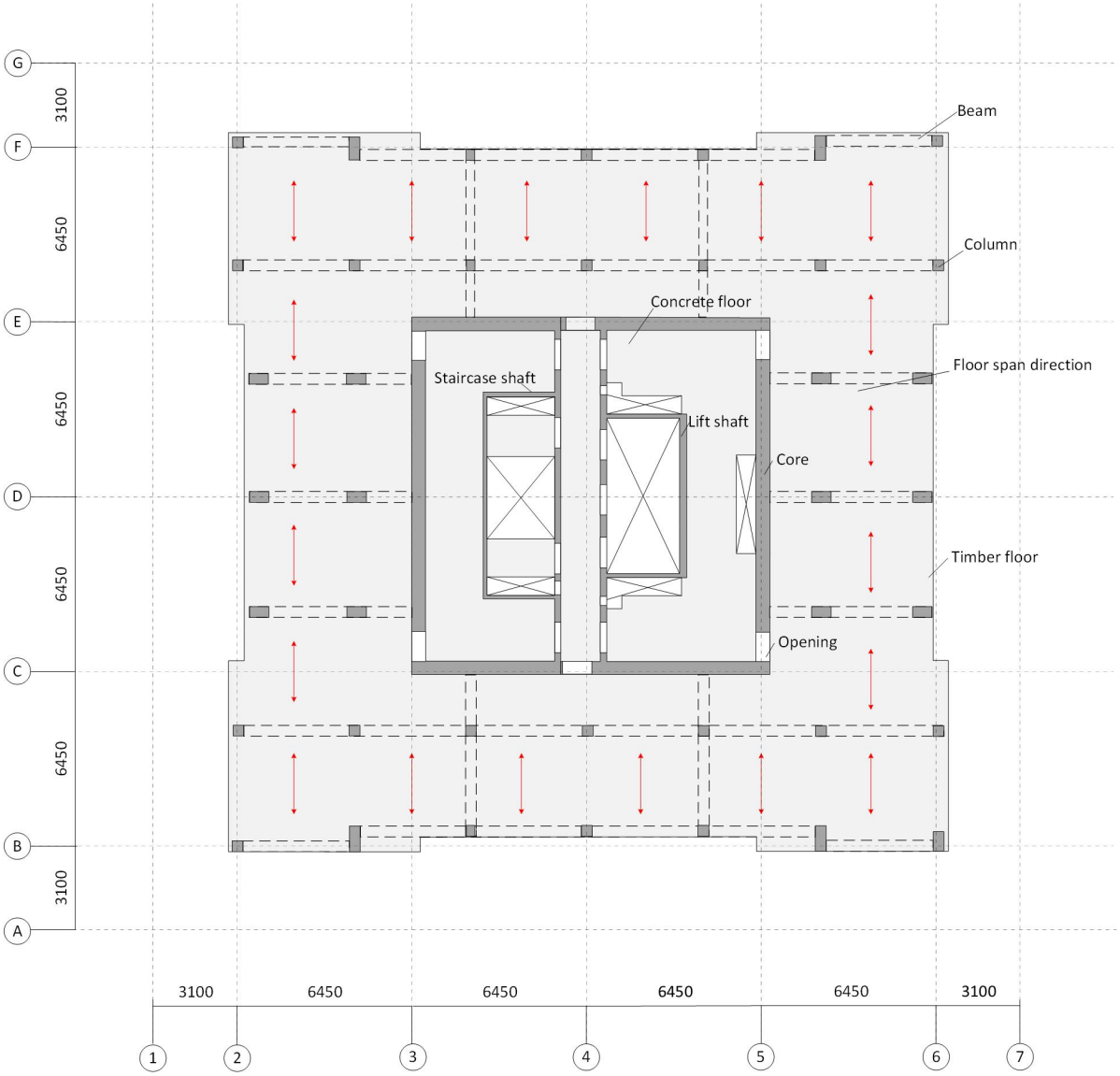

Figure L.4: Variant 4: 4.3 span

Figure L.5: Variant 5: 3.2 span - variant 1

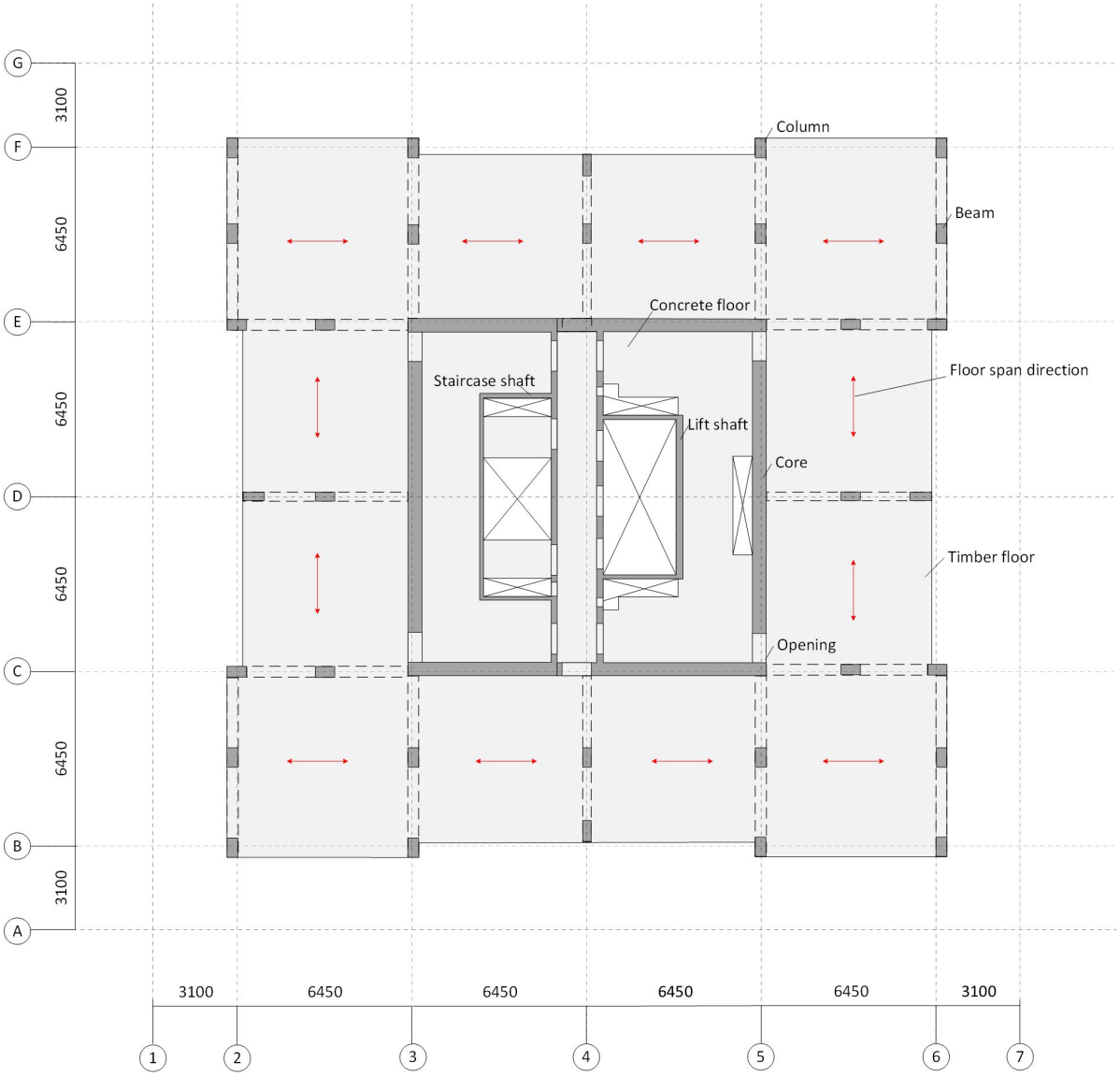

Figure L.6: Variant 6: 3.2 span - variant 2